STRUCTURAL AND SPATIAL ANALYSIS OF THE MICROBIAL COMMUNITIES IN
SOIL CONTAMINATED WITH POLYCYCLIC AROMATIC HYDROCARBONS

Juliet S. Swanson

A dissertation submitted to the faculty of the University of North Carolina at Chapel Hill in partial fulfillment of the requirements for the degree of Doctor of Philosophy in the Department of Environmental Sciences and Engineering.

Chapel Hill
2007

Approved by

Frederic K. Pfaender, Advisor
Michael D. Aitken, Reader
Louise M. Ball, Reader
R. Wayne Litaker, Reader
Ann G. Matthysse, Reader

ABSTRACT

Juliet S. Swanson

STRUCTURAL AND SPATIAL ANALYSIS OF THE MICROBIAL COMMUNITIES IN
SOIL CONTAMINATED WITH POLYCYCLIC AROMATIC HYDROCARBONS

Under the direction of Frederic K. Pfaender.

The microbial communities of an aged, creosote-contaminated soil (CMN) and an

uncontaminated soil (PMN) from nearby were compared. Polymerase chain reaction (PCR)

amplicons of small subunit ribosomal RNA-encoding genes were resolved on a denaturing

gradient gel (DGGE) and transformed into clone libraries. The CMN community was less

diverse than the PMN, as evidenced by 1) the finite number of DGGE bands versus the

smeared profile of the PMN and 2) the finite number of unique clones versus the flat rank

abundance of the PMN clones. The CMN clone library contained sequences belonging only

to the *Proteobacteria*, whereas the PMN sequences represented numerous phylotypes.

A soil-embedding technique was developed for visualizing microorganisms in soil that

preserved spatial arrangements as compared to conventional slurry-based methods. 16S

rRNA probes were hybridized to cells in three soils contaminated with polycyclic aromatic

hydrocarbons (PAH) and the uncontaminated soil after incubation with pyrene. Spatial

relationships between cells and pyrene were determined using a two-population stereological

analysis. Microbial localization with respect to pyrene was found to be nonrandom for the

slurry-based method and random for the aggregate method. This was likely due to the close

association of cells and pyrene with soil particles in the slurried samples. Other patterns also emerged: 1) the higher the background PAH contamination, the more cells clustered with respect to pyrene, and 2) the clustering tendency increased over time for the least contaminated soil and decreased for the others. These data suggest that better-adapted populations are present in more contaminated soils.

The change in the bacterial community structure of the spiked PMN was monitored by PCR-DGGE. The PMN profile became less diverse over time but never approached that of the CMN, even after an additional pyrene spike. The community did not recover its original diversity, indicating either permanent succession or an ongoing selection of certain populations due to constant contaminant availability in the soil. A group of pyrene degraders, PG3, was detected whose 16S rRNA gene copy number correlated with pyrene mineralization, suggesting that the appearance of this group following an acute exposure to PAH could be an indicator of remediation potential.

ACKNOWLEDGMENTS

I would like to thank all the members of my doctoral committee for their guidance, patience, and insight. I am grateful to the Pfaender/Aitken lab group members for their commiseration in the face of unsuccessful experiments and their assistance with my infamous lack of computer skills.

I would especially like to thank my parents, Thomas and Margaret Stumpf, and my in-laws, Thomas and Eunice Swanson, for countless hours of free babysitting. I am grateful to my friend Cindy Broderius for patiently listening to me talk about my research. Finally, I thank my husband, Andy, for never asking me when I was going to finish.

DEDICATION

I dedicate this work to all those in my past who served as mentors and encouraged my

interest in science, especially Drs. Thurman Thorpe and Ann Anderson.

TABLE OF CONTENTS

x

LIST OF TABLES

LIST OF FIGURES

LIST OF ABBREVIATIONS

16S rRNA – RNA from the small subunit of the ribosome; 16S, for prokaryotes and 18S for eukaryotes.

APS – ammonium persulfate; catalyst for the polymerization of acrylamide

BLAST -- Basic Local Alignment Sequence Tool; bioinformational algorithm that compares submitted sequences to those in the NIH database.

BTEX – benzene, toluene, ethylbenzene, xylene

CFB – *Cytophaga-Flavobacteria-Bacteroidetes* phylum

CEC – cation exchange capacity

CF – cystic fibrosis

CFU – colony-forming unit – using the conventional assumption that each colony arises from one bacterial clone, the number of CFUs is a measure of the number of cells per given unit of sample.

CMN – contaminated Minnesota soil

CNC – PAH-contaminated soil obtained from a former manufactured gas plant in Charlotte, NC.

C_T – in quantitative PCR, the cycle number at which dye-bound DNA reaches a pre-determined fluorescence threshold.

daime– Digital Analysis in Microbial Ecology; image analysis program developed by Holger Daims (University of Vienna, Dept. of Microbial Ecology).

DAPI – nucleic acid stain

DCM – dichloromethane

DGGE – denaturing gradient gel electrophoresis; technique used to separate DNA sequences based on their unique "melting domain" within a gradient of denaturant.

dNTP – deoxynucleotide phosphates; nucleotide bases with phosphate groups; used for DNA polymerization during PCR.

dpm – disintegrations per minute; the number of disintegrations of a radioactive compound that is read by a scintillation counter per minute; a measure of that compound's concentration in a sample.

EPA – Environmental Protection Agency

EBPR – enhanced biological phosphorus removal

EPS – extracellular polymeric substances

Eub338 – 16S rRNA probe for the detection of bacteria (eubacteria).

FBR – fluidized bed reactor

FISH – fluorescence *in situ* hybridization; in this thesis, DNA:RNA hybridization of 16S rRNA probes with fluorescent tags to organisms in soil.

FISH-MAR – fluorescence *in situ* hybridization-microautoradiography

FITC – fluorescein diisothiocyanate; a fluorescent compound used to tag biomolecules, such as oligonucleotides, or to stain whole cells.

G+C – abbreviation used to describe the mole percentage of guanine and cytosine in an organism's DNA; usually categorized as "low" versus "high".

HB – hybridization buffer; buffer in which oligonucleotide probes are hybridized to samples.

HOC – hydrophobic organic contaminant/compound

ID – index of dispersion; measure of the distribution of objects in an image.

KKY – creosote-contaminated soil; further information unavailable

K_{ow} – octanol-water partition coefficient, a measure of a compound's partitioning behavior between natural organic and aqueous phases.

LMW – low-molecular weight

MNND – mean nearest neighbor distance; the average of the distances from each object in an image to its nearest neighbor.

NAP(L) – non-aqueous phase (liquid)

O/E ratio – the ratio of the observed versus expected value of some parameter.

OTU – operational taxonomic unit; the term used to describe the "end of the branch" "species", or other designation, that is compared to others when conducting phylogenetic analyses.

PAH – polycyclic aromatic hydrocarbons; compounds of two or more fused benzene rings

PBS – phosphate-buffered saline

PCA – principal components analysis; method of ordination analysis whereby hypothetical variables, i.e. "principal components", are used to explain the maximum amount of variance in the data.

PCE – perchloroethylene

PCP – polychlorophenol

PCR – polymerase chain reaction; repeated denaturation, re-annealing, and elongation of a target DNA sequence in a buffered reaction mix containing dNTPs, *Taq* polymerase, primers, and Mg^{++}.

PLFA/FAME – phospholipid fatty acid analysis; fingerprinting technique wherein phospholipids are extracted from biomass, derivatized to methyl esters, resolved with GC, and used to identify groups of organisms based on signature lipids.

PMN – "pristine" Minnesota soil

PYR – pyrene

PG3 – pyrene-degrading Group 3

qPCR – quantitative polymerase chain reaction; a form of PCR where the amplification products are quantified by comparison to standards.

SET – Salt-EDTA-Tris solution; solution used to wash excess probe from a sample after hybridization.

SIP – stable isotope probing; the use of stable isotope-labeled substrate to measure its uptake by an organism.

SSU – small subunit; in this thesis, refers to ribosomal subunits (16S for prokaryotes, 18S for eukaryotes).

Taq – DNA polymerase from the bacterium *Thermus aquaticus*; a heat-stable enzyme used in PCR

TE – Tris-EDTA
TEM – transmission electron microscopy

TEMED – N,N,N',N'-tetramethylethylenediamine; catalyst for the polymerization of acrylamide.

TPH – total petroleum hydrocarbons

TRITC – tetramethylrhodamine isothiocyanate; fluorescent compound used to tag biomolecules, such as oligonucleotides.

Univ1390 – SSU rRNA probe for the detection of all organisms.

UPGMA – unweighted pair-group method using arithmetic averages; clustering method based on pairwise comparisons of similarity data.

VC – vinyl chloride

1.0 Introduction

The goals of microbial ecology are to characterize both the structural and functional diversity of community members in their natural environment; that is, which microorganisms are present, and what are they doing?

A community is an interactive group of organisms occupying a common habitat, such as soil. It is involved in complex physiological processes, including the biogeochemical cycling of elements or the oxidation of organic matter. To accomplish these functions, a community requires a collection of guilds, or populations of microorganisms with related metabolic processes. In soil, guild functions can include denitrification, methanogenesis, and sulfate reduction.

The soil environment is dynamic. Changes in temperature, moisture, or resource availability, among other parameters, lead to changes in the indigenous microbial community. In this way, the niche promotes the growth or adaptive mutation of species and increases the structural diversity of that environment. Simultaneously, a species can create a new niche, or role in the ecosystem, thus increasing the functional diversity of that environment. Both niche differentiation and adaptation promote community diversity and functional stability (Atlas and Bartha, 1993; Dykhuizen, 1998; Cohan, 2001; Bakker et al., 2004).

Another cause of change in the soil environment is perturbation, such the release of hazardous chemicals. The study of contaminant effects on community structure and

dynamics is termed "pollutant ecology" and comprises both the "ecology of pollutant degradation" (Watanabe and Hamamura, 2003) and the ecology of pollutant toxicity.

In studying pollutant degradation, it is not enough to simply know which organisms are present (community structure); one must also determine which are functionally important (community function). In fact, functional diversity may not always be reflected by changes in community structure, since all species are not equal (Tilman and Knops, 1997; Griffiths et al., 2001, 2004). Knowledge of a community's structure and function may be used to determine the remediation potential at a given site and to exploit it. This may be achieved with the addition of nutrients, surfactant, or even the introduction of genetically engineered microorganisms.

In the case of pollutant toxicity, community structure results from the loss or gain of member populations and/or their abundances due to the adverse effects of contaminant exposure and an inability to adapt. It is likely that both pollutant toxicity and degradative capability influence the microbial community structure at contaminated sites, with toxicity accounting for an initial significant change in structure and degradative capability causing slower changes thereafter.

Studying microorganisms *in situ* is thought to be the best approach to gaining a better understanding of their ecology, i.e. their interactions with each other and their surrounding environment (Amann et al., 1995; Amann and Ludwig, 2000; Wagner et al., 2006). While studying cultured isolates is of paramount importance, it does not paint a realistic picture of what is happening in the environment. Therefore, techniques other than traditional, culture-based methods are continuously being developed to obtain a more accurate representation of the organisms present and to gain insight into their potential interactions.

1.1 Scope and Objectives

The focus of this research is to gain a better understanding of the microbial community within a specific environmental sample, i.e. a soil contaminated with polycyclic aromatic hydrocarbons (PAH). By identifying the types and relative amounts of organisms present, and their spatial relationships with one another and with the contaminant, one may speculate on the activities and contributions of each community member, as they pertain to the degradation or transformation of the organic pollutants present in the soil.

The objectives of this research are as follows:

1) to compare the microbial community profiles of both an aged, PAH-contaminated soil and an uncontaminated soil from the same site to determine the influence of aged PAH contamination on community structural diversity;

2) to describe changes in the microbial community profile of the uncontaminated soil over time after a single spike with pyrene to assess the acute effects of the contaminant, and after a repeated pyrene spike to assess potential long-term effects on the community structure;

3) to develop a method for the *in situ* visualization of microorganisms in PAH-contaminated soils that involves limited disturbance of the soil aggregate structure and communities therein, in order to obtain a more meaningful interpretation of member contributions to community function and to reduce the chances of misinterpreting findings that result from sample manipulation or homogenization;

4) to apply the above method to microcosm incubations of an uncontaminated soil spiked with pyrene to describe the spatial relationships of community members with respect to the contaminant.

1.2 Significance

The significance of such experimental work is manifold for both the fields of soil microbiology and environmental engineering. First, microbiologists have realized that there is a great deal of as yet undiscovered diversity in soil (Borneman and Triplett, 1997; Insam, 2001; Rappé and Giovannoni, 2003). Consequently, many publications have aimed to describe the diversity in various samples (Borneman et al., 1996; Barns et al., 1994; Øvreås and Torsvik, 1998; Dunbar et al., 2000; Madrid et al., 2001). Although solely descriptive, the value of these publications cannot be discounted, as new species are continually being discovered while knowledge of the prevalence of others is growing rapidly (Dojka et al., 2000; Hugenholtz et al., 2001; Dunbar et al., 2002; DeSantis et al., 2007).

Second, by studying microorganisms in their natural habitat, insights may be gained into possible interactions. For example, there is continuing evidence that the spatial relationships between ammonia-oxidizing and nitrite-oxidizing bacteria are predictive of their functions, whether in soil or in activated sludge (Grundmann and Debouzie, 2000; Daims et al., 2006).

Third, a great deal is still unknown about the interactions between soil microbes and their environment. Soil is a dynamic and heterogeneous matrix. Both its components, including soil organic matter, and its aggregate structure are greatly influenced by and also influence microbial activity. In turn, soil structure and microbial activity also affect contaminant availability (Guthrie et al., 1999; Coates et al., 2000; Kim and Pfaender, 2005).

This leads to the significance of this work to the field of environmental sciences. Bioremediation potential is dependent upon both community structural and functional diversity. By studying the former, one may make inferences about the latter. In other words, can changes in the microbial community be indicative of remediation and/or toxicity? Can

4

the identification of contaminant degraders be used to enhance their activity? Can their

spatial arrangements with respect to a contaminant be used to infer degradative activity? The

answers to these questions may help determine the best technology for remediating a given

site and may also provide a means of monitoring its progress.

2.0 Literature Review

2.1 Microbial Diversity and rRNA Phylogeny

Diversity measurements rely on knowledge of the numbers and types of species present within a given population or sample. This information allows the determination of sample richness (the number of different species within a sample) and evenness (the relative abundance of organisms within that species). These measurements are a reflection of the community's structure, function, and stability. However, before these diversity indices can be calculated, one must justify the use of "species" as the operational taxonomic unit (OTU).

Simply put, a species is a group of physiologically related organisms that occupy a common ecological niche, exchange genetic information, and differ from other species in their evolutionary fates (Cohan, 2002). Conventional species delineation is based on phenotype. For bacteria, those characteristics may include, but are not limited to, morphology; Gram stain reactions; nutritional classifications and the ability to use various carbon, nitrogen, or sulfur sources; cell wall chemistry; lipid chemistry; habitats; and immunological characteristics (Madigan et al., 2000). In contrast, modern means of species classification are based on genotype. Two bacteria belong to the same species if they exhibit greater than 97% similarity in their 16S rRNA sequence (i.e. less than 3% dissimilarity) and more than 70% homology by DNA:DNA hybridization (Lengeler et al., 1999; Madigan et al., 2000; Stackebrandt et al., 2002). Using these techniques, it is unnecessary to culture the organism; one simply classifies it according to its closest relatives. This classification

scheme, termed phylogeny, is based on genealogical relatedness, or the evolutionary distances of organisms from each other and from a common ancestor.

With the advent of molecular technology, it has become clear that neither definition of species is adequate (Schlöter et al., 2000; Morris et al., 2002). For example, an organism cannot even be given a species name until it has been isolated in pure culture, even if its functional potential differs dramatically from any known species. This simply may not be possible for many environmental microorganisms; therefore, many of these have only achieved "candidate status" (Dojka et al., 2000; Hugenholtz et al., 2001; Dunbar et al., 2002).

Another reason for the inadequacy of "species" is that the bacterial genome is dynamic. Although rare, gene duplication, *de novo* genesis, losses, and recombination events all occur (Snel et al., 2002). Furthermore, the promiscuity with which bacteria exchange genetic information is well documented. It has been proposed that between 5 to 15% of any given bacterial genome was derived through horizontal transfer and that transfer is possible between organisms with as much as 25% divergence in DNA sequence (Cohan, 2002). Since phylogenetic classification is based on the vertical transfer of genes over time from a common ancestor, the dynamic attributes of the bacterial genome are especially problematic.

The use of ribosomal phylogeny was established by Woese et al. in the early 1970's and led to the discovery of the three distinct domains of life-- the *Eukarya*, the *Eubacteria*, and the *Archaebacteria* (Woese and Fox, 1977). Woese and his colleagues first reasoned that translation, a requisite process for cell viability, was one of the first systems to evolve. Therefore, ribosomes, which are an integral component of the cell's translational machinery, must be ubiquitous (Sogin et al., 1972; Fox et al., 1977). Furthermore, because of their importance, it is unlikely that they have changed significantly throughout evolution and also

unlikely that their encoding sequences would be viable targets for lateral genetic exchange (Fox et al., 1980; Woese, 1998). These attributes, coupled with the fact that ribosomes occur in large numbers that correlate with cell growth and activity, and are easily isolated, were initially what made them the choice target for DNA sequencing and phylogenetic studies. Later, it was determined that they contained regions whose sequences had been highly conserved throughout evolution, in addition to regions of great variability (Fox et al., 1977). This sequence variability, however minute, permitted the discrimination of "species" and their subsequent phylogenetic classification.

Ribosomal RNA phylogeny has been questioned by many for its appropriateness in taxonomic studies (Doolittle, 1999; Snel et al., 2002; Wolf et al., 2002). This argument is based most heavily on the impact of lateral gene transfer. Alternative phylogenetic trees have been drawn that are based on the sequences of known functional genes, gene content, gene order, signature sequences, the fraction of shared genes, and metabolic pathway reaction content (Huynen et al., 1999; Gupta and Soltys, 1999; Raymond et al., 2002; Wolf et al., 2002; Hong et al., 2004). Although the resulting trees differ somewhat in their deep branching, they are remarkably similar in their overall structure, and all support the three-domain paradigm. Today, small subunit rRNA phylogeny is still the most widely accepted means of analysis and, with due consideration, this phylotype will be used as the operational taxonomic unit for this research.

2.2 Characterizing Microbial Diversity: the Application of Molecular Methodology to Environmental Samples

2.2.1 Culture-based versus culture-independent methods Although tried and true in the clinical setting, culture-based techniques for the identification of microorganisms have

numerous disadvantages in the environmental arena. In a landmark study, Torsvik et al. (1990a, 1990b) used DNA:DNA hybridization kinetics of the nucleic acids extracted from forest soil to estimate that the number of standard genomes present in the sample was 4,000. From this analysis and comparisons to bacterial isolates, the authors determined that the cultured fraction represented less than 1% of the total diversity. Torsvik's data have been reevaluated extensively with notable modifications: Dykhuizen (1998) claims that the actual bacterial diversity within her soil sample was about 20,000 predominant species with approximately half a million rare ones. Others simply contend that the true diversity will never be realized (Doolittle, 1999).

The discrepancy between direct, microscopic counts and viable cell counts, or the "Great Plate Count Anomaly", is due to both the presence of viable but noncultivable bacteria and bacteria whose requisite conditions for growth have not yet been realized (Staley and Konopka, 1985, as cited in Amann et al., 1995). The inability to culture all the bacteria from a soil sample is chiefly attributed to the inability to replicate environmental conditions in the laboratory. Laboratory bias is inevitably introduced by the choice of culture media, incubation atmospheres, and temperatures, among other things, not to mention the bias introduced by simply trying to isolate a species that in nature cannot exist by itself. Further, these conditions change periodically in the environment. Therefore, the resulting microbial profile typically shows those organisms that grow best under the imposed conditions but may not be representative of the true community that is present.

The use of molecular methods will inevitably result in a different community profile than culture-based methods (Wagner et al., 1993; Smit et al., 2001). Felske et al (1999) found no correlation between 165 members of a 16S rRNA gene clone library and 659 cultured

isolates from the same soil. Similarly, 37% of 16S rRNA clones obtained from an Austrian experimental soil field were from the *Holophaga/Acidobacterium* family of bacteria; only three *Acidobacteria* have been cultured thus far (Sessitch et al., 2001). Snaidr et al. (1997) showed that *Acinetobacter spp*. accounted for only 3-9% of individual counts from *in situ* hybridizations of sludge; whereas, their numbers accounted for 30-60% of CFU's from the cultured sludge. As of this writing, the National Center for Biotechnological Information 16S ribosomal RNA database contains over 400,000 submitted sequences, the majority of which are from uncultured bacteria in environmental samples (www.ncbi.nlm.nih.gov).

The use of cultivation-independent techniques to describe the microbial flora in environmental systems has become standard within the past two decades. These techniques avoid the laboratory bias mentioned above. Studies have shown their utility in identifying new, previously uncultured organisms in environmental media, including fresh and salt waters, sediments and soils (Ludwig et al., 1997; Hugenholtz et al., 1998; Dojka et al., 2000; DeSantis et al., 2007). However, these techniques are not without their own disadvantages, especially when applied to environmental samples. This study used the following molecular techniques: DNA extraction, polymerase chain reaction (PCR), denaturing gradient gel electrophoresis (DGGE), clone libraries, and fluorescence *in situ* hybridization (FISH). Their advantages and disadvantages are addressed below, with emphasis on their relevance to soil samples.

2.2.2 Nucleic acid extraction from soils The extractability of DNA from soil is affected by many factors, such as mineralogy, pH, ionic strength, and the presence of organic matter (Sayler et al., 1992). Nucleic acids tend to adsorb more readily to clays than silicates, potentially causing lower yields of extractable DNA from this type of soil (Zhou et al., 1996;

Frostegård et al., 1999). Montmorillonite clays, especially, have been shown to retain more

nucleic acids than other clays, possibly due to their expandability and increased surface area.

Soil pH and ionic strength influence the charged versus uncharged state of DNA, thereby

affecting its adsorption onto the soil mineral matrix. A high pH of either the soil or the

extraction buffer results in a higher DNA yield but also more humics coextracted (Khanna

and Stotzky, 1992; Frostegård et al., 1999). Also, both soil pH and ionic strength affect the

state of natural organic matter, i.e. humic substances, in the soil, which in turn can lead to the

coextraction of these substances and any contaminants therein, and interfere with

downstream molecular methods.

Soil organic carbon content has been shown to correlate positively with DNA yields

(Zhou et al., 1996). Both these and the humics themselves may be coextracted with nucleic

acids and interfere with quantification measurements, PCR, or *in situ* hybridizations.

Finally, extracellular nucleases naturally present in soil may cause the degradation of

targeted nucleic acids even when care has been taken to use nuclease-free reagents and

laboratory equipment. Some protection from nuclease activity is afforded by binding with

clays or sand (Picard et al., 1992; Pietramellara et al., 1997), but the extraction procedure

itself may cause release of the nucleic acids from the mineral matrix and result in

vulnerability to nuclease attack.

Numerous protocols exist for the extraction of nucleic acids from soils and sediments,

and many papers have been published in an attempt to optimize them (Moré et al., 1994; van

Elsas and Smalla, 1995; Holben, 1997; Miller et al., 1999; Martin-Laurent et al., 2001). It is

apparent from reading them that each protocol must be optimized for a particular soil

(Ogram, 2000). Initially, methods involved separating cells from soil first and then

extracting the nucleic acids from the cells. Currently, most methods involve the direct

extraction of nucleic acids from bulk soil samples. These protocols vary in the rigor of their

lysis step and, therefore, may preferentially extract the nucleic acids from organisms that are

most easily lysed or those unprotected by soil structures. This is certainly true for fungi,

archaea and Gram-positive bacteria, whose cell walls, S-layers, and thick membranes,

respectively, lend more difficulty to the procedure. Also, lysis efficiency may vary with cell

size (Moré et al., 1994). Differential lysis efficiency may result in unrepresentative

sampling. Rigorous extraction techniques may also result in DNA shearing. High quality

(i.e. high-molecular-weight, intact, and pure) DNA is required for further molecular analyses,

such as PCR and DGGE.

2.2.3 rRNA-dependent methodologies: advantages and disadvantages of PCR, DGGE, Cloning and FISH

The choice of ribosomal DNA as the target sequence for organism identification has been

reviewed extensively elsewhere (Amann et al., 1995) and discussed earlier.

While the advantages of PCR are undeniable, there are also drawbacks. These have also

been reviewed extensively (Amann et al., 1995; Amann and Ludwig, 2000; Moter and Göbel,

2000). For the purposes of this study, the disadvantages are as follows: interference from

coextracted soil substances; the need for a nested protocol; primer selection bias, sensitivity

and specificity; differential amplification of genes; and the formation of chimeras. The first

two issues are discussed in a later section on methods.

Primers have been designed based on known sequences in existing databases. With the

supposed dramatic underestimation of existing bacterial species and the continued discovery

of new ones, it seems impossible to have primers that will amplify genes from all bacteria.

However, primer design was not within the scope of this study. The bacterial primers used in

this study were those used successfully by previous researchers on a variety of environmental samples (Hugenholtz et al., 1998; El-Fantroussi et al., 1999; Fraga, 2000), and their sensitivity and specificity have been tested against pure cultures (Marchesi et al., 1998). Fungal and archaeal primers were chosen based on the literature (Vertriani et al., 1998; Borneman and Hartin, 2000), current experimental work, and the recommendations of others (B. Whitman and colleagues, University of Georgia, personal communication; A. Grunden, North Carolina State University, personal communication).

Given the number of resulting amplicons from PCR (~10^9 or more), there is the potential for organisms that are present in low numbers to be masked by those that are more abundant due to preferential amplification of those present in larger numbers. This can also result from extraction bias, e.g. unrepresentative sampling. Additionally, the copy numbers of the ribosomal operon differ in bacteria and range between 1-15, in known, sequenced organisms (Ogram, 2000; Aciñas et al., 2004), again resulting in differential amplification. The use of nested PCR, or the amplification of a sequence within a sequence, may either resolve this problem by increasing the amplicons from organisms present in low numbers or those with low *rrn* copy numbers, or enhance it by even more masking. It has been suggested that rRNA operon copy number positively correlates with growth rate, such that for microorganisms in organic poor environments, the number would be low and would potentially minimize this bias (Klappenbach et al., 2000). This issue has not been resolved by current research in the literature; therefore, it can only be acknowledged in this study.

Chimeras are PCR amplicons formed from the sequences of more than one species or even between different copies of the SSU rRNA from the same organism (Wang and Wang, 1997). The probability of their occurrence is increased in low-molecular weight DNA

samples (i.e. < 10kbp), during PCR with short elongation periods, and by selecting primers that encode lengthy conserved regions of the rRNA gene (Amann et al., 1995). Extraction techniques that yield high-molecular-weight DNA should minimize chimera formation (Zhou et al., 1996).

Extensive clone libraries have been constructed from the 16S rRNA genes found in environmental samples and have yielded most of the findings that support the overwhelming bacterial diversity in soil (Borneman and Triplett, 1997; Liles et al., 2003). Cloning involves the ligation of an amplified target sequence (e.g. 16S rRNA gene) into a plasmid vector that is then transformed into *E. coli*. After cell growth, high copy numbers of the target sequence exist. These can be purified and sequenced, yielding a library with large amounts of data that can be analyzed statistically. Clone libraries are subject to the same problems as other molecular techniques, such as DNA extraction and PCR bias, and cost. Cloning is also prone to unique problems, such as a low percentage of transformants, and multiple steps, such as screening of ambiguous transformants and plasmid screening. However, new kits and methods have minimized the amount of manual screening necessary and maximized the percentage of transformants. Cloning remains the "gold standard" for characterizing genetic diversity in environmental samples.

Denaturing gradient gel electrophoresis is an ideal means of picturing differences in community diversity and for monitoring changes in diversity over time (Muyzer et al., 1993; Muyzer and Smalla, 1998). PCR-amplified rRNA gene fragments migrate until they reach a level of denaturant at which partial melting occurs and further movement through the gel is hindered. This "melting domain" differs with even minute variations in base pair sequence.

Theoretically, different DNA sequences represent different organisms; therefore, each band represents a different member of the microbial community.

Obvious disadvantages of DGGE include its dependency on representative extraction methods and optimal PCR amplification; therefore, quantification methods, such as measuring band intensity, may not be accurate. It has also been argued that not every band is a different species, since an organism may produce more than one band due to heterogeneous rRNA operons, such that even pure cultures have resulted in multiple DGGE bands (Cilia et al., 1996; Nübel et al., 1996). Overall, this might lead to an overestimation of diversity by as much as 2.5 to 3 times the actual amount present (Aciñas et al., 2004). However, it has also been argued that this type of heterogeneity in an environmental sample is actually due to the presence of "closely related, yet ecologically distinct," organisms (Yang and Crowley, 2000; Casamayor et al., 2002). In a contaminated sample, this functional diversity may become a selective advantage for the population. Others suggest that stable environments tend to result in bacteria with less rRNA operon sequence divergence, while extreme conditions result in extreme divergence (Aciñas et al., 2004).

DGGE is not ideal for profiling highly diverse communities due to the potential comigration of bands or a smeared image from too many bands. Even sequences with different base pair compositions can show similar migrating behavior in the gel resulting in an underestimation of diversity (von Wintzengrode et al., 1997).

Compared to cloning, DGGE offers more complete coverage of the community structure, that is, the entire community is shown on one gel, whereas the entire community may not be represented in a clone library (Dunbar et al., 2002). However, resolution at the OTU level may not be possible with DGGE, especially in a diverse sample. Cloning is advantageous in

this respect. Additionally, cloning can produce copies of a complete 16S rRNA gene sequence. DGGE is optimized for separating bands of between 200-500 bases; therefore, only partial rRNA gene sequences are obtained. Which technique the researcher chooses should depend on what question is being asked and on what resources are available.

Fluorescence *in situ* hybridization (FISH) permits the direct identification of different groups of microorganisms in an environmental sample and, when coupled with microscopy, also allows the spatial relationships between these organisms to be examined. FISH has been used extensively for aqueous samples and for soil and sediment slurries (Hicks et al., 1992; Amann et al., 1995; Amann et al., 1990a, 1990b, 1996; Christensen et al., 1999; Nogales et al., 2001). The importance of *in situ* studies has been touted by many (Amann and Ludwig, 2000; Wagner et al., 2003). The ability to visualize microbes in their habitat offers unique insight into their interactions with each other, with plants, with soil or sediment particles, or with other natural or synthetic surfaces.

Briefly, cells are fixed, pretreated if necessary, hybridized with an oligonucleotide probe complementary to the sequence of interest, washed, and visualized microscopically through the use of a fluorescent tag covalently attached to the end of the probe. Multiple probes with different tags may be used, allowing the researcher to visualize different populations simultaneously. Probes are chosen based on the study objective. Identification probes may target small subunit rRNA sequences that are unique to specific groups of organisms, while functional probes may target mRNA transcripts encoding an enzyme of interest. Both may be used simultaneously to determine "who is doing what and where".

Microbial consortia have been analyzed with functional probes to determine the contributions of each member to the consortium (Snaidr et al., 1997; Ravenschlag et al.,

2000; Kleikemper et al., 2002; Ginige et al., 2004). Similar studies have been conducted on stromatolite biofilms (Decho and Kawaguchi, 1999), flow chamber biofilms (Møller et al., 1998), and plant root systems (Briones et al., 2003). *In situ* hybridizations have also led to the discovery of symbiotic interactions and other interesting relationships between bacteria and fish, insects, humans, protozoa, and archaea, as well as between archaea and protozoa (Amann et al., 1995, and references therein).

However, there are weaknesses associated with the FISH technique, the biggest of which are probe penetration and access to target RNA, low cell numbers, and low cell activity. Cells can be fixed and made permeable using formaldehyde and/or ethanol solutions with or without lysozyme or heat pretreatment. Once again, cell wall structure determines how easily cells are made permeable; Gram-positive bacteria become more permeable with the use of ethanol or ethanol/formalin, while Gram negatives require formaldehyde or paraformaldehyde (Moter and Göbel, 2000). The added bulk of the attached fluorochrome can also make penetration more difficult. Once the probe has entered the cell, it must access the target RNA; therefore, the site of probe annealing should not be located on loop and hairpin structures or in areas of protein-RNA interaction (Moter and Göbel, 2000).

The numbers of microorganisms in contaminated soils may be fewer than those present in pristine soils. This presents a problem for *in situ* hybridizations for which signal intensity is dependent upon cell numbers. Typically, a slurry of soil or sediment or a large volume of water is filtered to concentrate cell numbers prior to fixation and hybridization. Alternatively, multiple probes, probes with multiple labels, or probes whose labels are unusually intense can be used.

Hybridization is indirectly influenced by the nutritional status of the cell, since rRNA content may vary with cell physiology (Oda et al., 2000; Hansen et al., 2001). Ribosomal numbers have been shown to correlate well with the cell's growth rate (Schaecter et al., 1958; Amann and Ludwig, 2000). Slow growing cells may not have RNA contents comparable to faster growing bacteria and may result in low signals or false negatives (Amann and Ludwig, 2000). Additionally, stressed or starved cells are less likely to be good candidates for *in situ* hybridization (Oda et al., 2000).

Finally, some prokaryotes--notably some methanogens, cyanobacteria, and pseudomonads--and even some eukaryotes, autofluoresce; therefore, tags must be chosen with care.

FISH is subject to the same difficulties as other molecular techniques when used in contaminated soils. That is, humic matter and organic contaminants may interfere with the hybridization reaction. They may also autofluoresce, providing a background from which the probes must be distinguished. Mineral components, such as aluminum oxides, carbonates, or clays, have also been shown to autofluoresce (Li et al., 2004). Finally, the monovalent cationic content of the soil may interfere with the hybridization process by causing oligonucleotide precipitation.

A serious, but little addressed, disadvantage of existing FISH methods is that the soil "aggregate" is disrupted before the technique is applied. By convention, either the soil is diluted in a slurry form or cells/nucleic acids are extracted from the soil prior to hybridizing. However, the distribution of microorganisms in soil is not uniform, and measurements on bulk soil may be misleading (Becker et al., 2006). For example, significant differences have been shown in the predominant organisms found in large versus small soil particle size

fractions and in soil macroaggregates versus inner microaggregates (Sessitch et al., 2001; Mummey et al., 2006). Furthermore, bulk soil measurements defeat the purpose of determining spatial relationships between groups of organisms or between organisms and soil components. Such relationships must be preserved if microbial distribution is to be related to microbial function (Harris, 1994; Grundmann and Debouzie, 2000).

Many studies of plant rhizospheres have shown the utility in preserving sample higher structure. Assmus et al. (1995) used FISH and confocal laser scanning microscopy to show that the distribution of three different strains of *Azospirillum brasiliense* in wheat rhizospheres varied with their purported function. Corgié et al. (2004) found that the degradative abilities of bacteria in phenanthrene-contaminated rhizospheres were modified spatially. It seems only logical that spatial relationships of bacteria outside rhizosphere soil should be as informative. However, few environmental studies have attempted to preserve the aggregate structure of soil. For the most part, this type of research has been conducted by agricultural scientists. Their studies employ methods such as biological thin sections, core sampling, and staining (Fisk et al., 1999; Nunan et al., 2001; Li et al., 2003). The advantage to these methods is that the soil higher structure is minimally disturbed. The chief disadvantages are that these techniques measure dead, as well as live, cells, and bacteria can only be distinguished by morphology and stain reaction, if hybridization methods are not used. A more detailed description of the bacteria, e.g. their genus or even domain, cannot be given.

2.3 Factors Influencing Microbial Community Development and Diversity in Soil

Among the factors that influence microbial community structure in soil are: soil type and particle size distribution; resources, such as carbon sources and other nutrients; cultivation practices and plant presence; the presence of terminal electron acceptors, including oxygen; seasonal variation, including temperature and moisture; spatial isolation; and the presence of pollutant compounds.

2.3.1 Soil type Soil type has been named the key factor in determining the bacterial community composition of arable soils, regardless of geography or cropping regimes (Liesack et al., 1997; Bossio et al., 1998; Girvan et al., 2003). Since most soils are mineral soils, type is determined largely by the size distribution of its particulate components, i.e. sand, silt, and clay. Differences in bacterial community diversity have been shown between different particle size fractions in topsoil with the lowest diversity in the sand fraction and the highest in the clay (Sessitch et al., 2001). The authors' explanation for this finding was: first, that the small size fraction might lend protection against protozoan predators, second, that many filamentous bacteria are able to adhere to clay particles, and third, that there may be more nutrients and water available in the smaller size fraction. Interestingly, fungi predominated in the sand, aerobic bacteria were present in both the larger and smaller size fractions, and anaerobes were limited to the smallest size fractions. Mummey and Stahl (2006) also found that the organisms present in soil macroaggregates differed from those present in microaggregates. *Acidobacteria* dominated the macroaggregates of three geographically distinct soils, whereas *Gemmatomonadetes* and *Rubrobacteridae* (Actinobacteria) were found in microaggregates.

2.3.2 Soil organic matter The presence, amount, and character of natural organic matter in soil may also influence the soil microbial community structure. A wider variety of carbon sources are present in higher organic soils. An analysis of 16S rRNA gene sequences from surface soils of differing carbon content showed that high-carbon sites had no predominant species, regardless of moisture content or depth (Zhou et al., 2002). This was attributed to the lack of competition for abundant and heterogeneous resources, and to spatial isolation of the organisms themselves.

Using phospholipid fatty acid analysis (PLFA), significant differences in community profiles were observed between soils of high and low organic content that were not detected using functional assays (Bossio et al., 1998). Øvreås and Torsvik (1998) also described richer and more even bacterial communities in an organic soil versus a sandy soil using amplified ribosomal DNA restriction analysis (ARDRA) and DGGE. However, they found more functional diversity in the sandy soil than the organic soil, possibly due to the narrower range of substrates present there.

2.3.3 Cultivation effects Several researchers have focused on the effects of land cultivation practices on microbial community structure. Buckley and Schmidt (2001) used 16S rRNA probes to show that any type of cultivation, regardless of short-term land management or crop cover, had a long-term impact on soil microbial communities as compared to no cultivation at all. It is thought that species are influenced by the presence of plant exudates but also by land practices such as tilling and crop rotation. The presence of healthy crops is thought to increase the nitrogen and phosphorus content of a soil, which become available to microorganisms as nutrients during plant decomposition (Smith, 2002). McCaig et al. (1999)

showed a reduction in *α-Proteobacterial* diversity in rhizosphere samples that had been amended with fertilizer compared to those that had not.

Different DGGE profiles were observed between different plant rhizospheres and bulk soil (Smalla et al., 2001). The rhizosphere pattern exhibited several dominant populations and fewer less prevalent populations, while bulk soils contained one or two dominant members but many less prevalent populations with equal abundance. This study also showed that different plant species enriched different populations of bacteria in the rhizosphere and that the enrichment could be enhanced with repeated cultivation of that same crop.

Another study found an association between the presence of specific catabolic genes (those encoding hydrocarbon and nitroaromatic degradation) and endophytic bacteria (Siciliano et al., 2001). This association was also dependent on both plant type and contaminant concentration, suggesting a plant-mediated selection of bacteria.

2.3.4 Terminal electron acceptors Many researchers have looked at the effects of redox gradients and anoxic zones on microbial community structure. These studies have been conducted chiefly on sediments where these gradients routinely exist. However, these studies are relevant to soils as well, since they cannot be guaranteed to be aerobic all of the time. Soil aeration can be affected by many factors, such as oxygen diffusion rates, available carbon sources and their microbial oxygen demands, temperature, soil type and porosity, the presence of aggregates, and water content. Anaerobic regions occur as two-dimensional layers in sediments and marshes due to the influx and efflux of water, but anaerobic microsites may occur as "three-dimensional mosaics" within many soils (Smith and Arah, 1985).

Water content, often dependent on soil type, is a major contributing factor to the anaerobicity found in soil. Fine soils tend to retain water. Soils that promote aggregation, even if well drained, may also be water-saturated within the aggregates. Low-clay soils and others that do not promote aggregation have been shown to have zones of anaerobicity in areas furthest from air-filled pores (Smith and Arah, 1985).

Changes in bacterial community structure have been shown to correlate with oxygen depletion and depth in the upper 2 mm of a soil (Lüdemann et al., 2000). In contrast, others have found minor differences in the 16S rRNA gene sequences of sediment denitrifying communities along a dramatic change in redox gradient, possibly due to vertical mixing by invertebrates (Braker et al., 2001). However, there was a significant amount of diversity in the nitrate reductase gene within the oxygen and nitrate gradients, indicating a functional diversity not linked to structure.

2.3.5 Seasonal variation and spatial isolation Seasonal variability, as measured by changes in temperature and moisture content, has also been found to correlate with changes in microbial community structure. MacGregor et al. (2001) measured an increase in rRNA concentration in Michigan lake sediments during seasons of greater nutrient input as well as changes in eukaryotic RNA (dominant in winter and early spring) versus bacterial (dominant for the remainder of the year). Repeated drying and rewetting of soil can also influence the bacterial/microbial diversity (Fierer et al., 2003). One explanation for this is that spatial isolation is promoted by decreases in moisture content (Treves et al., 2002). This may result in competition between species, such that different species predominate under different moisture conditions.

Finally, type, structure and aggregation all influence how water travels through a given soil. "Preferential flow paths" are known to exist and have been shown to be "hot spots" for microbial activity (Bundt et al., 2001). This may be due to differences in the physical and chemical properties along the flow paths, such as increased organic carbon and nitrogen content, increased solute input, and enhanced cation exchange capacity and base saturation. That being said, Bundt et al. found little difference in the microbial diversity of 16S rRNA genes along flow paths versus bulk soil, except among certain species of bacteria. Functional analyses were not conducted. The "hot spot" theory has been supported by other studies, including Nunan et al. (2002) whose *in situ* images from soil biological thin sections showed small, non-random clusters of bacterial growth at the microscale in an arable subsoil, and more random distribution at the macroscale, suggesting that hot spots are microscopic areas conducive to unrestricted bacterial population growth in a potentially larger area of limited nutrient availability (Nunan et al., 2001).

2.3.6 Microbial communities in soil Microorganisms make up less than 0.5% (w/w) of soil mass but constitute 90% of the total biomass (Liesack et al., 1997; Tate, 2000). Bacteria range from 10^6 to 10^{12} cells per gram of dry soil. Within the *Bacteria*, actinomycete numbers range from 10^7 to 10^9 per gram dry soil. Among eukaryotes, the fungi make up the majority of biomass due to their large size. Fungal propagules may reach between 10^{11} and 10^{12}, while total hyphal length can reach 25 km. Protozoan counts range from 10^4-10^6; while algal counts range from 10^3-10^4, but have reached 10^8 in some soils (Meyer, 1993; Wollum, 1999; Tate, 2000; Young and Crawford, 2004). For all but the protozoa, the higher counts were obtained from rhizosphere samples as opposed to bulk soil. Prokaryotes tend to dominate the rhizosphere.

Typical cultivable soil bacteria include: a) spore-forming, low-G+C, Gram-positives, such as *Bacillus* and *Clostridium* species among rods, and *Sporosarcina* among cocci; b) high-G+C Gram-positives, such as *Corynebacterium*, *Arthrobacter* (both non-spore-formers), and *Mycobacterium* species, in addition to the filamentous *Actinomycetes*; c) photosynthetic bacteria, such as the cyanobacteria; and d) Gram-negative aerobic rods and cocci, such as the pseudomonads, *Rhizobacteria*, or *Azotobacteria* (Alexander, 1999; Madigan et al., 2000; Tate, 2000). Several other *Proteobacteria*, such as nitrifiers and sulfate-reducers, can be found depending on the soil environment. As mentioned earlier, these numbers are a gross underestimate of the true, but unknown, soil microbial diversity.

2.4 Contaminant Influence on Soil Microbial Diversity

2.4.1 Resistance and resilience It has been proposed that the microbial response to the presence of contaminant compounds is two-staged (Griffiths et al., 2004). The immediate impact of the exposure is reflected in the community's "resistance", or its ability to withstand the contaminant. Over time, the community's "resilience" is measured by its ability to recover to its original structure.

Community resistance is reflected in the ability of its members to either detoxify a contaminant or withstand its adverse effects. The toxic effects of PAH and their metabolites to bacteria have been previously shown (Weissenfels et al., 1992; Bispo et al., 1999; Schweigert et al., 2001). It is thought that PAHs act primarily on the cell membrane, due to their high K_{ow} and their resulting lipophilicity. The accumulation of PAHs in the membrane may disrupt the bilayer either by expansion or vesiculation and adversely affect lipid-lipid and lipid-protein interactions (Sikkema et al., 1995, and references therein). Membrane

integrity is an obvious prerequisite for membrane function (e.g. transport, ATP synthesis) and cell survival.

Other toxic effects may include genetic disruption by adduct formation, or the formation of reactive oxygen species during redox cycling of quinone or catechol intermediates (Schweigert et al., 2001; Penning et al., 1999).

Bacterial responses to PAH toxicity are not well understood. Some have suggested a role for glutathione (Zablotowicz et al., 1995; Vuilleumier, 1997; Parales et al., 2002) in creating a soluble conjugate that is then removed from the bacterial system. Others have supported this suggestion by finding an association between the presence of glutathione-S-transferase-encoding genes and naphthalene and phenanthrene catabolic genes (Lloyd-Jones and Lau, 1997; Lloyd-Jones et al., 1999).

Still other studies report the presence of active efflux systems in some PAH-degrading bacteria (Bugg et al., 2000; Hearn et al., 2003). Although these studies did not deem PAHs to be toxic to bacteria, the results showed selectivity in the efflux system toward the 3- and 4-ring PAHs tested, but not for naphthalene or toluene. Interestingly, not all organisms tested possessed the efflux system, although all were members of the *Proteobacteria*.

Fungi respond similarly to other eukaryotes when exposed to PAHs. PAH presence induces the expression of genes encoding cytochrome P450 monooxygenases. These enzymes catalyze the addition of oxygen to the aromatic ring, resulting in a more soluble intermediate, albeit often a more toxic one. *Cunninghamella elegans*, a zygomycete, is able to eliminate some PAHs as glucoside conjugates (Cerniglia et al., 1986), while other fungi may form glucuronide and sulfate conjugates (Sutherland et al., 1995).

Community resilience measures the ability of a community to return to its original structure once the initial impact of the exposure has passed. Obviously, this would depend on how much of the community was affected by the original insult, for example whether or not there was a significant loss of species or a loss of "keystone" species (Bond, 1993; Tilman and Knops, 1997), and whether the physico-chemical characteristics of the soil remain altered. The concept of resilience may not be as readily applied to the case of PAHs for all these reasons. First, sites contaminated with non-volatile hydrocarbons may remain physically altered for some time. For example, creosote-contaminated soils often form "tar balls", due to the sticky and viscous nature of creosote (Johnsen et al., 2005). The presence of these, or any non-aqueous phase, may lead to the spatial isolation of microbial communities. Second, contaminant availability is questionable. If PAHs are bound by organic matter and unavailable, perhaps the community will recover. If, for whatever reason, they become available again, then the insult is ongoing and the community adapts instead. In this case, community succession takes place as a result of the continued presence of the contaminant.

2.4.2 Examples from literature Several papers describe the resultant microbial community diversity in hydrocarbon-contaminated environments (Dojka et al., 1998; Margesin et al., 2003; Nogales et al., 2001; Zhu et al., 2003; Saul et al., 2005), while other studies have followed the succession in community structure post-exposure and during remediation efforts (MacNaughton et al., 1999; Thompson et al., 1999; Ringelberg et al., 2001; Abed et al., 2002; Röling et al., 2002; Maruyama et al., 2003; Kaplan and Kitts, 2004). Interestingly, the findings are consistent with respect to an initial loss of diversity, but are not always consistent with respect to the resulting dominant species.

MacNaughton et al. (1999) used PLFA and 16S rRNA gene analysis to show a decrease in microbial diversity in beach plots contaminated to simulate an oil spill. Overall biomass, but especially eukaryotic, decreased with time, and the bacterial community shifted from a predominance of Gram-positive organisms with a minority of Gram-negatives (*Cytophaga-Flavobacteria-Bacteroides* phyla and γ- *Proteobacteria*) to an enrichment of Gram-negatives (α - *Proteobacteria* with complete disappearance of γ- *Proteobacteria*; CFBs only appearing in nutrient-amended plots). A similar study on an actual oil spill yielded differing results: an increase in γ- *Proteobacteria* that dominated the contaminated environment (Maruyama et al., 2003).

Bacterial community succession in a petroleum land treatment unit was followed using 16S rRNA gene analysis (Kaplan and Kitts, 2004). Shifts in community structure corresponded to three distinct phases of total petroleum hydrocarbon (TPH) degradation. The initial, rapid phase, whose rate was reportedly limited by enzyme kinetics rather than contaminant availability, was dominated by *Flavobacteria*, *Pseudomonas spp*. and *Azoarcus 2*. A transitional phase correlated with members of the *Alcaligenes*, *Microbacterium*, and *Bacteroides* genera. Lastly, the final phase of slow and stable TPH degradation rates, limited by contaminant desorption and availability, was dominated by *Azoarcus 1*, *Thermomonas* and *Rhodanobacter*. Extraction bias toward Gram-negative organisms was discounted, since the same protocol had previously retrieved Gram-positive organisms. The authors concluded that their results support a successive trend from a low-diversity/high dominance (i.e. poor and uneven) community that rapidly degrades the contaminant to a high diversity/low dominance (rich and even) community when contaminant desorption is slow. This suggests that the community adapted over time to the varying degrees of contaminant availability and

that there was no competition between species for resources when the contaminant was scarce.

A different study on community changes associated with oil spill bioremediation efforts found that the extent of oil degradation was greater in laboratory microcosms than in the field, especially for PAHs (Röling et al., 2004a). It also found that there were fewer actual changes in the community structure in the field than were shown in the laboratory, except when a slow-release fertilizer was added as a nutrient amendment. An extension of this same study showed a decrease in the abundance of *Archaea* at the site, suggesting that this domain may be used as an indicator of site recovery after a spill event (Röling et al., 2004b). This was the first study to address a possible role for *Archaea* at contaminated sites.

In a study on a bioslurry reactor containing PAH-contaminated dredge harbor sediments, three distinct microbial communities were detected by PLFA analyses (Ringelberg et al., 2001). These communities were associated with the disappearance of different PAHs based on their molecular weight. The first community to appear consisted mostly of Gram-negative organisms and corresponded to a loss of 5- to 6-ring PAHs. The second community was a mix of Gram-negatives and Gram-positives with a high abundance of Actinomycetes. This community corresponded to a decrease in 3-ring PAHs. Finally, a third community appeared that consisted of a different mix of Gram-negative and Gram-positive signatures. This community was associated with a loss of 3- to 4-ring compounds. Overall, there was a decrease in Gram-negatives, an increase in Gram-positives, and a decrease in eukaryotes.

The bacterial community found in clone libraries generated from hydrocarbon-contaminated Antarctic soil was dominated (76%) by *Proteobacteria*, especially *Pseudomonas*, *Sphingomonas*, and *Variovorax*. The clone library generated from a soil

sample nearby was far more diverse and dominated by *Fibrobacter/Acidobacterium* and CFB phyla, but only 6% of its clones were from the *Proteobacteria* (Saul et al., 2005).

Results from a study on soil organisms enriched on a hydrocarbon-containing medium, including naphthalene, also showed a reduction in evenness after enrichment (Greene et al., 2000). The authors also demonstrated that enrichments using pristine and contaminated soils evolved into similar communities, regardless of whether the soils had a history of pre-exposure. These communities shifted from an initial predominance of *γ-Proteobacteria* to that of *β-Proteobacteria*.

Dosing regimes have also been shown to have an effect on community structure (Thompson et al., 1999). Using PLFA and plate counts, the authors showed that a single dose of 1,2-dichlorobenzene led to a decrease in Gram-positives, except *Bacillus* species, an increase in *Pseudomonas* species, and an increase in degradation rates. Multiple doses were deemed more stressful to the community, resulting in both a decrease in numbers and a narrowing of the range of *Pseudomonas* species present in addition to a decrease in degradation rates and metabolic potential (as measured by substrate utilization patterns). In a separate study, Powell (2006) found that a single spike of salicylate into a soil slurry from a PAH-treating bioreactor resulted in the enrichment of both *γ-* and *β-Proteobacteria* sequences in a clone library; whereas, a continuous infusion of salicylate enriched only *γ-Proteobacteria*. Some of the sequences retrieved from the continuously-infused sample were also found in the singly-spiked sample, but the reverse was not observed. It appears that Powell's continuous infusion acts similarly to the multiple-dosing regime of Thompson et al. by exerting constant selection pressure on the community.

Sphingomonas species are well-known degraders of PAHs that have been isolated from many contaminated media. Leys et al. (2004) found that high levels of PAH contamination in soil led to less diverse and less even *Sphingomonas* populations, while low to moderate levels of contamination were associated with a highly diverse community with equally abundant species.

Gentry et al. (2003) incubated a silty loam with spiked pyrene and phenanthrene. Fatty acid methyl ester (FAME) analyses and plate counts showed a decrease in low-G+C, Gram-positive organisms, such as *Bacillus* and *Micrococcus*, followed by a gain in the numbers of high-G+C, Gram-positives (*Cellulomonas* and *Arthrobacter*) and *β-Proteobacteria* (*Burkholderia*). No change was noted in the overall numbers of bacteria, fungi, or actinomycetes, but an increase in the percentage of actual degraders was evident.

Finally, it has been suggested that the bacterial populations at PAH-contaminated sites are selected based on the bioavailability of the contaminants (Tang et al., 1998; Bastiaens et al., 2000; Friedrich et al., 2000; Uyttebroek et al., 2006b). Cultures grown in the presence of PAH strongly sorbed to acrylic beads or hydrophobic membranes, and therefore limited bioavailability, resulted in the enrichment of mycobacterial degraders; whereas, weakly sorbed phenanthrene enriched the growth of *Burkholderia* sp. Grosser et al. (2000) also enriched for different microbial communities between liquid cultures with sorbed and nonsorbed phenanthrene. Bioavailability is discussed in more detail in a later section.

The table below is a sampling of some PAH-degrading organisms isolated from enrichment cultures. It is by no means comprehensive. It is also not a given that the organisms enriched by laboratory experiments are the same ones playing a major role *in situ* (Röling et al., 2001).

Table 2.1. PAH-degrading Organisms Isolated from Enrichment Cultures.

Organism	Isolated From	Reference
Firmicutes/High G+C Gram positives		
Rhodococcus sp.	PAH-contaminated soil	Walter et al., 1991
	manufactured gas plant soil	Bouchez et al., 1995
	pristine lagoon sediment	Dean-Ross et al., 2002
	garden soil	Bouchez et al., 1995
	crude oil contaminated soil	Yuste et al., 2000
Nocardia sp.	pristine salt marsh rhizosphere	Daane et al., 2001
Coryneform bacillus	MGP soil	Bouchez et al., 1995
Microbacterium sp.	polluted soil-steel refinery	Zhang et al., 2004
Mycobacterium flavescens	pristine river sediment	Dean-Ross et al., 2002
Gordona sp.	HC-contaminated soil	Kästner et al., 1994
Gamma Proteobacteria		
Pseudomonas fluorescens	oil-contaminated soil	Ramirez et al., 2001
	petroleum effluent discharge	Yuan et al., 2000
Pseudomonas aeruginosa	oil-contaminated soil	Ramirez et al., 2001
	crude oil contaminated soil	Yuste et al., 2000
Pseudomonas stutzeri	MGP soil	Boonchan et al., 2000
Pseudomonas saccharophila	creosote-contaminated soil	Stringfellow, 1994
Pseudomonas sp.	polluted soil-wood processing plant	Zhang et al., 2004
Stenotrophomonas maltophilia	creosote-contaminated soil	Boonchan et al., 2000
Xylella fastidiosa	crude oil contaminated soil	Yuste et al., 2000
Acinetobacter calcoaceticus	crude oil contaminated soil	Yuste et al., 2000
Leclercia adecarboxylata	oily-sludge contaminated soil	Sarma et al., 2004
Haemophilus sp.	petroleum effluent discharge	Yuan et al., 2000
Flavobacteria		
Weeksella sp.	crude oil contaminated soil	Yuste et al., 2000
Beta Proteobacteria		
Burkholderia cepacia	crude oil contaminated soil	Yuste et al., 2000
Low G+C/Bacilli		
Bacillus cereus	oil-contaminated soil	Stringfellow, 1994
Paenibacillus sp.	pristine salt marsh rhizosphere	Daane et al., 2001
Alpha Proteobacteria		
Paracoccus sp.	polluted soil-oil refinery	Zhang et al., 2004
Sphingomonas paucimobilis	creosote contaminated soil	Mueller et al., 1989
Fungi		
Penicillium janthinellum	creosote-contaminated soil	Boonchan et al., 2000
Cunninhamella elegans	crude oil-contaminated marine sediment	Cerniglia & Perry, 1973, as cited in Cerniglia, 1984

Many are studying the link between structure and function in impacted environments (Griffiths et al., 2001; Morasch et al., 2002; Griffiths et al., 2004; Singleton et al., 2005, 2006; Wagner et al., 2006). It is unclear whether species loss also results in a loss of function or whether functional integrity is maintained by redundancy in species type, abundance, or gene content. It would seem logical that the more organisms capable of carrying out some task, the less that task would suffer after an impact. However, it has been shown that a decrease in diversity in a hydrocarbon-contaminated soil did not affect its ability to degrade a wider range of substrates than its pristine counterpart (Griffiths et al., 2001). This suggests an element of functional diversity within certain groups of organisms.

2.5 General Background on PAHs: Properties, Sources, Fate, and Health Effects

2.5.1 Sources Polycyclic aromatic hydrocarbons are formed from the incomplete combustion of organic matter. Sources of PAHs are both natural and anthropogenic. Natural sources include volcanoes, forest fires, and natural oil seeps, while the more numerous anthropogenic sources range from coal gasification and liquification processes, to automobile exhaust, cigarette smoke, and barbecue. Deposition of airborne particle-associated PAHs is the major means of global contamination by these compounds, and deposition rates correlate well with the burning of fossil fuels (Wilcke, 2000). PAHs almost never occur singly in nature.

2.5.2 Properties affecting fate PAHs are composed of two or more fused benzene rings. This aromatic structure lends resonance stabilization to the compounds. Their nonpolarity results in low aqueous solubility and high octanol-water coefficients (K_{ow}). The high K_{ow} is also reflected in their affinity for organic carbon. As a general rule, high-molecular-weight

PAHs tend to be less water-soluble. Altogether, these attributes make PAHs recalcitrant to

degradation and persistent in the environment. A sampling of carcinogenic PAHs in the

environment can be seen in the table below.

Table 2.2. Measured PAHs in a Sampling of Different Environmental Media and
Geographical Locations.

Medium	Range of Concentrations
Water	ng L^{-1}
surface water	0.1-830
groundwater	0.2-6.9
drinking water	0.1-62
Air	ng m^{-3}
outdoor published studies	0.2-65
indoor home	0.6-29
indoor home with tobacco smoke	7-29
Soil	mg kg^{-1} dry wt
forest	0.01-1.3
rural	0.01-1.01
urban	0.06-5.8
road dust	8-336
Sediment	
published studies	
near contaminated sites	0.003-232

Modified from Menzie et al., 1992.

Within the temperate zone, the mean and median levels of the EPA priority-listed PAHs

are given below.

Table 2.3. Levels of EPA-PAHs in Temperate Soils by Soil Type (μg kg^{-1}).

Arable		Grassland		Forest		Urban	
mean	median	mean	median	mean	median	mean	median
328	216	284	194	904	410	4420	1103

Modified from Wilcke, 2000.

2.5.3 Health effects The health effects of many PAHs have been studied in great detail. The earliest associations between PAH-containing substances and cancer were made by Dr. John Hill (1761) in a tract on snuff and nasal lesions and Sir Percivall Pott (1775) in his observations of scrotal cancers among chimney sweeps (Redmond, 1970). It was not until the early 1900's that a specific compound (1,2,5,6-dibenzanthracene) was isolated from coal tar and identified as the first cancer-causing agent, resulting in skin tumors on rabbits (as cited in Cerniglia, 1984). The EPA has designated sixteen PAHs as priority pollutants; among these, eight are considered class B2, or possible carcinogens, by the International Agency for Research on Cancer (Keith and Telliard, 1979; Boffeta et al., 1997).

The most common routes of exposure to PAHs are inhalation, dermal absorption, and ingestion. In mammalian systems, PAHs induce production of, and are transformed by, the cytochrome P450 monooxygenase enzyme family. This transformation occurs predominantly in liver endoplasmic reticulum. This results in a dihydrodiol compound by way of an arene oxide. These new electrophilic metabolites then undergo conjugation with an endogenous compound (e.g. sulfate, glucoside, or glucuronide) and are eliminated from the system. Unfortunately, the electrophilic intermediates may react with nucleophilic sites on proteins or nucleic acids, inhibiting the intended function of the former or resulting in erroneous transcription of the latter. They may also generate reactive oxygen species (Parkinson, 2001).

Due to their adverse effects, exposure to PAHs from contaminated environments is a public and environmental health concern. Soils and sediments are areas of high priority because of the aforementioned characteristics (e.g. high affinity for organic carbon and low aqueous solubility).

2.6 Factors Affecting Contaminant Bioavailability

Clearly, in order to be degraded, the contaminant must be both accessible and palatable to microorganisms. Bioavailability is thought to be a major limiting factor affecting the degradation of contaminants in the environment, and many have questioned the need for remediation at sites whose contaminants are not easily extractable except by rigorous procedures (Hatzinger and Alexander, 1995; Chung and Alexander, 1998; Alexander, 2000) or whose rates of release are so slow that the site is deemed "biostabilized" (Luthy et al., 1997). Bioavailability is affected by many factors, including soil physicochemical factors, the state of the natural organic matter within the soil, contaminant "aging" and sequestration into pores, and microbial mechanisms for achieving accessibility.

2.6.1 Soil Characteristics

2.6.1.1 Physico-chemical characteristics Characteristics of the soil matrix, such as texture, density, porosity, pH, cation exchange capacity, and percent and quality of organic carbon have an impact on the bioavailability of organic compounds, since they directly affect sorption phenomena and indirectly affect moisture content, oxygen gradients, and temperature. Soil texture, a measure of the particle size distribution of the inorganic soil components, affects soil density, which in turn affects soil pore volume. Pore space can allow or impede the flow of water, nutrients, particulate organics, and dissolved organic compounds. It can also facilitate or impair the diffusion of gases, such as oxygen. Obviously, these affect moisture content and oxygen tension within pore spaces. The clay content of the soil is extremely important, since the large surface area of clays enhances the sorption of organic matter, while the clay's small particle size can serve to block the flow of aqueous substances.

The association of PAHs with certain particle size fractions or their location within a soil aggregate may also influence PAH accessibility to microorganisms. PAHs may be distributed unevenly between particle size fractions with a high concentration of PAH associated with fine silt or clay (Amellal et al., 2001; Uyttebroek et al., 2006a). Amellal et al. showed that PAH-degrading bacteria were significantly associated with the fine silt and clay fractions, tenfold higher than those found within the sand fraction. Transmission electron microscopy (TEM) images revealed bacteria trapped within aggregates or embedded in organic matter. The authors hypothesized that mere physical disruption of aggregates could potentially increase the bioavailability of the PAHs to local degraders. These results have been supported by the work of others who showed a strong correlation between the extent of PAH mineralization and soil size fraction, with the lowest percentage of mineralization occurring in bulk soils containing the highest percentage of silt and clay (Carmichael and Pfaender, 1997).

It is assumed that the silt and clay fractions are highly associated with contaminants because they are also the fractions that sorb most of the soil organic matter. A clear association between contaminants and soil organic matter has been shown previously (Luthy et al., 1997; Ortega-Calvo and Saiz-Jimenez, 1998; Breedveld and Karlson, 2000; Wilcke, 2000).

Microorganisms also adsorb strongly to clay particles. This may limit their access to organic substrates and lead to the secretion of extracellular enzymes into the soil environment. Alternatively, they may be conveniently located near PAHs that are sorbed onto clay-associated organic matter (Ortega-Calvo and Saiz-Jimenez, 1998). Aged, PAH-contaminated soil has been shown to contain a higher proportion of PAH-degrading

Mycobacteria in its clay fraction than in sand or silt (Uyttebroek et al., 2006a). The authors suggest that increased cell surface hydrophobicity aids in adherence to either the clay substratum or the PAH itself, thus increasing bioaccessibility. Others have concluded from microscopic analyses that bacteria build "hutches" from extracellular polymeric substances (EPS) and clay in which they "store" their hydrophobic organics and use the clay as "carbon shuttles" (Lünsdorf et al., 2000).

2.6.1.2 Organic carbon content and character The naturally occurring organic carbon in soil may cause chemical interactions with PAHs, depending on its level of aromaticity and the presence of polar groups. Nam and Alexander (1998) showed that phenanthrene bioavailability was reduced in soils with greater than 2% organic carbon. Additionally, partially oxidized PAH metabolites secreted into the extracellular medium by microorganisms have been shown to bind covalently to particulate organic matter, thereby reducing their bioavailability and leading to a decrease in mineralization rates (Ressler et al., 1999). In contrast, some have shown that the increased solubility of oxidized metabolites results in an increased availability (Meulenberg et al., 1997).

Xing and Pignatello (1996, 1997) contend that natural organic matter can exist in two phases, a condensed, rigid, glassy polymer or an expandable, amorphous rubbery polymer. The former state contains voids into which solutes, such as contaminant PAHs, may enter. It is thought that the solutes displace water molecules, since these studies have shown that more solute is taken up when the organic matter is dry and that there is less swelling of the organic matter in the presence of solute than of water. Water softens the glassy nature of the organic matter to its rubbery state and, in doing so, alters the availability of the solutes in the pores.

At low ionic strength and high pH, charge repulsion from carboxyl and hydroxyl groups will enhance the open configuration of natural organic matter. The opposite conditions neutralize the repulsion, resulting in a coiled configuration. This latter change may release "entrapped" hydrophobic organic contaminants (HOCs) into pore waters where they become bioavailable (Coates et al., 2000). Additionally, high pH may cause organic matter, specifically humic acid, to act as a surfactant, resulting in increased solubility of PAH (Liang et al., 2007).

Coates et al. also showed that a reduced environment alters the configuration of humic substances, thereby increasing their surface tension and enhancing their solubility. In support of this, Pravecek et al. (2005) and Kim and Pfaender (2005) found a correlation between oxidation-reduction potential in anaerobic microcosms and an increase in PAH desorption from soils, presumably from an increased solubility of the natural organic matter carrying along with it the hydrophobic contaminant PAH. This compound mobilization into the aqueous phase presumably renders it available to microorganisms, at least until it is resorbed.

2.6.1.3 Sequestration The presence of micro- and nanopores within the mineral matrix has been implicated by some studies as an aggravating factor in the availability of HOCs (Hatzinger and Alexander, 1997; Nam and Alexander, 1998; Alexander, 2000). The movement of PAH out of these pores then becomes the rate-limiting step in their degradation. Soils that have been aged with PAHs show a tendency toward lower extractability, i.e. decreased availability, with increasing age (Hatzinger and Alexander, 1995; Carmichael and Pfaender, 1997; Chung and Alexander, 1998; Ressler et al., 1999). Whether this is due to sequestration within pores or humification of PAH metabolites is unknown (Guthrie et al., 1999).

2.6.2 Microbial characteristics Finally, the microbes themselves influence contaminant availability either by going to the carbon source, staying near the source, or making the source come to them. Bacteria employ processes such as adhesion or motility, high-affinity uptake systems, or the secretion of biosurfactants or altering cell surface hydrophobicity (Marshall, 1980; Rosenberg et al., 1980; Al-Tahhan et al., 2000; Bugg et al., 2000; Wick et al., 2002; Wu et al., 2003; Miyata et al., 2004).

2.6.2.1 Adhesion and biofilms Nutrient levels are higher on surfaces than in pore waters, especially for poorly soluble, sorbed PAHs. Therefore, it is to the organism's advantage to remain where there is food. This can be accomplished by the secretion of polysaccharide adhesins and/or the formation of biofilms. Simply being near a sorbed contaminant can enhance its rate of degradation (Bosma et al., 1997). Biofilm formation and PAH degradation have been reported for soil bacteria grown on pyrene and phenanthrene crystals (Stringfellow, 1994; Eriksson et al., 2002) and pure culture bacteria grown on anthracene crystals (Wick et al., 2002).

Biofilms may be used to "store" carbon sources for future use. Wolfaardt et al. (1994) measured the accumulation of the organic herbicide diclofop within a laboratory-grown biofilm and showed that, when the flow of herbicide into the system was discontinued, the biofilm-bound contaminant was utilized (Wolfaardt et al., 1995).

2.6.2.2 Motility and chemotaxis Chemotaxis, or the movement of an organism either toward or away from a chemical stimulant, is another means of ensuring substrate availability by seeking out the source. In fact, bacteria have been shown to be chemotactic toward substrates, such as naphthalene and biphenyl, and recently movement toward phenanthrene has been suggested (Grimm and Harwood, 1997; Wu et al., 2003; Uyttebroek et al., 2006b).

2.6.2.3 Substrate uptake A recent study has shown that a PAH-degrading *Mycobacterium* sp. utilizes a high-affinity uptake system for the transport of phenanthrene into the cell (Miyata et al., 2004). A high substrate affinity may be indicative of an organism that will benefit when the substrate is scarce (Lengeler et al., 1999), such as in a soil with slow, but continuous contaminant desorption.

2.6.2.4 Cell surface hydrophobicity and biosurfactant production It has been suggested that cell surface hydrophobicity can be used as a measure of affinity to hydrocarbons by degrader populations (Rosenberg et al., 1980). However, results are variable, and even non-degraders have been shown to adhere to select compounds causing a decrease in their availability to degrader populations (Stringfellow and Alvarez-Cohen, 1999). At higher cell densities, bacteria may adhere to one another, rather than to the contaminant compound (Wu et al., 2003). In contrast, alterations in cell surface hydrophobicity were responsible for the ability of a *Mycobacterium* species to form a biofilm directly on the surface of anthracene crystals (Wick et al., 2002). The bacteria did not exhibit this attribute when grown on glucose as the sole carbon source, and no biosurfactant was detected. Increased cell surface hydrophobicity may also permit the organism to dwell at a non-aqueous phase liquid (NAPL)-water interface where it has the double advantage of utilizing organics within the NAP and soluble nutrients and gases carried in the pore water.

Biosurfactants may act in two ways: first, by enhancing the solubility of HOCs so that they move into the aqueous environment where they are more readily accessible, and second, by changing the cell-surface hydrophobicity such that it more easily associates with the HOC. The former mechanism is suspected in the case of a soil *Sinorhizobium* whose exopolymer contained both lipid and polysaccharide components, although no mechanism or

evidence of actual PAH transport in the soil was provided (Janecka et al., 2002). Others were unable to show a correlation between biosurfactant formation and enhanced rates of PAH degradation (Stringfellow, 1994). A *Pseudomonas* species grown on hexadecane in the presence of a rhamnolipid surfactant changed its cell surface hydrophobicity by releasing the lipopolysaccharide component of its outer membrane (Al-Tahhan et al., 2000). Finally, an increase in PAH tolerance (as measured by growth) was noted in a strain of *Rhodococcus rhodocrous* that produced extracellular polymeric substances as compared to non-EPS-producing strains (Iwabuchi et al., 2000, 2002).

Some have suggested that compound availability may select for the growth of certain organisms (Tang et al., 1998; Friedrich et al., 2000; Grosser et al., 2000). As mentioned earlier, bacteria enriched from media containing phenanthrene sorbed to acrylic beads were able to degrade phenanthrene in contaminated sediment, whereas bacteria enriched from medium containing nonsorbed phenanthrene were not. Additionally, the rates of initial desorption were less than mineralization rates, indicating that the organisms had some means of facilitating compound accessibility, such that degradation rates were not limited by desorption rates. These findings have been supported by others. Vacca et al. (2005) found that bacterial isolates enriched from nonsorbed phenanthrene were not the same as those enriched from humic acid-sorbed phenanthrene, and that the former isolates were also not "competent" to mineralize the sorbed PAH. Guerin and Boyd (1992) long ago warned against making generalizations about the bioavailability of sorbed contaminants after they showed differential naphthalene availability between two naphthalene-degrading bacterial species.

2.7 Factors Affecting Biodegradation Rates

Two camps exist with regard to the chief rate-limiting factor in biodegradation: 1) mass transfer versus 2) microbial activity. This work will not address mass transfer quantitatively. A qualitative evaluation is given in section 2.6 ("factors affecting contaminant bioavailability").

The microbial factors affecting degradation rates include, but are not limited to, prior exposure, the presence of a second organic substrate, the accumulation of dead-end or toxic metabolites, the presence and numbers of specific bacterial or fungal strains, the presence of inducers, and the rhizosphere effect.

2.7.1 Prior exposure Prior exposure of microbial populations to a contaminant leads to enhanced initial rates of degradation most likely because of a diminished lag period during the initial phase post-exposure. While the enzymes responsible for PAH degradation may or may not be constitutive, repeated exposure to a compound leads to an acquired adaptive capability. Johnsen and Karlsen (2005) found that soils near industrialized areas contained enough pyrene, even at low levels, to sustain degradative genes within the indigenous community. However, prior exposure does not always lead to increased rates of degradation, depending on how the studies are performed. Smith et al. (1999) added known PAH degraders to crude-oil contaminated soils and found preferential degradation of other oil substituents besides PAH. Viñas et al. (2002) also found that an enrichment of degraders from specific fractions of oil (e.g. aromatic) did not make them more efficient degraders of that particular fraction when augmented into an oil-medium emulsion.

2.7.2 Degrader numbers The measure of PAH-degrader numbers as a reflection of PAH degradation or disappearance can be misleading. While some have shown that an increased

number of degraders leads to increased degradation rates (Gentry et al., 2003; Del Panno et al., 2005), others have found a poor correlation between numbers and degradation (Carmichael and Pfaender, 1997). Huesemann et al. (2002) showed a decrease in the ratio of hydrocarbon degraders to total heterotrophs over time for most of the soils they tested. Furthermore, this increase in numbers may not always be attainable or sustainable. For example, energy resulting from the initial phase of rapid degradation of a PAH mixture may be needed for cell maintenance rather than growth, once the usable carbon (e.g. low-molecular-weight PAH) has been depleted or is no longer available. It may be that functional redundancy or cometabolic effects rather than numbers play a more significant role.

2.7.3 Substrate competition Competition for the enzyme active site by two PAHs may account for reduced rates of degradation of one of the compounds (Bouchez et al., 1995, 1996) and was cited as the reason for a decrease in phenanthrene degradation by a mixed culture when a second PAH was present (Stringfellow, 1994) and a decrease in the pyrene degradation rate by *M. flavescens* in the presence of fluoranthene (Dean-Ross et al., 2002). Bouchez et al. (1999) found that the rate of mineralization decreased as the oxygen/carbon ratio decreased, for example with the addition of a second carbon source. Pyrene was cometabolized in the presence of anthracene as the primary carbon source but not when fluoranthene or phenanthrene was present.

2.7.4 Presence of inducers Salicylate is the most commonly studied inducer of PAH metabolism. It is an intermediate in many degradation pathways, and its production induces the lower pathway for naphthalene degradation. Its effects do not appear to be consistent and may depend on the PAH, the salicylate concentration, and the organisms present. The addition of salicylate led to increased removal of phenanthrene, fluoranthene, pyrene,

44

benz[a]anthracene, chrysene, and benzo[a]pyrene by *Pseudomonas saccharophila* P15 in liquid culture (Chen and Aitken, 1999). However, Carmichael and Pfaender (1997) were unable to show any effect of its addition on phenanthrene and pyrene degradation in soil microcosms. Repeated additions of salicylate induced the greatest extent of pyrene mineralization in soil microcosms as compared to a single spike (Vanderford, 2001).

2.7.5 Presence of metabolites "Dead-end" metabolites, or those that are degraded no further, have been shown to accumulate in some systems during the initial period of fast cell growth and compound degradation. Some of these have been deemed toxic to down-stream metabolizers. Kazunga and Aitken (2000) showed that the formation of cis-4,5-dihydro-4,5-dihydroxypyrene (PYRdHD) by bacterial isolates from a PAH-contaminated soil caused inhibition of phenanthrene degradation by some of the strains, while both PYRdHD and pyrene-4,5-dione (PYRQ) resulted in the inhibition of benzo[a]pyrene degradation by others. This latter finding was supported by Vanderford (2001) who used Microtox assays to show that PYRQ caused a decrease in the ATP-dependent production of luciferase by test organisms at levels well below its aqueous solubility. Although the above metabolites result from oxidation at bay- and K-regions of the PAH, others have shown that attack at non-bay- and non-K-regions may also result in toxic, dead-end metabolites (Kim et al., 2005). Increased degradation of a PAH mixture was reported for a consortium of PAH degraders as compared to a mixed, but defined, co-culture of bacteria, possibly due to a build-up of toxic metabolites that the defined culture was ill-suited to degrade (Bouchez et al., 1999).

2.7.6 Presence of fungi The presence of fungi in a mixed culture has been shown to have differing effects. As mentioned earlier, fungi may play a role in the initial oxidation step of PAHs, in their incorporation into humic matter, or in the formation of toxic metabolites.

PAHs may adsorb to fungal mycelia, leading to a decrease in availability to bacterial degraders. Hyphae also play an important role in the formation, maintenance, and destruction of soil aggregates. This can lead to the spatial isolation of some bacteria, thereby decreasing their accessibility to contaminants. The presence of organic-rich matter in soils was shown to stimulate ligninolytic fungi and, as a result, enhanced rates of PAH degradation. Fungi in organic-poor soils had an inhibitory effect on degradation, possibly due to the lower production of oxidative enzymes by mycelia under these conditions and the repression of bacterial degraders. In either event, the presence of fungi may alter the evolving bacterial community (Gramss et al., 1999).

2.7.7 Plant presence Some have studied the effects of plant residues ("the rhizosphere effect") on bacterial populations in contaminated soils. Joner et al. (2002) measured enhanced degradation of 3- and 4-ring PAHs after the addition of phosphorus, nitrogen, and root exudates and the increase in the ratio of PAH-degrading bacteria to total heterotrophs. Corgié et al. (2004) found that different bacterial communities were selected as a function of the distance to plant roots and that those located closest to roots had greater phenanthrene degrading abilities, possibly due to stimulation by root exudates.

2.8 Microbial Metabolism of PAHs, Specifically Pyrene

2.8.1 General aerobic Many pathways have been delineated for the aerobic degradation of polycyclic aromatics by various bacteria and fungi (Sutherland et al., 1995, and references therein). In bacteria, the initial reaction generally involves the incorporation of atmospheric oxygen into the aromatic ring to form a *cis*-dihydrodiol. This reaction is catalyzed by a dioxygenase enzyme. The site of attack differs with the molecule, due to steric hindrance of

the compound and the regio-specificity of the dioxygenases. From this point in the pathway, the molecule can be dehydrogenated by dihydrodiol dehydrogenases to form a diphenol. Ring cleavage of this catechol form is catalyzed by yet another dioxygenase and occurs either *ortho* or *meta* to the hydroxyl groups resulting in an acid or semi-aldehyde, respectively (Schwarzenbach et al., 2003).

Some bacteria, notably the cyanobacteria and mycobacterial species, are able to form *trans*-dihydrodiols via a monooxygenase. Cyanobacteria metabolize PAHs under photoautotrophic conditions.

Among fungi, cytochrome P450 catalyzes the incorporation of one atom from molecular oxygen to form an epoxide (Sutherland et al., 1995; Moody et al., 2001). This form can undergo a non-enzymatic rearrangement to a phenol or be catalyzed by epoxide hydrolase to form a *trans*-dihydrodiol. The former is excreted as a conjugate with an endogenous glucoside, glucuronide, or sulfate. The latter can be dehydrogenated to a catechol via dihydrodiol dehydrogenase or undergo an additional epoxidation to form a diol epoxide.

White-rot fungi, such as *Phanerochaete chrysosporium*, may use lignin peroxidases to metabolize PAHs to quinones. *P. chrysosporium* can also transform PAHs to phenols and *trans*-dihydrodiols under non-ligninolytic conditions (Hammel et al., 1986). It has been suggested that the lignin peroxidase reaction proceeds by way of a cation radical intermediate through to the quinone product (Hammel et al., 1986).

Cationic radicals reportedly form DNA adducts in eukaryotic systems, and quinone redox cycling produces reactive oxygen species. These findings may have important ramifications in the decision whether to use natural attenuation or bioaugmentation with fungi as a remediation strategy. Fungal transformation of PAHs may result in a compound that is more

toxic than the parent compound itself. However, cometabolism of benz[a]anthracene and benzo[a]pyrene by *Penicillium janthinellum* growing on pyrene in the presence of a bacterial co-culture resulted in a decrease in mutagenicity of the extractable fraction, possibly due to induction of BaP catabolic enzymes (Boonchan et al., 2000).

2.8.2 General anaerobic Anaerobic biodegradation of unsubstituted aromatic compounds was once thought improbable (Zehnder and Colberg, 1985; Mihelcic and Luthy, 1988). Although there is still a dearth of knowledge on the pathways and enzymes responsible, there are many studies that have shown that transformations do occur.

Under anaerobic conditions, molecular oxygen is not present for either accepting electrons or promoting the initial attack on the organic compound. The aromatic compound is transformed initially via one of several reactions: hydration, dehydration, or carboxylation, to a central intermediate, such as benzoyl-CoA, resorcinol, or phloroglucinol. These compounds are then reduced to alicyclics. Since oxidative cleavage of the aromatic ring is impossible, reduction occurs instead (Heider and Fuchs, 1997). Cleavage occurs next by hydrolysis by atomic hydrogen or a cofactor such as NADPH. Finally, beta-oxidation transforms these to central metabolites, such as acetyl-CoA. Unlike aerobic degradation, there is no catechol intermediate.

2.8.3 Pyrene transformation In 1988, Heitkamp and Cerniglia isolated the first known bacterium capable of degrading pyrene. They measured 60% mineralization of radiolabeled pyrene by *Mycobacterium sp*. PYR-1 (now *M. vanbaalenii* PYR-1) after a lag phase attributed to enzyme induction. Intermediates of both ring oxidation and ring fission were identified, including both a *cis*-4,5- and *trans*-4,5-dihydrodiol, and pyrenol from ring-oxidation; and 4-hydroxyperinaphthenone, 4-phenanthroic acid, phthalic acid and cinnamic

acid from ring fission. Since then, other organisms have been isolated and pathways have

been proposed for pyrene metabolism by both bacteria and fungi (see Figure 2.1). For

bacteria, the predominant site of enzymatic attack is between carbons 4 and 5; however,

hydroxylation has been shown to occur at carbons 1 and 2 (Walter et al., 1991) or 9 and 10 in

some organisms (Khan et al., 2001).
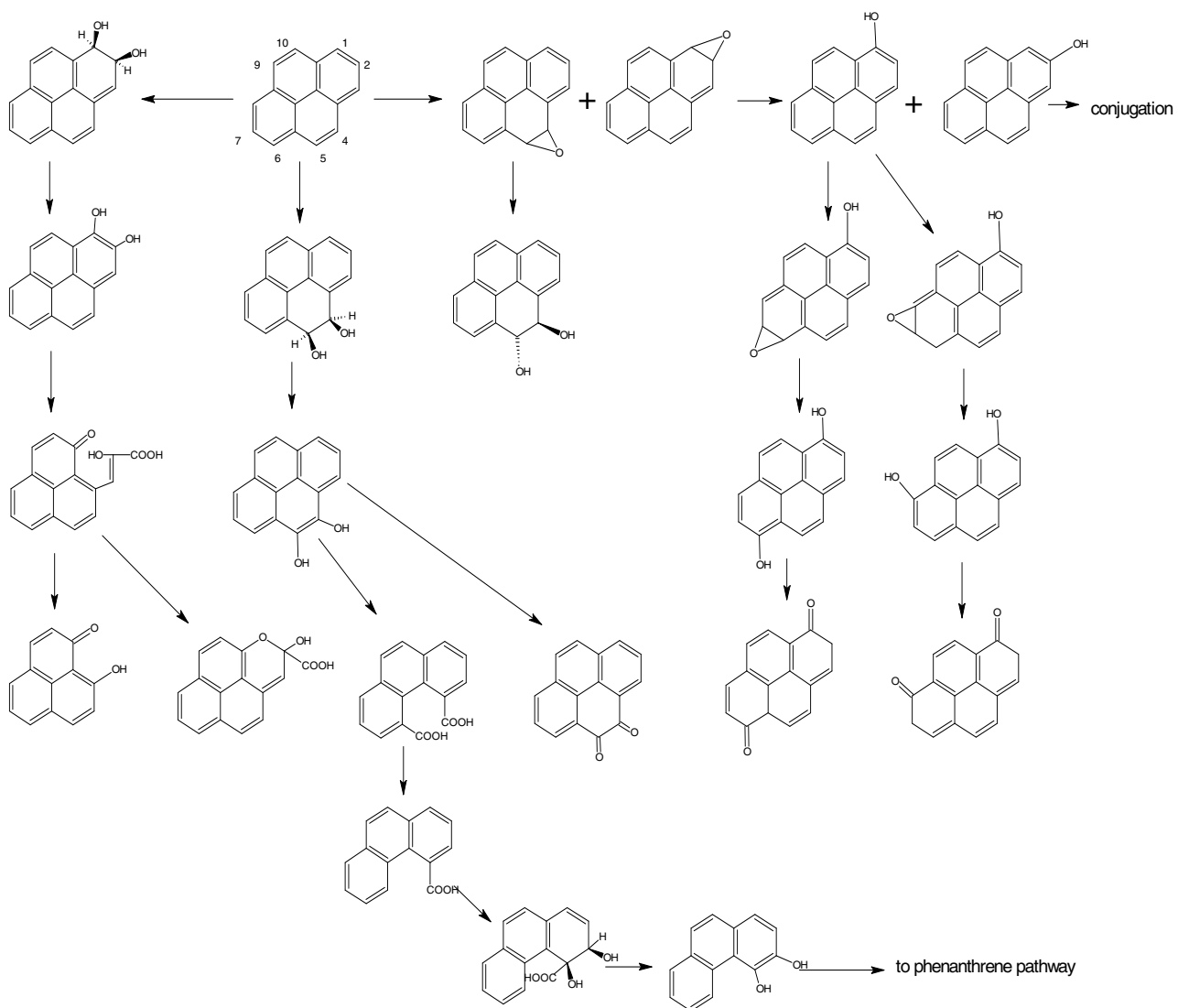
Figure 2.1. Proposed Pathways for the Microbial Transformation of Pyrene.

It has been suggested that the majority of bacteria capable of utilizing pyrene as their sole carbon source tend to fall within the Gram-positive Actinomycetes (Kästner et al., 1994; Bouchez et al., 1995; Dean-Ross and Cerniglia, 1996; Kanaly and Harayama, 2000, and references therein; Zhang et al., 2004; Uyttebroek et al., 2006a, 2006b), including *Mycobacterium* sp. strains RJGII-145, KR2, BB1, VF1, and CH1, *Mycobacterium flavescens, Mycobacterium pyrenivorans*, and other *Rhodococcus* and *Gordona* species. Kazunga and Aitken (2000) found that *M. vanbaalenii* PYR-1 can also produce a pyrene-4,5-quinone, possibly by way of a 4,5-dihydroxypyrene. This same organism was screened for enzymes responsible for PAH degradation, and it was found that the initial oxidation step can be catalyzed by either a dioxygenase or monooxygenase (Khan et al., 2001) yielding both the *cis-* and *trans*-dihydrodiols in either the 4,5 or 9,10 positions.

Rhodococcus sp. UW1 mineralized 72% of pyrene in liquid culture within two weeks, forming 1,2- and 4,5-dihydroxypyrene, cis-2-hydroxy-3-(perinaphthenone-9-yl) propenic acid, and 2-hydroxy-2-(phenanthren-5-one-4-enyl)-acetic acid (Walter et al., 1991).

Gram-negative bacteria have also been shown to transform pyrene in some studies. *Pseudomonas stutzeri* P16 formed cis-4,5-dihydro-4,5-dihydroxypyrene (PYRdHD), while *Sphingomonas yanoikuyae* and *Pseudomonas* (now *Pelomonas*) *saccharophila* were able to form both PYRdHD and PYRQ (Kazunga and Aitken, 2000). Other Gram-negative degraders include *Flavobacterium* sp., *Cycloclasticus*, and *Burkholderia cepacia* (Kanaly and Harayama, 2000). Recently, an enteric bacterium, *Leclercia adecarboxylata*, capable of degrading pyrene was isolated from an oily sludge (Sarma et al., 2004), and a *Paracoccus* sp. capable of utilizing pyrene as its sole carbon source was found in an oil-refinery soil (Zhang et al., 2004).

Cometabolism of pyrene, or its transformation by cells not using it as a carbon source, has also been shown to occur. Bouchez et al. (1999) isolated a bacterial strain from the site of a former manufactured gas plant that mineralized pyrene while growing on anthracene. A large percentage of fluoranthene-degraders isolated from various PAH-contaminated soils cometabolized pyrene (Ho et al., 2000). In contrast, cometabolism of pyrene by *Mycobacterium flavescens* was inhibited by the presence of fluoranthene, possibly due to competitive inhibition (Dean-Ross et al., 2002).

Fungal transformation of pyrene has also been reported. The zygomycete *Cunninghamella elegans* produces 1-hydroxypyrene and both 1,6- and 1,8-pyrenequinones, as well as three glucoside conjugates of 1-hydroxypyrene, 1,6- and 1,8-dihydroxypyrene (Cerniglia et al., 1986). Other species of fungi have also been shown to metabolize pyrene, but those intermediates have not been identified (Cerniglia et al., 1986). White rot fungi, such as *Phanerochaete chrysosporium*, oxidize pyrene to its 1,6- and 1,8-quinones (Hammel et al., 1986) via lignin peroxidase, instead of monooxygenases.

2.8.4 Genes involved in PAH degradation Studies on the genes involved in PAH degradation have focused on the naphthalene-degrading genes of *Pseudomonas putida*. The *nah* regulon comprises the *nah* operon and the *sal* operon. The former encodes the upper metabolic pathway involving the metabolism of naphthalene to salicylate. The *sal* operon encodes the lower metabolic pathway that takes salicylate through catechol to pyruvate and acetaldehyde. The regulator gene, *nahR*, is located between the two operons. It encodes the *nah* regulatory protein which, in the presence of an inducer, salicylate, activates transcription of the *nah* operon. The *nah* genes are usually located on self-transmissible NAH plasmids. Naphthalene dioxygenase, encoded in *Pseudomonas* sp. by *nahA*, was found to have a

significantly different primary structure than its analogue in a *Rhodococcus* sp., while the tertiary structure is apparently conserved (Parales et al., 2002).

The *nag* genes found in *Ralstonia sp.* strain U2 encode the naphthalene pathway to salicylate, but then salicylate is degraded via gentisol, not catechol. *Nag*-like gene copy number was found to correlate positively with naphthalene concentrations in coal-tar contaminated sediments (Dionisi et al., 2004).

The genes responsible for the degradation of pyrene have not been extensively studied. In *Mycobacterium vanbaalenii* PYR-1, the dioxygenase genes are located chromosomally, not on a plasmid, as with the *nah* genes, and they apparently show no homology to dioxygenase genes from other organisms, especially Gram-negatives (Khan et al., 2001). The dioxygenase encoded by these *nid* genes was shown to cause pyrene transformation to the *cis*-4,5-dihydrodiol.

Many have used degradative genes as biomarkers for PAH metabolism. Mesarch et al. (2000) and Ringelberg et al. (2001) probed for catechol-2,3-dioxygenase genes in petroleum-contaminated soils and dredged harbor sediments, respectively, to monitor bioremediation. The latter study found that an increase in gene copy numbers correlated with phenanthrene disappearance. However, equating the presence of degradative genes with degradation can be misleading due to the ubiquity of the genes themselves, the fact that many are located on transmissible plasmids, and due to the likely existence of, as yet undiscovered and unsequenced degradative genes (Lloyd-Jones et al., 1999; Khan et al., 2001; Ní Chadhain et al., 2006). Measuring transcripts is preferable but more difficult because of short half-lives, interference from soil nucleases or contaminants, and the potentially low cell numbers resulting from contaminant toxicity or poor metabolism. In spite of these difficulties,

Sanseverino et al. (1993) and Fleming et al. (1993) were able to correlate *nahA* gene frequency and *nahA* transcript levels with ^{14}C-naphthalene mineralization rates and disappearance from manufactured gas plant soils. In a later study, Wilson et al. (1999) developed *nahAc* probes and were able to hybridize those with cDNA from homologous dioxygenase mRNA transcripts extracted from groundwater. Bakermans and Madsen (2002) used tyramide signal amplification to enhance the detection of naphthalene dioxygenase mRNA transcripts in contaminated groundwater.

3.0 Comparison of the Microbial Communities in an Aged, PAH-Contaminated Soil and an Uncontaminated Soil from within the Same Site

3.1 Introduction

Polycyclic aromatic hydrocarbons are found in virtually every environmental matrix. They result from the incomplete combustion of the organic matter found in both natural and anthropogenic sources. Due to their resonance stabilization, low water solubility, and interaction with organic matter, these compounds are recalcitrant to degradation and persist in the environment. This is of concern to public health specialists, since some PAHs are known or suspected carcinogens and mutagens (Keith and Telliard, 1979; Boffeta et al., 1997; Parkinson, 2001).

The presence of PAHs in soil is largely due to atmospheric deposition but may be a result of many other causes, such as oil seeps or the disposal of poorly treated coal tar waste (Wilcke, 2000). Because they are so persistent in soils, it is important to know if and how PAH presence affects the indigenous flora, especially since microorganisms are responsible for the transformation and degradation of organic matter in this environment (Schwarzenbach et al., 2003). To understand the effects of PAH presence on the microbial community, one must first describe the community.

Profiling the microbial community in any soil environment is important for many reasons. First, the true diversity of bacteria in soil is unknown, due to the largely uncultivable fraction, and potentially magnitudes greater than originally thought (Rappé and

Giovanonni, 2003). Second, microbes exist as communities in nature, not as individuals, and likely function this way, as well (Møller et al., 1998; Yuan et al., 2000). Their activity may differ between their natural habitat and pure, or even mixed, laboratory cultures (Bakermans and Madsen, 2002). Finally, knowing the community structure may help infer community member functions which, in turn, may aid in predicting a community's response to future environmental perturbations.

The microbial communities present in contaminated soils may be described immediately following or long after an insult has occurred. In the former case, one may follow community succession after contaminant exposure, since these changes may be indicative of contaminant toxicity to indigenous microorganisms. Long-term changes may reflect community adaptation to an insult, either through enzyme induction, genetic transformation, or the natural selection of organisms with the desired metabolic or degradative capabilities (Spain and van Veld, 1983; Macleod and Semple, 2002; Joynt et al., 2006). These community profiles may also help to identify active contaminant degraders, since organisms that are capable degraders in pure cultures may not play the most significant role *in situ* (Johnsen et al., 2002). Such information can then be used to predict the bioremediation potential of a given site or to evaluate its ongoing remediation effectiveness (Watanabe and Hamamura, 2003). Finally, profiling the microbial community in a contaminated soil may provide insight into its functional diversity, even if the structural diversity is low.

Most often, comparisons are made between the same soil before and after controlled spiking in the laboratory or field (MacNaughton, 1999; Thompson et al., 1999; Röling et al., 2002, 2004a). The obvious disadvantage is that these experiments are simulations. Alternatively, many researchers focus on the "after" picture once a spill or other

contamination event has occurred (Stephen et al., 1999; Maruyama et al., 2003; Röling et al., 2004a). Unfortunately, these cases have no "before" picture with which to compare the results. Rarely, one may have access to samples from the same site—both contaminated and uncontaminated (Kasai et al., 2005; Saul et al., 2005). It is these studies that should provide an ideal focus for community profiling and comparison.

The objective of this study was to use culture-independent methods to compare the microbial communities present in an uncontaminated soil and an aged, creosote-contaminated soil from the same vicinity. It was hypothesized that the contaminated soil would be less diverse with a selection for specific groups of bacteria, e.g. the *Proteobacteria*.

3.2 Materials and Methods

3.2.1 Soils Both experimental soils were obtained from the site of the former Reilly Tar and Chemical Corporation (St. Louis Park, MN). This Superfund site is highly contaminated with polycyclic aromatic hydrocarbons from its 50-year history as a creosote-producing and wood-preserving facility. The contaminated soil (CMN) was excavated from the southeast corner of the site in August, 1999 from under 6 feet of topsoil capping. The uncontaminated soil (PMN) was removed in September, 2002 from the surface at the northwest corner of the same site. Groundwater flow is east southeast (S. Anderson, Utilities Superintendent, City of St. Louis Park, MN, personal communication) thus suggesting no flow of contaminants from the affected area to the pristine soil. Characteristics of both soils are given in Table 3.1 below.

Table 3.1. Characteristics of Experimental Soils.

	CMN	PMN
soil class	mineral	mineral
soil texture	sand	sandy loam
% sand	89	63
% silt	8	24
% clay	3	13
% moisture	5.49 ± 0.85	4.57 ± 0.61
% organic matter	2.7	1.5
% carbon by weight	9.01 ± 1.20	1.77 ± 0.14
pH	7.5	8.1
CEC (meq 100cm^{-3})	22	13/22.3
BET surface area (m^2 g^{-1})	8.89	7.75
Density (g cm^{-3})	1.28	1.28/1.31
total PAH (mg kg^{-1})	4393 ± 693	20.4 ± 4.6
pyrene concentration	463 ± 100	3.49 ± 0.28

Soil texture, pH, percent organic matter, cation exchange capacity, and sample density were determined by the University of Wisconsin-Madison Soil and Plant Analysis Laboratory, Madison, WI. The second measurements of CEC, pH, and pore volume for the PMN soil were obtained from the North Carolina Department of Agriculture Agronomic Division, Raleigh, NC. Percent carbon by weight, percent moisture, and surface area were measured by Clear Science, Baton Rouge, LA. PAHs were analyzed by Eno River Laboratories, Durham, NC, using EPA method 8270. Total PAH refers to the following 16 EPA-listed priority compounds: acenaphthene, acenaphthylene, anthracene, benzo[a]anthracene, benzo[b]fluoranthene, benzo[k]fluoranthene, benzo[g,h,i]perylene, benzo[a]pyrene, chrysene, dibenzo[a,h]anthracene, fluoranthene, fluorene, indeno[1,2,3-cd]pyrene, naphthalene, phenanthrene, and pyrene.

Soils were stored in plastic garbage bags in the dark at 4°C until use. Prior to use, they were passed through a 2 mm sieve.

Pretreated soils were washed once with an equivalent volume of dichloromethane (soil gram wet weight to milliliters DCM). Soils were vortexed for one minute at medium speed, centrifuged for 5 minutes at 1,048 x g and allowed to air dry in the fume hood for 10 minutes prior to use.

3.2.2 DNA extraction DNA was extracted from ~0.3-0.6 g aliquots of sieved soil using the Ultra Clean Soil DNA Kit (MoBio Laboratories, Solana Beach, CA) and following the manufacturer's directions. Homogenization was performed with a bead-beater (Biospec Products Mini Beadbeater) set at 2500 beats per minute (bpm) for 5 minutes. Soils used for

archaeal analysis were pretreated with DCM as outlined above. Yields and DNA size were

estimated by agarose gel electrophoresis alongside a HindIII digest of λ-phage DNA.

Densitometric measurements were made in Adobe Photoshop 7.0 using FoveaPro software

(Reindeer Graphics, Asheville, NC). DNA was stored in Tris at -20°C if analyses were not

performed immediately.

3.2.3 Polymerase chain reactions (PCR) Amplification of 16S and 18S rRNA gene

segments from the contaminated soil was performed by nested PCR. The uncontaminated

soil did not require a nested approach. Primer sets for each domain are listed in Table 3.2

and were synthesized by Invitrogen Life Technologies (Rockville, MD).

Table 3.2. Primers for the PCR Amplification of Extracted Soil DNA.

Primer		Sequence (5'-3')	Domain	Reference
27f	(outer)	AGAGTTTGATCCTGGCTCAG	Bacteria	Lane, 1991
1492r	(outer)	GGTTACCTTGTTACGACTT	Universal	Lane, 1991
63fGC	(inner)	CAGGCCTAACACATGCAAGTC	Bacteria	Marchesi et al., 1998
518r	(inner)	ATTACCGCGGCTGCTGG	Universal	Neefs et al., 1990
25f	(outer)	CTGGTTGATCCTGCCAG	Archaea	Sowers & Schreier, 1995
1392r	(outer)	ACGGGCGGTGTGTRC	Universal	Olsen et al., 1986*
344fGC	(inner)	ACGGGGCGCAGCAGGCGCGA	Archaea	Raskin et al., 1994
806r	(inner)	GGACTACVSGGGTATCTAAT	Archaea	Takai & Horikoshi, 2000
0305f	(outer)	CTGCCCTATCAACTTTCGA	Fungal	Gargas and DePriest, 1996
1536r	(outer)	ATTGCAATCCYCTATCCCCA	Fungal	Borneman & Hartin, 2000
817fGC	(inner)	TTAGCATGGAATAATRRAATAGGA	Fungal	Borneman & Hartin, 2000
1196r	(inner)	TCTGGACCTGGTGAGTTTCC	Fungal	Borneman & Hartin, 2000

f = forward primer; r = reverse primer; GC = 40-base GC-rich clamp, Muyzer et al., 1993
(5'CGCCCGCCGCGCGCGGCGGGCGGGGCGGGGGCACGGGGGG3').
All prokaryotic primer designations are based on the *E. coli* numbering system; fungal designations are based
on *Saccharomyces cerevisiae* 18S numbering. *as cited in Lane, 1991.

The inner bacterial primer set amplified a segment of the 16S rRNA gene covering

hypervariable regions V1, V2, and V3 with an expected length of 495 base pairs; while the

archaeal inner set spanned V3 and yielded expected products of 481 bp. Fungal inner

58

primers covered part of V4 and all of V5 of the 18S rRNA-encoding gene to generate products of approximately 422 bp. All PCR reagents were obtained from Applied Biosystems (Foster City, CA) and were certified nuclease-free. Bacterial PCR was performed in 1X PCR buffer (10 mM Tris-HCl, 50 mM KCl, pH 8.3), 2 mM MgCl$_2$, 250 μM of each deoxynucleotide phosphate (dNTP), 500 nM of each primer, and 2.5 U of DNA polymerase from *Thermus aquaticus* (*Taq*) with an annealing temperature of 55°C. The reaction mix for archaeal PCR was similar except for an increased concentration of MgCl$_2$ to 2.5 mM. The outer reaction used on the contaminated soil employed a 54°C annealing temperature, while the nested reaction annealed at 48°C. Fungal PCR reactions used 200 μM of each dNTP, 300 nM of each primer, and a 56°C annealing temperature. The forward primer used in each nested reaction also contained a 40-base GC-rich clamp.

3.2.4 Denaturing gradient gel electrophoresis (DGGE) Once amplified, PCR products were separated electrophoretically using BioRad's DCode System (Hercules, CA) on a polyacrylamide gel (acrylamide:bisacrylamide ratio of 37.5:1) containing a urea-formamide denaturant gradient (full-strength denaturant contains 7 M urea and 40% formamide). Bacterial and archaeal PCR products were run on a 6% gel, and fungal products were separated on an 8% gel. After initial screening on a 0-80% denaturing gradient gel, gradients were chosen as follows: 30-55% for bacteria, 45-55% for archaea, and 0-40% with a 0% stacking gel for fungi. Segments were separated over 1000 volt-hours. DGGE bands were excised, eluted overnight in TE buffer (10 mM Tris, 1 mM EDTA) and reamplified by PCR. PCR products displaying "pure" bands on gels were cleaned using QIAQuick Spin PCR Purification Kit (Qiagen; Valencia, CA) following the manufacturer's directions.

3.2.5 Clone libraries Bacterial PCR products (63fGC-518r) were inserted into the pCR®4-TOPO® vector using the TOPO TA Cloning Kit for Sequencing (Invitrogen Life Technologies; Rockville, MD), following the manufacturer's directions, and transformed into *E. coli* DH5α™-TR® chemically competent cells. Plasmids were purified from 10 randomly selected transformants using Qiagen's Qiaprep Spin MiniPrep Kit (Qiagen; Valencia, CA) and digested with EcoRI for screening. Once a minimum of 90% of the screened plasmids was shown to contain the desired insert, the cultures were sent to a commercial laboratory for sequencing. Transformant cultures were stored in Luria-Bertani broth containing kanamycin (50 μg ml^{-1}) and 15% glycerol at –20°C.

3.2.6 DNA sequencing DNA sequences obtained by DGGE were sent to the Genome Analysis Facility at the University of North Carolina-Chapel Hill. Sequencing reactions were initiated from the Bac63fGC primer. Transformant cultures were sent to SeqWright (Houston, TX) for plasmid purification and subsequent clone sequencing from the M13f primer.

3.2.7 Sequence analysis Results from all sequencing reactions were reviewed for quality and "cleaned" within Sequencher, version 4.5 (Gene Codes Corporation; Ann Arbor, MI) prior to identification. Sequences were screened for chimeras using both Chimera_Check version 2.7, release 9 (Niels Larson; www.rdpii.msu.edu) and Bellerophon (Huber et al., 2004; huber@maths.uq.edu.au). Those reported by both programs to be putative chimeras were eliminated from the data set. Those reported only by Bellerophon were verified manually and subsequently eliminated. Sequences were then matched with their closest relatives from ribosomal databases using BLASTn (Altschul et al., 1997) through the National Center for Biotechnology Information web interface (www.ncbi.nlm.nih.gov). A

progressive multiple sequence alignment was performed within the Clustal X Multiple Sequence Alignment Program version 1.83 (Higgins and Sharp, 1988). The resulting distance matrix was then used as input for a neighbor-joining program that inferred the phylogenetic trees. Confidence was achieved by bootstrapping 1000 times. Trees were displayed in Treeview, version 1.6.6 (http://taxonomy.zoology.gla.ac.uk/rod/treeview).

3.2.8 Diversity analysis Community richness was determined presumptively by counting the number of DGGE bands in the profile. Band presence was verified by generating a histogram profile of the density along the length of the gel, using FoveaPro software in Adobe Photoshop 7.0 (Reindeer Graphics; Asheville, NC). Each peak in density was assumed to represent a band. Richness was also estimated from the number of unique clones in each library.

When possible, the DGGE profile similarity between the two soils was compared using Sorensen's similarity coefficient, $S_{AB} = 2C/(A + B)$, where C is the number of bands in common between the two DGGE profiles, and A and B are the number of bands unique to each profile (McCaig et al., 1999). The Shannon index (H') was calculated for each soil and was used to measure the relative diversity of the two clone libraries: $H' = -\Sigma(p_i \ln p_i)$, where $p_i = n_i/N$ or the proportion of members that a particular operational taxonomic unit (OTU) contributes to the total in the sample, n_i is the number of clones of the ith OTU, and N is the total number of clones (Shannon and Weaver, 1963; Casamayor et al., 2002). The index was also calculated for the CMN using the DGGE profile; n_i is the peak height of the ith band, and N is the total peak height (Ibekwe et al., 2001).

Community evenness was estimated from the distribution of cloned sequences among different phylogenetic groups. Evenness was calculated as $E = H'/\log S$, where H' is the Shannon index and S is the number of unique OTUs within the sample (Smit et al., 2001).

Species loss or gain, as measured by the absence or presence of corresponding DGGE bands or phylogenetic groups, between the pristine and the contaminated samples was reviewed qualitatively.

3.3 Results

3.3.1 DGGE The original bacterial DGGE profile generated from the contaminated soil is shown in Figure 3.1. Twelve of the seventeen total bands, including four of the five dominant bands, were purified and sequenced.
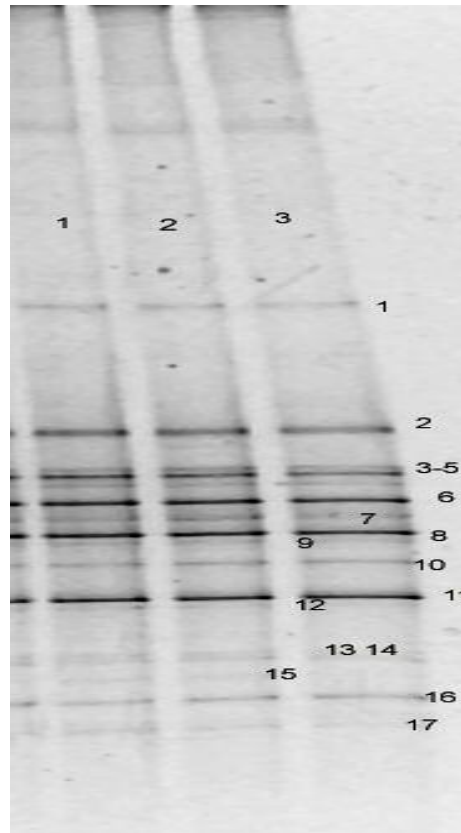
Figure 3.1. DGGE Profile of Bacterial Amplicons from CMN. Lanes 1-3 represent replicate DNA extraction protocols.

DGGE profiles of bacterial amplicons from the PMN resulted in a smear down the length

of the gel. It was necessary to dilute the original DNA extract prior to bacterial PCR in order

to generate discernible bands on DGGE.
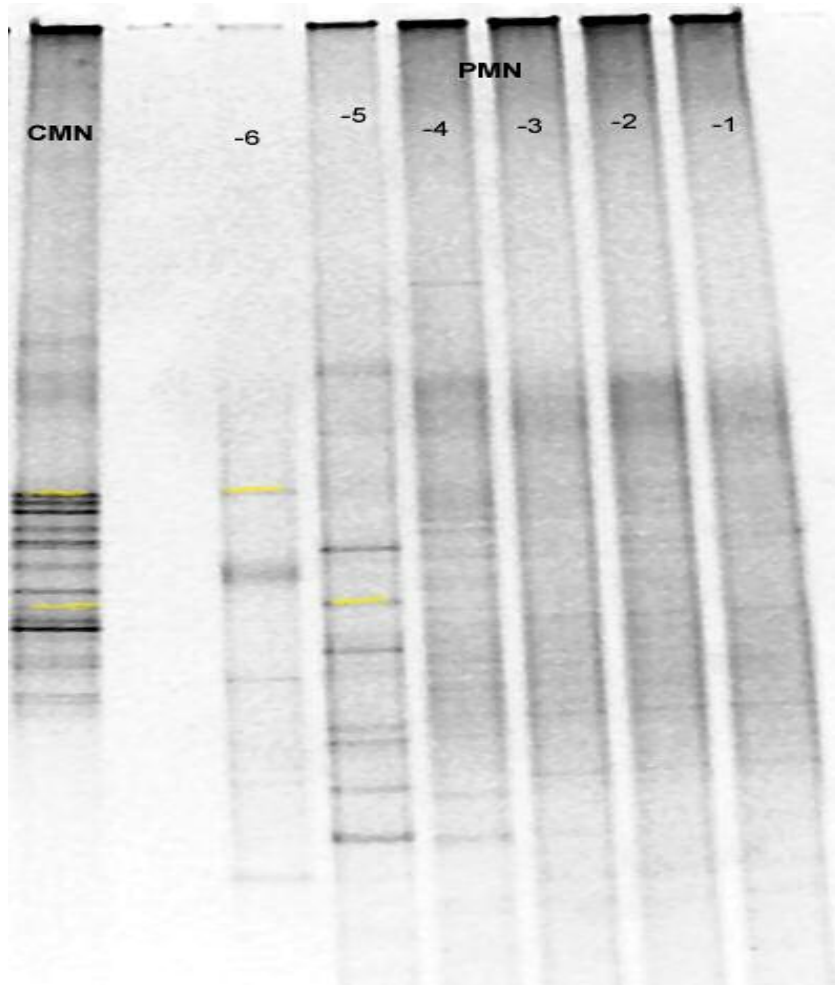
Figure 3.2 Bacterial Profile of CMN and Dilutions of PMN. Shared bands are highlighted. Lanes -1 through -6 represent dilutions 10^{-1} through 10^{-6} of the original PMN extract prior to PCR-DGGE.

Numerous attempts to purify and sequence DGGE bands from the PMN dilutions were

mostly unsuccessful. Only two bands could be sequenced.

By measuring distance along the length of the gel, it appears that two bands in the CMN

profile migrated to the same position in the PMN profile, as highlighted. The top band

corresponds to CMN1 (see Table 3.4 below). The second highlighted band could not be purified.

The DGGE profile of archaeal amplicons from both soils is shown in Figure 3.3.
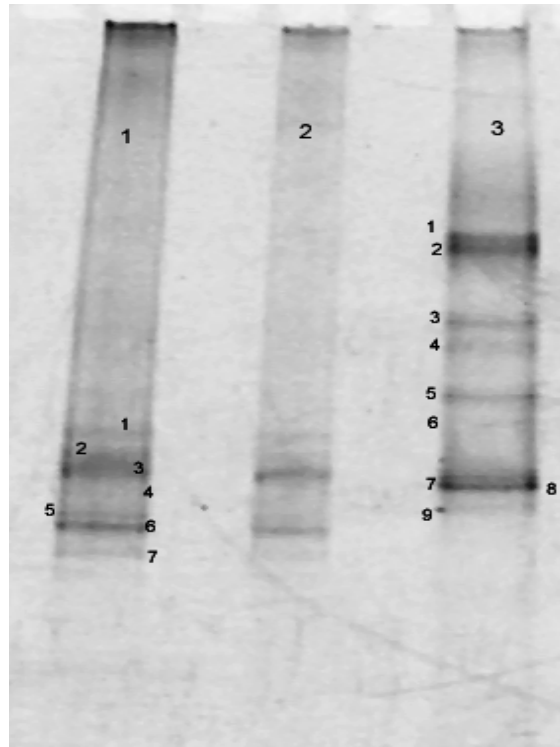
Figure 3.3. Archaeal DGGE Profile of Both PMN (lane 1) and CMN (lane 3) Soils. Lane 2 is a PMN duplicate with half the template mass loaded onto the gel.

Nine distinct bands can be seen in the CMN profile. However, only one band could be purified and sequenced. Seven bands were discernible in the PMN archaeal profile. Initial attempts to purify these bands were unsuccessful and, therefore, abandoned. There are no common bands between the two soil profiles.

Fungal PCR products could not be obtained from the CMN soil after many attempts. The fungal profile generated from the PMN PCR products was of very poor quality but appears to show 5 bands (see Figure 3.4). This was verified using the histogram profile of band density.

Figure 3.4. DGGE Profile of Fungal PCR products from PMN.

Results of DGGE sequence analysis of both soils are given in Table 3.3. CMN bacterial
sequences matched exclusively with members of the *Proteobacteria*: eight of the twelve
sequenced bands were from the *β-* subgroup, and four were from the *γ-* subgroup. Bands 6,
8, and 10 resulted in the same BLAST matches. One of the two PMN sequences obtained by
DGGE was for a *β-Proteobacterium* (*Ralstonia* sp.), while the other matched an uncultured
Acidobacterium.

3.3.2 Clone libraries and phylogenetic trees Results from the CMN clone library are
given in Table 3.4. Three of the sequenced plasmids contained no insert, and five sequences
were eliminated as chimeric, leaving a total of 40 acceptable clone sequences. Of these, six
groups of sequences were defined as contiguous (i.e. from which a consensus sequence could
be created with a percentage match set at 100% similarity). These are shown in Appendix I,
along with six groups defined as contiguous at 97% similarity. Group 5 of the 100%
similarity contiguous sequences falls within Group 2 of the 97% similarity sequences, and
Group 6 at 100% falls within Group 1. Four DGGE bands—6, 8, 10, and 11-- correlate with
cloned sequences CMN1 (6, 8, 10) and CMN6 (11).

The phylogenetic tree constructed from the multiple sequence alignment data for the CMN soil is shown in Figure 3.5. Only 100% contiguous groupings were used in the tree, along with 25 singleton sequences.

The PMN clone library results are given in Table 3.6, and the inferred tree is shown in Figure 3.6. There was only one possible contiguous group of two sequences that could be formed from the PMN clones; therefore, these sequences were not grouped together.

There were no matches between any of the clones between the CMN and PMN libraries. A phylogenetic tree constructed from the alignment of all CMN and PMN bacterial clones is given in Figure 3.7.

Table 3.3. Results of rRNA Gene Sequence Analysis of DGGE Bands

DGGE Designation	Closest Match in Ribosomal Database [GenBank Accession Number]	Percent Similarity	Phylogenetic Class of Closest Match	Source
CMNBac3	*Variovorax paradoxus* EP1 [AY190135]	95%	*β-Proteobacteria*	rhizosphere of diesel phytoremediants
CMNBac4	*Pseudomonas aurantiaca* VKMB152 [AM000006]	97%	*γ-Proteobacteria*	pure culture
CMNBac5	uncultured bacterium clone 14 [AY853674]	92%	*γ-Proteobacteria*	naphthalene-contaminated soil
CMNBac6	uncultured bacterium clone L-2 [AY625146]	98%	*β-Proteobacteria*	PCE-contaminated groundwater
CMNBac7	uncultured bacterium clone SO92 [AY037615]	98%	*γ-Proteobacteria*	earthworm burrows/cast in agricultural soil
CMNBac8	uncultured bacterium clone L-2 [AY625146]	98%	*β-Proteobacteria*	PCE-contaminated groundwater
CMNBac9	uncultured bacterium clone SX2-10 [DQ469201]	99%	*β-Proteobacteria*	mine water
CMNBac10	uncultured bacterium clone L-2 [AY625146]	94%	*β-Proteobacteria*	PCE-contaminated groundwater
CMNBac11	uncultured bacterial clone W18 [AY770958]	94%	*γ-Proteobacteria*	oil field injection well water
CMNBac12	Achromobacter sp. SHIBATA-9 [AB181502]	98%	*β-Proteobacteria*	human stool
CMNBac13	uncultured bacterial clone HN57 [AB089949]	96%	*β-Proteobacteria*	aquarium
CMNBac15	uncultured bacterium clone BANW406 [DQ264411]	92%	*β-Proteobacteria*	groundwater undergoing Cr bioremediation
CMNArc7	uncultured archaeal clone 5LOC9 [AY835826]	99%	Crenarchaeota	anaerobic granular sludge
PMNBac1	*Ralstonia insidiosa* [AJ539233]	99%	*β-Proteobacteria*	
PMNBac2	uncultured bacterium clone BAC-14A1 [AY214904]	99%	Acidobacterium	soil metagenomic library

CMN = contaminated MN soil; PMN = pristine MN soil; Bac = found with bacterial primer set; Arc = found with archaeal primer set

Table 3.4. Results of CMN Clone Library

Clone Designation	Closest Match in Ribosomal Database [GenBank Accession Number]	Percent Similarity	Phylogenetic Class of Closest Match	Source
CMN1	uncultured bacterium clone L-2 [AY625146]	98%	*β-Proteobacteria*	PCE-contaminated groundwater
CMN2	uncultured bacterium clone 1013-1-CG1[AY532535]	99%	*α-Proteobacteria*	uranium-contaminated aquifer
CMN3	uncultured bacterium clone M07_pitesti [DQ378229]	99%	*γ-Proteobacteria*	oil-polluted soil
CMN4	uncultured bacterium clone IAFR510 [AF270959]	99%	*γ-Proteobacteria*	PCP-contaminated soil
CMN5	uncultured bacterium clone M07_pitesti [DQ378229]	99%	*γ-Proteobacteria*	oil-polluted soil
CMN6	uncultured bacterium clone W18 [AY770958]	100%	*γ-Proteobacteria*	oil field injection water
CMN7	*Sphingomonas* sp. ROL7 [AJ634942]	99%	*α-Proteobacteria*	coal-tar-contaminated soil
CMN9	uncultured bacterium clone IAFR510 [AF270959]	99%	*γ-Proteobacteria*	PCP-contaminated soil
CMN11	*Stenotrophomonas* sp. 1-2004 [AY563052]	99%	*γ-Proteobacteria*	pure culture
CMN12	uncultured *β-Proteobacteria* clone TH480 [AJ888547]	99%	*β-Proteobacteria*	lake sediment
CMN13	uncultured bacterium clone W18 [AY770958]	100%	*γ-Proteobacteria*	oil field injection water
CMN15	*Stenotrophomonas* sp. 1-2004 [AY563052]	99%	*γ-Proteobacteria*	pure culture
CMN16	uncultured freshwater bacterium clone...[DQ064933]	98%	*α-Proteobacteria*	freshwater
CMN18	*Collimonas* sp. CT0113 [AY281151]	99%	*β-Proteobacteria*	soil isolate
CMN20	uncultured bacterium clone W18 [AY770958]	100%	*γ-Proteobacteria*	oil field injection water
CMN21	uncultured bacterium clone W18 [AY770958]	100%	*γ-Proteobacteria*	oil field injection water
CMN22	uncultured bacterium clone 178up [AY212629]	98%	*β-Proteobacteria*	manure-contaminated water
CMN23	*Pseudomonas* sp. A1Y13 [AJ278814]	100%	*γ-Proteobacteria*	BTEX-contaminated soil
CMN24	uncultured bacterium clone W18 [AY770958]	100%	*γ-Proteobacteria*	oil field injection water
CMN25	uncultured bacterium clone W18 [AY770958]	100%	*γ-Proteobacteria*	oil field injection water
CMN26	uncultured bacterium clone W18 [AY770958]	100%	*γ-Proteobacteria*	oil field injection water
CMN28	*Pseudomonas mandelii* [AY179326]	100%	*γ-Proteobacteria*	nonylphenol degrader
CMN29	*Pseudomonas lini* [AY035996]	99%	*γ-Proteobacteria*	soil isolate, nov. sp.
CMN30	uncultured bacterium clone M07_pitesti [DQ378229]	99%	*γ-Proteobacteria*	oil-polluted soil
CMN31	uncultured bacterium clone W18 [AY770958]	100%	*γ-Proteobacteria*	oil field injection water
CMN32	uncultured bacterium clone IAFR510 [AF270959]	99%	*γ-Proteobacteria*	PCP-contaminated soil
CMN35	uncultured bacterium clone W18 [AY770958]	100%	*γ-Proteobacteria*	oil field injection water
CMN36	uncultured bacterium clone IAFR510 [AF270959]	99%	*γ-Proteobacteria*	PCP-contaminated soil
CMN37	uncultured bacterium clone W18 [AY770958]	100%	*γ-Proteobacteria*	oil field injection water
CMN40	uncultured bacterium clone W18 [AY770958]	100%	*γ-Proteobacteria*	oil field injection water
CMN41	*Sphingomonas* sp. ROL7 [AJ634942]	99%	*α-Proteobacteria*	coal-tar-contaminated soil
CMN42	uncultured bacterium clone M07_pitesti [DQ378229]	99%	*γ-Proteobacteria*	oil-polluted soil

CMN43	uncultured bacterium clone W18 [AY770958]	100%	*γ-Proteobacteria*	oil field injection water
CMN44	uncultured bacterium clone IAFR510 [AF270959]	99%	*γ-Proteobacteria*	PCP-contaminated soil
CMN45	uncultured bacterium clone M07_pitesti [DQ378229]	99%	*γ-Proteobacteria*	oil-polluted soil
CMN46	uncultured bacterium clone L-2 [AY625146]	98%	*β-Proteobacteria*	PCE-contaminated groundwater
CMN47	uncultured bacterium clone IAFR510 [AF270959]	99%	*γ-Proteobacteria*	PCP-contaminated soil
CMN48	*Dyella japonica* [AM086243]	97%	*γ-Proteobacteria*	ectomycorhizzal endophyte
CMN49	uncultured bacterium clone W18 [AY770958]	100%	*γ-Proteobacteria*	oil field injection water
CMN50	uncultured bacterium clone W18 [AY770958]	100%	*γ-Proteobacteria*	oil field injection water
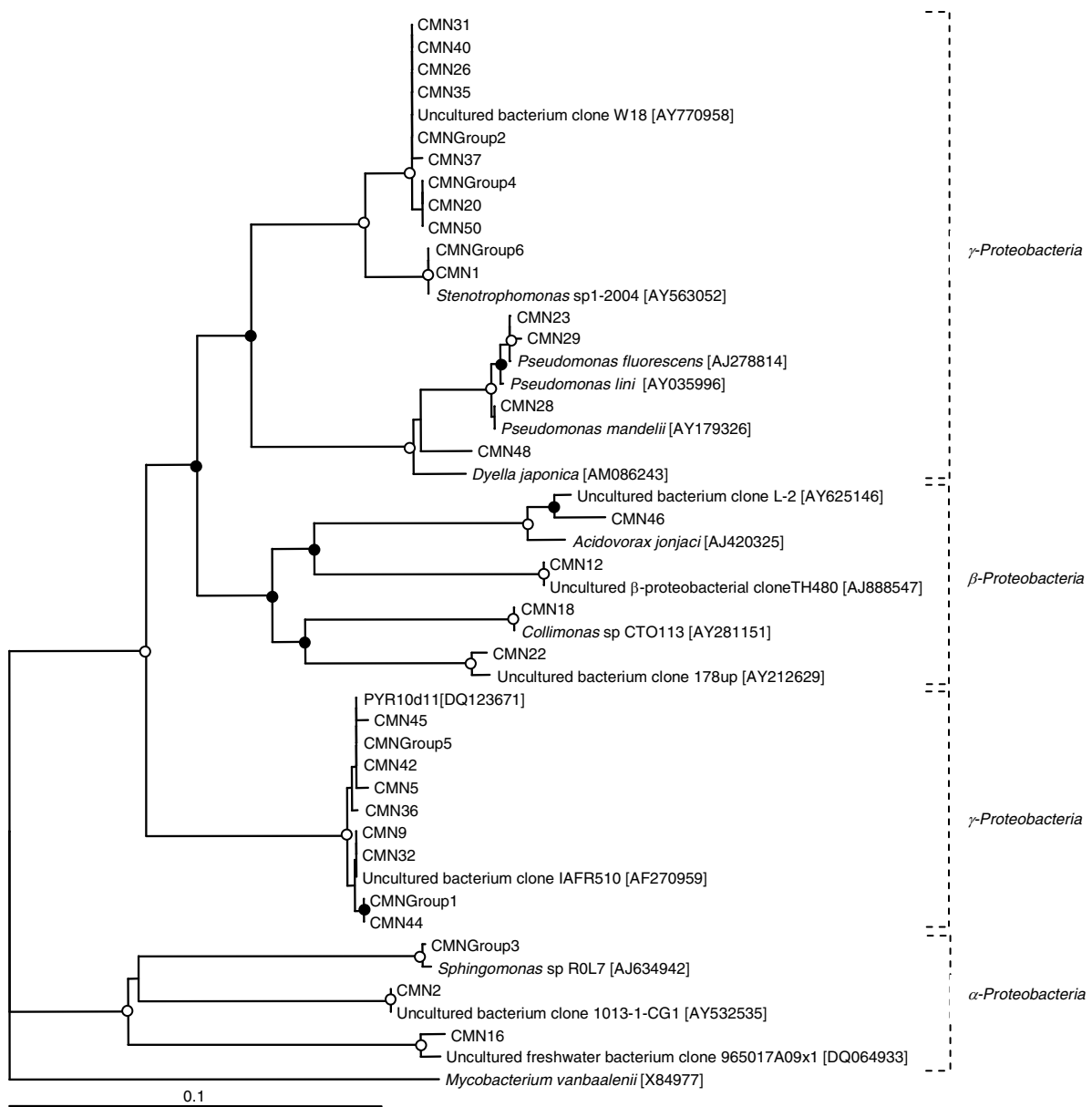
Figure 3.5. Phylogenetic Tree Inferred from CMN Clone Library. *Mycobacterium vanbaalenii* is included as an outgroup from which the tree is rooted. Also included are reference sequences most closely related to the CMN clones. Solid circles indicate greater than 70% bootstrap support; open circles indicate greater than 95% bootstrap support.

Table 3.6. Results of PMN Clone Library

Clone Designation	Closest Match in Ribosomal Database [GenBank Accession Number]	Percent Similarity	Phylogenetic Class of Closest Match	Source
PMN1	uncultured bacterium clone Niitsu0-51 [AB187648]	92%	*Proteobacteria*	garbage compost
PMN3	uncultured bacterium clone L1A.12E07 [AY989413]	98%	*Actinobacteria*	Alaskan soil
PMN4	uncultured bacterium clone L1A.7F03 [AY989063]	93%	*Acidobacteria*	Alaskan soil
PMN5	unidentified eubacterium [AF010120]	94%	*Actinobacteria*	soil
PMN9	uncultured bacterium clone L1A.5E01 [AY988917]	98%	*Planctomycetacia*	Alaskan soil
PMN10	uncultured bacterium clone L1A.9E11 [AY989203]	94%	*γ-Proteobacteria*	Alaskan soil
PMN11	uncultured bacterium clone 26BSF24 [AJ863267]	97%	*α-Proteobacteria*	flooded soil
PMN12	uncultured bacterium clone L1A.15G10 [AY989631]	97%	*α-Proteobacteria*	Alaskan soil
PMN13	uncultured α-proteobacterium clone EB1015 [AY395334]	91%	*α-Proteobacteria*	pasture soil
PMN17	uncultured bacterium clone RFS-C310 [DQ154623]	96%	*β-Proteobacteria*	forest soil
PMN21	uncultured bacterium clone CJRC123 [DQ202185]	93%	*α-Proteobacteria*	FBR treating U-contaminated groundwater
PMN24	uncultured bacterium clone 661258 [DQ404803]	90%	*Planctomycetacia*	contaminated sediment
PMN25	uncultured bacterium clone S089 [AY037612]	99%	*Acidobacteria*	soil earthworm cast
PMN26	uncultured α-proteobacterium clone glen99_6 [AY150881]	95%	*α-Proteobacteria*	soil disturbed by coal mining
PMN27	uncultured Acidobacterium clone AKYG990 [AY922086]	97%	*Acidobacteria*	farm soil next to silage bunker
PMN29	uncultured bacterium clone ML-7-121 [DQ235074]	90%	*α-Proteobacteria*	eutrophic bay
PMN31	uncultured eubacterium clone DS3-25 [DQ444105]	97%	*Chloroflexi*	benzene-contaminated sediment
PMN33	uncultured bacterium clone L1A.15A12 [AY989586]	87%	*α-Proteobacteria*	Alaskan soil
PMN34	agricultural soil bacterium clone SC-I-47 [AJ252637]	99%	*γ-Proteobacteria*	transgenic potato plant rhizosphere
PMN35	uncultured bacterium clone CWT STO2_C09 [DQ129163]	97%	*α-Proteobacteria*	forest soil
PMN36	uncultured bacterium clone RB210 [AB240319]	99%	*Acidobacteria*	phragmites rhizosphere
PMN37	*Pseudomonas frederickbergensis* OUCZ24 [AY785733]	100%	*γ-Proteobacteria*	pure culture
PMN39	uncultured bacterium clone C34.095M [AF432645]	94%	*Planctomycetacia*	pine rhizosphere
PMN40	uncultured β-proteobacterium clone JABCS30 [AY734338]	94%	*β-Proteobacteria*	soil
PMN41	uncultured Chloroflexi bact. clone AKYH834 [AY921869]	98%	*Chloroflexi*	farm soil next to silage bunker
PMN42	uncultured Planctomycete clone 6 [AF271339]	99%	*Planctomycetacia*	forest soil
PMN43	uncultured bacterium clone WIT-MS-78 [AY309186]	97%	*α-Proteobacteria*	peat
PMN44	uncultivated soil bacterium clone S114 [AF013562]	97%	*Bacteroidetes*	arid soil
PMN45	*Lysobacter* sp. L40 [DQ249997]	90%	*γ-Proteobacteria*	cavern
PMN48	uncultured Acidobacterium clone AKYG1538 [AY921884]	90%	*Acidobacteria*	farm soil next to silage bunker
PMN49	uncultured bacterium clone L1A.13B03 [AY989447]	96%	*Acidobacteria*	Alaskan soil

Clone Designation	Closest Match in Ribosomal Database [GenBank Accession Number]	Percent Similarity	Phylogenetic Class of Closest Match	Source
PMN51	uncultured bacterium clone 25BSU8 [AJ863206]	99%	*Verrumicrobiae*	poplar tree soil microcosm
PMN53	uncultured bacterium clone Tc26 [AF445096]	92%	*β-Proteobacteria*	metal-contaminated soil rhizosphere
PMN54	uncultured bacterium clone CDF3 [AF392739]	97%	*Acidobacteria*	swiss chard rhizosphere
PMN55	uncultured proteobacterium clone PLTA13 [AY193176]	96%	*γ-Proteobacteria*	lake
PMN56	uncultured forest soil bact. clone DUNSSU024 [AY913244]	92%	*α-Proteobacteria*	forest soil
PMN57	uncultured bacterium clone 48 [DQ413107]	93%	*Proteobacteria*	EBPR sludge bioreactor
PMN58	uncultured α-proteobacterium clone AKYG1791 [AY921654]	98%	*α-Proteobacteria*	farm soil near silage bunker
PMN59	uncultured Acidobacterium clone VC47 [AY211077]	98%	*Acidobacteria*	anaerobic VC-degrading enrichment
PMN60	uncultured bacterium clone B2C7OD1 [AY957895]	96%	*α-Proteobacteria*	drinking water biofilm
PMN62	uncultured bacterium clone BS03 [AY963441]	96%	*Acidobacteria*	soil
PMN64	uncultured bacterium clone 26BSF1 [AJ863266]	100%	*α-Proteobacteria*	flooded soil
PMN65	Streptomycetaceae bacterium CNQ732 [AY464539]	91%	*Actinobacteria*	marine sediment isolate
PMN66	uncultured δ-proteobacterium clone BIrii41 [AJ318168]	96%	*δ-Proteobacteria*	industrial waste-gas biofilter
PMN67	uncultured Planctomycete clone JABEAA26 [AY697676]	93%	*Planctomycetacia*	soil
PMN69	uncultured bacterium clone 3NL-80 [AY651821]	97%	*α-Proteobacteria*	contaminated groundwater plume
PMN70	uncultured bacterium clone BS03 [AY963441]	96%	*Acidobacteria*	soil
PMN72	uncultured *Sphingomonas* clone BL004B14 [AY806002]	99%	*α-Proteobacteria*	lavaged sputum-CF patient
PMN73	α-Proteobacterium clone S23419 [D84621]	94%	*α-Proteobacteria*	pure culture
PMN76	uncultured Sphingobacteria bact. clone F4 [DQ003153]	97%	*Bacteroidetes*	soil mineral surface
PMN78	uncultured bacterium clone L1A.13C08 [AY989459]	95%	*α-Proteobacteria*	Alaskan soil
PMN79	*Pseudomonas plecoglossicida* strain P9 [AY972231]	98%	*γ-Proteobacteria*	activated sludge
PMN82	uncultured bacterium clone 655894 [DQ404682]	95%	*Acidobacteria*	contaminated sediment
PMN84	uncultured α-proteobacterium. clone KCM-B-15 [AJ581585]	98%	*α-Proteobacteria*	metal-contaminated soil
PMN88	uncultured soil bacterium clone UC8 [DQ297986]	97%	*Planctomycetacia*	HC-contaminated soil
PMN89	uncultured soil bacterium clone RFS-C313 [DQ154626]	98%	*α-Proteobacteria*	forest soil
PMN90	uncultured bacterium clone LAA2 [AF392629]	100%	*α-Proteobacteria*	crop lettuce rhizosphere
PMN91	unidentified eubacterium [AF010100]	92%	*Acidobacteria*	soil
PMN92	uncultured Actinobacteria bacterium AKYG1901 [AY921723]	97%	*Actinobacteria*	farm soil near silage bunker
PMN93	uncultured soil bacterium clone 597-1 [AY326608]	99%	*α-Proteobacteria*	Amazon soil
PMN95	uncultured soil bacterium clone SO53 [AY037586]	99%	*γ/β-Proteobacteria*?	agricultural soil earthworm cast
PMN98	uncultured earthworm cast bacterium clone c259 [AY154612]	95%	*β-Proteobacteria*	earthworm cast
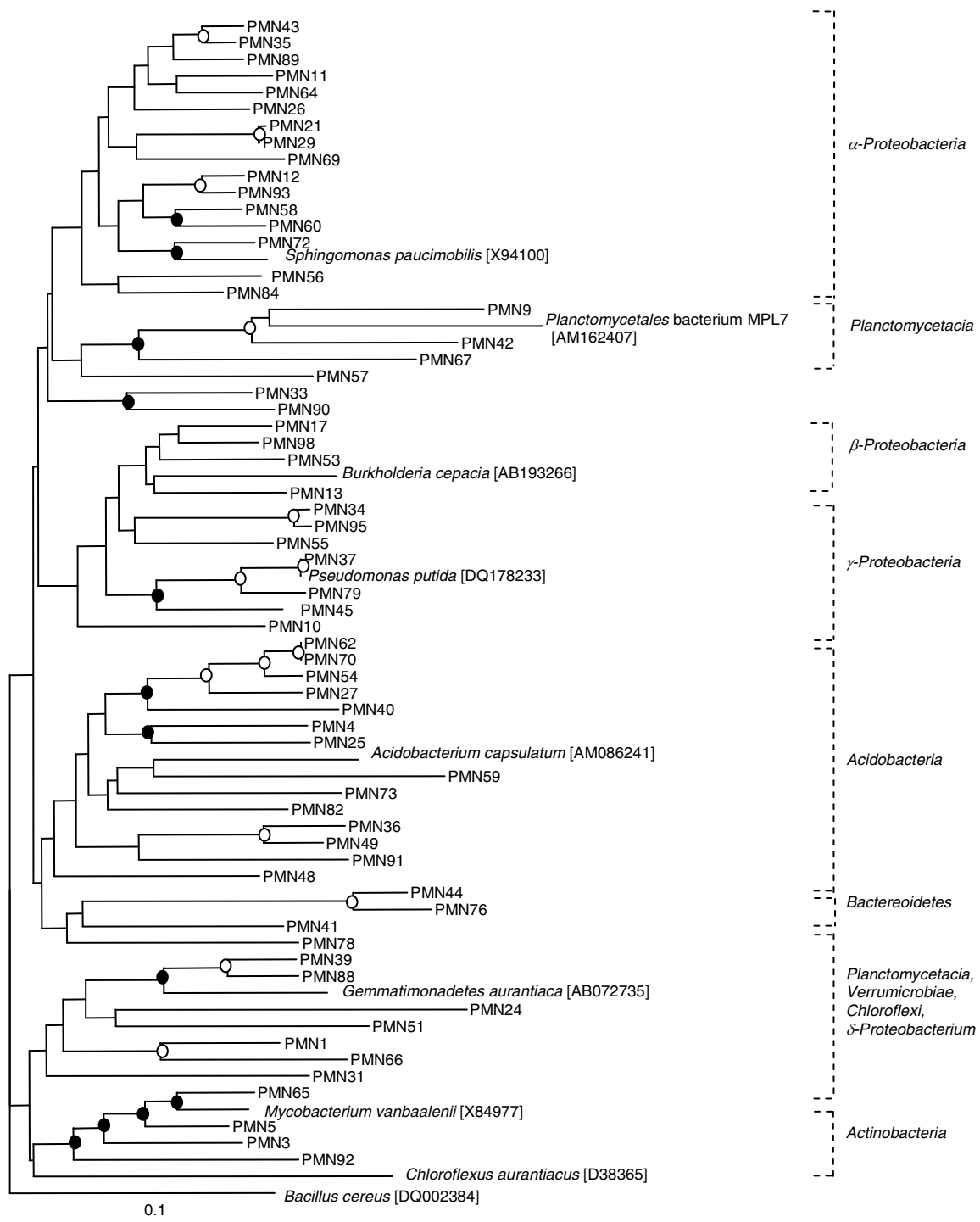
Figure 3.6. Phylogenetic Tree Inferred from PMN Clone Library. *Bacillus cereus* is included as an outgroup from which the tree is rooted. Also included are reference sequences most closely related to several PMN clones. Solid circles indicate > 70% bootstrap support; open circles indicate > 95% bootstrap support.

73
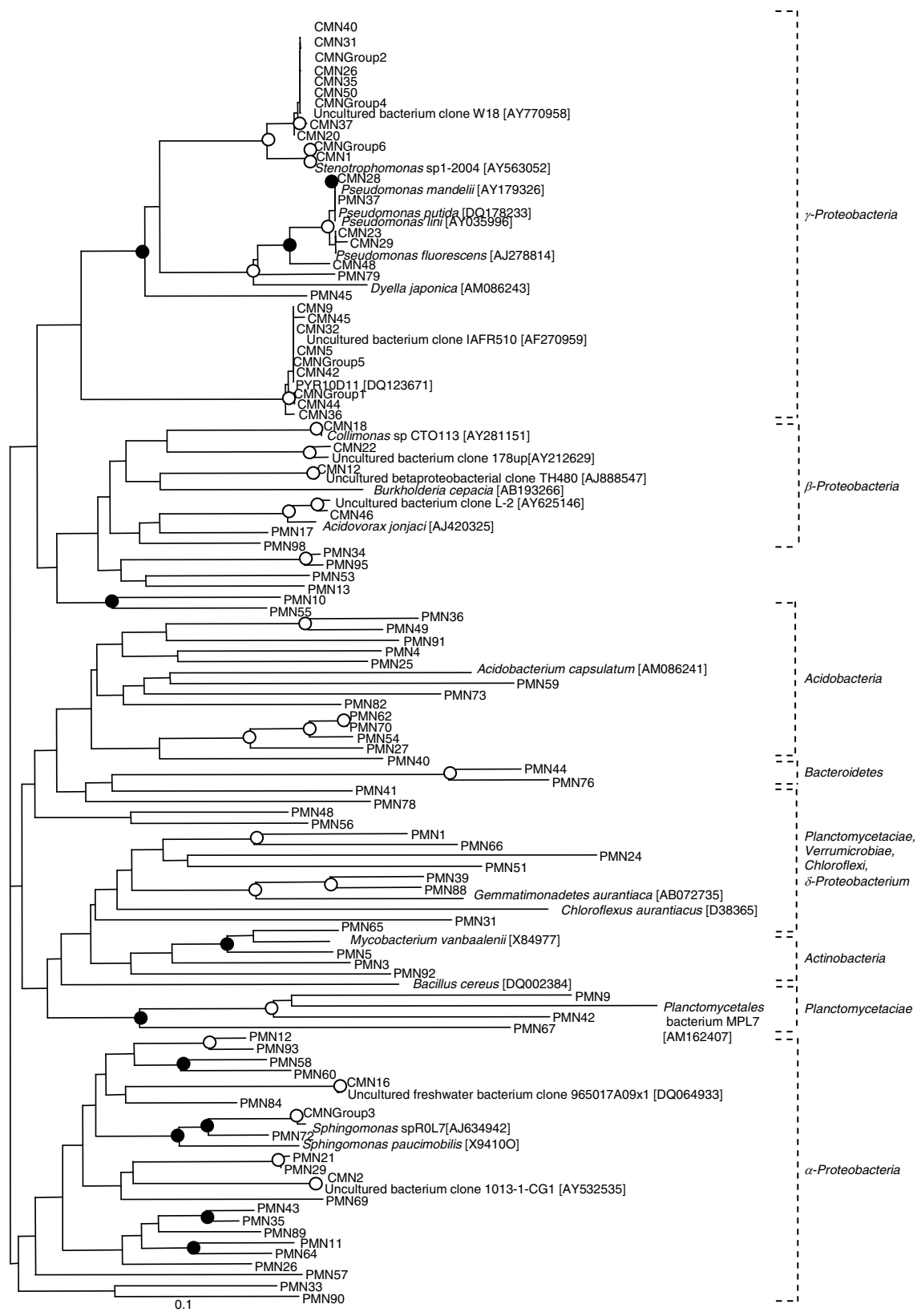
Figure 3.7. Phylogenetic Tree Inferred from both CMN and PMN Clone Libraries.

74

3.4 Discussion

Soils contain extremely diverse microbial communities whose vast membership has not been fully characterized (Dunbar et al., 2002; Liles et al., 2003; DeSantis et al., 2007). Contaminated soils have been shown to contain less diverse communities as a result of the natural selection of organisms tolerant of or able to utilize a contaminant compound (Wünsche et al., 1995; Margesin et al., 2003; Saul et al., 2005; Joynt et al., 2006). This is clearly the case with the two soils used in this study. In summary, the CMN community differed dramatically from the PMN. While the PMN exhibited a high level of diversity, the CMN community diversity was low and uneven, with only the *Proteobacteria* represented.

3.4.1 Comparison of DGGE profiles and clone libraries Apart from the obvious differences in DGGE profiles and clone libraries, two other factors were indicative of a greater diversity within the PMN community. First, a bacterial DGGE profile could not be obtained from the PMN unless PCR was performed on dilutions beyond 1:10,000 of the original genomic extract; whereas, profiles of the CMN were easily obtainable on amplicons from the direct genomic extract. Second, the clone library generated from the CMN produced a rank abundance plot that suggests the total diversity of the CMN was fully represented in the one grab sample used to generate the library (see Figure 3.8; Magurran, 1988). This was not the case with the PMN, where the rank abundance distribution was flat (i.e. the library was composed exclusively of singleton sequences) and additional unique sequences could have been identified had more clones been sequenced. The probability that a clone library of this size, generated from a soil with ~10^9 cells per gram, should contain all unique sequences is highly likely (Pr = 0.99) if the

number of species present in the PMN is 10^5 and reasonable (Pr = 0.82) if the number of species is 10^4. This is indicative of a "hyperdiverse" soil (Dunbar et al., 2002; Lunn et al., 2004).
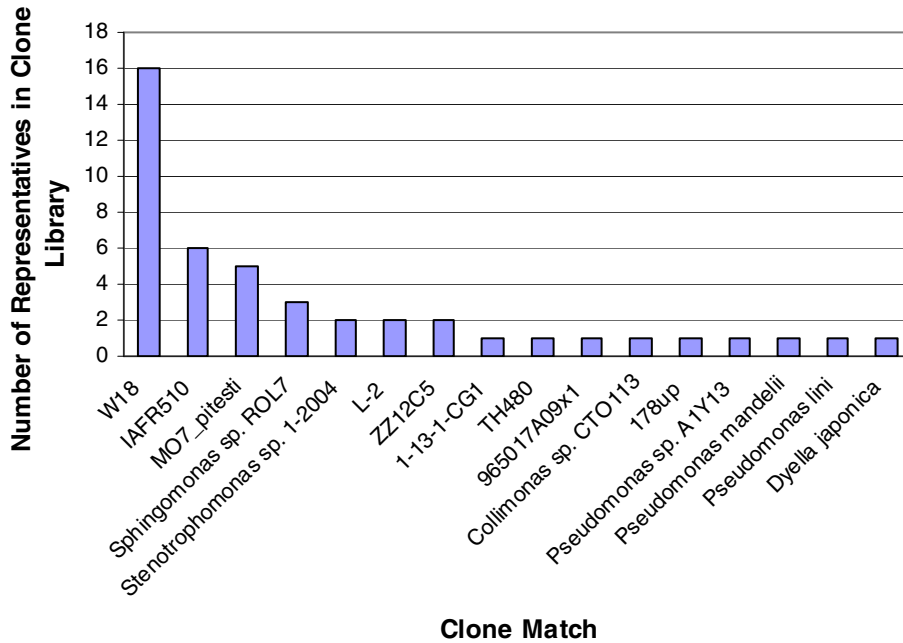
Figure 3.8. Rank Abundance Plot for CMN Clone Library.

Although it appears that two bands from the CMN profile are also in the PMN profile (see Figure 3.2), there were no common sequences within the clone libraries. The PMN clone library contained representatives from many different phylogenetic classes (*Acidobacteria*, *Proteobacteria*, *Actinobacteria*, *Chloroflexi*, *Planctomycetacia*, *Verrumicrobiae*, and *Bacteroidetes*), while the CMN was exclusively limited to the *Proteobacteria* (see Figure 3.9 below). Among the *Proteobacteria*, the majority in the CMN were from the γ-subgroup, while those in the PMN comprised mostly the α-subgroup.
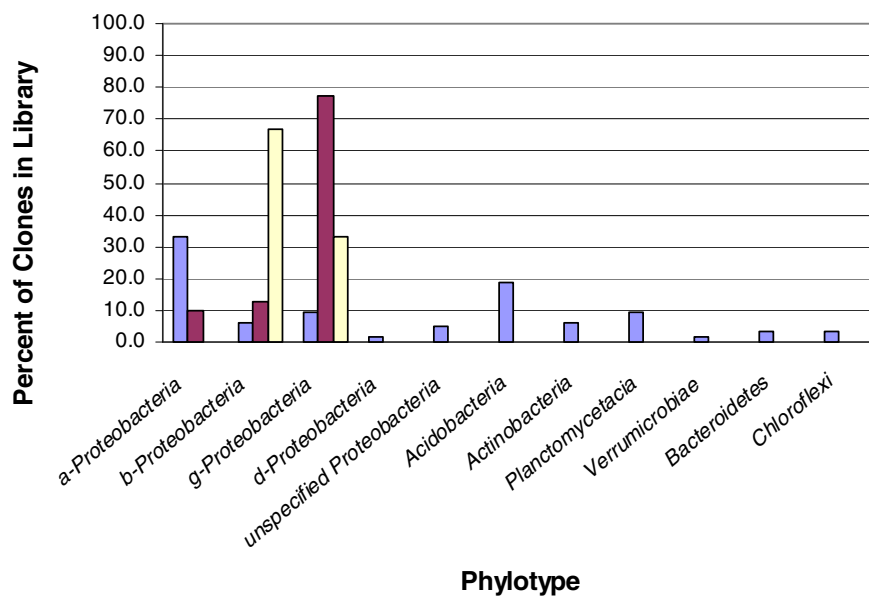
Figure 3.9. The Distribution of Clones/DGGE Bands across Common Soil Phylotypes. Blue: PMN clones; fuschia: CMN clones; beige: CMN DGGE bands.

The phylogenetic tree inferred from both clone libraries together (see Figure 3.7) is yet another reflection of the communities' dissimilarity. While the *Proteobacteria* are well represented in both communities, all other groups occur only in the PMN.

3.4.2 Diversity measurements If one assumes that the two sets of highlighted bands in Figure 3.2 represent the same OTUs, the resulting Sorensen's coefficient calculated by using only the discernible PMN bands in dilutions 10^{-5} and 10^{-6} (n = 12) is 0.14. This coefficient ranges from 0 (no shared OTUs) to 1 (identical populations). Even using this minimal number of PMN bands, the coefficient is low. It is possible that common bands exist but are not discernible due to the PMN smear. Because there are no shared clone sequences, the Sorensen's coefficient for the libraries is zero. However, it is possible that common sequences might have appeared had a larger number of PMN clones been sequenced. Since the archaeal DGGE profiles shared no bands and since no fungal PCR

products could be obtained from the CMN, the Sorensen's coefficients were 0 for each of these domains.

The Shannon index, H', was calculated for both the CMN DGGE profile and the CMN clone library. The library index was 2.19, and the DGGE index was 2.40. The Shannon index for the PMN was 4.15. Values for this index in soils usually range from 1.50 to 3.50 (increasing values indicate greater diversity) and rarely exceed 4.50. While there is no apparent difference between the two values generated for the CMN, there was an obvious difference between the CMN and PMN values for each library. The evenness of the CMN library was calculated to be 1.86, while that of the PMN was 2.50, indicating a less even distribution of OTUs within the CMN.

3.4.3 Species loss Although one cannot say that the CMN profile used to be the same as the PMN, it is reasonable to assume that they were once more similar, since they were located only ~0.5 km apart. What is interesting, then, is which organisms were absent in the CMN but were present in the PMN—high G+C Gram-positive bacteria, Bacteroidetes, and Fungi. Known, isolated PAH-degraders include many members of these groups, such as the high G+C *Actinobacteria* (Cerniglia, 1992; Dean-Ross et al., 2002; Miller et al., 2004), Flavobacteria (Yuste et al., 2000), and the well characterized *Cunninghamella elegans* fungus (Cerniglia, 1984).

The role of the Actinobacterial class, specifically *Mycobacterium* species, in the degradation of PAHs has been studied extensively. These organisms have been isolated from many PAH-contaminated soils and have been shown to degrade a variety of PAHs, including those of higher molecular weight, i.e. 4-rings and above (Dean-Ross and Cerniglia, 1996; Ho et al., 2000). However, a negative correlation was shown between

78

Mycobacterial diversity and PAH concentration in soils with much lower levels of PAH than the CMN (Cheung and Kinkle, 2001), and Mycobacteria have been conspicuously absent from other soils as well (Johnsen et al., 2002). Leys et al. (2005) found that Mycobacteria were present in lower numbers in soils containing high concentrations of low-molecular-weight (LMW) PAH. LMW PAH comprised 31% of the CMN contamination, suggesting that Mycobacteria may be selected against even at relatively lower concentrations of the more available compounds.

Creosote is used to preserve wood from degradation specifically by fungi and other cellulose-degrading organisms. It should not be a surprise, therefore, that no fungi were found in the CMN. However, many fungal species have been shown to degrade PAHs through the use of lignin or manganese peroxidases or oxygenase enzymes (Hammel et al., 1986; Sutherland et al., 1991) in either pure or bacterial co-cultures (Boonchan et al., 2000). However, fungi may oxidize PAHs as a means of detoxification rather than assimilation and growth. It is possible that the levels of PAH were too high for too long in this soil for fungal species to survive. Additionally, the CMN had been capped with 6' of topsoil on site, and the resulting diminished oxygen levels may have also been detrimental to fungi.

Although not as common, low G+C Gram-positive bacteria, such as *Bacillus* species, have also been isolated from PAH-contaminated soils and shown to have degradative abilities (Stringfellow, 1994; Daane et al., 2001). Because this group was not recovered from either soil, it was concluded that method bias in DNA recovery was the cause. Bacilli are spore-formers, and it is probable that the extraction method was unable to lyse these forms. Vegetative cells and spores of *Bacillus cereus* were inoculated into separate

aliquots of CMN soil to test for the adequacy of the MoBio kit in recovering this organism's DNA. DNA was recovered only from the vegetative cells. Others have shown a discrepancy between the high percentage of Gram-positive organisms cultivated and the low percentage found using molecular techniques (Felske et al., 1999; Smit et al., 2001).

3.4.4 Archaea It is interesting to note that both soils contain diverse Archaea. Although the proportion of Archaea in the overall PMN community could not be determined since the bacterial bands were uncountable, it can be assumed that they account for a small percentage of total possible bands in the PMN. In contrast, archaeal OTUs make up 35% of the total OTUs observed in the CMN profile (9 bands out of 26 total). While this domain has the potential to degrade hydrocarbons (Kasai et al., 2005), it has not been implicated in PAH degradation, and in fact, was ruled out as an active player in sediment contaminated with oil (Röling et al, 2004b) and in the CMN soil when incubated aerobically with pyrene (Jones et al., 2007, submitted). Nonetheless, these organisms are present and their DGGE profiles were different, suggesting some sort of selection for certain organisms. It is possible that under anaerobic conditions, this group plays a significant role in PAH transformation or degradation that has yet to be described.

3.4.5 Reasons for changes in the CMN structure There are many reasons why a microbial community may shift to a poor and uneven composition. Among these are stressors, such as competition, based on habitat alteration, limited resources, or differential growth rates (Tilman, 1993; Langworthy et al., 2002; Zhou et al., 2002); exposure to toxic compounds; or selection based on inherent or acquired metabolic capability (MacNaughton et al., 1999; Langworthy et al., 2002; Viñas et al., 2002).

Creosote is a non-aqueous phase liquid that, when applied to soil, may cause many physico-chemical changes in the microbial environment. Tar "droplets" have been observed in PAH-contaminated soils, including the CMN, that may cause sticky aggregates to form (Johnsen et al., 2005). Zones of anaerobicity may form due to poor oxygen diffusion or water retention, or a decrease in moisture content due to the impermeability to water. These conditions can lead to habitat fragmentation, in which larger communities may be divided at the microscale. This results in a loss of population interaction and an induction of competition between the remaining species for the limited access to resources such as oxygen or water with soluble nutrients (Tilman, 1993).

Substrate competition is the most common type of competition between microorganisms in nature (Lengeler et al., 1999). It is possible that competition for carbon sources once occurred in the CMN. Other components of creosote, e.g. alkanes or simple aromatics, and natural organic matter in the soil would have been degraded in preference to PAHs. Once their supply had diminished, competition may have ensued. Theoretically, there is still a sufficiently high concentration of "bioavailable" carbon, including low molecular weight PAHs, in the CMN soil to support the growth of many species without inducing competition. It seems more likely that this overabundance of carbon itself could be a source of stress to the community by causing differential and unbalanced growth rates of certain groups to the detriment of others (Stephen et al., 1999).

The effects of PAH toxicity to indigenous microbes are probably manifested early after an exposure and may result in significant damage to or complete loss of certain populations. Because of community interdependency, it is likely that other populations

81

suffer as a result. Toxic effects are also concentration dependent. At low or intermediate

levels, PAHs may stimulate the growth or activity of microorganisms in soil (Langworthy

et al., 2002; Johnsen et al., 2002). However, given the high levels of PAH in the CMN, it

is not unreasonable to assume that toxicity played a large role in affecting diversity

(DelPanno et al., 2005).

Apart from toxicity, the most likely reason for the dramatic shift in community

structure is the selection of specific groups that are capable of metabolizing PAHs. Low

substrate specificity and functional complexity may provide advantages to certain

organisms. Over time, a community may become adapted to an environmental insult,

especially a contaminant. Organisms may be selected that already possess the metabolic

capabilities to deal with the compound or that can acquire this capability, for example

through horizontal gene transfer. Repeated exposure to a contaminant results in quick

enzyme induction, if the required enzymes are not constitutively expressed.

The organisms that have survived in the CMN soil fall within the *Proteobacteria*.

This phylum is the largest and phenotypically most diverse of all *Bacteria*, with widely

varied habitats and means of energy acquisition (Kersters et al., 2005). Members of the

α-subclass include the *Sphingomonas* species, some of which are known PAH-degraders.

Burkholderia species, members of the β-subclass, are ubiquitous in nature, and some

members are also known aromatic degraders. The γ-subclass is the largest within the

Proteobacteria and comprises the *Pseudomonas* species. This genus is well known for

its "metabolic diversity and genetic plasticity" (Moore et al., 2005). (The β- and γ-

subclasses are now considered one broad complex called the *Chromatibacteria*, which

may explain the difficulty in assigning PMN95 to a class).

One reason for the selection of *Proteobacteria* is the phenotypic diversity exhibited by this group. If a community loses member populations, it can benefit from the functional redundancy of the remaining members. The greater the functional complexity of a community, the more resilient it is in response to disturbance (Tilman and Knops, 1997).

Microbial community succession in soil proceeds from *r*-selected to *K*-selected organisms (Garland et al., 2001). *r*-Strategists are opportunists with a broad niche width, who expend their energy on rapid reproduction during times of high resource availability. *K*-strategists are considered equilibrium organisms, or those who predominate when resources are limited and who prefer to direct their energy toward maintenance by adaptation and niche specialization (Andrews, 1984, as cited in Atlas and Bartha, 1993).

This theory may help to partially explain the resulting community in the CMN soil. Many *Proteobacteria*, especially members of the γ-subgroup, such as *Pseudomonas* sp., are considered to be *r*-strategists. Gram-positives, such as the *Mycobacteria*, are theorized to be the *K*-strategists. The presence of only *r*-organisms and the complete absence of *K*-organisms in the CMN soil suggest that *K*-organisms were eliminated in the past due to periodic desorption, or "flushes", of PAH from the soil matrix into the microenvironment. It is assumed that these "flushes" continue today. Otherwise, one might expect to find *Mycobacteria* dominating in this soil as in other aged, PAH-contaminated soils (Leys et al., 2005; Uyttebroek et al., 2006a; Johnsen et al., 2007).

3.4.6 Anaerobic effects The 6' capping on the CMN has undoubtedly played a role in the selection of certain organisms. It is probable that an oxygen gradient existed causing the selection for certain groups, e.g. Archaea, and against others, e.g. Fungi. The

Proteobacteria include aerobes, facultative anaerobes, microaerophiles, and anaerobes; thus, it is easy to see why they were not excluded from this type of environment. Many other groups of soil organisms found in the PMN—such as the Planctomycetes, Verrumicrobia, Actinomycetes, and Bacteroidetes-- contain members who can survive and proliferate in anaerobic environments. However, the Mycobacteria and Nocardia are obligate aerobes.

3.4.7 Storage effects Storage conditions may also have played a role in decreasing or altering the diversity of both soils (Petersen and Klug, 1994; Ringelberg et al., 2001). The CMN was initially characterized in 2002, but the process was repeated two years later. The resulting DGGE profiles (compare Figures 3.1 and 3.2) were different, although BLAST results for many of the sequenced bands were identical and all fell within the same Proteobacterial groups in roughly the same proportion. However, the PMN soil was not stored long prior to processing, and its profile still did not match either CMN profile generated.

3.5 Method Limitations

A large percentage (25%) of the PMN sequences generated from the clone library was determined to be chimeras. The CMN library was found to contain 11% chimeric sequences. There are several possible causes for the high level of chimera formation in these samples. First, the rigorous bead-beating during extraction may have yielded short DNA fragments, as samples containing smaller fragments have been shown to form more chimeras (von Wintzingerode et al., 1997). Second, the number of cycles (35) of PCR or an insufficient elongation step (1 minute each) may have been conducive to chimera

formation by increasing the opportunities for non-target fragments to anneal and elongate (Wang and Wang, 1997). Third, others have reported that highly complex templates, such as soil genomic DNA, yield a high percentage of chimeras (von Wintzingerode et al., 1997). Fourth, the forward primer used to generate the fragment DNA for cloning was the same used for DGGE, and thus contained the GC-clamp. It is possible that the clamp prevented complete denaturation during PCR, allowing the chimeric fragment to continue forming during elongation. Nevertheless, there were no chimeras discovered in the sequenced DGGE bands.

In hindsight, DGGE was not the best tool with which to compare the community diversity of this sample set. It was adequate for the less diverse contaminated soil but not the highly diverse "pristine" soil. While cloning has the distinct disadvantage of high cost, the results were more conclusive than those from the DGGE profiling and are more conducive to statistical analysis.

Another limitation to this study was the need for a nested PCR protocol when profiling the CMN. When this soil is incubated with a supplemental carbon source to encourage growth, the nested protocol is not required. Nesting may have produced bias in the relative abundances of bands profiled by DGGE and in the actual number of bands. However, without nesting, PCR products could not be obtained for this soil.

Additionally, the size of the clone library obtained for the PMN was not an adequate representation of the overall diversity of this soil, as evidenced by its nonasymptotic rarefaction curve (see Figure 3.10).
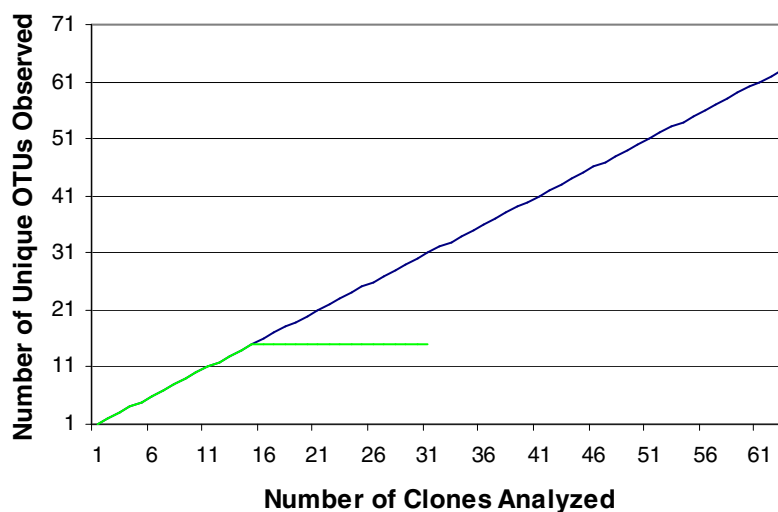
Figure 3.10. Rarefaction Curves of Observed OTUs in PMN and CMN Soils. Blue: PMN clones; green: CMN clones.

However, it was not within the scope of this project to do a full profiling of the PMN soil, so much as to provide a contrast to the low level of diversity within the CMN.

Finally, the sampling of these soils only provides a snapshot in time at one location. It might have been more meaningful had both soils been retrieved and analyzed at the same time, since storage conditions may alter the resulting DGGE profiles and/or clone libraries. Additionally, multiple samples from within the contaminated and uncontaminated areas should have been profiled to measure within-site variability.

3.6 Future Research

Future work on these soils could include a detailed profiling of the Archaea using clone libraries. Archaea have not been shown to play a role in PAH degradation, yet they have survived in a highly contaminated soil. The distinct differences between the CMN

and PMN DGGE profiles for this domain in conjunction with the relative richness within

the CMN, suggests that selection for certain groups may have taken place.

4.0 Comparison of a Slurry-based Method and an Aggregate Method for the *in situ* Visualization of Microorganisms in PAH-contaminated Soils

4.1 Introduction

Soil is a heterogeneous matrix, and neither microbial distribution nor activity is uniform within. This is not to say that a soil aggregate is without order. Indeed, soil has been described as a "self-organized" complex, because its heterogeneous structure both controls and is controlled by the microorganisms therein (Preston et al., 1999; Young and Crawford, 2004; Feeney et al., 2006).   For example, bacterial decomposition of soil organic matter leads to an increase in porosity, while bacterial extracellular polymers act as temporary adhesives to hold this new structure together (Martens and Frankenberger, 1992; Feeney et al., 2006). By ordering pore structure, bacteria facilitate the transport of substances in soil (Feeney et al., 2006). However, variable levels of oxygen and other nutrients introduced into these newly-formed pores lead to patchy bacterial colonization. Thus, a consequence of soil heterogeneity is the spatial variability of organisms and their activities (Ettema and Wardle, 2002).

In light of this, scientific measurements made on bulk soil are not always reflective of the undisturbed microscale and may lead to incorrect interpretations of microbial community structure and function (Parkin, 1993; Harris, 1994; Ashman et al., 2003; Becker et al., 2006; Mummey et al., 2006). In microenvironments, there may be variations in cell numbers, phylotypes, or functional roles. These may be associated with

depth, porosity, particle size fractions, geochemistry, and nutrient availability (Bundt et al., 2001; Nunan et al., 2001, 2002, 2003; Sessitch et al., 2001; Mummey et al., 2006). As a result, it would seem advantageous to use techniques that provide accurate information at the microscale level, or the level at which microbial life has an immediate impact.

The importance of examining microorganisms *in situ* extends to contaminated soils and sediments as well. Now that the organisms and genes responsible for contaminant degradation are being identified without the bias of cultivation, it may be possible to use these cultivation-independent techniques to determine the spatial relationships between active degraders, the contaminant, and the soil matrix. Tools such as fluorescence staining, *in situ* hybridization with fluorescent probes, and microautoradiography are fundamental to this area of study (Dechesne et al., 2003; Wagner et al., 2006). However, they are still limited by the fact that, in most cases, sample processing causes disturbance, thereby making any *in situ* examination impossible.

Many soil scientists utilize techniques such as biological thin sections or soil smears, and staining or immunodetection followed by microscopy to gain a more realistic picture of the spatial organization of microorganisms within the larger, relatively undisturbed, soil aggregate structure or horizon (Altemüller and van Vliet-Lanoe, 1990; Fisk et al., 1999; Nunan et al., 2001; Li et al, 2004). Again, while these studies yield valuable results, they are often unable to identify the organisms except by morphology, and may not even be able to tell live from dead. Some stains exist which are able to differentiate between live and dead cells, but they are still unable to identify specific groups of organisms.

Fluorescence *in situ* hybridization (FISH) has been used widely on aqueous samples, and is increasingly used on sediment and soil samples as well. However, there are many problems inherent in performing FISH on soil or sediment, such the high background caused by probe adsorption onto particulate surfaces, or the autofluorescence of soil particles (Moter and Göbel, 2000). Most researchers avoid these difficulties by creating a slurry from the soil or sediment and using only microliter volumes of the slurry for hybridization (Amann, 1995). However, this convention may not result in the most accurate representation of the larger picture because it destroys any existing spatial relationships.

In an attempt to correlate microbial activity with spatial arrangement, Macnaughton et al. (1996) devised a technique that preserved the spatial arrangement of bacteria at the root:soil interface. This involved immobilizing the plant root in agarose prior to hybridization. Decho and Kawaguchi (1999) used the same immobilization concept by embedding stromatolite biofilms in resin after staining. They were able to show a close spatial relationship between cyanobacteria and heterotrophic bacteria in their samples. More recently, the embedding technique was used on activated sludge to maintain the three-dimensional structure of flocs (Daims et al., 2006). After FISH, the clustering of ammonia- and nitrite-oxidizers was measured, providing supporting evidence of their related functional roles.

The aim of this research was to attempt to visualize the organisms present in soil while preserving, as much as possible, the soil's aggregate structure, thus allowing examination of the spatial relationships therein. This was accomplished by creating an

90

aggregate-based method ("Aggregate FISH") which was then compared to an established slurry-based method ("Slurry FISH").

4.2 Materials and Method Optimization

4.2.1 Soils The soils used for this experiment came from three different sites around the United States. Two soils, CMN and KKY, were obtained from wood-preserving facilities (see chapter 3 for further information on CMN). The third, CNC, came from the site of a former manufactured gas plant in Charlotte, NC. A limited characterization of these soils is given in Table 4.1 below. A shortage of CNC precluded a detailed analysis of this soil.

Table 4.1. Characteristics of Experimental Soils.

	CMN	CNC	KKY
% moisture	5.49 ± 0.85	22.60	0.61 ± 0.28
% carbon by weight	9.01 ± 1.20	3.55	18.44 ± 0.95
pH	7.5	7.0	7.8
total PAH (mg kg^{-1})	4393 ± 693	360	12,408 ± 3465
pyrene content (mg kg^{-1})	463 ± 100	42.4 ± 0.29	1826 ± 368

All CNC analyses were performed by H. Zhu and J.K. Park, University of North Carolina-Chapel Hill, Department of Environmental Sciences and Engineering, personal communication. pH measurements of CMN and KKY soils were made by the University of Wisconsin-Madison Soil and Plant Analysis Laboratory, Madison, WI. Percent carbon and moisture were measured by Clear Science, Baton Rouge, LA. PAHs were analyzed by Eno River Laboratories, Durham, NC, using EPA method 8270. Total PAH refers to the following 16 EPA-listed priority compounds: acenaphthene, acenaphthylene, anthracene, benzo[a]anthracene, benzo[b]fluoranthene, benzo[k]fluoranthene, benzo[g,h,i]perylene, benzo[a]pyrene, chrysene, dibenzo[a,h]anthracene, fluoranthene, fluorene, indeno[1,2,3-cd]pyrene, naphthalene, phenanthrene, and pyrene. PAH measurements were performed on triplicate samples.

4.2.2 Chemicals and reagents All chemicals used for FISH, with the exception of acrylamide, were of molecular grade and certified by the manufacturer to be nuclease-free. FISH reagents were filtered through 0.2 μm nylon membranes. A 20% acrylamide stock solution (200:1, acrylamide: bisacrylamide) was made in filter-sterilized, deionized

water and stored at 4°C in the dark until just before use. Crystalline pyrene was obtained from Sigma-Aldrich (St. Louis, MO) and was the highest purity available.

4.2.3 Probes A combination of bacterial, Eub338 (5' GCTGCCTCCCGTAGGAGT 3'), and universal, Univ1390 (5' GACCGGGCGGTGTGTACAA 3'), probes was used (Amann et al., 1990a). Oligonucleotides were synthesized and gel-purified by Oligos Etc., Inc. (Wilsonville, OR). Fluorescent tags were covalently attached at the 5' end-- fluorescein isothiocyanate (FITC; excitation at 495 nm, emission at 519 nm) for Univ1390 and tetramethylcarboxyrhodamine (TAMRA or TRITC depending on the manufacturer, ex. 547 nm, em. 572 nm) for EUB338. Probes were reconstituted in TE buffer (Tris 10 mM, EDTA 1 mM, pH 8) and stored at -20°C until use.

4.2.4 Filter apparatus A filter-based apparatus was constructed from a solid-phase extraction manifold. Fifteen-milliliter conical, polypropylene tubes were cut at their bases to a diameter of 13 mm and glued to the upper component of a Swinnex filter housing (Millipore, Burlington, MA) whose conical portion had been cut (see Figure 4.1; Miller and Scholin, 1998).
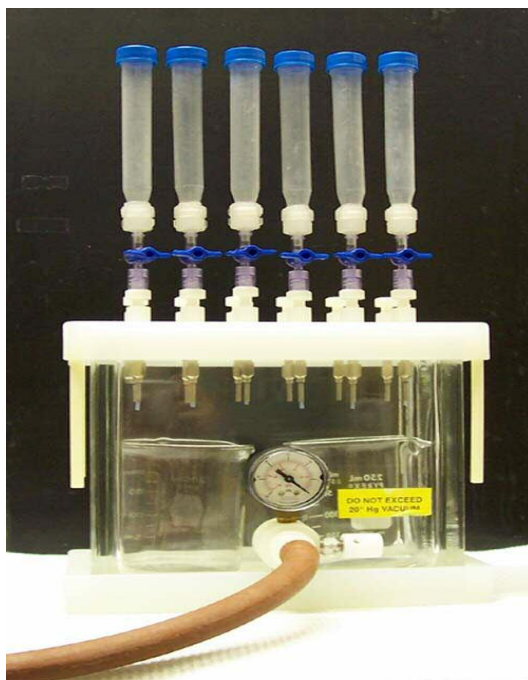
Figure 4.1 Miller-Scholin Apparatus for Filter-based Hybridizations

The base of the filter housing was secured to the manifold by a luer-lock stopcock inserted into the teflon liner. A 13 mm silicone gasket was placed in the base of the conical tube. Slurries were filtered through 0.2 μm white isopore polycarbonate membrane filters under 3-5 inches Hg vacuum. The vacuum was increased at the end of each step to no greater than 10 inches Hg, depending on the mass of soil covering the filter.

4.2.5 Microscopy Microscopy was performed on an Olympus IX71 epifluorescence microscope equipped with a 100W mercury lamp, an inverted stage, and a 12.5 MegaPixel DP70 digital camera. Samples were viewed at 1000-fold magnification using the following filter sets (Chroma Technology Corp; Brattleboro, VT): Pyrene (excitation 360 nm with a 40 nm bandwidth, emission 480 nm with a 60 nm bandwidth; dichroic longpass beamsplitter at 400 nm); FITC/EGFP/Biodipy/Fluo3/DiO (ex. 480 nm with a 40 nm bandwidth, em. 535 nm with a 50 nm bandwidth, longpass beamsplitter cut-on of 505

nm); TRITC (Rhodamine)/DiI (ex. 535 nm with a 50 nm bandwidth, em. 610 nm with a

75 nm bandwidth, longpass beamsplitter cut-on at 565 nm); and DAPI/Hoechst/AMCA

(ex. 360 nm with a 40 nm bandwidth, em. 460 nm with a 50 nm bandwidth, dichroic

longpass beamsplitter cut-on at 400 nm). Samples were stored at 4°C after analysis.

4.2.6 Image processing and analysis Processing, other than contrast and brightness

adjustment, was not necessary during method optimization tests. Images were analyzed

for the ratio of cell to background fluorescence. Fluorescence can be described in terms

of both color (fluorochrome brightness) and luminance (grayscale intensity) (Russ, 2002).

These measurements were made using FoveaPro software in Adobe Photoshop 7.0

(Reindeer Graphics, Asheville, NC). The ratios of organism color and luminance to

background color and luminance were calculated and summed for each method parameter

tested. Theoretically, the larger the ratio, the easier it is to discern objects from

background. The objective of this optimization step was to maximize the ratio. Bacteria

were selected from each image using either the "magic wand" or "oval marquée" tool.

The inverse of the selected features was measured in the same way as the background.

For slurried samples, soil particles were eliminated from the inverse image.

4.2.7 Statistics Significance testing of the difference between means was conducted

using Student's *t* test.

4.3 Method Optimization

4.3.1 Choice of fluorochrome The CMN was screened for background fluorescence,

i.e. soil constituents and PAHs, in order to determine which fluorescent tags would be

suitable for use. Soil smears in water were examined with an epifluorescence microscope

94

that was fitted with a selection of filters that spanned the visible spectrum. At the time of this initial screening, neither the CNC nor KKY soil was available for examination.

The CMN was found to fluoresce over all wavelengths tested. It is unknown whether the observed background is due to autofluorescent soil constituents, such as carbonates, iron compounds, organic matter or the PAHs therein (see Figure 4.2 below; Altemüller and van Vliet-Lanoe, 1990). Regardless, this fluorescence left few choices for fluorochrome tagging. Fluorescein was chosen based on the relatively low fluorescence of the CMN soil using the FITC filter, its well-established use in soils and for FISH, and its reasonable cost.

(a)   (b)

(c)   (d)
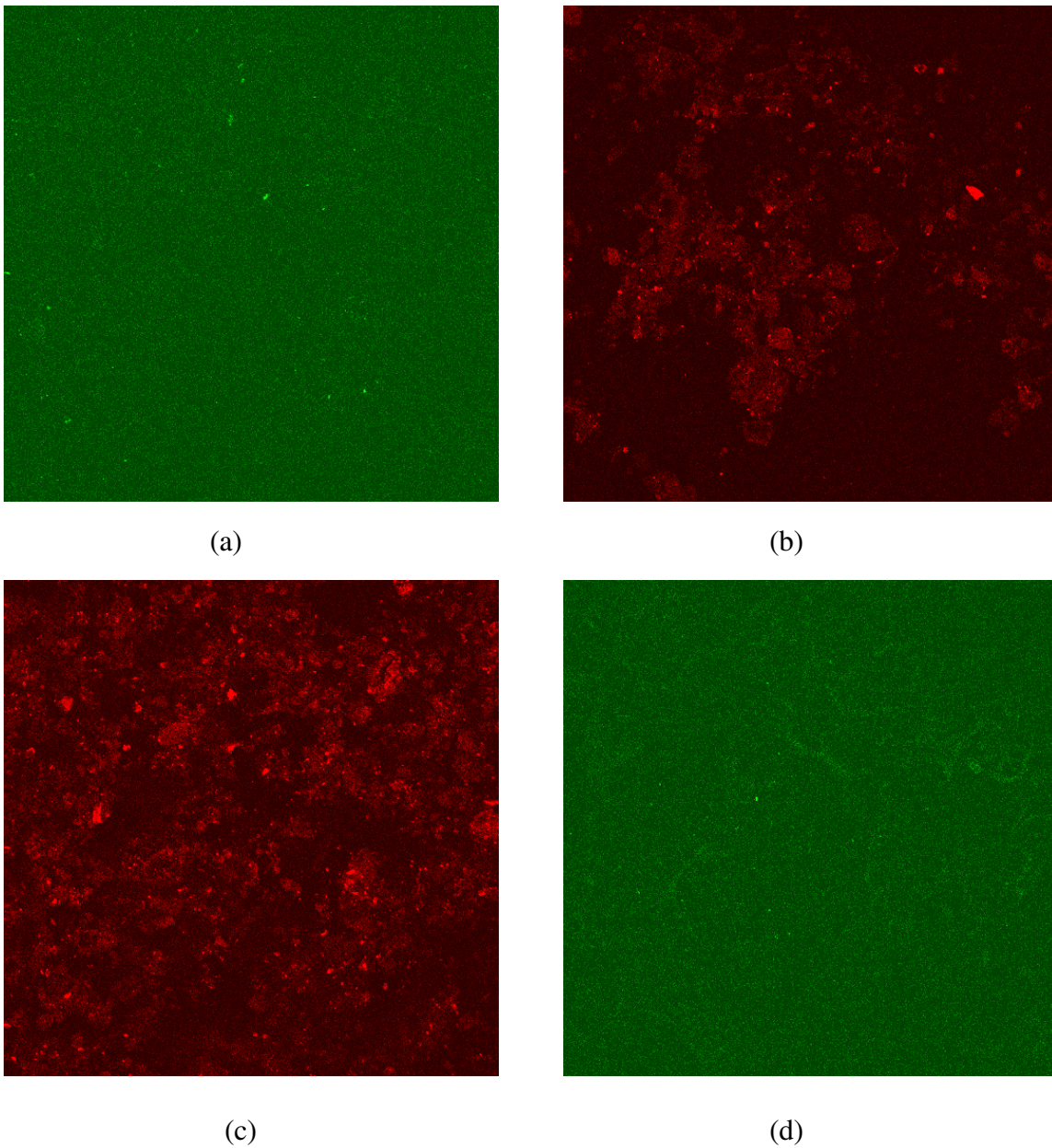
Figure 4.2 Autofluorescence of CMN Soil. Soil smears in water were visualized using the following filters: a) FITC, b) TRITC, c) Cy 3 ex. 520, em. 570, d) Lucifer Yellow ex. 425, em. 528.

TRITC, or TAMRA, was chosen as the second fluorochrome based on the low

fluorescence of the CMN soil when visualized with this filter and its reasonable spectral

separation from FITC and pyrene. The CNC and KKY soils were not screened for

background fluorescence. It is possible that they would have exhibited different levels of autofluorescence, due to their varied soil constituents and PAH concentrations.

4.3.2 The embedding method

4.3.2.1 Sample preparation by embedding A sterile brass corer (inner diameter ~11 mm) was inserted into the center of a given vial containing soil and secured manually. The soil was embedded by the slow introduction of the reagent to be tested from the bottom of the core, using a Pasteur pipette. The reagent was allowed to polymerize for 30 minutes prior to removal. After its removal, additional reagent was used to "cap" the ends of the embedded "plug" (see Figure 4.3 below).

Figure 4.3 Acrylamide-embedded Soil "Plug"

4.3.2.2 Choice of embedding reagent A comparison of Noble agar (15 g L^{-1} and 7.5 g L^{-1}), purified bovine gelatin (50 g L^{-1} and 100 g L^{-1}), and acrylamide (37.1:1 and 200:1 ratio of acrylamide:bisacrylamide) was carried out by embedding 1 gram of CMN in each matrix. Different concentrations of the polymerizing catalysts, ammonium persulfate (APS) and N,N,N',N'-Tetramethylethylenediamine (TEMED), were also tested on the acrylamide solutions. Samples were examined for integrity after embedding. Those

deemed firm enough were fixed in 4% paraformaldehyde (w/v) in phosphate-buffered

saline overnight (PBS: 130 mM NaCl, 7 mM Na_2HPO_4, 3 mM NaH_2PO_4, pH 7.2;

Amann, 1995). After fixation, the supernatant was analyzed for "leached", or extracted,

PAHs by high-pressure liquid chromatography (HPLC). The samples were then

incubated at the hybridization temperature (45^oC) for 4 hours, after which the integrity of

the embedding matrix was again examined.

   None of the lower concentrations of any of the embedding reagents were able to

adequately maintain the aggregate structure of the soil. Additionally, none of the lower

concentrations of APS/TEMED were sufficient to polymerize the acrylamide. While the

supernatant in the gelatin samples showed the least amount of leaching from the soil after

an overnight fixation step, the gelatin could not withstand incubation at the required

hybridization temperature. The Noble agar appeared less firm than the acrylamide after

fixation, although it did survive the entire protocol intact. The acrylamide-embedded

sample was the firmest of the three and was the least affected by either the fixing or

hybridization steps.

4.3.2.3 Validation of the embedding method Once acrylamide was chosen as the

optimal embedding reagent, its effect on the spatial arrangement of microorganisms

within the soil aggregate was examined. This was accomplished by seeding 30 grams of

an uncontaminated soil (PMN) with a known inoculum of bacteria (2.14×10^9 CFU from

a mixed culture consisting of *Bacillus cereus*, *Sphingomonas yanoikuye*, and *Pelomonas*

saccharophila). The soil was then embedded in acrylamide, fixed in

paraformaldehyde/PBS, and stained with 4',6-diamidino-2-phenylindole (DAPI;

Invitrogen/Molecular Probes, Oregon). Four transects were made along the length of the

core (designated 1-4, with 1 being closest to the point of acrylamide introduction), and direct cell counts were taken microscopically using the epifluorescence microscope equipped with a DAPI filter.

Cells were counted manually from the images taken of 20-32 fields at each transect. The total number of cells per gram of soil was back-calculated as follows:

a) for slurry samples: $N = (N_fAD)/aV$, where: N_f = cells counted per field, A = effective filtering area, D = dilution factor of soil in slurry form, a = area of microscopic field, and V = volume of slurry filtered; and

b) for embedded samples: $N = (N_fAT)/aS$, where: N_f = cells counted per field, A = area of transected core slice, T = number of transected slices per soil core, a = area of microscopic field, S = grams of soil in a core. The number of transects per soil core was calculated as the core height/slice height. The height of a transect slice that can be visualized under a microscope is referred to as the "field of depth" ($= \lambda[\sqrt{(n^2-NA^2)}]/NA^2$). This parameter is dependent upon the maximum emission wavelength of each fluorochrome (λ), the refractive index of the immersion oil (n), and the numerical aperture (NA) of the microscope objective (Shillaber, 1944; R. Bagnell, Microscopy Services Laboratory, Department of Pathology and Laboratory Medicine, UNC-Chapel Hill School of Medicine, personal communication).

DAPI counts along the depths of duplicate acrylamide-embedded soil cores are shown in Figures 4.4a and b below.
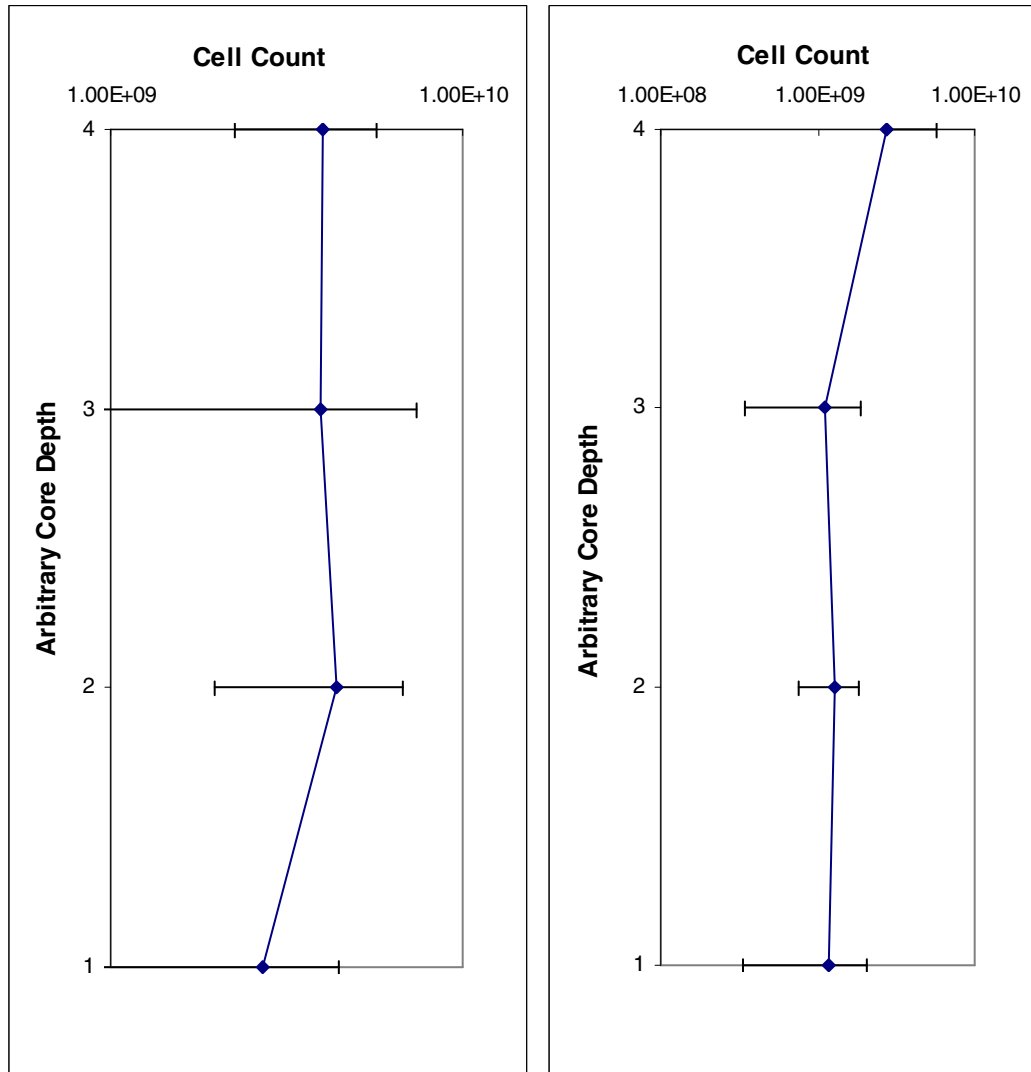
(a)   (b)

Figures 4.4 a and b Enumeration of DAPI-Stained Cells at Four Core Depths for
Duplicate Embedded Cores, A and B. Introduction of acrylamide begins at Arbitrary
Core Depth 1.

In Core A, counts at arbitrary depth 1 (i.e. the point of acrylamide introduction) were

significantly different from those at depths 2 and 4 (P<0.02). Counts at all other depths

were not significantly different from each other. In Core B, counts at arbitrary depth 4

(the point furthest from acrylamide introduction) were significantly different from counts

at all other depths along the core (P<0.05). It was noted that there was an initial rapid

addition of acrylamide in Core A, which could potentially explain the differences between depth 1 and the other depths (see Figure 4.4a). To compensate for this, acrylamide was added more slowly to Core B. However, due to its rapid polymerization, it was expelled more quickly at the top of Core B. This could explain the difference between counts at depth 4 and all other depths (see Figure 4.4b). Because of the differences in counts at the core ends and because there was no significant difference between counts at the cores' mid-sections, it was concluded that the speed with which acrylamide was added had a greater effect on cell displacement with depth than just the addition of acrylamide itself.

Therefore, the embedding method was deemed acceptable for maintaining the soil's aggregate structure without displacing resident cells, as long as the acrylamide could be dispensed at the same rate. To ensure that this would be the case, the mass of soil per core was decreased, so that the acrylamide did not polymerize until after it was all dispensed.

4.3.3 Optimization of hybridization buffer composition and pH, wash solution strength and pH The FISH method was optimized using the filter apparatus and a mixture of pure culture organisms (see section 4.3.2.3) obtained as isolates from other PAH-contaminated soils (Stringfellow, 1994) and *Candida albicans* as a negative control for the bacterial probe. The method was optimized on one of the soils, CMN, in slurry form.

The original hybridization buffer (HB) contained 0.75 M NaCl, 0.001% (v/v) IGEPAL, 0.003% (w/v) polyadenylic acid, and 15% (v/v) formamide (Miller and Scholin, 1998; Amann et al., 1990a). First, formamide was found to extract PAHs from

the soils. Therefore, a hybridization buffer without formamide was tested for comparison. Second, the pH of the hybridization buffer and wash solution (SET: 0.75 M NaCl; 5 mM EDTA; 100 mM Tris) were tested over a range from 8.0 through pH 9.5, at 0.5 increments. The wash solution was kept at a pH 0.5 units higher for increased stringency. Finally, the salt content of the wash solution was tested at three concentrations (5X, 2.5X, and 1X, where 5X = 0.75 M NaCl).

Images were generated of pure cultures and the CMN soil slurry after FISH, as described above (see 4.2.5), and attributes were measured in Photoshop. Results for the ratio of organism fluorescence to background fluorescence over all tested Slurry FISH conditions are given in Appendix II.

In pure culture tests, there was no significant difference between fluorescence ratios generated with or without formamide addition to the hybridization buffer (Appendix IIa). The same held true for fluorescence ratios generated from CMN slurry FISH images, except at 1X salt concentration using the TRITC-based probe (Appendix IIb). Formamide is added to FISH protocols to increase stringency, but its effect is probe-dependent. Its lack of significant effect for these samples was a fortunate finding, since the formamide also tended to extract PAH from the samples.

There was also no significant difference between fluorescence ratios of pure cultures for either probe at any of the tested wash solution salt concentrations. For the CMN Slurry FISH samples, fluorescence ratios were found to be higher after washing in 1X SET than in 5X but only for the TRITC-based probe. Significance could not be tested due to the low number of images. Ultimately, 5X SET was chosen because it was

thought that its increased stringency would be more effective at removing high-affinity probes from the soils.

The results of pH optimization tests on pure cultures were the same for both fluorochromes: optimal fluorescence ratios occurred with HB pH 9.0 and SET pH 9.5 (Appendix IIc). It was originally supposed that a higher pH might decrease the background fluorescence caused by FITC-based probes adsorbing onto soil components. Fluorescein is an anionic fluorochrome that, at high pH, is negatively charged and repelled by the similar charge on clay compounds and other soil constituents, but attracted to the positive charges of proteinaceous components (Altemüller and van Vliet-Lanoe, 1990; Haugland, 2002). While the fluorescence ratios at these pH were the highest, it was noted that the highest pH (9.5) also caused more precipitation of the FITC-based probe. As a result, the pH chosen for the study were pH 8.5 for HB and pH 9.0 for the wash. The TRITC-based probe generally yielded higher ratios than the FITC-based probe, although not always. This is not unreasonable, since TRITC is more photostable and is more excitable by the source wavelength of the mercury arc lamp of the microscope (Haugland, 2002). It is also possible that the proximity of FITC emission and TRITC excitation wavelengths led to fluorescence energy resonant transfer. This would lead to a decrease in FITC fluorescence coupled with an increase in TRITC fluorescence (Cullander, 1999; Haugland, 2002).

The fluorescence ratios of slurried CMN soil with variable pH varied widely (Appendix IId). The optimal pH range for HB in CMN slurry was pH 8.0-8.5, while the optimal SET pH was between 9.0-9.5. There were no apparent differences between the ratios from each fluorochrome.

It should also be noted that the ratios for slurried soil spiked with pure cultures were lower than those of pure culture suspensions, although the difference was significant only for the TRITC-based probe (P<0.05). This is likely due to the affinity of the probe for soil constituents regardless of method stringency. The two fluorochromes appeared to behave differently in these soils. They sorbed preferentially to different types of soil particulates, FITC was pH-sensitive, and TRITC was salt-sensitive.

4.4 Method Validation: Fluorescence *in situ* Hybridization of Cells in PAH-Contaminated Soils Spiked with Pyrene and Subsequent Examination of Spatial Relationships Therein

In order to provide "proof of principle" for the Aggregate FISH method, three PAH-contaminated soils were spiked with pyrene, stimulated by nutrient addition, and allowed to incubate statically for 7 weeks. At 2 and 7 weeks, samples were removed for plate counts and Slurry and Aggregate FISH. The resulting FISH images were analyzed for cell counts, the presence or absence of pyrene crystals, and cell distribution with respect to pyrene.

4.4.1 Spiking procedure The three PAH-contaminated soils were spiked as follows (Reid et al., 1998; Brinch et al., 2002). One-fourth of the soil mass to be used was air-dried in a fume hood for 24 hours. One-fourth of the air-dried soil was spiked with pyrene in 2 ml acetone to achieve a total concentration of 1000 mg kg^{-1} soil. The soil was mixed by hand with a glass rod for 10-15 minutes. The remaining air-dried soil was mixed by quarters into the spiked aliquot. The soil was covered loosely with aluminum foil, and the solvent was allowed to evaporate overnight. The next day, the remaining 3/4 of the total soil mass to be used was mixed in with the spiked aliquot by quarters, stirring

with a glass rod for 15-20 minutes after each addition. Spiking in this fashion reduced microbial exposure to the solvent carrier and ensured a great degree of mixing.

A separate nutrient solution was prepared for each soil that matched the pH of that soil and the nitrogen and phosphorus required to achieve a ratio of oxygen demand:N:P of 100:5:1 (M. Aitken, personal communication; Potter et al., 1999). Nitrogen was added as ammonium chloride, while phosphorus was added as 10 mM phosphate buffer (2:1 dibasic:monobasic). The OD had been previously calculated for each soil based on measurements of total organic carbon (see Table 4.1). The nutrient buffers were added to achieve 70% of the water holding capacity for each soil.

Soils were incubated without shaking at ambient temperature (25°C) in the dark until sampled.

4.4.2 Sample preparation and fixation First, soil was embedded in acrylamide as described above (section 4.3.2.1.) The embedded plug was transferred to a 50 ml polypropylene conical centrifuge tube and covered with 15 ml of 4% (w/v) paraformaldehyde in phosphate-buffered saline. Next, one-gram samples were removed and placed into two 15 ml polypropylene conical tubes. Fixative was added to one tube to achieve 10 ml of slurry. These samples were fixed overnight on a rotator at 4°C in the dark. Sodium pyrophosphate solution (0.1% w/v) was added to the second 15 ml tube to achieve 10 ml of slurry and to help detach cells from soil particles. The slurry was vortexed vigorously for one minute, allowed to sit for 30-45 minutes, and vortexed again. Serial dilutions were made in PBS and plated onto R2A agar. Colony forming units were counted after 2 weeks incubation at ambient temperature (25°C).

4.4.3 Sample pretreatment A 1:10 dilution in PBS was made of the fixed slurry, and 0.5-1.0 ml was drawn through the filter apparatus. This volume varied depending on the sample, due to clogging of the filter membrane. Samples were rinsed with PBS to remove any fixative prior to continuing. Samples were then incubated with a lysozyme solution (32,900 units in Tris 100 mM, EDTA 50 mM, pH 8; Wagner et al., 1998) at room temperature and rinsed.

4.4.4 Hybridization The incubated soils were hybridized at 45^oC with 5 ng μl^{-1} of Univ1390 and 2.5 ng μl^{-1} of Eub338 in hybridization buffer (HB).

4.4.5 Washing Excess probe was removed by washing twice in 5X SET at 45^oC.

4.4.6 Microscopy and image acquisition Membrane filters were removed from the filter manifold and placed onto slides with a No. 1.5 coverslip. Slow-Fade antifade reagent (Invitrogen/Molecular Probes, Eugene, OR) was added to minimize bleaching of samples. Embedded samples were sliced into ~2 mm sections, or transects. Each transect was placed into a cell culture dish with a 1.5 coverslip inserted into a 13 mm hole in its base (Mattek Corporation, Ashland, MA). Samples were examined as outlined in section 4.2.5. Multiple images were taken from fields chosen by "stairstep" movement of the microscope stage while under bright field. A minimum of ten images was obtained for each sample. However, not all images were processed. Images were occasionally omitted from analysis due to poor alignment of the fields under different filters, or because the files were corrupted and not retrievable.

4.4.7 Image processing FISH images of soil were processed in Adobe Photoshop 7.0 using Fovea Pro software. An image series consisted of triplicate images, each taken with a different filter (FITC, TRITC, and PYR). Slurry images and some aggregate

images comprised quadruplicate images with the addition of Bright Field as the fourth in the series.

Images were screened initially by splitting into color channels: red-R, green-G, and blue-B. Splitting channels resulted in images that were resolved more easily by the naked eye such that they could be used as references to the colored images. In theory, bacteria should have been visible in the red color channel of the TRITC-filtered image and in the green color channel of the FITC-filtered image, whereas pyrene crystals should have been visible in the blue color channel of the PYR-filtered image. However, in soil, these attributes were not as well defined as they were in pure culture. Since there was subjectivity involved in all image processing, a computer algorithm was not used. In general, feature overlap between the TRITC- and PYR-filtered images was due to sorption of the fluorochrome to soil particles. This was verified, when possible, by comparing both to the bright field image. Overlap in the TRITC- and FITC-filtered images was indicative of cells, and feature overlap in the FITC- and PYR-filtered images was due to pyrene. Occasionally, overlap was noted with all three filters. These features were often soil particles, eliminated by comparison to bright field images, but were occasionally attributed to pyrene crystals or cells. Soil particles tended to have a muted, diffuse fluorescence, whereas cells and pyrene were uniformly intense. Morphology was also considered in these cases to distinguish cells from soil and/or pyrene.

For measuring spatial relationships, cells and pyrene were "extracted" manually as features from their respective images. Background was subtracted, and the two images were added together to produce a "reduced" image.
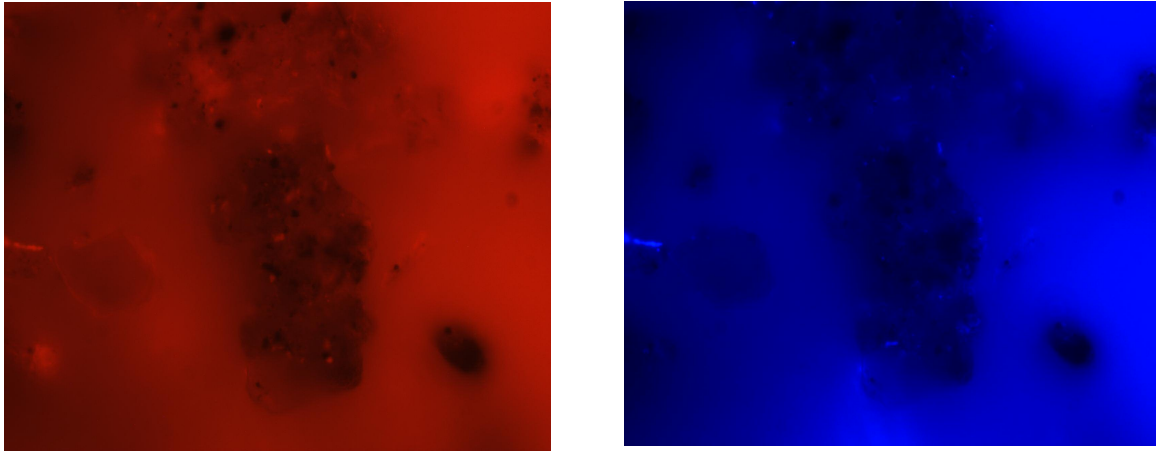
(a)

(b)
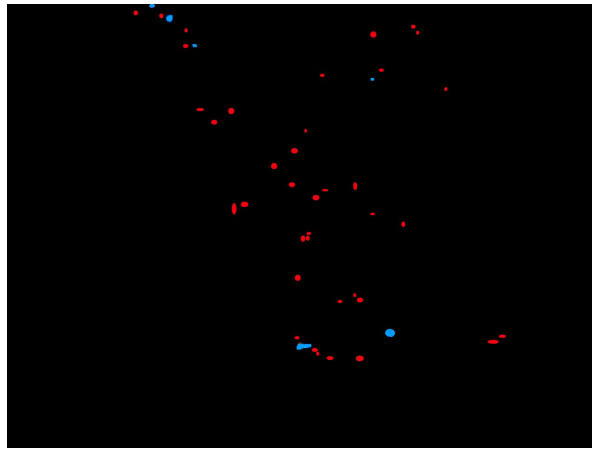
(c)

Figure 4.5 Example of Image Reduction: Extraction of objects from KKY Slurry FISH images taken with (a) TRITC filter to show cells and (b) PYR filter showing pyrene and added together to produce (c) the reduced image.

Reduced images (such as Figure 4.5c) were imported into the Digital Image Analysis in

Microbial Ecology program (*daime*; Daims et al., 2006), where they were automatically

segmented using the Rapid Automated Threshold Selection (RATS-L) biomass detection

algorithm followed by an associative map object detection algorithm. This segmentation

step permits the distinction of individual cells, i.e. biomass, from background and from each other by defining upper and lower thresholds for pixel intensity.

4.4.8 Image analysis During method validation, images were analyzed for the following: cell numbers, pyrene prevalence, overall object distribution, and the distribution of cells with respect to pyrene.

4.4.8.1 Cell enumeration Cells were counted manually for all images. Overall counts per gram of soil were calculated as discussed in section 4.3.2.3.

4.4.8.2 Pyrene prevalence Pyrene prevalence was measured as the percentage of images that contained presumptive pyrene crystals. Additionally, the image area occupied by pyrene was measured with FoveaPro and divided by the total image area. This relative measurement was viewed as a two-dimensional proxy for pyrene concentration.

4.4.8.3 Overall object distribution Overall object distribution was measured in two ways: a) by calculating an index of dispersion and b) by comparing computer-generated nearest neighbor distances. An Index of Dispersion, ID, was calculated for each image as follows: $ID = \sqrt{(2\chi^2)} - \sqrt{(2n-1)}$, where n is the number of fields in which bacteria were counted, $\chi^2 = \Sigma\ (x-X)^2/X$, where x is the number of bacteria counted in each field and X is the mean number of bacteria per field (Nunan et al., 2001). An index greater than 2 is an indication of aggregation as opposed to uniform distribution, and the greater the index, the greater the degree of non-uniformity (Harris, 1994; Nunan et al., 2001). An evenly distributed sample will generate an ID of less than zero.

FoveaPro was used to generate nearest neighbor measurements, or the distance between any given feature (cells and/or pyrene) and its nearest neighbor. These values

are reported as a mean, $0.5/\sqrt{(N/Area)}$, where N is the number of features counted within the image, and can be graphed as a frequency distribution over distance. FoveaPro also generates the mean value that would be expected if the distribution within that image were random. The ratio of the observed mean to the expected mean (O/E ratio) can be used to show a tendency of the objects to either cluster (O/E < 1) or avoid each other (O/E > 1). The mean value of a random distribution is less than that of a repellant population and greater than that of a clustering population (Russ, 2002).

4.4.8.4 Distribution of cells with respect to pyrene The distribution of cells with respect to pyrene was measured using the *daime* program. This program was designed for use with environmental samples to analyze the spatial relationships between members of the same microbial population or those of two different microbial populations. The objective of this research was slightly different--to see if a microbial community was randomly distributed with respect to pyrene. Because the *daime* program is based on the architectural analysis of any given features regardless of their animacy, it was deemed appropriate for these samples (Reed and Howard, 1999). The stereological analysis algorithm generates a set of linear dipoles radiating from the center of each population member and covering a range of designated lengths. A "hit" is a dipole that crosses two features of interest—in this study, both a cell and a pyrene crystal (see Figure 4.6).

(a)   (b)
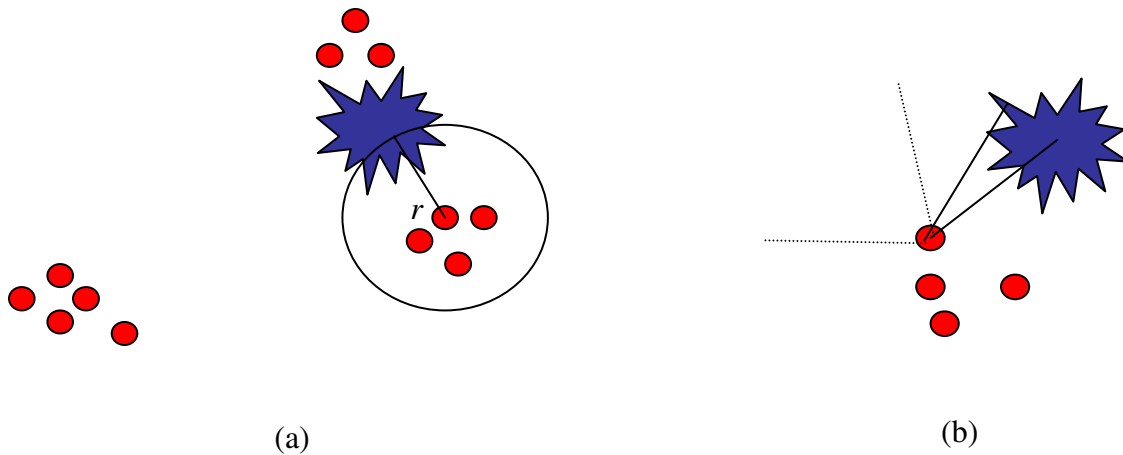
Figures 4.6a and b Illustration of *daime* Stereological Analysis. (a) A radius, *r*, from the center of a bacterial cell (red), is defined over a range. Pyrene crystals (blue) within this radius will be "hit" by a dipole of that length. (b) Hits are shown with a solid line, misses with dashed lines (from Daims et al., 2006).

The designated range and potential increments for dipole radii are automatically

established by the *daime* program and are based on the image size, magnification, and

pixel resolution. For the images in this study, the distances ranged from 0.11-69.79 μm

(image dimensions were 120 x 90 μm). Due to the required computing capacity, dipole

lengths were selected at increments of approximately 0.30-0.40 μm within this range.

A pair cross-correlation function, g(*r*), is generated for each distance and is based on

the probability that a dipole of length *r* hits both a bacterial cell and pyrene crystal. The

function is normalized for both cell density and pyrene concentration, given its

dependence on both. The correlation value is calculated as follows: $g(r) = P(r)/2BY$,

where $P(r) = H_r/T_r$, H_r being the number of hits, and T_r being the sum of both hits and

misses. B is defined as A_o/A_T, or the ratio of bacterial cell-occupied area (A_o) to total

image area (A_T), and is analogous to biomass concentration. Y is defined by the same

ratio, where A_o is the area occupied by a pyrene crystal, and is analogous to pyrene

concentration. Values less than 1 indicate repulsion, values greater than 1 indicate clustering, and values approximately equal to 1 indicate a random distribution.

daime also generated nearest neighbor measurements for cells with respect to pyrene, from which a histogram was plotted. A Poisson-like histogram is observed when objects are randomly distributed, and a narrowed histogram reflects clustering. A leftward shift in a distribution can also indicate clustering, whereas a shift to the right suggests avoidance (Russ, 2002).

4.4.9 Results and discussion of method validation test

4.4.9.1 Cell enumeration: plate counts, Slurry FISH and Aggregate FISH counts

A comparison of the plate counts and direct microscopic FISH counts for each soil at each time point are given in Table 4.2 below and depicted in Figures 4.7a-c.

Table 4.2. Cell Counts for Each Soil Over Time, as Determined by R2A Plate Counts and Slurry and Aggregate FISH Counts, using both Univ1390-FITC and Eub338-TRITC (average ± standard deviation).

Sample	Time (wk)	CFU/g wet soil	Slurry FISH (10^7)		Aggregate FISH (10^9)	
			Univ1390	Eub338	Univ1390	Eub338
CMN	2	$1.07 \pm 0.16 \times 10^8$	10.50 ± 7.00	9.07 ± 6.92	6.53 ± 2.47	6.75 ± 2.82
CMN	7	$1.31 \pm 0.37 \times 10^5$	3.56 ± 3.42	4.48 ± 4.88	6.95 ± 2.35	7.63 ± 2.81
CNC	2	$2.55 \pm 0.17 \times 10^7$	37.90 ± 18.10	30.50 ± 11.50	1.77 ± 1.39	3.48 ± 2.15
CNC	7	$1.21 \pm 0.10 \times 10^8$	4.05 ± 1.57	4.99 ± 1.87	2.91 ± 1.43	3.27 ± 1.36
KKY	2	$5.60 \pm 0.21 \times 10^8$	6.67 ± 5.30	11.20 ± 8.00	14.50 ± 5.60	10.60 ± 3.70
KKY	7	$2.86 \pm 0.09 \times 10^7$	8.26 ± 6.12	9.51 ± 7.47	16.10 ± 5.20	14.90 ± 5.10
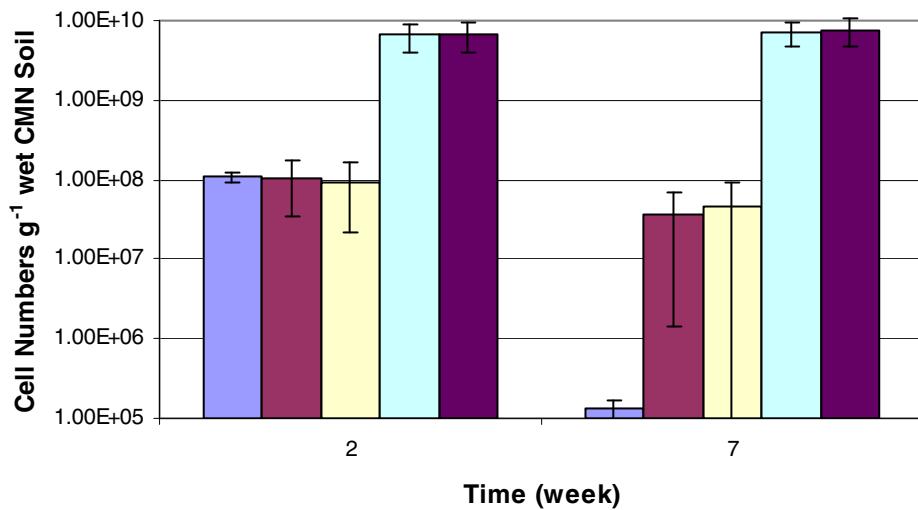
Figure 4.7a Comparison of Cell Counts in the CMN Soil Obtained by Plating, Slurry FISH, and Aggregate FISH. Separate Results are provided for each Probe. Blue: CFU; magenta: Slurry FISH Univ1390; beige: Slurry FISH Eub338; aqua: Aggregate FISH Univ1390; purple: Aggregate FISH Eub338.
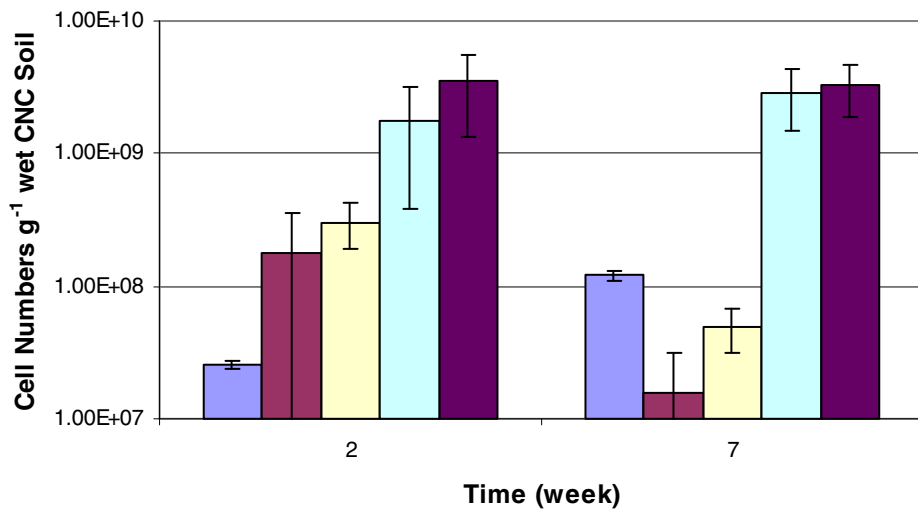
Figure 4.7b Comparison of Cell Counts in the CNC Soil Obtained by Plating, Slurry FISH, and Aggregate FISH. Separate Results are provided for each Probe. Blue: CFU; magenta: Slurry FISH Univ1390; beige: Slurry FISH Eub338; aqua: Aggregate FISH Univ1390; purple: Aggregate FISH Eub338.
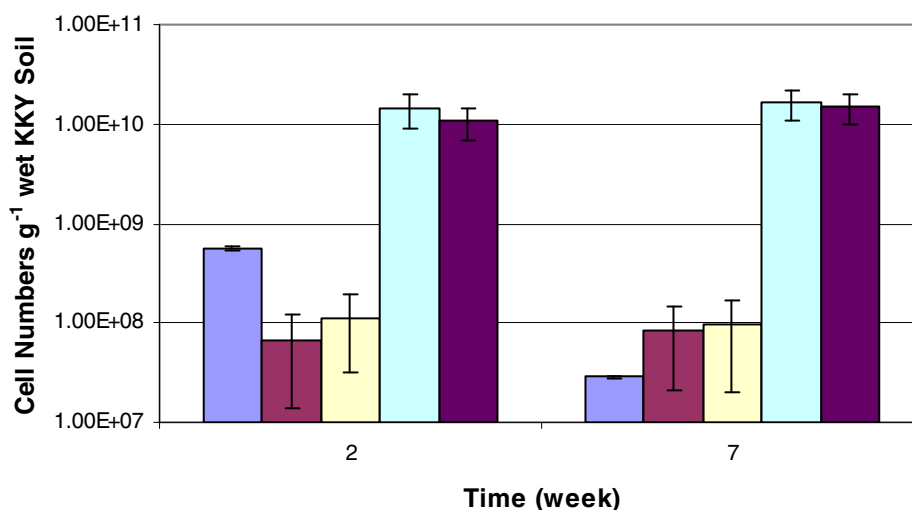
Figure 4.7c Comparison of Cell Counts in the KKY Soil Obtained by Plating, Slurry FISH, and Aggregate FISH. Separate Results are provided for each Probe. Blue: CFU; magenta: Slurry FISH Univ1390; beige: Slurry FISH Eub338; aqua: Aggregate FISH Univ1390; purple: Aggregate FISH Eub338.

CFU versus FISH Counts Plate counts ranged from one order of magnitude higher to two orders lower than Slurry FISH counts and two to four orders of magnitude lower than Aggregate FISH counts. Lower plate counts were not surprising, since many studies have shown direct count results to be orders of magnitude higher than plate counts, especially for environmental samples, where many of the organisms present are considered "viable but non-culturable." However, higher plate counts than Slurry FISH counts (see CNC week 7 and KKY week 2) were not anticipated. It is unlikely that hybridization efficiency is the cause of this, since the aggregate counts were all significantly higher than CFU counts. It is possible that hybridized cells were masked by soil particles in the Slurry FISH samples or that samples were poorly mixed prior to filtration, so that their numbers were underestimated. It is also possible that cells not adhering to soil particles were lost during sample dilution.

114

The difference between CFU counts and Slurry FISH counts were significant for the CNC soil at both time points (P < 0.01 at week 2, P < 0.001 at week 7) and for the KKY soil at week 2 (P < 0.001). The differences between CFU counts and Aggregate FISH counts were significant for the CMN soil at both time points (P < 0.01 for Eub338 counts and CFU at week 2, P < 0.001 for all other comparisons), and for the KKY soil at both time points (P < 0.01 for Univ1390 versus CFU at week 2, P < 0.001 for all other comparisons). Colony-forming unit counts for the CNC soil were not significantly different from Univ1390 FISH counts at week 2, but counts were different at all other time points (P < 0.02 for Univ1390 counts versus CFU at week 7, P < 0.02 for Eub338 counts versus CFU at week 2, and P < 0.01 at week 7).

Universal versus Bacterial Probe Counts FISH counts did not differ significantly between the universal and bacterial probes for either slurry or aggregate samples, except for CNC week 2 Aggregate FISH (P < 0.05). It was anticipated that Univ1390-FITC counts would be higher than the Eub338-TRITC, given that the latter is a subset of the former. However, this was not the case. In one sample where protozoa were observed, they did not fluoresce with the TRITC-tagged Eub338 probe and were not counted.

A recent review reported that the hybridization efficiency for Eub338 ranged from 1% to 75% in soil and sediment, and that recently identified bacterial phyla in soil, the *Verrumicrobiae* and the *Planctomycetaceae*, do not hybridize with Eub338 at all (Bouvier and del Giorgio, 2003). As a result, the literature currently recommends a suite of eubacterial probes (Eub338 I-III; Amann et al., 2001), although this is not routinely done. Previous profiling of the CMN did not show any members of these soil microbial classes present (see Chapter 3). It is unknown whether or not they were present in the

CNC or KKY soils. Although hybridization efficiency could not be measured for these samples due to the overlap between DAPI and pyrene fluorescence, the agreement between the universal and eubacterial probe counts suggests that, at the least, both probes hybridized equally well.

There are three possible reasons for the significant difference between universal and bacterial counts in CNC week 2 Aggregate FISH samples. First, the TRITC-based probe was found to adsorb strongly to some soil particles, and it is possible that particulate matter was incorrectly counted as a cell. Whereas bright field images were used as a "blank" from which soil particulate-sorbed probe was subtracted for slurry images, aggregate samples rarely had corresponding bright field images for comparison. Therefore, TRITC sorption to soil particles cannot be ruled out for these samples. Second, pure culture tests showed that the luminance values measured for the FITC-based probe tended to be less than those of the TRITC-based probe (see section 4.3.3). These intensity differences were also visually noted for some, but not all, cells in some soil images. It is possible that lower intensities were difficult to detect, e.g. masked by soil background fluorescence when soil was present in the samples, and that cells were undercounted. However, neither of these reasons can explain why the CMN and KKY soils did not show these differences between probes. Therefore, the most likely reason for the difference is the composition of the CNC soil itself.

Slurry versus Aggregate FISH Counts The FISH counts also varied between the slurry-based and aggregate methods for both probes. It was expected that Slurry FISH counts would be less than Aggregate FISH counts, since any cells not adherent to a soil particle could be washed out. The differences between slurry counts and aggregate

116

counts were significant for Univ1390-FITC at both time points (P < 0.001 for CMN and KKY; P < 0.01 for CNC at week 2 and < 0.001 at week 7). Slurry and Aggregate FISH counts for Eub338-TRITC were significantly different for all soils at each time point (P < 0.001).

It was not expected that the Slurry and Aggregate FISH counts would vary by up to two orders of magnitude. It is likely that the formula used to generate Aggregate FISH counts (see section 4.3.2.4) overestimated the actual number of cells. Core height (mm) was measured manually and was large compared to the calculated slice height (µm), such that an inexact measurement of the former would have affected the results greatly.

In summary, the cell enumeration data suggest that the current conventional methods for FISH, which rely on the formation of slurry, grossly underestimate true cell counts and could skew determinations of population proportions. Furthermore, if functional probes are used, they may also underestimate target gene prevalence.

4.4.9.2 Pyrene prevalence Presumptive pyrene crystals were counted in each field examined by Slurry or Aggregate FISH at each time point. The results for pyrene prevalence are given in Table 4.3 below.

Table 4.3 Pyrene Prevalence.

Soil	Time	Percentage of Images Containing Presumptive Pyrene Crystals		Percentage of Total Image Area Occupied by Pyrene	
		Slurry	Aggregate	Slurry	Aggregate
CMN	2	30	100	0.02 ± 0.04	0.49 ± 0.25
CMN	7	83	100	0.11 ± 0.11	0.36 ± 0.21
CNC	2	60	100	0.06 ± 0.07	0.38 ± 0.17
CNC	7	100	100	0.10 ± 0.09	0.34 ± 0.30
KKY	2	20	100	0.01 ± 0.03	0.41 ± 0.24
KKY	7	89	100	0.15 ± 0.16	0.41 ± 0.30

At week 2, pyrene was present in 30% of CMN, 60% of CNC, and 20% of KKY Slurry FISH images. These percentages decreased with increasing soil PAH concentration—that is, the more the original level of background PAH contamination, the less presumptive pyrene was observed (see Table 4.3). This was also the case with image area occupied by pyrene. One possible reason for this finding is that the spiked pyrene fluorescence may have been quenched by the high levels of other PAH present in the soil. Alternatively, the high level of PAH contamination may have reduced the number of binding sites for the spiked pyrene, such that it was unable to adsorb well and was diluted out during the FISH procedure.

At week 7, 83% of the CMN, 100% of the CNC, and 89% of KKY Slurry FISH images contained pyrene. This increase in pyrene prevalence with time suggests that, as pyrene is being degraded, it desorbs from the soil organic matter such that it is more easily visualized microscopically. Alternatively, early reversible sorption led to easier "washout" of pyrene during slurry formation at week 2 than at week 7. In contrast to week 2, the image area occupied by pyrene at week 7 is greatest when the background level of contamination is greatest. Again, this could be due to a greater amount of pyrene desorbed in the presence of populations that are more efficient degraders.

One hundred percent of the Aggregate FISH images contained pyrene at both time points. For week 2, this could suggest that, compared to Slurry FISH, no measurable amount of pyrene was lost during the Aggregate FISH procedure. However, this can only be supported indirectly by the larger surface area covered by pyrene in the Aggregate versus Slurry FISH images. This difference was statistically significant for all soils (P < 0.001). There was no significant change in pyrene prevalence over time in the Aggregate

FISH images, as measured by either percentage of images containing pyrene or pyrene-occupied area per image.

It was expected that the Slurry FISH images would show less pyrene than the Aggregate FISH images as a result of sample dilution. However, Slurry FISH seemed advantageous in that it was able to show whether or not pyrene was associated with soil particles. Association was defined, for the purposes of this study, as a distance less than one micron from a particle, as measured in the x,y-plane. At week 2, 80%, 56%, and 33% of visible pyrene was soil-associated in the CMN, CNC, and KKY soils, respectively. At week 7, 100% of pyrene was soil-associated in the CMN and KKY images, whereas 89% of the CNC images contained soil-associated pyrene. It was not possible to distinguish between sorbed and free pyrene in the Aggregate FISH images, since the entire image background was soil. Had confocal imaging been feasible, it is possible that this association could have been made.

4.4.9.3 Object distribution Aggregated, non-uniform cell distribution is expected in soils, where successful colonization is a result of favorable conditions and is, therefore, not random (Harris, 1994; Nunan et al., 2003). The objective of this study was to show that the aggregate method would represent a more accurate picture of the microscale environment than the slurry method, i.e. that it would be less random.

4.4.9.3.1 Dispersion indices The indices of dispersion are shown in Table 4.4.

Table 4.4 Dispersion Indices Based on Cell Counts for Each Image

| Soil | Time (week) | Index of Dispersion (ID) | | | |
| | | Slurry | | Aggregate | |
		Univ1390	Eub338	Univ1390	Eub338
CMN	2	10.44	10.72	14.30	16.91
CMN	7	16.36	22.26	13.39	17.24
CNC	2	12.28	6.98	15.15	17.19
CNC	7	8.73	10.08	10.03	9.29
KKY	2	5.12	6.58	21.64	16.04
KKY	7	10.68	12.89	19.85	21.37

The higher the index, the more non-uniform is the distribution of cells in the image. While the indices suggest nonrandom distribution regardless of the method (i.e. ID>2), those calculated for Aggregate FISH samples are higher than those of Slurry FISH samples in all cases except CMN and CNC week 7, suggesting a greater degree of non-uniformity. This should be the case if the original spatial arrangement of cells and pyrene was preserved. It is interesting to note that dispersion indices increase over time for the CMN and KKY soils and decrease over time for the CNC soil. This could potentially point to the level of adaptation of the microbial populations within each soil and their subsequent growth. The CNC is the least contaminated of the soils and might be expected to have less well-adapted microbial communities than the other two soils.

4.4.9.3.2 Nearest neighbor analysis: cell to cell and/or pyrene Mean nearest neighbor values and their standard deviations were calculated for each image and were compared to the expected mean values had the distribution been random. Table 4.5 provides a comparison of the observed to expected values (O/E ratios) for each sample set.

Table 4.5 Observed/Expected Ratios of Mean Nearest Neighbor Values

Soil	Time	Average Ratio of Observed to Expected Mean Nearest Neighbor Values (± sd)	
		Slurry	Aggregate
CMN	2	0.58 ± 0.40	0.82 ± 0.08
CMN	7	0.52 ± 0.17	0.89 ± 0.07
CNC	2	0.86 ± 0.14	0.91 ± 0.17
CNC	7	0.71 ± 0.17	0.88 ±0.07
KKY	2	0.66 ± 0.42	0.71 ± 0.14
KKY	7	0.46 ± 0.13	0.85 ± 0.10

The O/E ratios ranged from 0.12-1.03 for Slurry FISH and 0.52-1.09 for Aggregate FISH, but the majority of ratios were less than one (indicating object clustering). Only 3% of Slurry FISH values and 7% of Aggregate FISH values were greater than one (indicating object avoidance) and were only found in the CNC soil images (9% of Slurry and 20% of Aggregate FISH).

Almost all mean nearest neighbor values were less than those generated for random distributions (O/E <1), suggesting that all images depicted aggregation. However, only 41% of Slurry FISH (P < 0.05) and only 6.7% of Aggregate FISH (P < 0.02) images showed an observed value significantly lower than the expected, suggesting that Aggregate FISH images were more random in distribution than the Slurry FISH images. The relatively lower coefficients of variance (not shown) for Aggregate FISH images reflect the lower variance seen when there is uniformity in the spacing of objects, as opposed to the wider range found in Slurry FISH images.

Originally, it was hypothesized that O/E ratios for Aggregate FISH would be greater than those for Slurry FISH. However, this was not the case. This could be due to the close association of cells and pyrene with soil particles in the Slurry FISH images (see 4.4.9.2). If both are soil-associated and cells thrive, then clustering would be observed.

It could also be due to the possibility that pyrene was randomly distributed in the soils; this would only be evident in the undisturbed, Aggregate FISH images.

There was no significant difference in O/E ratios over time for each soil within each method. However, there was a significant difference between ratios generated by Slurry versus Aggregate FISH at week 7 for CMN and KKY soils ($P < 0.001$). Again, the higher O/E ratios for Aggregate FISH suggest a more uniform distribution.

4.4.9.4 *daime*: Spatial arrangement analysis of cells and pyrene

4.4.9.4.1 Pair cross-correlation values The pair cross-correlation values are plotted versus the lengths of dipole radii (distance) in Figures 4.8 through 4.10. Within each figure, (a) provides results at week 2 and (b) at week 7.
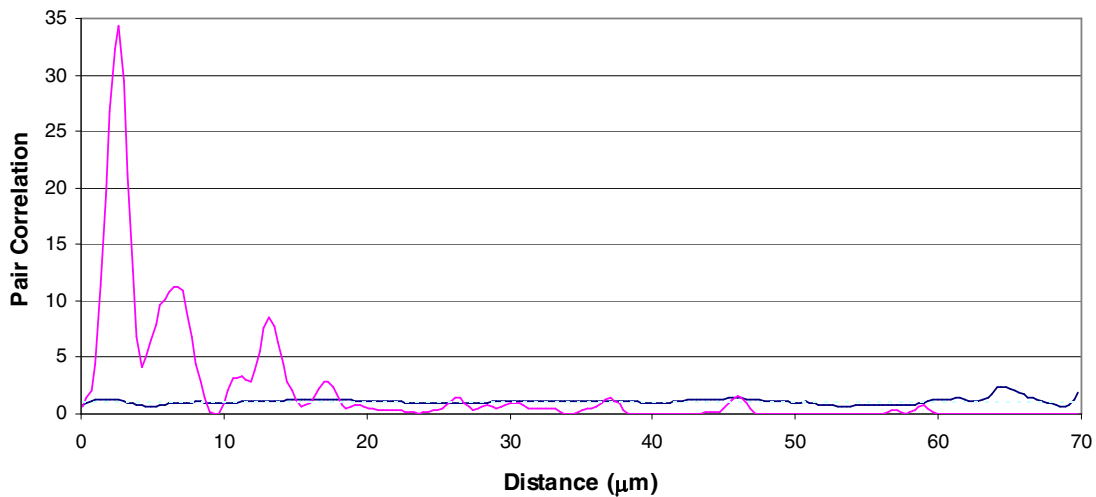
Figure 4.8a Cross-Correlation Values Calculated over Distance: A Comparison of Slurry FISH versus Aggregate FISH for CMN at Week 2. Blue: Aggregate FISH g(*r*) values; pink: Slurry FISH g(*r*) values; aqua dotted line: random distribution.
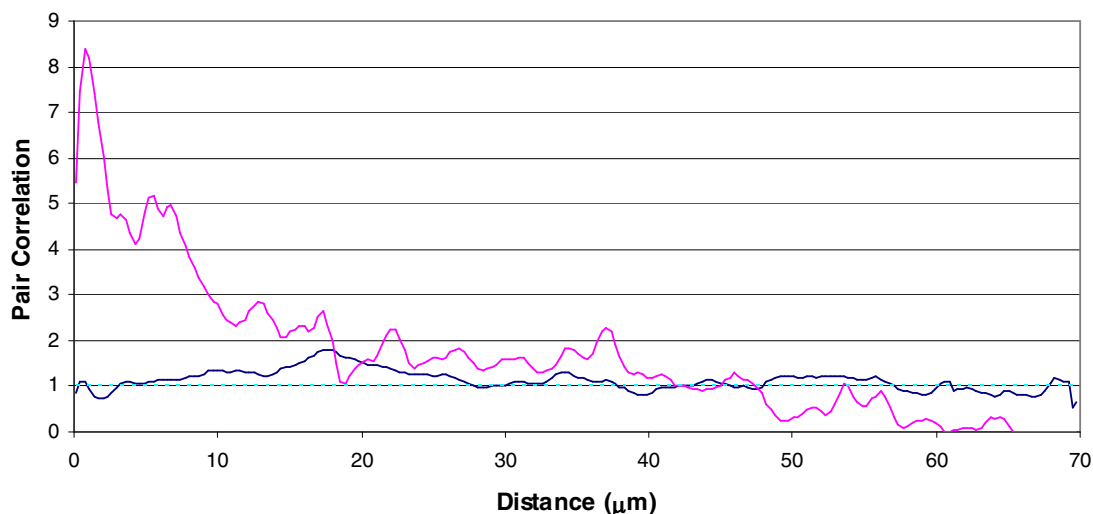
Figure 4.8b Cross-Correlation Values Calculated over Distance: A Comparison of Slurry FISH versus Aggregate FISH for CMN at Week 7. Blue: Aggregate FISH g(*r*) values; pink: Slurry FISH g(*r*) values; aqua dotted line: random distribution.

A summary of the g(*r*) values generated by each method at each time point for the CMN soil are given in Table 4.6 below.

Table 4.6 Average Pair Correlation Values (± standard deviation) and the Percentage of Values Exceeding 1 for the CMN Soil at a Given Distance from Pyrene. Comparison of Each FISH Method at Each Time Point.

Distance From Pyrene	SLURRY				AGGREGATE			
	Week 2		Week 7		Week 2		Week 7	
	g(*r*) value	g(*r*) > 1	g(*r*) value	g(*r*) > 1	g(*r*) value	g(*r*) > 1	g(*r*) value	g(*r*) > 1
< 5 μm	13.67 ± 11.81	94 %	5.71 ± 1.46	100 %	1.03 ± 0.24	56 %	0.94 ± 0.14	50 %
5-10 μm	6.11 ± 4.54	75 %	4.10 ± 0.87	100 %	0.92 ± 0.10	25 %	1.19 ± 0.09	100 %
0-70 μm	2.03 ± 5.02	27 %	1.70 ± 1.61	70 %	1.10 ± 0.27	65 %	1.25 ± 0.22	70 %

The CMN Slurry FISH images at week 2 show significant clustering at distances less than 10 microns and weak clustering from 10-20 microns. This may reflect an initial increased growth of pyrene-degraders. At greater distances, g(*r*) values become random or even suggest avoidance. At week 7, the g(*r*) values for Slurry FISH depict weaker clustering tendencies that decrease gradually with distance. Although the g(*r*) values

123

decline between weeks 2 and 7, clustering continues over greater distances at week 7. This may indicate continued but slow growth of pyrene- or metabolite-utilizing organisms. In contrast, the pair correlation values for CMN Aggregate FISH images at both time points are very low and suggest a random distribution of cells with respect to pyrene.

Pair cross-correlation data for the CNC soil are provided below.
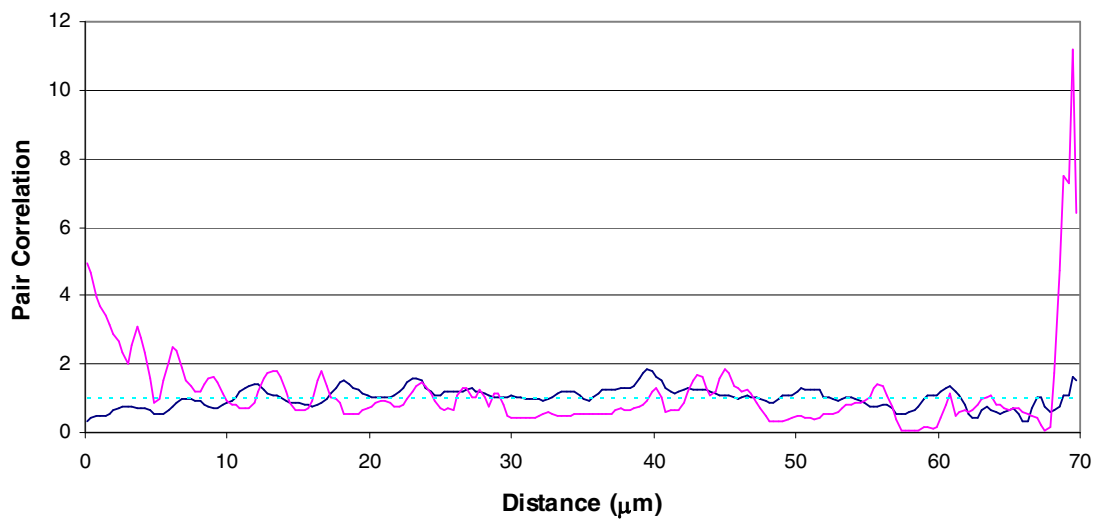
Figure 4.9a Cross-Correlation Values Calculated over Distance: A Comparison of Slurry FISH versus Aggregate FISH for CNC at Week 2. Blue: Aggregate FISH g(r) values; pink: Slurry FISH g(r) values; aqua dotted line: random distribution.
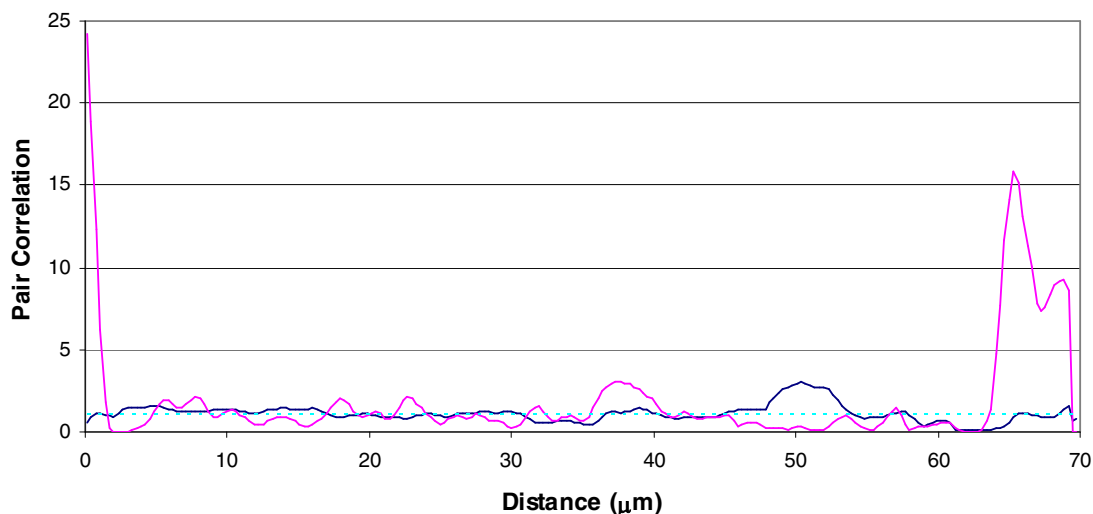
Figure 4.9b Cross-Correlation Values Calculated over Distance: A Comparison of Slurry FISH versus Aggregate FISH for CNC at Week 7. Blue: Aggregate FISH g(r) values; pink: Slurry FISH g(r) values; aqua dotted line: random distribution.

Table 4.7 Average Pair Correlation Values (± standard deviation) and the Percentage of Values Exceeding 1 for the CNC Soil at a Given Distance from Pyrene. Comparison of Each FISH Method at Each Time Point.

Distance From Pyrene	SLURRY				AGGREGATE			
	Week 2		Week 7		Week 2		Week 7	
	g(r) value	g(r) > 1	g(r) value	g(r) > 1	g(r) value	g(r) > 1	g(r) value	g(r) > 1
< 5 μm	2.94 ± 1.06	6 %	4.17 ± 7.58	38 %	0.61 ± 0.14	0 %	1.22 ± 0.30	75
5-10 μm	1.55 ± 0.46	13 %	1.58 ± 0.38	88 %	0.80 ± 0.15	0 %	1.32 ± 0.10	100
0-70 μm	1.16 ± 1.25	61 %	1.90 ± 3.36	59 %	1.01 ± 0.29	56 %	1.13 ± 0.53	40

Pair correlation values for CNC Slurry FISH images at week 2 exhibit weak clustering of cells with respect to pyrene up to ~8 microns and a random distribution of cells thereafter. A spike in g(r) values occurs between 68-70 microns. At week 7, the clustering signal is strong at a distance less than 1.5 microns from pyrene. The increase in clustering with time suggests that the CNC microbial population required time to adapt to the presence of pyrene. At greater distances, the clustering tendency is weaker, but a large peak in g(r) values occurs between 64-70 microns. The occurrence of the strong

clustering signal at the greatest distance from pyrene at both timepoints could mean that some community members do not benefit from a close association with the contaminant and do not adapt to its presence over time but may be able to use downstream metabolites as they diffuse through the soil matrix.

In contrast, Aggregate FISH images at week 2 show weak avoidance, as indicated by the g(r) values less than one. At distances greater than 10 microns, the distribution tends toward randomness. Although the average pair correlation values increase in the Aggregate FISH images at week 7, the tendency is still random, with weak clustering at greater distance. Again, this suggests a lag period of adaptation for the indigenous community.

Pair correlation data for the KKY soil are given below.
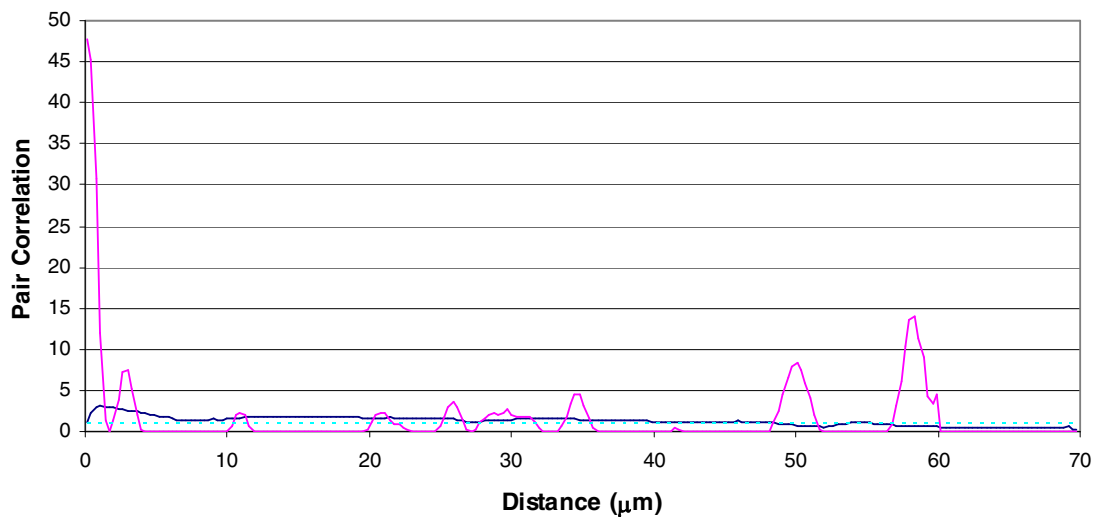
Figure 4.10a Cross-Correlation Values Calculated over Distance: A Comparison of Slurry FISH versus Aggregate FISH for KKY at Week 2. Blue: Aggregate FISH g(r) values; pink: Slurry FISH g(r) values; aqua dotted line: random distribution.
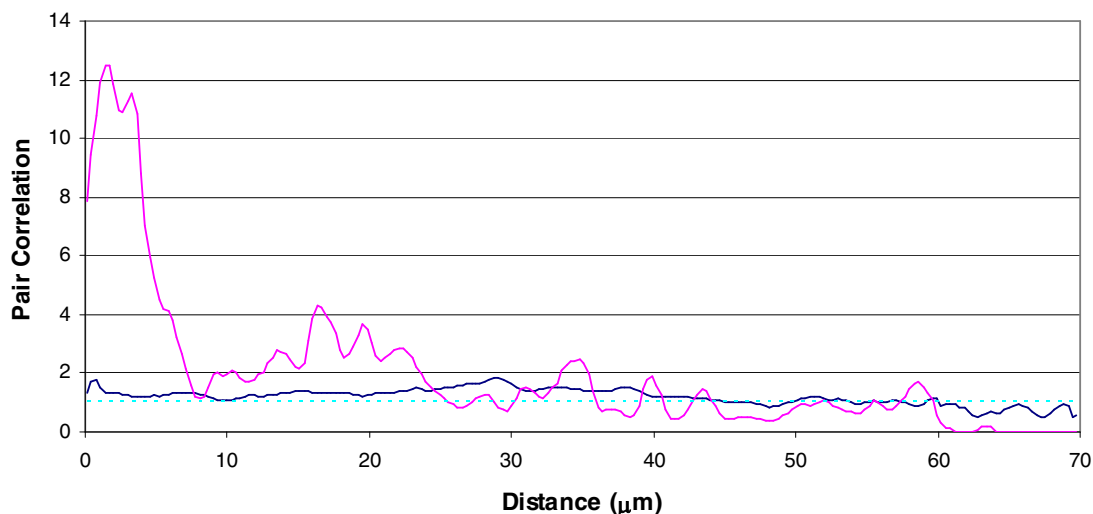
Figure 4.10b Cross-Correlation Values Calculated over Distance: A Comparison of Slurry FISH versus Aggregate FISH for KKY at Week 7. Blue: Aggregate FISH g(*r*) values; pink: Slurry FISH g(*r*) values; aqua dotted line: random distribution.

Table 4.8 Average Pair Correlation Values (± standard deviation) and the Percentage of Values Exceeding 1 for the KKY Soil at a Given Distance from Pyrene. Comparison of Each FISH Method at Each Time Point.

Distance From Pyrene	SLURRY				AGGREGATE			
	Week 2		Week 7		Week 2		Week 7	
	g(*r*) value	g(*r*) > 1	g(*r*) value	g(*r*) > 1	g(*r*) value	g(*r*) > 1	g(*r*) value	g(*r*) > 1
< 5 µm	10.28 ± 16.11	69 %	9.96 ± 2.32	100 %	2.49 ± 0.50	100 %	1.34 ± 0.18	100 %
5-10 µm	0.00 ± 0.00	0 %	2.45 ± 1.15	100 %	1.51 ± 0.17	100 %	1.24 ± 0.11	100 %
0-70 µm	1.71 ± 5.34	29 %	1.97 ± 2.54	57 %	1.30 ± 0.60	72 %	1.20 ± 0.28	78 %

Pair correlation graphs for KKY Slurry FISH images at week 2 are very spiky due to the large number of g(*r*) values equaling zero. A value of zero indicates that there were no "hits", i.e., no dipoles that crossed both a pyrene crystal and a cell, at those distances. The clustering signal is strong below 1.3 microns, and various clusters occur at distances greater than 10 microns. At week 7, strong clustering occurs to a distance of ~8 microns with weaker but consistent clustering up to ~45 microns. The values at week 7 are less than at week 2 but more sporadic, suggesting an initial increase in a degrader population

followed by their slow and steady decline. Pair correlation values for KKY Aggregate

FISH at week 2 exhibit weak clustering with a peak value at ~1.4 microns and a steady

decline thereafter. At week 7, the values point toward a random to extremely weak

clustering distribution. The clustering signal is greater at week 2 than at week 7. Slurry

FISH pair correlation values are much higher than those of Aggregate FISH.

A comparison of the pair correlation values of the three soils yielded interesting

results. Slurry FISH in CMN and KKY soils shows a decrease in the attraction over time,

while CNC shows the reverse. This may be due to the lag in obtaining a responsive

population in the CNC soil. The clustering signal for Slurry FISH tends to be strong but

erratic with very large confidence intervals (not shown). Regardless of the FISH method,

the highest $g(r)$ values at week 2 were obtained from the KKY soil images, followed by

CMN and CNC. This parallels their degree of PAH contamination and may reflect the

presence of adapted microbial communities.

4.4.9.4.2 Frequency distributions of nearest neighbor values The percentage of cells

at any given distance from a pyrene crystal, or the frequency distribution based on nearest

neighbor values, is given below in Figures 4.11-4.13. Within each figure, (a) depicts

results at week 2, and (b) represents week 7. In a random distribution, the locations of

any two cells are independent of each other, and the probability of finding a cell at any

given location is very small. Therefore, the histogram of a random distribution, e.g.

bacteria on a membrane filter or colonies on a Petri plate, assumes a Poisson distribution

(Rosner, 1986; Kepner and Pratt, 1994; Russ, 2002). If cells are proliferating within the

vicinity of a pyrene crystal, the probability of any two cells occupying proximal space is

increased and no longer random. This "clustering" phenomenon can be depicted by a narrow histogram that is shifted to the left.
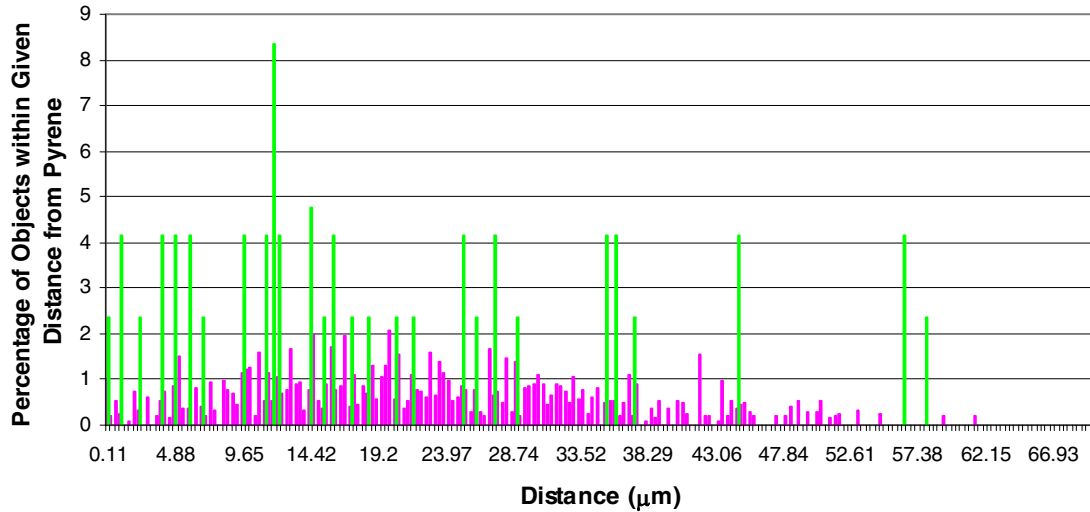
Figure 4.11a Nearest Neighbor Distribution versus Distance: A Comparison of Slurry FISH versus Aggregate FISH for the CMN Soil at Week 2. Pink: Aggregate FISH; green: Slurry FISH.
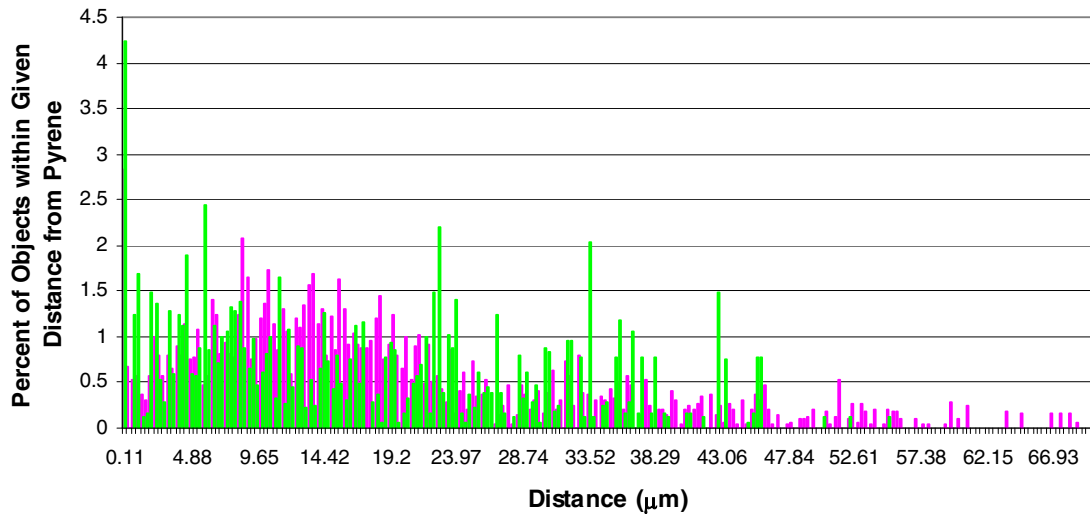
Figure 4.11b Nearest Neighbor Distribution versus Distance: A Comparison of Slurry FISH versus Aggregate FISH for the CMN Soil at week 7. Pink: Aggregate FISH; green: Slurry FISH.

At week 2, the CMN Slurry distribution is very spiky and without a discernible pattern. At week 7, the distribution is more structured with possible underlying distributions at 0-20, 20-28, and 28-39 microns. The Aggregate FISH percentages tend to be evenly distributed at both time points, but the histogram narrows and shifts slightly to the left at week 7, suggesting clustering with respect to pyrene and the presence of pyrene utilizers, even though the pair correlation graphs reflect a random distribution.

The histograms are affected by the percentage of objects involved in a positive "hit"--a dipole that touches both a pyrene crystal and a cell. A truly representative histogram should obtain a hit percentage of 95% or above (*daime* version 1.1, H. Daims, 2005). Hits depend on the dipole lengths that are used. This study used lengths that increased by ~0.30-0.40 microns. Unfortunately, an attempt to use all suggested dipole lengths (increments of 0.03-0.04 microns) was no more successful in generating a larger hit percentage, and it required a vast amount of computing time (~9-10 hours/image). This is likely a limitation of the *daime* software rather than the images themselves.

The Slurry FISH histograms were generated from "hit" values of 63 and 74%, for weeks 2 and 7, respectively. In contrast, the Aggregate FISH histograms resulted from "hits" of 92 and 88% for weeks 2 and 7, respectively. This may explain some of the spikiness in the Slurry FISH histograms. Alternatively, unevenness could be attributed to the occurrence of cell clusters at various distances from pyrene: a peak in the percentages at close distances could mean that cells are utilizing pyrene, whereas peaks at greater distances could indicate cell clustering independent of pyrene. This is also reflected in the "wavy" nature of the pair correlation graphs. The fact that clustering occurs away from pyrene suggests that cells may be utilizing some other carbon source or

a pyrene metabolite. However, given the destruction of the original spatial arrangement, this cannot be determined. In Slurry FISH images, this type of distribution might also be seen in cases where both cells and pyrene are adherent to soil particles, but the location of the particles on the filter membrane is random.

Mean nearest neighbor data for the CNC soil are depicted in Figures 4.11a and b below.
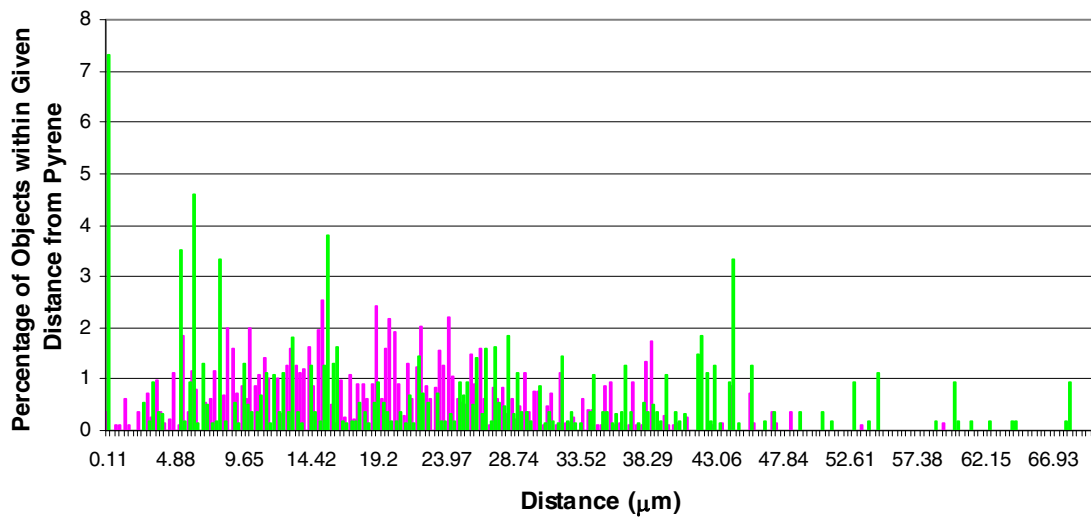
Figure 4.12a Nearest Neighbor Distribution versus Distance: A Comparison of Slurry FISH versus Aggregate FISH for the CNC Soil at week 2. Pink: Aggregate FISH; green: Slurry FISH.
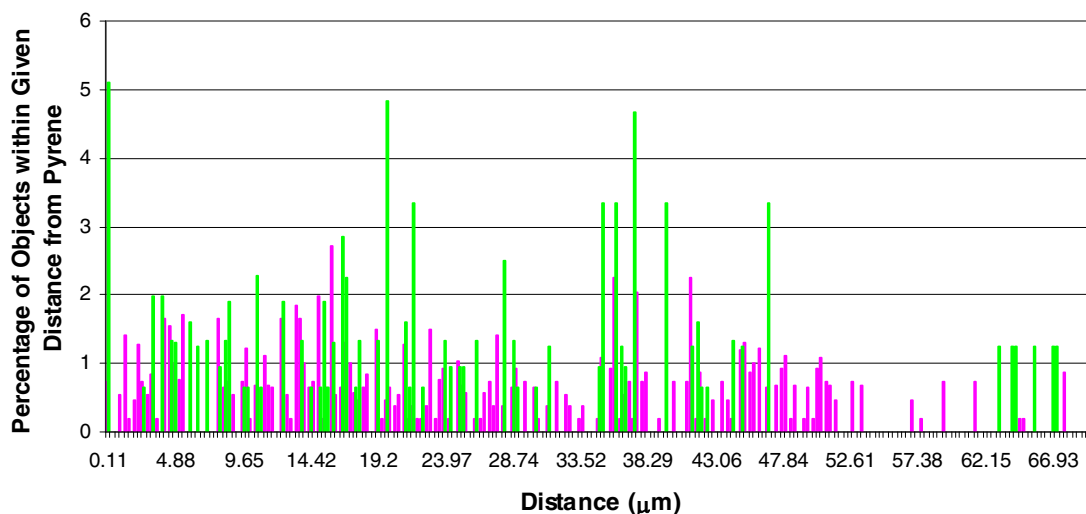
Figure 4.12b Nearest Neighbor Distribution versus Distance: A Comparison of Slurry FISH versus Aggregate FISH for the CNC Soil at week 7. Pink: Aggregate FISH; green: Slurry FISH.

The histogram generated from Slurry FISH images at week 2 is irregular and spiky but resulted from only a 46% hit rate. A large percentage of cells (7.31%) are located within 0.11 microns of pyrene, suggesting utilization. The distribution at week 7 is similarly irregular and also has a significant percentage (5.1%) of cells occupying the closest distance from pyrene. This distribution was generated from an 85% hit rate. The unevenness of these two distributions coupled with the increase in pair correlation values and their "waviness" over time is consistent with the close association of cells and pyrene to soil particles.

    The Aggregate FISH distribution at week 2 appears random with a peak in percentage values at ~15 microns and a possible secondary distribution between 32-48 microns. At week 7, Aggregate FISH images resulted in an irregular distribution. The hit rate for Aggregate FISH at week 2 was 91%, whereas the hit rate for week 7 was only 77%.

Given the low pair correlation values, it is likely that the low hit rate, rather than actual nonrandomness, accounts for the irregularity in the distribution at the later time point.

Mean nearest neighbor data for the KKY soil are depicted in Figures 4.13a and b below.
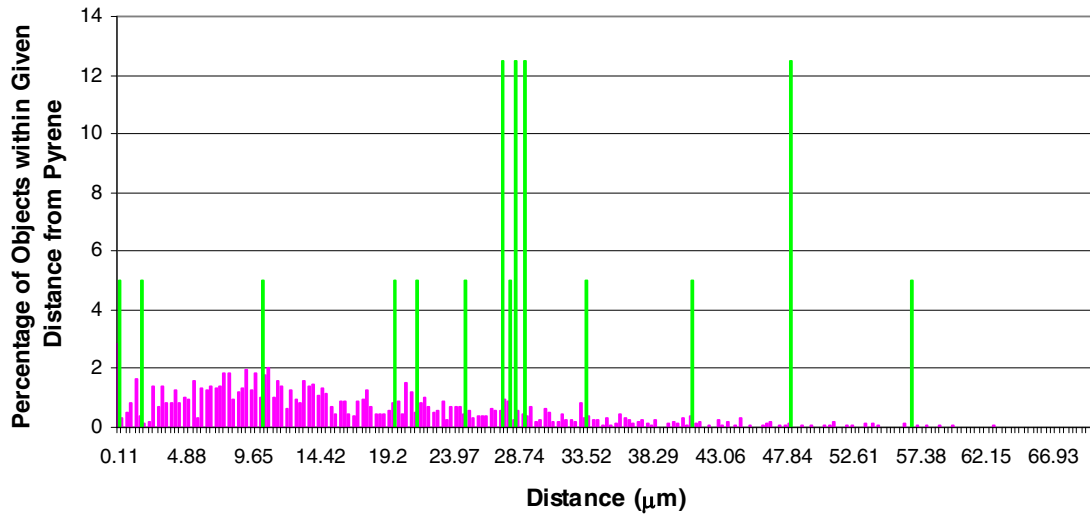
Figure 4.13a Nearest Neighbor Distribution versus Distance: A Comparison of Slurry FISH versus Aggregate FISH for the KKY Soil at week 2. Pink: Aggregate FISH; green: Slurry FISH.
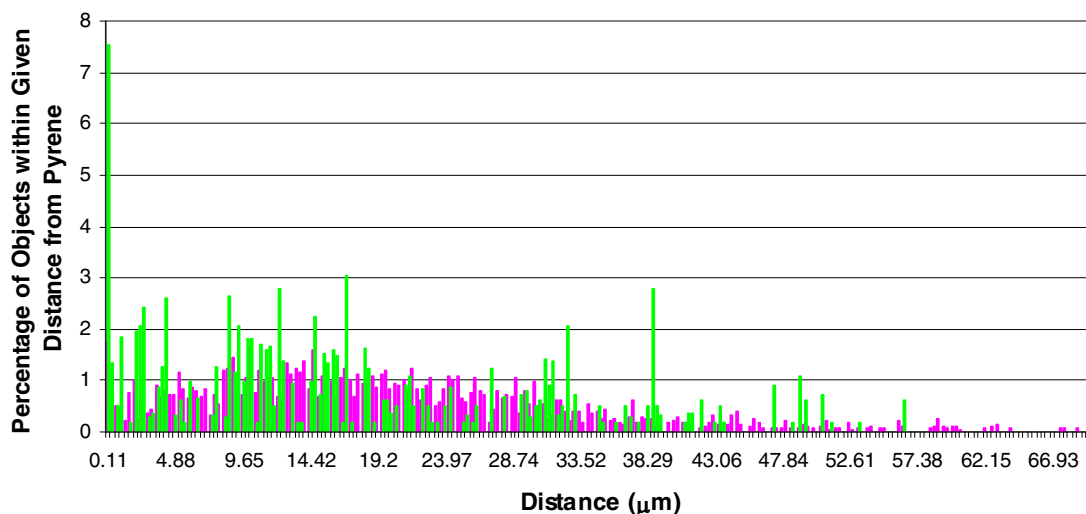
Figure 4.13b Nearest Neighbor Distribution versus Distance: A Comparison of Slurry FISH versus Aggregate FISH for the KKY Soil at week 7. Pink: Aggregate FISH; green: Slurry FISH.

At week 2, Slurry FISH images generated a very irregular and spiky histogram. Again, this could be due, in part, to the low hit percentage (51%). At week 7, the percentage of hits increased to 91; however, the Slurry FISH histogram is still irregular. There is a large (7.5%) percentage of cells located within 0.11 microns from pyrene. Again, this irregular distribution, coupled with very high pair correlation values at close distances from pyrene, suggests that clustering is due to the association of cells and/or pyrene with soil particles.

In contrast, the histograms generated from Aggregate FISH images are Poisson-like, suggesting a random distribution of cells with respect to pyrene. However, there is a slight shift in the histogram peaks from ~9 microns at week 2 to ~14 microns at week 7 which could indicate a closer association of cells with pyrene at the earlier time point. This could point to the presence of an adapted population that responds early to pyrene

presence. The stronger clustering signal from the pair correlation values at week 2 supports this finding.

4.4.9.5 Summary of spatial arrangement analyses Results from the *daime* spatial arrangement analyses conducted on images were unexpected. It was thought that Slurry FISH images would exhibit a more random distribution than Aggregate FISH images, as measured by the pair cross-correlation values and nearest neighbor values. This was not the case. In all instances, the Slurry FISH images had $g(r)$ values greater than 1, indicating clustering, whereas the Aggregate FISH images had $g(r)$ values approaching 1, indicating a random distribution. The most likely reason for this finding is the association of cells and pyrene with soil particles in the Slurry FISH images.

The $g(r)$ values were in contrast to the calculated indices of dispersion which were, on the whole, greater for Aggregate FISH. There are many possible explanations for this finding. First, the analysis did not take into account the association between pyrene, cells, and soil particles. In Aggregate FISH images, this association could not be comfortably made without confocal microscopy. It was not possible to distinguish between cells and/or pyrene floating in a plane above the soil. In Slurry FISH images, there was a distinct association of pyrene and soil particles (see section 4.4.9.2 above). This phenomenon would explain the large $g(r)$ values calculated at the shortest distances in the slurried samples and may also explain the large confidence intervals obtained for these samples. Whether this association was due to the increased contact between pyrene, cells, and soil particles during the fixation step of Slurry FISH or to the possibility that cells and pyrene were originally adherent to soil in the static incubation is unknown. Secondly, it is possible that the distribution of pyrene itself in the incubating

microcosms was random. In this case, cells responding to pyrene presence would also assume a random distribution. This phenomenon would not be observed in the Slurry FISH images, since the original spatial relationships in those samples would have been destroyed. Thirdly, the *daime* program has been utilized on images at a lesser degree of magnification than those of this study. It is possible that, over longer distances, the pair cross-correlation values of Aggregate FISH samples would show a greater tendency toward non-randomness. Initially, images were taken at a lower level of magnification in addition to 1000X. However, at this level, it was not possible to distinguish between cells, pyrene, or soil particles, such that these images could not be used for analysis. Fourthly, it is also possible that the greater areas occupied by cells and pyrene in the Aggregate FISH images led to lower cross-correlation values, even though this value is supposedly normalized for density (see equation in section 4.4.8). Not only do these ratios decrease the $g(r)$ value, but the numbers affect the totals of hits versus misses, which can also lower the cross-correlation value. Finally, Reed and Howard (1999) considered $g(r)$ values of ~1.8 to be highly positively correlated. Therefore, values such as those found in Aggregate FISH samples could very well indicate clustering, but not as significantly as with Slurry FISH.

4.5 Method Limitations The chief limitation to the Aggregate FISH method is its cost. Aggregate FISH requires a greater amount of probe than does Slurry FISH. Additionally, success of the embedding reagent is dependent upon soil type and moisture content. The higher the sand and the lower the clay contents of the soil, the easier the acrylamide can penetrate into a core. This was true for the CMN soil compared with the KKY soil and

especially with the CNC soil. Unfortunately, a textural analysis was not available for the latter. The presence of moisture also causes the acrylamide embedding to be less effective. The samples for this study contained 70% of each soil's water holding capacity. The higher a soil's clay content, the higher that holding capacity will be, thus exacerbating the problem of penetration. However, the embedding was shown to be effective on a separate clay soil (21%) that was dry. It appears that clay's expandability in the presence of moisture precludes acrylamide penetration and makes the embedded core less stable. Most FISH protocols have dehydration steps involving ethanol. However, these were not feasible for the contaminated soils, as ethanol tended to extract PAHs from the samples. Ideally, cores could be re-embedded in resin, then sectioned and examined with confocal laser scanning microscopy.

Because the CNC was not characterized, it is also difficult to say whether the differences in probe hybridization were due to the soil's physico-chemistry. However, core integrity was a problem when processing this soil, and it is likely that this is a key cause of differences between this soil and the others.

An additional cause of bias was the lack of random image generation. In order to compensate for the lack of an automated stage, the stage was moved manually while visualizing the sample with the bright field filter. The direction was usually in a "stairstep" pattern (up/down and over), until the edge of the sample was reached; then the stage was shifted either left or right, and the stairstep repeated. It is possible that samples were overcounted as a result of this process, but this error should still have been consistent across all samples.

4.6 Conclusions

Although FISH is widely used throughout all fields of microbiology to describe and assign functions to community members, it is severely limited in its ability to lend an interpretation of spatial relationships within samples. This is especially true in soils and sediments, where the method itself, i.e. the creation of a slurry, presumably alters these relationships.

An aggregate-based method was developed that was shown to maintain, albeit to a varying degree, the three-dimensional structure of its soil samples. The results showed that Slurry FISH significantly underestimates direct cell counts as compared to Aggregate FISH. Indices of Dispersion showed that the objects in Aggregate FISH images were more non-uniform in distribution than those in the Slurry FISH images. This is in agreement with many other studies on the non-uniformity of microbial distribution in soil (Nunan et al., 2002; Dechesne et al., 2003; Becker et al., 2006). Nearest Neighbor Analyses of object distribution showed the contrary; however, it is thought that this was due to the close association of pyrene and cells to soil particles in the Slurry FISH images.

Results from the *daime* spatial arrangement analysis showed that the Slurry FISH method yielded more clustered distributions of cells with respect to pyrene crystals than the Aggregate FISH method. Again, this could be due to the close association of all objects with soil particles. Overall, the spatial analyses support the use of Slurry FISH as opposed to Aggregate FISH; whereas, cell enumeration data support the opposite.

It was thought that the use of cell proximity and clustering in the presence of a contaminant might be a surrogate measurement for contaminant utilization, in the same

way that "hot spots" are considered as areas of higher microbial activity. For example, Amellal et al. (2001) found that PAH-degrading bacteria were embedded in soil aggregates where PAHs were abundant. Alternatively, proximity could at least indicate a lack of acute toxicity (Becker et al., 2006). Although this study cannot definitively say that those cells found closest to pyrene crystals were involved in the degradation process, the results of the Slurry FISH spatial analyses show that the location of these cells with respect to the pyrene crystals was not random. It is unknown whether the clustering is due to the presence of pyrene or sorption of both cells and pyrene to soil particles.

In order for bacterial colonization to occur, there must be access to a given location, resources, and a lack of adverse conditions (Harris, 1994). The bacteria were already present in the soil, and chance caused them to be located near an utilizable resource, i.e. pyrene when it was mixed into the soil. The excess pyrene spike could be considered adverse but only for populations unaccustomed to high levels of PAH contamination, while those better adapted to PAH would proliferate. This is reflected in the *daime* findings. Regardless of the FISH method, the week 2 pair correlation values at the closest distances to pyrene correspond to the level of PAH contamination within each soil, i.e. the higher the original level of PAH contamination, the stronger the clustering signal. This points to the presence of ready degraders in both the CMN and KKY soils, whereas the increase in $g(r)$ values over time for the CNC suggests that time was required to induce a similar community.

Future studies could use group-specific and/or functional probes in conjunction with microautoradiography to show a correlation between carbon utilization and assimilation, and spatial organization. Alternatively, studies could be carried out with functional

probes. However, given that pathways for pyrene metabolism are still being discovered,

as are new genes involved in its degradation (Ní Chadhain et al., 2006), this is currently

difficult.

5.0 The Change in Microbial Community Structure over Time in a Previously Uncontaminated Soil Spiked with Pyrene

5.1 Introduction

Microbial community succession following contaminant exposure can manifest itself in different ways, but the descriptor most often followed is diversity. Structural diversity focuses on the number and relative abundance of all species present, i.e., their richness and evenness, respectively. Following an exposure, there is often an overall loss of diversity, whether in species number or proportion, followed by alterations in population dynamics within the community (Röling et al., 2002; Gentry et al., 2003; Ní Chadhain et al., 2006).

The release of contaminants may alter the physical and chemical nature of the surrounding environment. For example, the presence of a non-aqueous phase (NAP), such as creosote, causes a decrease in the diffusion of gases through the soil matrix. Similarly, other nutrients, including water, will tend to remain outside the NAP or will only minimally diffuse. Hydrophobic organic contaminants, such as PAHs, will partition into the NAP, limiting them as potential carbon sources for degradation. Overall, NAP presence may result in the spatial isolation of some communities.

Indigenous communities will respond to these environmental changes. The mere presence of contaminants may have a toxic effect on some species, leading to their disappearance or decline. The loss of one species in a commensal, mutualistic, or predator-prey relationship may lead to the loss of other species. Competition will

ensue in the isolated communities as a result of limited resources. In areas where the contaminant is present, organisms that are inherently capable of degrading the contaminant, or that can acquire that ability through gene transfer, will be at a selective advantage. In any event, community richness, evenness, and population interactions will change.

It is important to monitor microbial community changes after contaminant releases into the environment. Community resilience to such occurrences reflects ecosystem homeostasis and stability (Woodward, 1993; Coleman et al., 1994; Norgerg et al., 2001), and stability is a result of functional complexity. The ultimate goal in environmental microbiology is to be able to relate structure to function. Monitoring changes in structure along with contaminant presence or disappearance allows these relationships to be studied, and, when elucidated, they may help to predict responses to further perturbations, to determine if bioremediation is feasible, and to define endpoints for recovery.

Recovery is an operational definition and is dependent on the soil, the pollutant, and the available remediation technology. It can mean the return of a community to its original level of diversity, regardless of structure (Röling et al., 2002); the reappearance of a lost indicator species or the increase in abundance of diminished ones (Griffiths et al., 2001); or the appearance and subsequent disappearance of selected groups of organisms, such as known degraders, that are only associated with the contamination event (Stephen et al., 1999; Maruyama et al., 2003).

For soils, determining the original community structure can be difficult, as they can be very diverse environments (Gelsomino et al., 1999; McCaig et al., 2001). Small subunit ribosomal DNA clone libraries may not provide adequate coverage of the community to obtain a baseline measurement of diversity, especially given the cost (Borneman and Triplett,

142

1997; Hughes et al., 2001; Dunbar et al., 2002). While gel separation of SSU rRNA genes may provide adequate coverage, it may be lacking in resolution. Therefore, it is easier to look at key organisms or populations.

Determining which organisms can be used as indicator species is also very difficult. Our knowledge of soil microbial communities and their interactions is severely limited by culture bias. Furthermore, communities are inherently dynamic in structure and interaction, so that an organism that is chosen as the indicator species under some given condition may not be a good choice under others. Therefore, it seems most reasonable to look for transient changes that parallel the effects of a perturbation. This could be the appearance, or increase in abundance, of known or presumed contaminant degraders. Their disappearance or decrease in abundance could then be defined as recovery and, if it corresponds to decreased contaminant concentrations to permissible levels, an endpoint for remediation.

An additional recommendation for measuring community recovery is that the analysis should be made with culture-independent techniques. Laboratory artifact may contribute to the erroneous attribution of roles or significance to organisms that are not primarily responsible for them *in situ*. For example, Kong et al. (2005) used FISH coupled with microautoradiography (FISH-MAR) to discover that certain *Actinobacteria* played an active role in phosphorus removal from wastewater and, in some treatment plants, were more abundant than the *β-Proteobacteria* previously credited with that removal. While this example is not from soil, the effects of culture bias can easily be seen. Many studies on PAH degradation have focused on pure cultures enriched from contaminated environments. These isolates routinely are Gram-positive organisms, especially the well-studied *Mycobacteria* (Cerniglia, 1992; Miller et al., 2004). While these organisms may be able to utilize PAH as

sole carbon sources *in vitro* and after augmentation into soils (Hall et al., 2005; Miller et al., 2004), their presence does not preclude the involvement of other species, nor does their absence preclude degradation. For example, using stable isotope probing (SIP) and quantitative PCR (qPCR), others have recently identified members of the *Proteobacteria* as the primary assimilators of labeled carbon from PAH in contaminated soils (Singleton et al., 2005, 2006; Jones et al., 2007, submitted).

Another reason for monitoring transient populations is that, with the exception of acute spill events, contaminants are rarely released into the environment all at once. This is especially the case at sites of former manufactured gas plants or wood preserving facilities, where waste was continually generated and discharged. These releases are periodic in nature and occur over the length of time spanning the facility's existence. Repeated or continuous contaminant exposure may lead to different community changes than single exposures (Thompson et al., 1999; Powell, 2006). However, if the transient population is always selected from that particular environment, one could monitor its changes more easily.

Finally, compounds released into the environment and presumably adsorbed onto soil particles may eventually be re-released. Although this may seem unlikely in the case of PAHs, given the hydrophobic nature of the compounds, it could occur easily when the compounds are particle-associated. For example, simple physical disruption of soil aggregates, such as might occur with site construction, water erosion and rainfall, or freeze-thaw cycles, has been shown to cause the release of PAHs (Amellal et al., 2001; Totsche et al., 2006). Additionally, reduced conditions, such as might be caused by soil capping or excess precipitation, result in an increase in dissolved organic matter, carrying with it the sorbed PAHs (Pravecek et al., 2005; Kim and Pfaender, 2005). Occasional monitoring for

144

these transient populations may provide an indication of whether the target compound has become bioavailable again.

The goals of this objective were threefold: 1) to determine if the shifts in bacterial community structure of a previously uncontaminated soil spiked with pyrene could be correlated with pyrene localization, 2) to determine if the transient appearance of a group of pyrene degraders was feasible for use as a recovery endpoint, either after a single or duplicate spike, and 3) to determine if spatial relationships of organisms with respect to pyrene were suggestive of their roles in its degradation.

5.2 Materials and Methods

5.2.1 Soils The soils used in this study, both contaminated (CMN) and "pristine" (PMN), were obtained from the site of the former Reilly Tar and Chemical Corporation (St. Louis Park, MN). This Superfund site is highly contaminated with polycyclic aromatic hydrocarbons from its 50-year history as a creosote-producing and wood-preserving facility. PMN was removed in September, 2002 from the surface at the northwest corner of the same site. Groundwater flow is east southeast (S. Anderson, Utilities Superintendent, City of St. Louis Park, MN, personal communication) thus suggesting no flow of contaminants from the affected area to the "pristine" soil. Characteristics of the PMN soil are given in Table 5.1 below. The CMN soil is described in Chapter 4.

Table 5.1. Characteristics of the PMN Soil.

soil class	mineral
soil texture	sandy loam
% sand (50-2000 μm)	63
% silt (2-50 μm)	24
% clay (<2 μm)	13

% moisture	4.57 ± 0.61
% organic matter	1.5
% carbon by weight	1.77 ± 0.14
pH	8.1
CEC (meq $100cm^{-3}$)	13/22.3
BET surface area ($m^2 \, g^{-1}$)	7.75
density ($g \, cm^{-3}$)	1.28/1.31
total PAH ($mg \, kg^{-1}$)	20.37 ± 4.63
pyrene concentration	3.49 ± 0.28

Soil texture, pH, percent organic matter, cation exchange capacity, and sample density were determined by the University of Wisconsin-Madison Soil and Plant Analysis Laboratory, Madison, WI. The second measurements of CEC, pH, and density for the PMN soil were obtained from the North Carolina Department of Agriculture Agronomic Division, Raleigh, NC. Percent carbon by weight, percent moisture, and surface area were measured by Clear Science, Baton Rouge, LA. PAHs were analyzed by Eno River Laboratories, Durham, NC, using EPA method 8270. Total PAH refers to the following 16 EPA-listed priority compounds: acenaphthene, acenaphthylene, anthracene, benzo[a]anthracene, benzo[b]fluoranthene, benzo[k]fluoranthene, benzo[g,h,i]perylene, benzo[a]pyrene, chrysene, dibenzo[a,h]anthracene, fluoranthene, fluorene, indeno[1,2,3-cd]pyrene, naphthalene, phenanthrene, and pyrene.

Soils were stored in plastic garbage bags in the dark at 4°C until use. Prior to use, they were passed through a 2mm sieve.

5.2.2 Chemicals and reagents Crystalline pyrene was obtained from Sigma-Aldrich (St. Louis, MO) and was of the highest purity available. $[4,5,9,10]^{14}$C-Pyrene (61mCi mmol^{-1}) was also obtained from Sigma. All chemicals used for polymerase chain reactions (PCR) were obtained from Applied Biosystems (Foster City, CA), of molecular grade and certified to be nuclease-free. All chemicals used for *in situ* hybridizations, with the exception of acrylamide, were also of molecular grade and nuclease-free.

5.2.3 Oligonucleotide synthesis Primers for conventional PCR were synthesized by Invitrogen Life Technologies (Rockville, MD). Primers for quantitative PCR were designed and synthesized as discussed in Singleton et al. (2006). Probes were synthesized and gel purified by Oligos Etc., Inc. (Wilsonville, OR). Fluorescent tags were covalently attached at the 5' end—fluorescein isothiocyanate (FITC; ex. 495 nm, em. 519 nm) for Univ1390 and tetramethylcarboxyrhodamine (TAMRA or TRITC, ex. 547nm, em. 572 nm) for Eub338. All oligonucleotide sequences are given below in Table 5.2.

Table 5.2. Oligonucleotides for PCR Primers and FISH Probes.

Oligonucleotide		Target Group	Sequence (5'-3')	Reference
Conventional PCR				
27f	(outer)	Bacteria	AGAGTTTGATCCTGGCTCAG	Lane, 1991
1492r	(outer)	Universal	GGTTACCTTGTTACGACTT	Lane, 1991
63fGC	(inner)	Bacteria	CAGGCCTAACACATGCAAGTC	Marchesi et al., 1998
518r	(inner)	Universal	ATTACCGCGGCTGCTGG	Neefs et al., 1990
Quantitative PCR				
341f		Bacterial	CCTACGGGAGGCAGCAG	Muyzer et al., 1993
518r		Standard	ATTACCGCGGCTGCTGG	Neefs et al., 1990
Eub338f		PYR Group 1	ACTCCTACGGGAGGCAGC	Amann et al., 1990a*
PG1r			TAGCAGGCCGTATTAAGAC	Singleton et al., 2006
PG2f		PYR Group 2	GCACAGGGTAGCTTGCTATC	Singleton et al., 2006
PG2r			CGCAGGCTCATCTTTCC	Singleton et al., 2006
PG3f		PYR Group 3	TAACGCTTGGGAATCTGCCTRTT	Singleton et al., 2006
PG3r			CATCTRTTAGCGCCAGGCCTTGC	Singleton et al., 2006
FISH				
Univ1390		Universal	GACCGGGCGGTGTGTACAA	Amann et al., 1990a
Eub338		Bacterial	GCTGCCTCCCGTAGGAGT	Amann et al., 1990a

f = forward primer; r = reverse primer; GC = 40-base GC-rich clamp, Muyzer et al., 1993
(5'CGCCCGCCGCGCGCGGCGGGCGGGGCGGGGGCACGGGGGG3').
All number designations are based on the *E. coli* numbering system. *as cited in Singleton et al., 2006.

5.3 Experimental Methods

5.3.1 Microcosm set-up and incubation The PMN soil was spiked as follows (Reid et al.,

1998; Brinch et al., 2002). One-fourth of the total soil mass to be used was air-dried in a

fume hood for 24 hours. One-fourth of this air-dried soil was spiked with pyrene in 2 ml

acetone to achieve a total concentration of 1000 ppm. The soil was mixed by hand with a

glass rod for 10-15 minutes. The remaining air-dried soil was mixed by quarters into the

spiked aliquot. The soil was covered loosely with aluminum foil, and the solvent was

allowed to evaporate overnight. The next day, the remaining 3/4 of the total soil mass to be

used was mixed in with the spiked aliquot by quarters, stirring with a glass rod for 15-20

minutes after each addition. Five grams of the final spiked soil were dispensed into 30 ml

EPA vials, with triplicate samples and controls for each time point. Spiking in this fashion reduced microbial exposure to the solvent carrier and ensured a great degree of mixing.

The spiking process was repeated with the "hot" microcosms with the exception that the pyrene solution was mixed with a trace amount of ^{14}C-pyrene to achieve 20,000 disintegrations per minute (dpm) per vial. Two grams of soil were dispensed into 30 ml glass centrifuge tubes providing duplicate samples and a single control for each time point. Into these tubes were placed 3 ml glass culture tubes. These contained fluted Whatman No. 1 chromatography paper saturated with 2N KOH.

The addition of nitrogen and phosphorus, as ammonium chloride and 10 mM phosphate buffer (2:1, monobasic:dibasic) respectively, was carried out to obtain a ratio of Oxygen Demand:Nitrogen:Phosphorus of 100:5:1 (M. Aitken, personal communication; Potter et al., 1999). The OD had been previously calculated based on measurements of total organic carbon (see Table 5.1). The pH was adjusted to match that originally measured in the PMN. The nutrient buffer was added to achieve 70% of the water holding capacity of the soil. The buffer used in control microcosms also contained 0.1% (w/v) of sodium azide to inhibit microbial activity.

5.3.1.1 Respiking After three months incubation, a subset of microcosms was re-spiked with the equivalent of 500 ppm of pyrene, added as 25% of the soil mass already contained within the microcosm. This experiment was conducted to see if repeated exposure to a contaminant resulted in further or irreversible changes in community structure.

Microcosms were monitored as outlined below. Vials were incubated statically at 24-25°C in the dark for 5 months.

5.3.2 "Hot" microcosm sampling: ^{14}C-pyrene measurements Every two weeks, samples were taken for the measurement of evolved $^{14}CO_2$ by removing the 2N KOH-saturated filter and placing it into 10 ml of scintillation cocktail (Scintisafe Plus 50%; Fisher Scientific, Atlanta, GA). Samples were counted on a Hewlett Packard TriCarb 1900TR Scintillation Counter (Meriden, CT) that automatically adjusts counts per minute to dpm based on a set of standards run concomitantly with the samples.

After the culture tube was removed, two ml of autoclaved, deionized water was added to the sample. The vials were shaken at 180 rpm on an orbital shaker for 24 hours. At the end of this time, samples were centrifuged at 2054 x g for 5 minutes. One ml of supernatant was withdrawn by glass pipette and transferred to a scintillation vial containing 7 ml of scintillation cocktail. The pipette was then rinsed twice with scintillation cocktail, and the rinsate was collected in the scintillation vial. The remaining supernatant in the microcosm vial was decanted, and the soil was allowed to air dry in the fume hood for 2 weeks. Aqueous samples were measured on the scintillation counter, and disintegrations per minute were corrected for the total volume of moisture contained within each vial (i.e. initial nutrient solution plus water for aqueous extraction).

Once the soil was dry, aliquots of ~0.4-0.7 g were removed and combusted with a Harvey Biological Oxidizer (RJ Harvey Instrument Corp.; Hillsdale, NJ). Carbon dioxide was collected in 15 ml of OX 161 scintillation cocktail (RJ Harvey); the collection reservoir was rinsed twice with methanol, and the rinsate was decanted into the scintillation vial. Combustion efficiency was measured during each session with calibration standards (100 μl of ^{14}C-glucose of known dpm added to 100 mg mannitol) placed at the beginning, middle, and end of the sample set. Samples were counted on the HP Scintillation Counter.

Disintegrations per minute were corrected for combustion efficiency and total soil mass in each vial.

5.3.3 "Cold" microcosm sampling: DNA extraction, PCR-DGGE, quantitative PCR, plate counts, and FISH At the end of each month, triplicate parallel cold sample vials were sacrificed.

5.3.3.1 DNA extraction DNA was extracted from 0.3-0.6 g aliquots of soil from each vial using the Ultra Clean Soil DNA Kit (MoBio Laboratories; Solana Beach, CA) and following the manufacturer's directions. Homogenization was performed with a bead-beater (Biospec Products Mini Beadbeater; Bartlesville, OK) set at 2500 beats per minute for 5 minutes. DNA concentration was determined densitometrically by agarose gel electrophoresis alongside a HindIII digest of λ-phage DNA. Densitometric measurements on the gel were made in Adobe Photoshop 7.0 using FoveaPro Software (Reindeer Graphics, Asheville, NC). DNA was stored in Tris buffer at -20°C until analyses could be performed.

5.3.3.2 Polymerase chain reaction-denaturing gradient gel electrophoresis (PCR-DGGE) A segment of the 16S rRNA gene was amplified from the genomic extract using PCR with the following primer sets and conditions: 1X PCR buffer (10 mM Tris-HCl, 50 mM KCl, pH 8.3), 2 mM $MgCl_2$, 250 μM of each dNTP, 500 nM of each primer (see Table 5.2), and 2.5 U of *Taq* DNA polymerase with an annealing temperature of 55°C. CMN extracts were PCR-amplified using a nested protocol with primer set 27f and 1492r as the outer set. Once amplified, PCR products were separated electrophoretically using BioRad's DCode System (Hercules, CA) on a 6% polyacrylamide gel (acrylamide:bisacrylamide ratio of 37.5:1) containing a urea-formamide denaturant gradient (full-strength denaturant contains 7M urea and 40% formamide) ranging from 30-55%. Reproducibility of DGGE profiles

between triplicate microcosms was verified initially; after verification, extracts from only one microcosm (A) at each time point were profiled to generate a single image.

5.3.3.3 Quantitative polymerase chain reaction (qPCR) The dominant band was excised from the denaturing gradient gel and allowed to elute overnight in TE buffer (10 mM Tris; 1 mM EDTA) at 4°C. One microliter of eluate was used as the template in Quantitect^{TM} SYBR$^®$ PCR Master Mix (Qiagen; Valencia, CA), and conventional PCR was performed with the Pyrene Group primer sets given in Table 5.2. Quantitative PCR was performed on Cepheid's SmartCycler System (Sunnyvale, CA) with the PG3 primer set at 600 nM, and an annealing temperature of 60°C. C_T values for both Bacteria and Pyrene Group 3 were generated. The C_T value corresponds to the cycle number at which a pre-determined threshold for the fluorescence of dye-bound DNA is reached. Gene copy numbers were calculated from a previously generated standard curve (Singleton et al., 2006). This curve was established by plotting the C_T value versus gene copy number of a dilution series of linearized plasmid DNA containing an insert of either bacterial or the Pyrene Group-specific 16S rRNA gene. Amplification efficiencies were measured as the slopes of the best-fit lines and found to match each other, thus validating the use of this curve.

5.3.3.4 Plate counts One-gram aliquots of soil were removed from the triplicate vials and added to 0.1% sodium pyrophosphate solution (w/v) to achieve a 10 ml slurry. The slurry was vortexed vigorously, serial dilutions were made in phosphate-buffered saline, and the dilutions were plated onto R2A agar. Colony-forming units were counted after 2 weeks incubation at 25°C.

5.3.3.5 Fluorescence *in situ* hybridization (FISH) At two months incubation, additional cold samples were also sacrificed for FISH. A sterile brass corer (inner diameter ~11mm)

was inserted into the center of each replicate vial and secured manually. The soil was embedded by the slow introduction of acrylamide, ammonium persulfate (APS), and N,N,N',N'-tetramethylethylenediamine (TEMED) from the bottom of the core, using a Pasteur pipette. The acrylamide was allowed to polymerize for 30 minutes. After its removal, additional acrylamide was used to "cap" the ends of the embedded "plug". The plug was transferred to a 50 ml polypropylene, centrifuge tube and covered with 15 ml of 4% paraformaldehyde in phosphate-buffered saline (130 mM NaCl, 7 mM Na_2HPO_4, 3 mM NaH_2PO_4, pH 7.2). One gram of soil from each replicate vial was transferred into each of three 15 ml polypropylene tubes. Fixative was added to achieve 10 ml of slurry. These samples were fixed overnight on a rotator at 4^oC in the dark.

A 1:10 dilution in PBS was made of the fixed slurry, and 0.5-1.0 ml was drawn through the filter apparatus. Both slurried and embedded soils were rinsed with PBS to remove any fixative prior to continuing. Samples were then incubated with a lysozyme solution (32,900 units in Tris 100 mM, EDTA 50 mM, pH 8.0) at room temperature and rinsed. Probes were hybridized at 45^oC at a concentration of 5 ng μl^{-1} for Univ1390 and 2.5 ng μl^{-1} for Eub338. Attempts to remove excess probe were made by washing twice in 5X SET (0.75 M NaCl; 5 mM EDTA; 100 mM Tris) at 45^oC.

5.3.3.6 Microscopy and image acquisition Membrane filters from Slurry FISH were removed from the filter manifold and placed onto slides with a No. 1.5 coverslip. Slow-Fade antifade reagent (Invitrogen/Molecular Probes; Eugene, OR) was added to minimize bleaching of samples. Embedded samples were sliced into ~2 mm sections, or transects. Each transect was placed into a cell culture dish with a 1.5 coverslip inserted into a 13 mm hole in its base (Mattek Corporation; Ashland, MA). Samples were examined with an

Olympus IX71 epifluorescence microscope equipped with a 100W mercury lamp, an inverted

stage, and a 12.5 MegaPixel DP70 digital camera. Samples were viewed at 1000-fold

magnification using the following filter sets (Chroma Technology Corp; Brattleboro, VT):

Pyrene (excitation 360 nm with a 40 nm bandwidth, emission 480 nm with a 60 nm

bandwidth, dichroic longpass beamsplitter at 400 nm); FITC/EGFP/Biodipy/Fluo3/DiO (ex.

480 nm with a 40 nm bandwidth, em. 535 nm with a 50 nm bandwidth, longpass beamsplitter

cut-on of 505 nm); TRITC (Rhodamine)/DiI (ex. 535 nm with a 50 nm bandwidth, em. 610

nm with a 75 nm bandwidth, longpass beamsplitter cut-on at 565 nm); and

DAPI/Hoechst/AMCA (ex. 360 nm with a 40 nm bandwidth, em. 460 nm with a 50 nm

bandwidth, dichroic longpass beamsplitter cut-on at 400 nm).

Multiple images were taken from fields chosen by "stairstep" movement of the

microscope stage while under bright field light. A minimum of ten images was obtained for

each sample. However, not all images were processed. Images were occasionally omitted

from analysis due to poor alignment of the fields under different filters, or because the files

were corrupted and not retrievable.

5.3.3.7 Image processing FISH images were processed in Adobe Photoshop 7.0 using

Fovea Pro software. An image series from Slurry FISH consisted of quadruplicate images—

bright field and each of the three fluorochrome filters (FITC, TRITC, and PYR). An image

series from Aggregate FISH comprised the fluorochrome-filtered images only.

Images were screened initially by splitting into color channels: red-R, green-G, blue-B.

Splitting channels resulted in images that were resolved more easily by the naked eye such

that they could be used as references to the colored images. Theoretically, bacteria should

have been visible in the red color channel of the TRITC-filtered image and in the green color

153

channel of the FITC-filtered image, whereas pyrene crystals should have been visible in the blue color channel of the PYR-filtered image. However, in soil, these attributes were not as well defined. Since there was subjectivity involved in all image processing, a computer algorithm was not used. In general, feature overlap between the TRITC- and PYR-filtered images was due to sorption of the fluorochrome to soil particles. This was verified, when possible, by comparing both to the bright field image. Overlap in the TRITC- and FITC-filtered images was indicative of cells, and feature overlap in the FITC- and PYR-filtered images was due to pyrene. Occasionally, overlap was noted with all three filters. These features were generally soil particles, eliminated by comparison to bright field images, but were occasionally attributed to pyrene crystals or cells. Soil particles tended to have a muted, diffuse fluorescence, whereas cells and pyrene were uniformly intense. Morphology was also considered in these cases to distinguish cells from soil and/or pyrene.

For measuring spatial relationships, cells and pyrene were "extracted" manually as features and copied onto a blank image with a black background (see Figure 4.5 for example). "Reduced" images were imported into the Digital Image Analysis in Microbial Ecology program (*daime*; Daims et al., 2006), where they were automatically segmented using the Rapid Automated Threshold Selection (RATS-L) biomass detection algorithm followed by an associative map object detection algorithm. This segmentation step permits the distinction of individual cells, i.e. biomass, from background and from each other by defining upper and lower thresholds for pixel intensity.

5.3.3.8 Image analysis Images were analyzed for the following: cell numbers, pyrene prevalence, overall object distribution, and the distribution of cells with respect to pyrene.

154

Cells were counted manually, and the total number of cells per gram of soil was back-calculated as follows:

1) for slurry samples: $N = (N_f AD)/aV$, where: N_f = cells counted per field, A = effective filtering area, D = dilution factor of soil in slurry form, a = area of microscopic field, and V = volume of slurry filtered;

2) for embedded samples: $N = (N_f AT)/aS$, where: N_f = cells counted per field, A = area of transected core slice, T = number of transected slices per soil core, a = area of microscopic field, S = grams of soil in a core. The number of transects per soil core was calculated as the core height/slice height. The height of a transect slice that can be visualized under a microscope is referred to as the "field of depth" ($= \lambda[\sqrt{(n^2-NA^2)}]/NA^2$). This parameter is dependent upon the maximum emission wavelength of each fluorochrome (λ), the refractive index of the immersion oil (n), and the numerical aperture (NA) of the microscope objective (Shillaber, 1944; R. Bagnell, Microscopy Services Laboratory, Department of Pathology and Laboratory Medicine, UNC-Chapel Hill School of Medicine, personal communication).

Pyrene prevalence was measured as the percentage of images that contained presumptive pyrene crystals. Additionally, the image area occupied by pyrene was measured with FoveaPro and divided by the total image area. This relative measurement was viewed as a two-dimensional proxy for pyrene concentration.

Overall object distribution was measured in two ways: 1) by calculating an index of dispersion and 2) by comparing computer-generated nearest neighbor distances. An Index of Dispersion, ID, was calculated for each image as follows: $ID = \sqrt{(2\chi^2)} - \sqrt{(2n-1)}$, where n is the number of fields in which bacteria were counted; $\chi^2 = \Sigma[(x-X)^2/X]$, where x is the number of bacteria counted in each field, and X is the mean number of bacteria per field

(Nunan et al., 2001). An index greater than 2 is an indication of aggregation as opposed to uniform distribution, and the greater the index, the greater the degree of non-uniformity (Harris, 1994; Nunan et al., 2001). An evenly distributed sample will generate an ID of less than zero.

FoveaPro was used to generate nearest neighbor measurements, or the distance between any given feature (cells and/or pyrene) and its nearest neighbor. These values are reported as a mean, $0.5/\sqrt{(N/Area)}$, where N is the number of features counted within the image, and can be graphed as a frequency distribution over distance. FoveaPro also generates the mean value that would be expected if the distribution within that image were random. The ratio of the observed value to the expected value (O/E ratio) can be used to show a tendency of the objects to either cluster (O/E<1) or avoid each other (O/E>1). The mean value of a random distribution is less than that of a repellant population and greater than that of a clustering population (Russ, 2002).

The distribution of cells with respect to pyrene was measured using the *daime* program. The stereological analysis algorithm generates a set of linear dipoles radiating from the center of each population member and covering a range of designated lengths. A "hit" is a dipole that crosses two features of interest—in this study, both a cell and a pyrene crystal (see Figure 4.6). The designated range and potential increments for dipole radii are automatically established by the *daime* program and are based on the image size, magnification, and pixel resolution. For the images in this study, the distances ranged from 0.11-69.79 μm (image dimensions were 120 x 90 μm). Due to the required computing capacity, dipole lengths were selected at increments of approximately 0.30-0.40 μm within this range.

A pair cross-correlation function, g(r), is generated for each distance and is based on the probability that a dipole of length r hits both a bacterial cell and pyrene crystal. The function is normalized for both cell density and pyrene concentration, given its dependence on both. The correlation value is calculated as follows: g(r) = P(r)/2BY, where P(r) = H_r/T_r, H_r is the number of hits, and T_r is the sum of both hits and misses. B is defined as A_o/A_T, or the ratio of bacterial cell-occupied area (A_o) to total image area (A_T), and is analogous to biomass concentration. Y is defined by the same ratio, where A_o is the area occupied by a pyrene crystal, and is analogous to pyrene concentration. Values less than 1 indicate repulsion, values greater than 1 indicate clustering, and values approximately equal to 1 indicate a random distribution.

daime also generated nearest neighbor measurements for cells with respect to pyrene, from which a histogram was plotted. A Poisson-like histogram is observed when objects are randomly distributed, and a narrowed histogram reflects clustering. A leftward shift in a distribution can also indicate clustering, whereas a shift to the right suggests avoidance (Russ, 2002).

5.3.4 Statistical analyses The correlation between the community structures at each time point, as measured by DGGE banding patterns, was established using hierarchical cluster analysis. First, the presence or absence of dominant bands in each lane of the denaturing gradient gel was determined. From this, a pairwise similarity matrix was created using Sorensen's Similarity Coefficient (S_{AB} = 2C/(A+B), where C = the number of bands in common between two DGGE lanes, A and B = the number of bands unique to lanes A and B, respectively. The similarity coefficients were clustered using the unweighted pair-group method with arithmetic averages algorithm (UPGMA; Ibekwe et al., 2001; Fromin et al.,

2002; Kasai et al., 2005) in ProStat (Version 3.0b; Polysoftware International, Inc.; Pearl River, NY), and a dendrogram was constructed in Excel.

In order to verify the previous findings without the subjective reading of DGGE bands, the variation in community structure over time was measured by comparing the density profiles along a denaturing gradient gel. A horizontal density profile for each lane was created in Adobe Photoshop 7.0 using FovePro software. The measurements were analyzed by Principal Components Analysis (PCA) using ProStat Version 3.0b (Polysoftware International, Inc.; Pearl River, NY; Rosswall and Kvillner, 1978; McCaig et al., 2001; Ní Chadhain et al., 2006). A correlation matrix was created from the loadings of each principal component, and the Eigenvalues for the two dominant principal components were graphed to show possible clustering.

The relationship between pyrene mineralization and degrader abundance, i.e. Pyrene Group 3 gene copy number, was established with linear regression (Yang and Crowley, 2000). Linear regression was also used to correlate the spatial relationship of cells and pyrene (as determined by mean nearest neighbor distance) with the overall prevalence of pyrene (image area occupied by pyrene) for both Slurry FISH and Aggregate FISH images.

Significance testing of the difference between two means was conducted using Student's *t* test.

5.4 Results and Discussion

5.4.1 ^{14}C-Pyrene compartmentalization

5.4.1.1 Mineralization The cumulative production of $^{14}CO_2$, as a percentage of the original radiolabel added, can be seen in Figure 5.1 below.
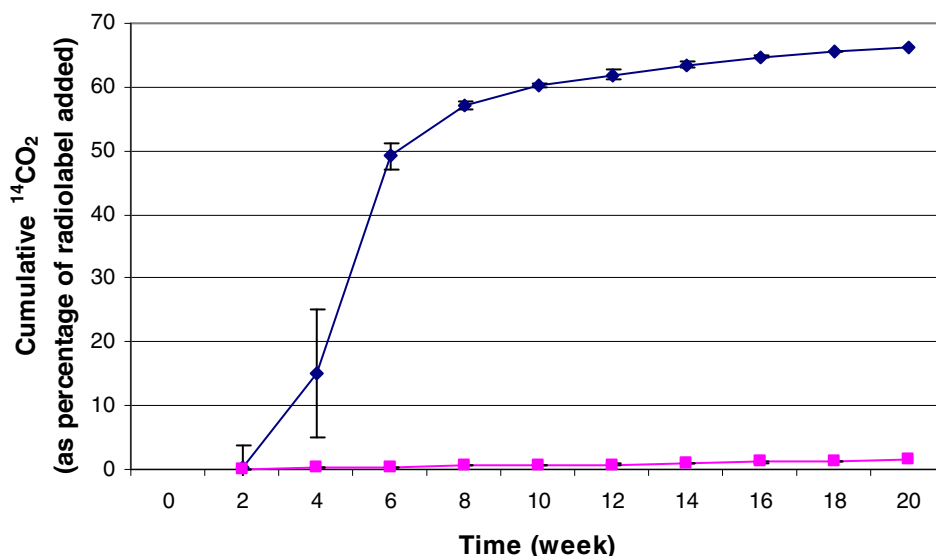
Figure 5.1. Pyrene Mineralization Curve. Measurements shown are the average and standard deviation of multiple replicates. Blue: sample microcosms; pink: control microcosms.

There was a lag period of two weeks before mineralization began. The live microcosms achieved 66.18% mineralization of pyrene with an initial rate of 1.05% per day (between weeks 2 and 4) and a maximum rate of 2.44% per day (between weeks 4 and 6). Mineralization began to plateau at around 10-12 weeks. The inactivated controls achieved 1.43% overall mineralization.

It was originally hypothesized that the PMN would exhibit a significant lag period of perhaps a month followed by a slow rate of mineralization. This hypothesis was based on the assumption that this soil contained populations unadapted to the contaminant compounds. Roper and Pfaender (2001) spiked a pristine soil with 100 ppm pyrene and found a 140 day lag period before mineralization began, whereas Carmichael and Pfaender (1997) spiked the

same soil with 1000 ppm pyrene and measured only 0.5% mineralization over 4 weeks. It was somewhat surprising, then, to see only a two-week lag period, a fairly rapid rate of mineralization, and a large extent of overall pyrene mineralized. These findings could be due to two things: readily available pyrene, not yet incorporated into the soil organic matter, and/or the presence of an adapted (or adaptable) population. Given that the spiked soil was not aged prior to setting up the microcosms and that pyrene was spiked at a high concentration, availability should not have been a rate-limiting factor. At this stage, binding of pyrene to the soil organic matter would be reversible, and pyrene transfer into the surrounding medium would occur as a result of the concentration gradient created by local degradation.

The fact that pyrene mineralization begins as early as week two suggests that its availability is not the only reason for the absence of a significant lag period and the presence of substantial mineralization. Whether or not the PMN contained a pre-adapted population of microorganisms was not determined, since a DGGE profile could not be established at t = 0, and the small proportion of its diversity represented by a clone library did not contain any known PAH-degraders (see Chapter 3). However, the mineralization data suggest that there was an adapted community present.

Contaminant levels in the parts per billion have been shown to constitute a "pre-exposure" in other soils (Spain and van Veld, 1983; Johnsen and Karlsen, 2005). It is possible that the proximity of the site from which the PMN was retrieved to the actual contaminated Reilly site or to an adjacent highway led to the adaptation of indigenous PMN microbiota. The PMN contains 3.49 mg kg^{-1} of pyrene (20 mg kg^{-1} of total PAH) at its

baseline, and this may be a significant enough background to have induced and maintained a level of degradative genes within its population (Johnsen and Karlsen, 2005).

A comparison of the mineralization rates between the contaminated soil from the Reilly site (CMN) and the PMN, similarly incubated, are given below in Table 5.3.

Table 5.3. Comparison of Mineralization Data for CMN, PMN, and Respiked PMN.

Soil	Lag Period	k_0	k_{max}	Overall % of mineralization
CMN	1 week	0.05	2.36	42.9 ± 0.03
PMN	2 weeks	1.05	2.44	66.2 ± 0.07
Respiked PMN	None	4.53	4.53	78.8 ± 0.37

Rates are given as percent mineralized per day. Initial rates for CMN are for days 0-7; for PMN, days 7-14; for respiked PMN, days 0-7. Maximum rates occur for CMN between days 7-14; for PMN, between days 14-21; and for respiked PMN between days 0-7. Overall extent for CMN was taken from measurements at 7 weeks; PMN at 20 weeks; respiked PMN at 8 weeks. CMN data from Jones, 2006.

Compared with the PMN, the CMN showed less lag time, a lower initial rate of mineralization, a similar maximum rate of mineralization, and a lower overall extent of mineralization. It should be noted that the CMN incubations did not continue as long as those in this study; however, they did appear to be approaching a plateau.

There are abiotic differences between the CMN and PMN soils that might account for some of the observed mineralization data, especially the lower overall extent of mineralization. First, the CMN contamination was a result of creosote waste, not the spiking of a single compound. The presence of this non-aqueous phase (NAP), in addition to the multitude of other PAHs contained therein, results in a higher level of organic carbon in the CMN soil ($f_{oc} = 0.13$ for CMN, 0.02 for PMN). This may have resulted in a loss of sorption sites for the spiked pyrene, thus making it more available for mineralization in the short run, but yielding less overall mineralization in the long run after partitioning into the NAP.

Second, the CMN is an aged, contaminated soil. Decades of humification processes within this soil would have resulted in changes to the organic matter that would make it easier to "encapsulate" pyrene over time (Guthrie et al., 1999).

The most likely reason for the difference in mineralization rates between the two soils is the presence of an adapted population in the CMN. This will be discussed in more detail in a later section. Briefly, an adapted population would not require time for enzyme induction (hence, no lag time), but its low density would account for a lower initial rate of mineralization while cell numbers are increasing. It is unknown whether the similar maximum degradation rates are due to sheer cell numbers or pyrene transformation efficiency.

5.4.1.2 Aqueous phase-associated radioactivity Association of the radiolabeled pyrene with the aqueous phase is shown in Figure 5.2 below. The sample and control values appear to mirror each other, with an exception at 18 weeks. A "peak" in aqueous phase-associate radiolabel was observed at 10 weeks in both sample and control microcosms.
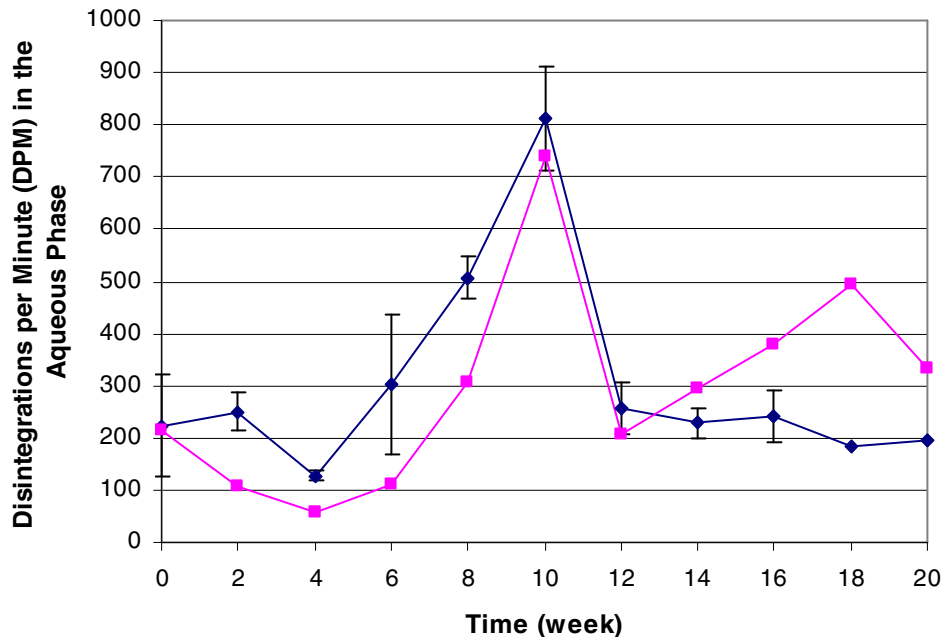
Figure 5.2. Aqueous Phase-Associated Radioactivity. Blue: sample; pink: control. Sample measurements shown are the average of duplicate microcosms. Error bars represent the range. Control measurements were not replicated.

The aqueous phase-associated radiolabel in the samples mirrored that in the control microcosms. Significance testing was not possible due to the lack of replicates. Still, the values for samples range from 1.6 to 2.7 times higher than those of the control microcosms between weeks 2 and 8. It was thought that an increase in radioactivity in the aqueous phase might point to oxidation of the parent compound to a more polar metabolite, thus reflecting microbially induced transformation. However, if this difference is not significant, this would suggest that there was no biotic influence on the amount of pyrene that ended up in the aqueous phase. The parallel plots suggest that this is probable.

The percentage of aqueous phase-associated radiolabel (0.9 to 4.1%) was very small relative to the total radiolabel added and could, as a result, be deemed insignificant.

However, the fact that levels in both the sample and control aqueous phases exceed pyrene solubility warrants consideration. If not due to microbial activity, these high levels of label in the aqueous phase could be due to 1) chemical oxidation to a more polar form, 2) undissolved pyrene crystals that remained in suspension after centrifugation, or 3) association of the pyrene with soil particles or dissolved organic matter (DOM). Chemical oxidation was not measured but cannot be ruled out. Undissolved pyrene crystals, soil particles with "attached" pyrene, and DOM containing pyrene could have been withdrawn by the pipette during removal of the supernatant and subsequently detected by scintillation counting. This is a likely scenario, given that the measurements for the radiolabeled pyrene in the control aqueous phase (29.5 mg L^{-1} at their maximum, 4.4 mg L^{-1} at their minimum) far exceed the solubility limit of the parent compound in water (0.13 mg L^{-1}). Originally, the supernatant was passed through a glass fiber filter to remove all soil particles prior to adding it to the scintillation cocktail. However, this extra step resulted in a significant loss of sample; therefore, it was omitted from the protocol. Although there was no visible carryover of soil particles from the microcosm vial to the scintillation vial, it cannot be ruled out.

The fact that the parent compound was mineralized at all indicates that metabolites had to have been generated. These could account for a fair amount of the sample aqueous phase associated radioactivity, as metabolites would be more soluble than the parent compound, and may also account for the observed difference in sample versus control values, whether or not they are significant.

5.4.1.3 Solid phase-associated radioactivity Radiolabel within the solid phase compartment can be seen in Figure 5.3 below. The values are closely related until 4 weeks, at which point they diverge. Solid phase-associated radioactivity in samples decreases

dramatically between 4-6 weeks, after which time it remains relatively constant. That in the control microcosms slowly increases. The sample decrease parallels the increased compound mineralization, whereas the control increase points to gradual incorporation into the soil over time.
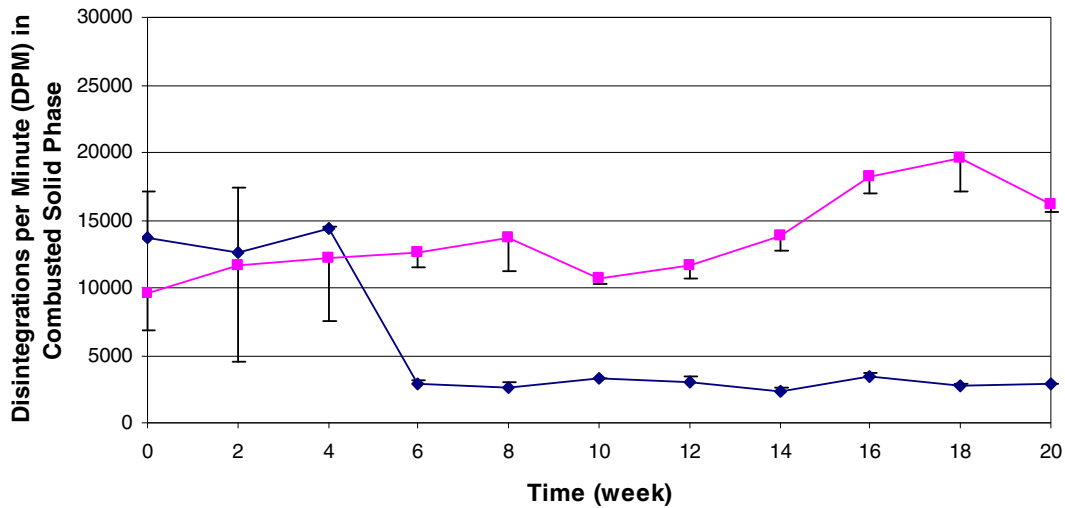
Figure 5.3. Solid Phase-associated Radioactivity. Blue: sample; pink: control. Sample measurements shown are the average and standard deviation of triplicate subsets from each of duplicate microcosms. Control measurements are the average and standard deviation of triplicate subsamples from within a singular microcosm. Error bars are given in one direction only for ease of reading at the earlier time points.

5.4.1.4 Respiked microcosms Mineralization of pyrene after respiking the microcosms is shown below in Figure 5.4.
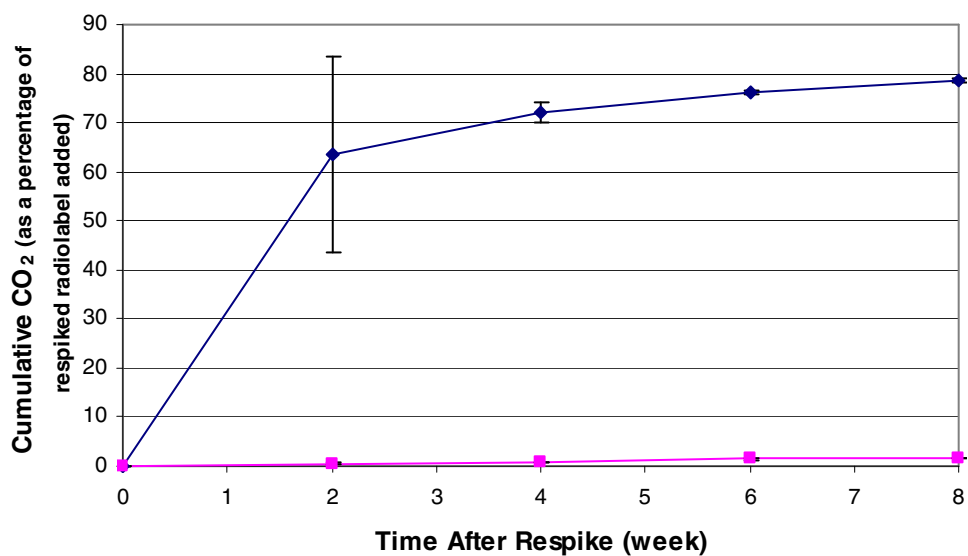
Figure 5.4. Mineralization Curve for Respiked Pyrene. Blue: sample; pink: control. Measurements shown are the average and standard deviation of multiple replicates.

After spiking a second time, the overall extent of pyrene mineralization rose to 79% with a maximum rate of 4.5% per day. There was no lag period before mineralization began, and the initial rate was also the maximum.

Aqueous phase-associated radiolabel for the respiked microcosms is shown below in Figure 5.5.
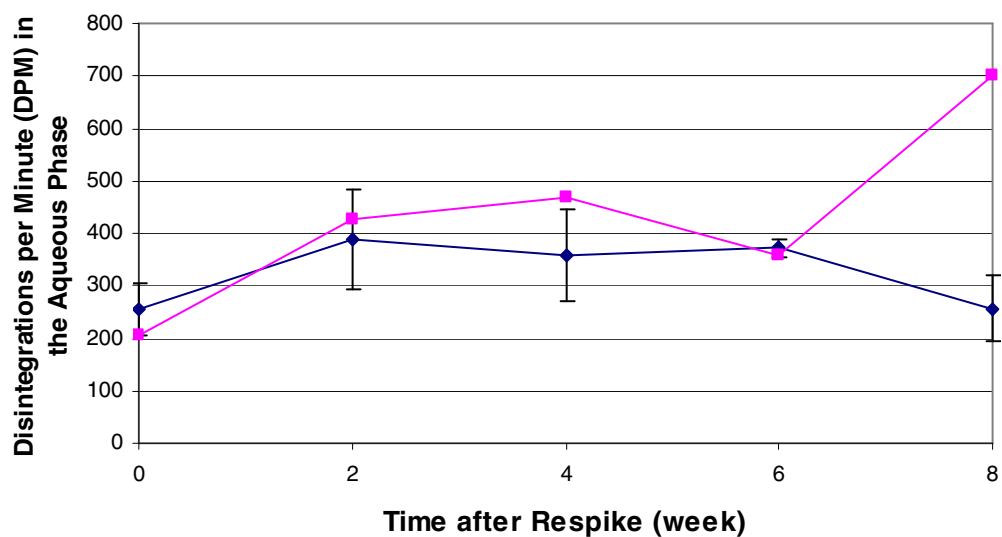
Figure 5.5. Aqueous phase-Associated Radioactivity in Respiked Microcosms. Blue: sample; pink: control. Measurements shown are the average and range of duplicate microcosms. Control microcosms were not replicated.

Again, the sample and control microcosms parallel one another but diverge at 8 weeks after respiking.

Solid phase-associated radiolabeled pyrene for the respiked microcosms is shown below in Figure 5.6.
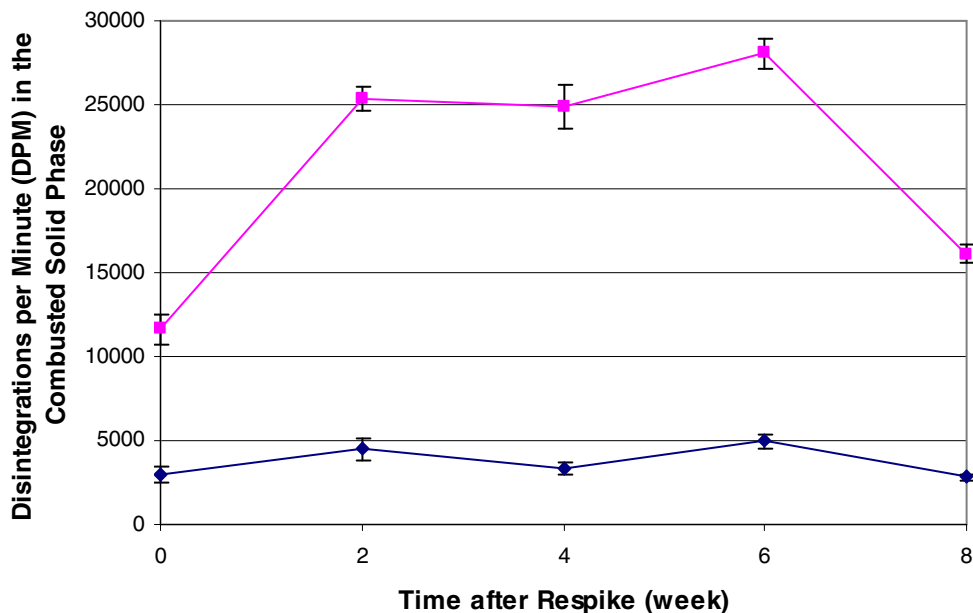
Figure 5.6. Solid Phase-associated Radioactivity in Respiked Microcosms. Blue: sample; pink: control. Sample measurements shown are the average and standard deviation of triplicate subsets within each of duplicate microcosms. Control measurements are the average and standard deviation of triplicate measurements taken from one microcosm.

The radiolabel combusted from the solid phase in sample microcosms appears to remain the same over time after respiking. That in the control microcosm solid phase increases up to 2 weeks after respiking, then decreases at 6 weeks after respiking.

The respiked microcosms did not exhibit any lag period. Their maximum rate of mineralization was twice that of the originally spiked PMN, and the overall extent of mineralization reached ~80% of the re-spiked pyrene, as compared to the 66% reached in the singly-spiked microcosms. This is in contrast to the findings of Thompson et al. (1999) who found that repeated exposure of a soil community to 1,2-dichlorobenzene yielded lower mineralization rates than a single exposure. This they attributed to a decreased bioavailability, and therefore reduced toxicity, with the single exposure. The reverse finding

in this study points to an adapted population of sufficient cell density to be able to immediately mineralize pyrene at a higher rate (MacLeod and Semple, 2002; Johnsen et al., 2007).

5.4.1.5 Mass balance of pyrene The mass balance of added radiolabeled pyrene is shown in Figure 5.7 below.
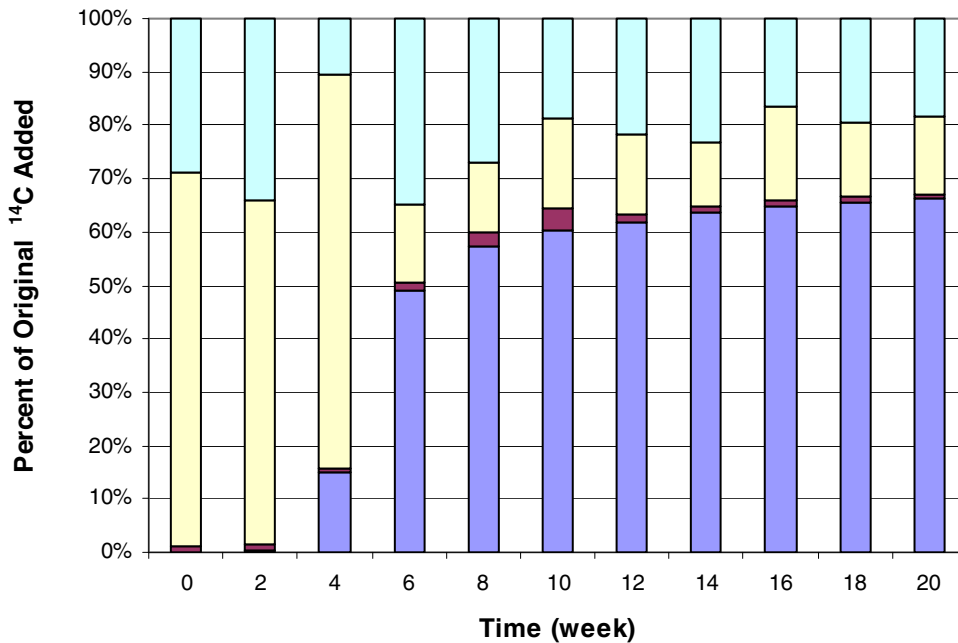
Figure 5.7. Mass Balance of Spiked ^{14}C-Pyrene in Incubated Microcosms Over Time. Blue: $^{14}CO_2$-associated radiolabel; fuschia: aqueous phase-associated label; beige: solid phase-associated radiolabel; aqua: unaccounted for radiolabel.

The mass balances range from 65-89%, leaving a considerable percentage of unaccounted for radiolabeled pyrene at all time points. This could be due to carbon dioxide loss during trap exchange, leaky vials, or the delay in soil combustion. The latter is probably the most significant cause of pyrene unaccountability. Soils had to be fully dried prior to combustion, per the manufacturer's directions. At the time the microcosms were set up, the Bio-oxidizer was inoperable, and samples were set aside for drying until they could be analyzed. Once the

Bio-oxidizer was in operation (t = 1 month), two aliquots of the spiked soil were measured as time zero: an original aliquot of pyrene-spiked soil without nutrient amendments added, and an aliquot with nutrients added on day 0 and air-dried (called t = 0). The aliquot without amendments contained 97.5% of the original spike upon combustion, whereas the "t = 0" samples contained $70 \pm 18\%$ of the original dpm added. Mineralization extent was calculated based on the original ~20,000 dpm spike, instead of the "t = 0" ~14,000 dpm measurement, since the control microcosms at later time points approached 20,000 dpm. If the approximately 30% loss during drying is taken into account, mass balances improve dramatically. In order to be consistent with sample handling, the remaining time points were also allowed to sit for two weeks prior to combustion. In hindsight, the soils should have been dried overnight in an oven at a temperature low enough to prevent volatilization (i.e. 60°C) and then combusted. In any event, some of the unaccounted for radiolabel in live microcosms is likely due to additional mineralization in the drying soils, but should not have affected either the original mineralization measurements or the aqueous phase-associated measurements. However, the delay would explain the larger standard deviations found at t = 0-4 weeks.

5.4.2 Plate counts and direct cell counts

Plate counts rose at one month and remained steady over the next two months, dropping significantly at months 4 and 5 (P < 0.01). The spurt in cell growth occurred just before the onset of the maximum rate of pyrene mineralization, suggesting that the observed lag period may be a result of biomass production (see Figure 5.8).
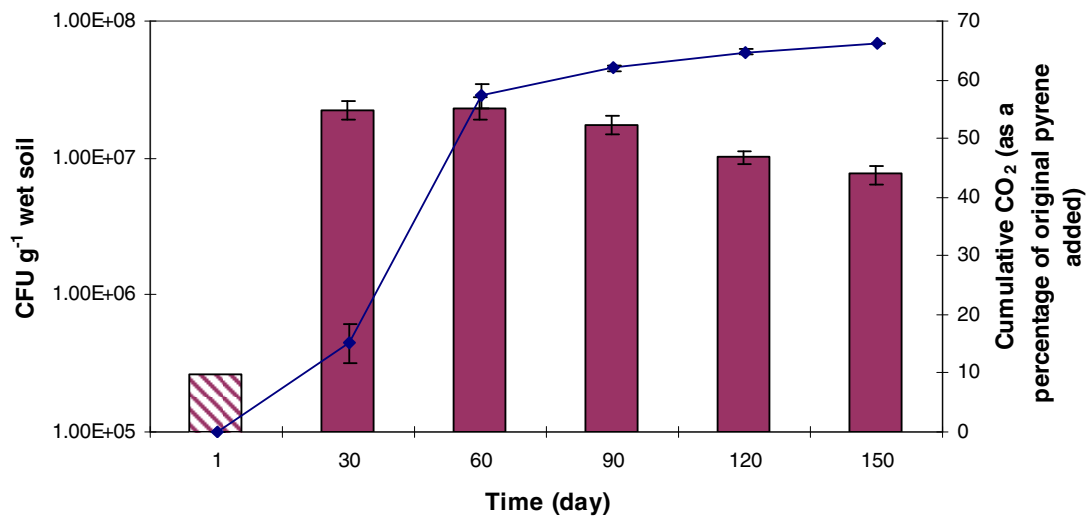
Figure 5.8. Plate Counts and Percent Mineralization over Time. CFU values (solid columns) are the average and standard deviation of triplicate plate counts from triplicate microcosms; mineralization values are the average and standard deviation of multiple replicates at each time point. CFU value at t = 1 day (striped column) is based on a theoretical plate count of 300 CFU on a 10^{-4} dilution plate (10^{-5} dilution yielded no growth).

The numbers of CFU do not significantly drop as pyrene mineralization initially levels off (i.e., t = 2 or 3 months), but this is likely due to the maintenance of other organisms, not primary degraders, utilizing pyrene metabolites or other carbon sources. Colonies were not screened for their degrading abilities. However, other studies have shown conflicting results when trying to correlate overall biomass, degrader abundance, and mineralization (Spain and van Veld, 1983; Carmichael and Pfaender, 1997; Huesemann et al., 2002; Gentry et al., 2003). Respike plate counts are not significantly different from those seen at t = 4 or 5 months. This suggests a lack of a toxic response to the respiked microcosms, again pointing to an adapted population.

Since FISH was only performed at one time point, a comparison of counts over time is not possible. At two months, the CFU count (2.32×10^7) was significantly lower than the

Slurry FISH count (1.96×10^8, P < 0.001) which was significantly lower than the Aggregate FISH count (3.32×10^9, P < 0.001).

   Four distinct cell morphologies were observed in the PMN soil images. First, there were cells similar in appearance to those seen in the contaminated soils (see Chapter 4). These were coccoid and very small (< 0.3 microns in diameter) and some larger coccobacilli. These cells appeared in varying numbers in almost all images, regardless of the FISH method employed. Second, there were coccoid cells that were much larger than any seen in the uncontaminated soils although not necessarily large by pure culture standards (e.g. 1-3 microns in diameter). These appeared in ~37% (11/30) of the Slurry FISH images but only appeared in 5% (2/40) of the Aggregate FISH images (see Figure 5.9).
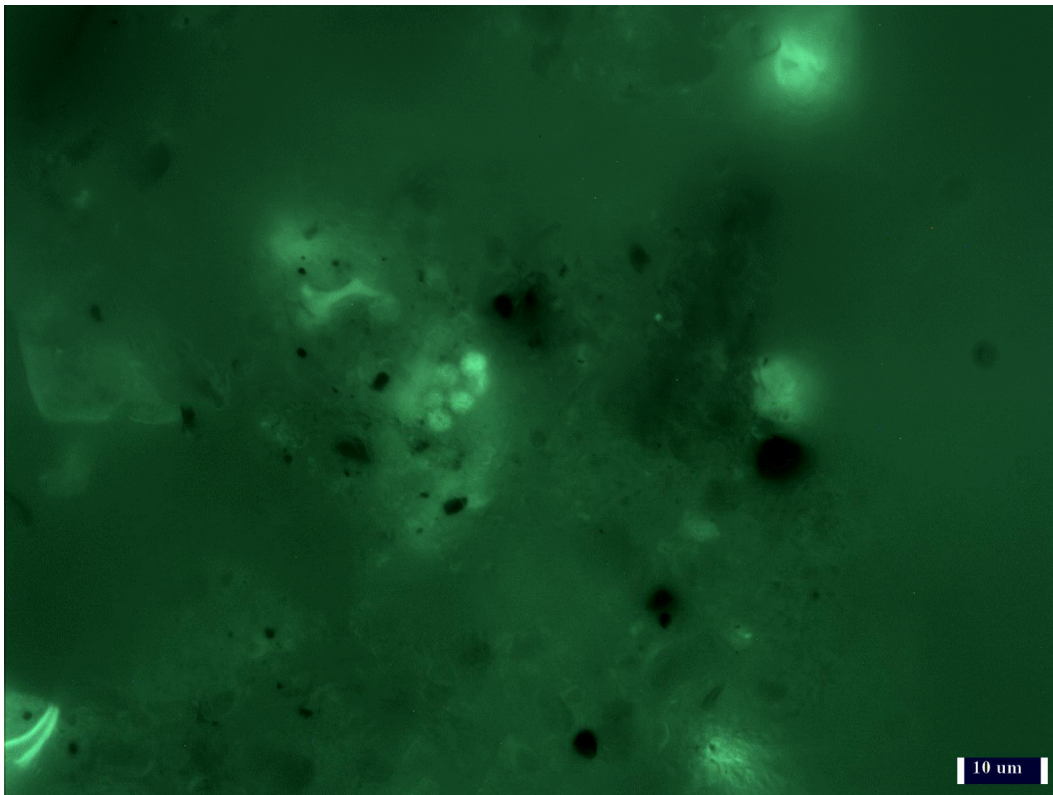
Figure 5.9. Example of Larger Cells Seen in Microcosm A (overlay of FITC-filtered image and its corresponding Green channel image).

These cells were only noted in images obtained from Microcosm A. This finding suggests that an insufficient number of microscopic fields was examined for Aggregate FISH or for microcosms B and C, or that the cells may have been associated with soil particles and therefore not diluted out by slurrying, or that the hybridization conditions within slurried samples were optimal for this group. In three of the Slurry FISH images, these cells only hybridized with the Univ1390 probe, whereas in two others, the signal from Eub338 was present but weak. The cells in the remaining images hybridized with both probes. It is possible that these cells were of eukaryotic origin. Still, they were much smaller than the either the protozoa or fungal spores previously observed in this soil.

Finally, there were narrow and elongated cells (~0.5 x 3 microns) that appeared in ~53% (21/40) of the Aggregate FISH images but did not appear at all in the Slurry FISH images (see Figure 5.10 below) and in only one image from microcosm A. This suggests that either an insufficient number of fields was examined in the Slurry FISH samples of microcosm A, or that these cells are less soil-associated or lower in number and were diluted out of the slurry samples, or that hybridization conditions within the Aggregate samples were optimal for this group. The cells also appeared when visualized under UV light, suggesting either that they are autofluorescent in nature or that pyrene uptake has rendered them fluorescent. Many soil-borne organisms are autofluorescent. The most notable are the pseudomonads, of which *Ps. putida*, *Ps. aeruginosa*, *Ps. fluorescens*, and *Ps. stutzeri* are known PAH-degraders (Campbell et al., 1995; Boonchan et al., 2000; Ramirez et al., 2001). Fluorescence resulting from pyrene uptake during degradation has not appeared in the literature. However, the use of pyrene derivatives to stain cellular lipids and as molecular beacons for oligonucleotides is well established (Haugland, 2002; Seo et al., 2006).
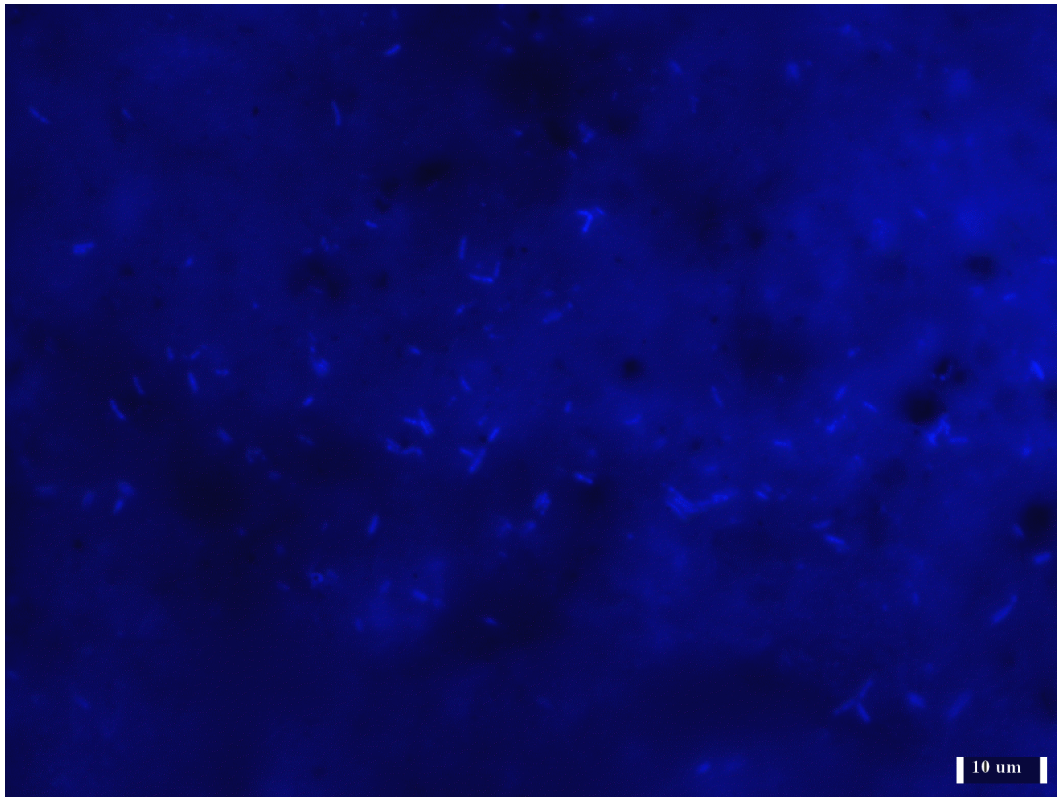
Figure 5.10. Example of Rod Morphology that Predominated Aggregate FISH Images. Image taken with PYR filter shows cell fluorescence under UV light.

The appearance of small cells in any of these samples is not surprising. Visualization of soil samples by electron microscopy showed that 72% of cells were extremely small coccobacilli with diameters less than 0.3 microns (as cited in Kepner and Pratt, 1994), while others used FISH to show that 68-77% of the actively growing bacteria in two soils had diameters between 0.25 and 0.5 microns (Christensen et al., 1999). This morphology is an obvious advantage to life in nutrient-poor environments, where large surface area-to-volume ratios maximize the diffusion of substrate and nutrients into the cell (Koch, 1990). The addition of a large amount of pyrene accompanied by nutrients into this soil may have resulted in the appearance of other cell morphologies and sizes, consistent with growth on pyrene and/or its metabolites.

5.4.3 Community diversity comparisons: DGGE profiles

Figure 5.11 depicts the change in bacterial community profile over time for the PMN soil and

compares it with the CMN soil and Respiked PMN samples.
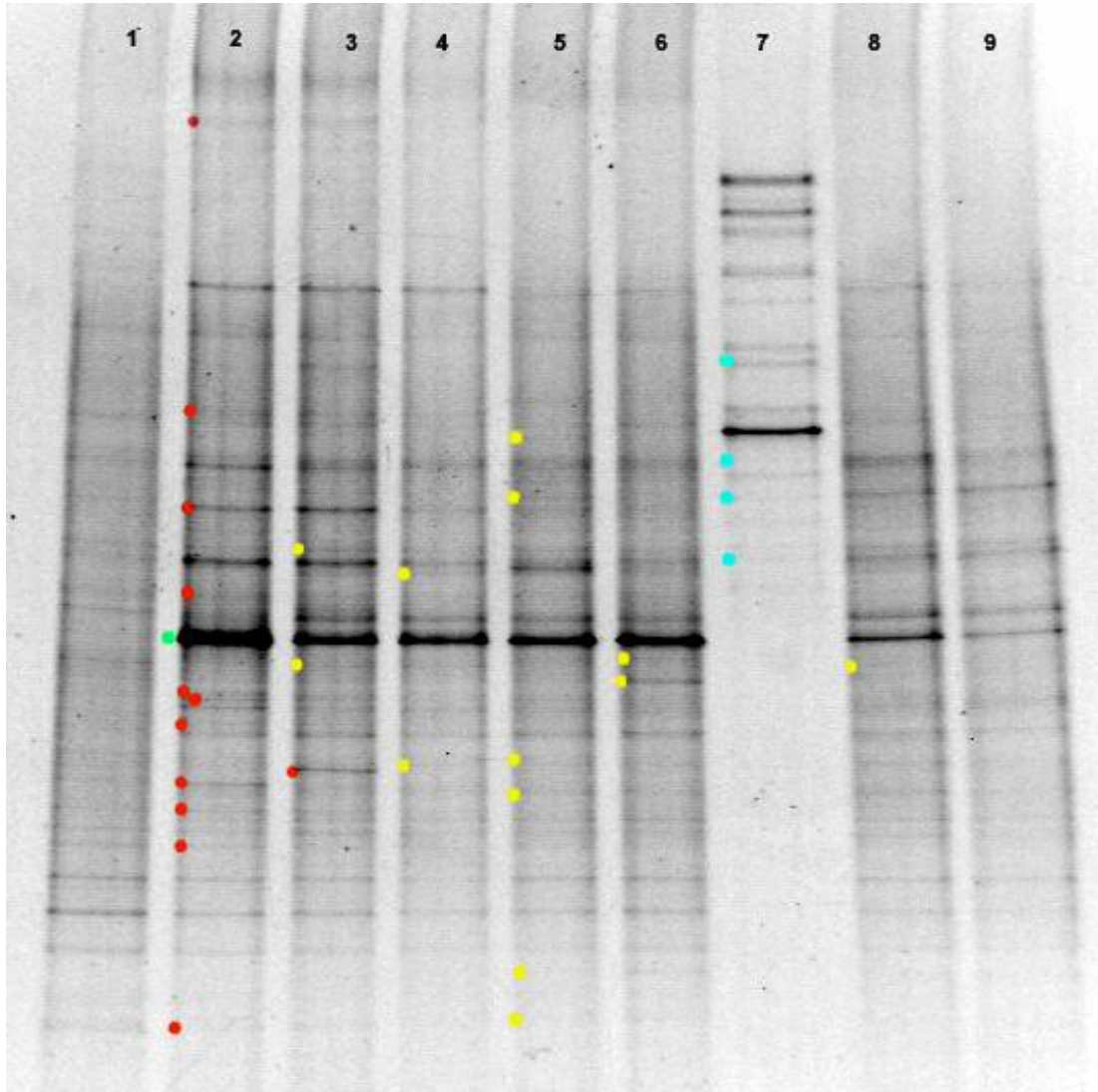
Figure 5.11. DGGE Profiles of Spiked PMN over Time, CMN, and Respiked PMN. Lanes 1-6, PMN at times 0-5 months, one-month interval per lane; lane 7, CMN; lane 8, respiked PMN at 1 month; lane 9, respiked PMN at 2 months. The meaning of the colored dots is described in the text.

Dominant bands are difficult to discern in the PMN t = 0 sample due to the high level of

diversity. There are changes that appear over time: for example, the disappearance of

several bands (red dots); and the appearance, however brief, of many others (yellow dots). What is most striking is the appearance of a dominant band (green dot), that persists over the entire incubation but is not discernible in the time zero PMN profile. Figure 5.11 also provides a comparison of the PMN profile over time to that of the contaminated Minnesota soil from the same site. There are four bands (blue dots) that appear in both the CMN and PMN. Two of these appear in the PMN at all time points. One appears only at t = 2 months, and the final common band appears at t = 4 months and in both respiked profiles. The banding patterns in the Respiked PMN soil at 1 and 2 months are nearly identical and share some representatives with the PMN incubations, especially at t = 5 months.

Although it was difficult to discern bands in the original profile, a change in operational taxonomic unit (OTU) richness and evenness is still apparent over time. Many other studies have shown such changes after contaminant exposures (Stephen et al., 1999; Margesin et al., 2003; Joynt et al., 2006). The change in evenness over time can best be shown by comparing density profiles (see Figure 5.12 below).
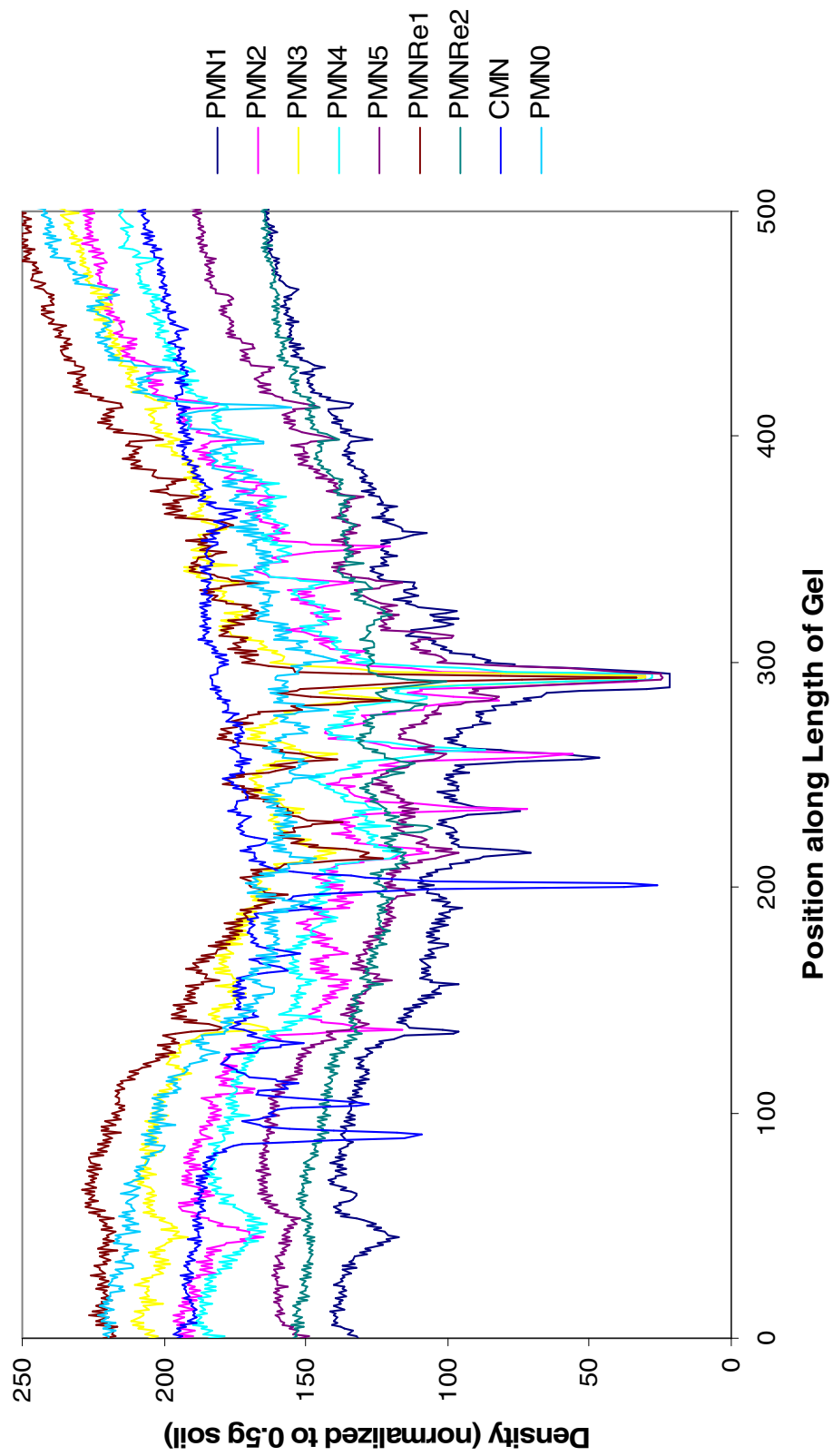
Figure 5.12. Density Profiles of PMN Time Series, Respiked Samples, and CMN along the Length of the Denaturing Gradient Gel.

177

Where the original profile contains no dominant species, the spiked community structure evolves to one that is dominated by few bands and one dominant band (seen at position 293).

The PMN profiles did not at all approach that of the CMN, even after respiking. It was thought that the two soils would be structurally related given their proximity at the Reilly site and that eventually the spiked and respiked soils would become more similar to the CMN structure. Although there were 4 common bands in the DGGE profiles, none represented a dominant OTU for the CMN, and the overall similarities were very low at all time points. This could be due to the aging of the soil with PAHs, to the fact that it has been subjected to attempts at remediation, and to the addition of only one PAH to the PMN, as opposed to creosote itself.

Respiking resulted in an even less diverse community whose shared OTUs decreased. This is presumably due to the selection for and against certain groups. The profiles of the respiked samples appear the same at months 1 and 2.

The similarity matrix created from Sorensen's Similarity Coefficient is shown below in Table 5.4. Coefficients were not calculated using PMN t = 0, due to the difficulty in distinguishing bands. Presumably, the profiles at each time point for the PMN are a subset of t = 0, but there is no way to count the total number of bands present in that lane.

Table 5.4. Similarity Matrix of Sorensen's Similarity Coefficients Calculated from a Pair-wise Comparison of DGGE Banding Patterns.

Time	PMN t = 1	2	3	4	5	CMN	Respiked PMN t = 1	2
1	--	0.91	0.76	0.69	0.60	0.10	0.63	0.61
2	--	--	0.79	0.69	0.60	0.14	0.63	0.61
3	--	--	--	0.77	0.76	0.11	0.74	0.73
4	--	--	--	--	0.83	0.15	0.72	0.71
5	--	--	--	--	--	0.11	0.84	0.79
CMN	--	--	--	--	--	--	0.15	0.16
Re1	--	--	--	--	--	--	--	0.95
Re2	--	--	--	--	--	--	--	--

A dendrogram constructed from the similarity matrix using UPGMA is shown in Figure 5.13

below.
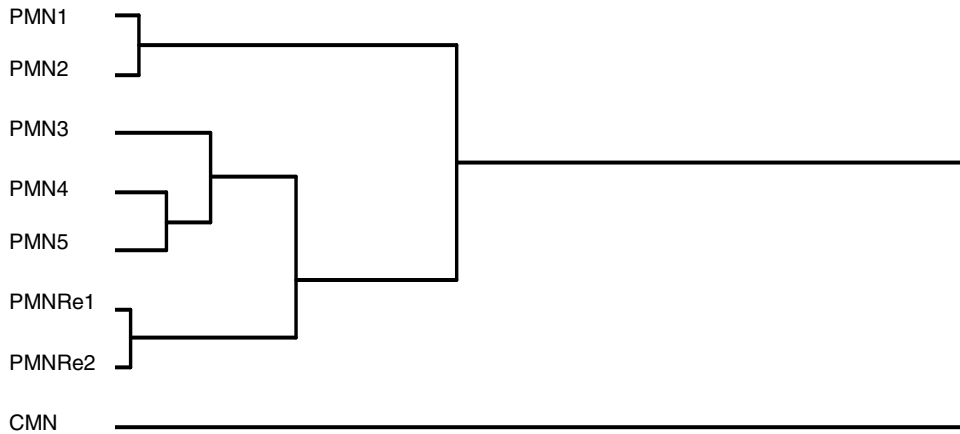
Figure 5.13. Dendrogram Constructed from the Sorensen's Similarity Coefficient Matrix, using UPGMA.

Each PMN profile is most closely related to the one from the previous month, and the

respiked profiles are nearly identical ($S_{4,5} = 0.95$). The CMN profile acts as an outlier due to

its low similarity coefficient.

The profiles of the respiked soil most closely resembled that of the singly spiked microcosms at 5 months but were less diverse and still dissimilar ($S_{5, Respike1}$ = 0.84; $S_{5, Respike2}$ = 0.79). They did not approach the CMN ($S_{CMN, Re1}$ = 0.15; $S_{CMN, Re2}$ = 0.16). It is possible that with continuous respiking, as would occur with repeated waste discharge into the soil, these might have become more similar to the CMN. However, this was not observed during the course of this experiment and could easily be due to the fact that the PMN was spiked with only one compound versus the complex mixture of hydrocarbons within creosote.

Principal components analysis of all the DGGE intensity profiles showed that 85.9% of the variance across profiles can be explained by principal component one (PC1). Another 8.9% of the variance is explained by principal component two (PC2). The CMN profile is well separated from all the other profiles. The respiked profiles are also shifted to the left on the PC2 axis. Interestingly, PMN0 is shifted farther to the left than PMNRe1, suggesting that even less of the variance in this profile than in PMNRe1 can be explained by PC2. PMN1-5 cluster together. If the CMN profile is omitted from the data (pink squares), then PMN0, PMNRe1, and PMNRe2 are all separated from the remaining cluster of PMN1-5. In this case, 93.7% of the variance is explained by one principal component (PC1), and another 3.6% of the variance is explained by PC2. Figure 5.14 below shows the loadings generated at each time point for PC1 and PC2. This analysis supports the results of the similarity matrix and suggests that there was little bias in reading the DGGE banding patterns. It is also consistent with others' findings that the use of unweighted data (presence/absence of bands) versus weighted data (intensity profiles) does not affect the overall results (McCaig et al., 2001).
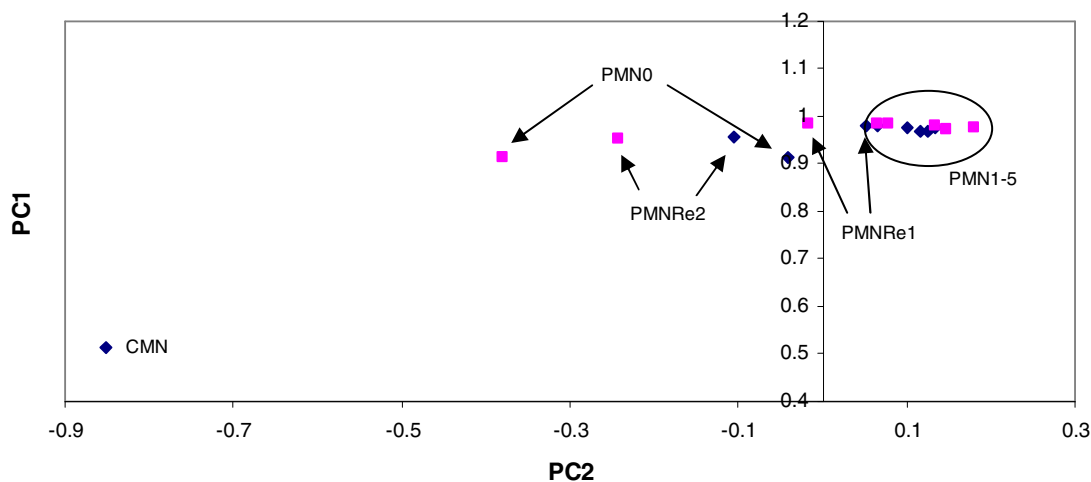
Figure 5.14. Plot Showing Relative Loadings from Two Principal Components (PC1 and PC2) at Each Time Point for the Incubated PMN; Based on Density Profile Data. Blue: component loadings when CMN is included in the analysis; pink: component loadings without CMN included.

5.4.4 Appearance of pyrene degraders The appearance of a dominant band at each time point in the PMN incubation (see Figure 5.11) suggested that the OTU represented by this band was involved in pyrene degradation. DNA extracts from the incubated PMN and from the eluate of the dominant band were screened for the presence of uncultivated pyrene-degrading organisms using primer sets specific for previously identified Pyrene Groups 1-3 (Singleton et al., 2006; see Table 5.2). PYR Group 2 was found to be the dominant group in the CMN soil incubated under the same conditions as the PMN in this experiment (Jones et al., 2007, submitted). Thus, it was assumed that the PMN would also contain PYR Group 2 representatives, given its proximity to CMN at the Reilly site. However, this was not the case. The incubated PMN and the dominant band eluate yielded PCR products only for PYR Group 3 (PG3).

Quantitative PCR was then performed on the extracts at all time points. The results are given in Figure 5.15 below. The number of PG3 gene copies increases 2 orders of magnitude

181

from time zero to t = 1 month, then decreases gradually over time, remaining 1 order of

magnitude higher than the original number after 5 months of incubation. Gene copy numbers

of PG3 and Bacteria in the respiked samples are not significantly different from the singly

spiked microcosms at t = 4 and 5 months for either group.
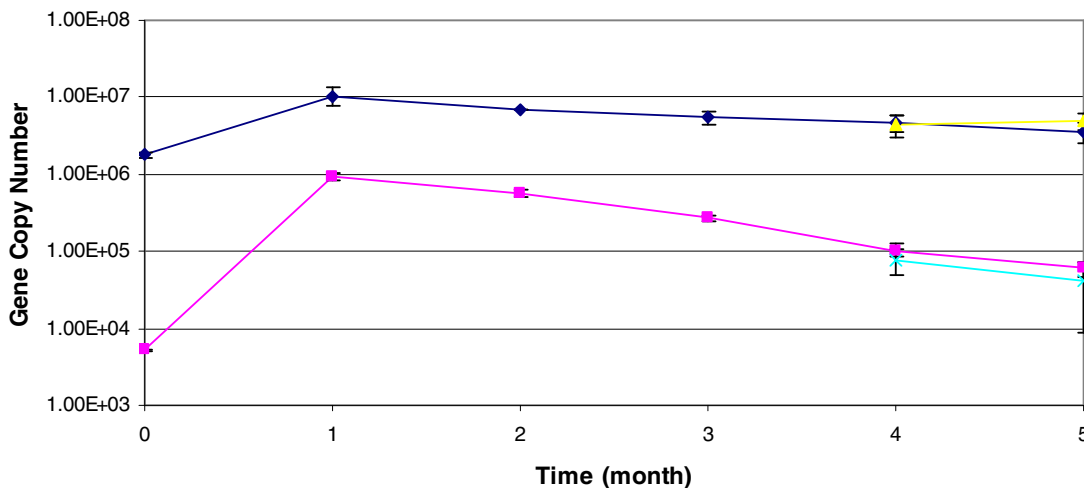
Figure 5.15. Number of Bacterial and Pyrene Group 3 16S rRNA Genes over Time. Blue:
bacterial gene copy number; pink: pyrene group 3 gene copy number; yellow: bacteria after
respiking; aqua: pyrene group 3 after respiking. Values for t = 1-5 represent the average and
standard deviation of reactions from triplicate microcosm extracts; values at t = 0 represent
the average and standard deviation of triplicate reactions from a single extract.

The increase in gene copy number precedes both the increase in aqueous phase-

associated pyrene and the onset of pyrene mineralization (see Figures 5.16 and 5.17 below)

suggesting that it may be involved in the transformation and/or mineralization of pyrene.

Linear regression of pyrene mineralization and Group 3 gene copy number supports this

relationship ($R^2 = 0.97$). Bacterial gene copy numbers also correlated with mineralization

data, but not as strongly ($R^2 = 0.89$). If the aqueous phase data are shifted to the left,

assuming a delay in soluble metabolite production following bacterial growth, a correlation

can be made with PG3 copy number and bacterial copy number ($R^2 = 0.90$ for PG3, $R^2 =$

0.92 for Bacteria) that is somewhat stronger for bacteria. Without this time shift, there is no

correlation.
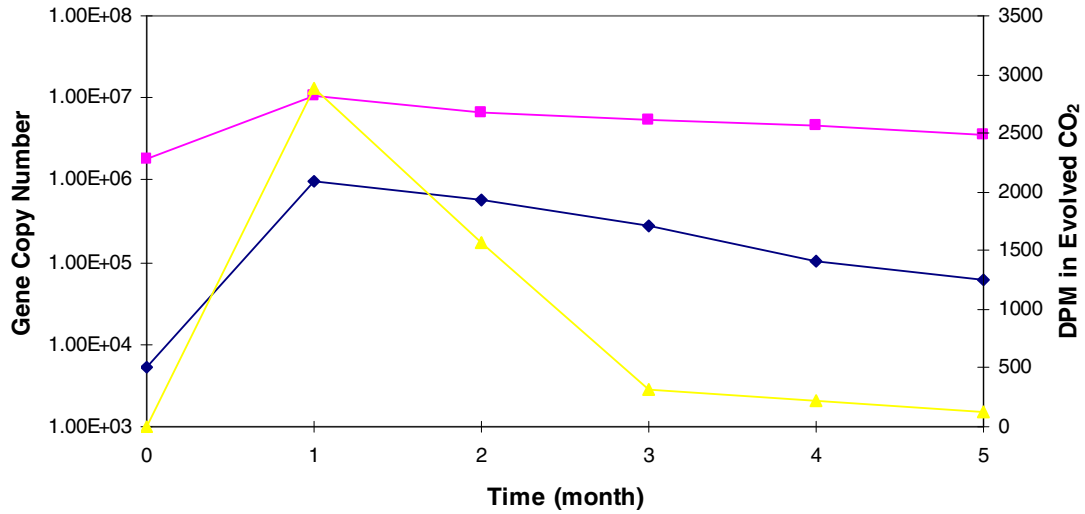
Figure 5.16. Pyrene Mineralization and 16S rRNA Gene Copy Numbers over Time. Pink: bacteria; blue: PG3; yellow: dpm.
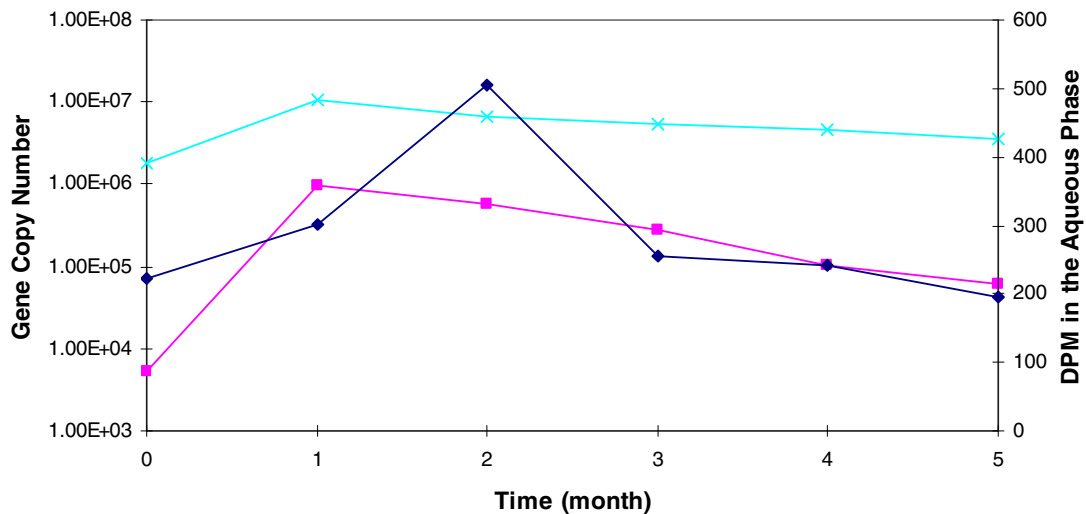
Figure 5.17. Aqueous Phase-Associated Radioactivity and Pyrene Group 3 Gene Copy Numbers over Time. Blue: aqueous phase-associated pyrene; aqua: bacterial gene copies; pink: PG3.

These data suggest that aqueous phase-associated radioactivity is influenced by microbial activity, such that the greater values seen for samples may in fact significantly differ from controls.

The drop in gene copy number of Pyrene Group 3 as pyrene mineralization plateaus suggests that cell growth may have ceased. The fact that plate counts and Bacterial 16S rRNA gene copies do not decrease significantly during the 1-3 month time points suggests that the colonies represent organisms other than the degrading population.

Pyrene Group 3 was first identified in a clone library derived from ^{13}C-pyrene incubations of a PAH-contaminated soil being treated in a slurry bioreactor (Singleton et al., 2006). Members of this group were hypothesized to be primary assimilators of the labeled pyrene. The appearance of this group under very different incubation conditions--static versus shaken, field-wet versus slurry, 10-day time course versus 5 months, nutrient levels of 0.024 mg N g^{-1} soil versus 0.5 mg N g^{-1} soil, and ~21μg pyrene ml^{-1} slurry (equivalent to 260 μg g^{-1} soil) versus 1,000 μg g^{-1} soil--suggests that it is not selected for by the incubation conditions, nutrient addition, or pyrene concentration. The only common denominator between these incubations was the availability of pyrene and the addition of nutrients. However, the nitrogen levels in these microcosms were ~20-times higher than in the bioreactor slurry. It is possible that these organisms respond to highly available pyrene and would not be the primary assimilators in an aged soil. It is also possible that they are the beneficiaries of cometabolism by other organisms. Others have shown that richer growth media enhance PAH cometabolism by *Sphingomonas* strains (Zhong et al., 2007). The addition of nutrients may have had this effect.

The eluate from the dominant band was not purified and sequenced, so it is unknown how similar these degraders would be to others in the ribosomal databases or in Group 3. Pyrene Group 3 is composed of γ-Proteobacteria, the majority of which are termed "unclassified", while the others belong to the *Xanthomonadaceae*. The Group 3 primer set amplifies only 0.06% of all γ-Proteobacteria currently listed in the Ribosomal Database Project (version 9) as determined by Probe Match, suggesting that their prevalence in nature is either limited or as yet undiscovered. The sequences belonging to this group have been retrieved from coral reefs, tannery effluents, compost, sediments and soils.

Previous 16S rRNA gene profiling of the CMN soil resulted in a clone library comprising organisms known to be capable of degrading PAHs (see Chapter 3). Further characterization of pyrene degraders by stable isotope probing showed that all organisms assimilating labeled carbon from pyrene were members of Pyrene Group 2 (PG2; Jones et al., 2007, submitted). PCR using primer sets for PG 1-3 showed that PG3 was not present in the CMN (as evidenced by lack of a product). Differences in original community structure may lead to the formation of different degrading consortia after exposure, such that the enrichment of Pyrene Groups 2 or 3 could have been dependent upon the other organisms originally present in the CMN and PMN, respectively. The role of either group in the degradation of pyrene has not yet been delineated, making it difficult to determine the reason for differential selection.

Recovery of the original level of community diversity was not possible to measure, given the poor DGGE profiling of the PMN at time zero and the inadequate coverage by its clone library. However, recovery as defined by the disappearance of a transient group of pyrene degraders was measurable. Nevertheless, by this definition, recovery did not completely occur over the time course of this experiment. It is possible that had samples been taken at

later times, recovery might have been shown. Taken together with the mineralization data,

the disappearance of Pyrene Group 3 could be used as an endpoint for remediation for this

soil. Since there was only 66% overall mineralization of the parent compound, it would be

advisable to perform analyses on extractable PAHs in addition to the mineralization data, in

order to determine if the remaining label is sorbed onto the soil, whether as parent compound

or insoluble metabolites, and considered unavailable (Roper and Pfaender, 2005). The

remainder would likely have been assimilated into biomass.

The relative abundance of Pyrene Group 3 (PG3) genes compared to Bacterial genes is

shown in Figure 5.18 below.
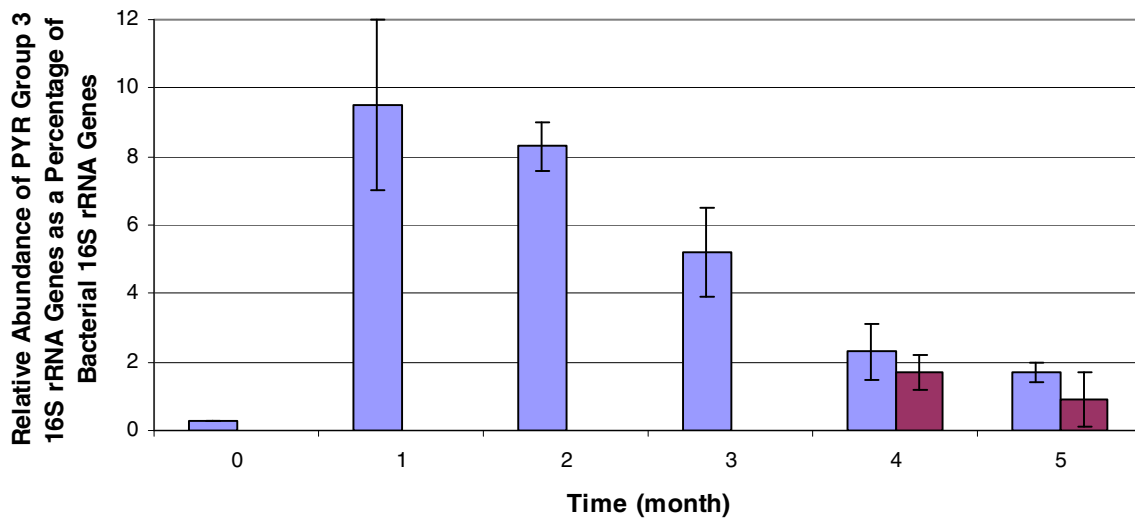
Figure 5.18. The Relative Abundance of Pyrene Group 3 16S rRNA Genes to Overall
Bacterial 16S rRNA Genes. Blue: singly-spiked microcosms; fuschia: respiked
microcosms. Values for t = 1-5 represent the average and standard deviation of reactions
from triplicate microcosm extracts; values at t = 0 represent the average and standard
deviation of triplicate reactions from a single extract.

The relative abundance of PG3 genes also increases dramatically from 0.3% of the total

eubacterial 16S rRNA genes at time zero to 9.5% at t = 1 month, then gradually decreases to

1.7% at month 5. The relative abundances of PG3 in the respiked microcosms are not

significantly different from those at times 4 and 5 months.

5.4.5 Presence or absence of pyrene Presumptive pyrene crystals were identified during

the examination of each microscopic field after FISH (see section 5.3.3.8). The results for

pyrene prevalence are given in Table 5.5 below. The percentage of images containing pyrene

and the image area occupied by pyrene were viewed as two-dimensional proxies for pyrene

concentration. The percentage of images containing pyrene varied across microcosm

replicates: pyrene was present in 91-100% of Slurry FISH images, whereas 57-100% of

Aggregate FISH images exhibited pyrene.

Table 5.5. Pyrene Prevalence in FISH Images.

Replicate Microcosm	Percentage of Images Containing Presumptive Pyrene Crystals		Percentage of Total Image Area Occupied by Pyrene	
	Slurry	Aggregate	Slurry	Aggregate
A	100	100	0.03 ± 0.04	0.03 ± 0.02
B	91	87	0.04 ± 0.03	0.08 ± 0.22
C	100	57	0.06 ± 0.03	0.10 ± 0.15

The overall percentage of images containing presumptive pyrene crystals (97% for Slurry,

81% for Aggregate) was not significantly different, due to the variability between replicate

microcosms for Aggregate FISH. The trend seen previously in the contaminated soils was

that the lower the initial level of PAH contamination before spiking with pyrene, the higher

the percentage of visualized pyrene in Slurry FISH images at the earlier time point and the

lower the percentage at the later time point (see chapter 4). The PMN also exhibits this later

time point behavior and shows less visible pyrene than the least of the contaminated soils,

CNC. It was suggested previously that, due to the high background PAH contamination,

binding sites for spiked pyrene were few, and that much of the spike was lost during slurry

formation at the early time point. The appearance of more pyrene at the later time points in the most contaminated soils was hypothesized to be due to the desorption of pyrene in larger amounts from a larger concentration gradient created by local adapted degraders.

The variation across replicate microcosms in Aggregate FISH images containing pyrene could be due to an insufficient number of fields examined, or simply to soil or microbial heterogeneity between the replicates. Inadequate mixing of the spiked pyrene was ruled out by measuring the radiolabel in the original spike by combustion. Microbial heterogeneity of the bulk sample was ruled out by comparative DGGE profiling of the replicates; however, heterogeneity at the microscale is certain. There was a greater percentage of Slurry FISH images than Aggregate FISH images that contained pyrene. This is in contrast with the contaminated soils and could be due to the fact that the spiked pyrene could more easily associate with the PMN soil and was not diluted out during Slurry FISH.

The overall percentage of image area occupied by pyrene was also not significantly different between Slurry FISH and Aggregate FISH images (0.04% for Slurry, 0.07% for Aggregate). The percentage of Slurry FISH image area occupied by a presumptive pyrene crystal was not different across the three replicate microcosms. The percentage of Aggregate FISH images containing pyrene was most different for replicate C (57% versus 100% of A and 87% of B). Although fewer Aggregate FISH images from microcosm C contained pyrene, the image area occupied by pyrene was greater than in microcosms A and B.

In summary, the PMN followed the trend seen with the contaminated soils (see Chapter 4): the lower the level of background PAH contamination, the less pyrene was visualized in Slurry FISH images at a later time point. Additionally, more Slurry FISH images contained

pyrene than Aggregate FISH images, although the differences were not significant. This was probably due to the great variability within and between the replicate microcosms.

5.4.6 Object distribution and spatial analyses FISH samples were taken from the incubated PMN at 2 months. This corresponded to the end of the peak mineralization rate, after pyrene was less associated with the solid phase, while cell numbers were still high, and just before the peak in aqueous phase-associated pyrene label. This was in hopes of capturing the active players in pyrene metabolism. However, due to financial constraints, FISH could not be performed at any other point during the incubation period, leaving no possibility of comparison with other time points.

5.4.6.1 Dispersion indices Dispersion indices were calculated for the image sets generated from each microcosm replicate--A, B, and C (see Table 5.6 below). A value greater than 2 indicates aggregation of the objects in the sample. The greater the index value, the greater the non-uniformity. The Aggregate FISH IDs were greater than Slurry FISH IDs for microcosms B and C, indicating a more non-uniform distribution of objects in the images from these microcosms. All indices, whether from Slurry or Aggregate FISH images, indicate non-uniform object distribution. This is to be expected in soils where resources are unevenly distributed and cells are most likely adhering to particles. However, the ID values for Aggregate FISH are more likely to be based on undisturbed spatial relationships.

Table 5.6. Indices of Dispersion for Replicate Microcosms.

Replicate Microcosm	Index of Dispersion	
	Slurry	Aggregate
A	11.3	5.0
B	23.7	44.2
C	9.8	16.4

5.4.6.2 Nearest neighbor analysis: cell to cell and/or pyrene Mean nearest neighbor values and their standard deviations were calculated for each image and compared to similar values generated for an expected random distribution. Table 5.7 provides a comparison of the observed and expected values (O/E ratio) for each microcosm replicate.

Table 5.7. Observed/Expected Ratios of Mean Nearest Neighbor Values.

Replicate Microcosm	Average Ratio of Observed to Expected Mean Nearest Neighbor Value (± sd)	
	Slurry	Aggregate
A	0.77 ± 0.27	0.69 ± 0.24
B	0.72 ± 0.38	0.84 ± 0.22
C	0.69 ± 0.26	0.75 ± 0.26

The O/E ratios ranged between 0.27-3.07 for Slurry FISH images and between 0.20-1.29 for Aggregate FISH images. None of the Slurry FISH images showed significant avoidance, as indicated by O/E > 1, whereas eight images (26.7% of images containing pyrene) showed significant clustering (O/E < 1; $P < 0.001$).

For Aggregate FISH images as well, none of the images showed significant avoidance. Ten images (25.7% of images containing pyrene) were significant for clustering tendencies (P values varied, all were less than 0.05: six at a level of P<0.001, two with $P < 0.01$, one at $P < 0.02$, and one at $P < 0.05$).

It was hypothesized that cell clusters proximal to pyrene might indicate utilization or, at a minimum, a lack of toxicity. This was tested with regression analysis of the observed mean nearest neighbor values (MNND) for the significantly clustered images and the image area occupied by pyrene. A clear relationship was established, but only for Aggregate FISH images. Significantly clustered Aggregate FISH images from microcosm A (n = 3) showed a strong negative correlation with pyrene-occupied image area ($R^2 = 1$). Microcosm B also

showed a negative correlation, although it was not as strong ($R^2 = 0.88$; n = 5). Microcosm C did not generate any images with significant clustering that also contained pyrene; therefore, it was not included in the analysis. Overall, this suggests that cells clustered strongly in areas of greater pyrene occupation. While this may not directly point to utilization, it does suggest cell proliferation in areas of high pyrene concentration, which certainly indicates a lack of toxicity.

Regression analysis was also performed on the Slurry FISH images with significant clustering. In these images, a strong correlation is only meaningful if both the cells and the pyrene are associated with the same soil particle, since the formation of a slurry would have destroyed any initial spatial relationship that existed. That being said, there was a strong correlation between MNND and pyrene-occupied image area for Slurry FISH images of microcosm A ($R^2 = 0.99$; n = 4). However, this was a positive correlation, indicating that cells were clustered in areas of low pyrene concentration. While this could indicate toxicity, it cannot rule out a decrease in pyrene concentration due to utilization. There was no correlation for Slurry FISH images of Microcosm B, and it was not possible to determine a relationship from microcosm C (n = 1 significantly clustered image).

As shown above, the correlation between mean nearest neighbor distances and pyrene prevalence is ambiguous. If negative (i.e. the more pyrene the more clustering among cells), this can only suggest growth in the presence of pyrene. However, if the correlation is positive (i.e. the more pyrene the less clustering), then two inferences can be made: 1) growth occurs in the absence of pyrene, indicating toxicity, or 2) growth led to the disappearance of pyrene, indicating utilization. Because of this ambiguity, an attempt was made to correlate cell density with pyrene prevalence. In this case, a positive correlation (i.e.

more pyrene, more cells) indicates utilization. A negative correlation (i.e. less pyrene, more cells) suggests toxicity.

There was a negative correlation between the image area occupied by pyrene and that occupied by cells in the Aggregate FISH images ($R^2 = 0.83$) but only at the highest cell density (n = 4 images). This suggests that the greatest cell density was observed in areas of low pyrene concentration. If this trend had continued over all pyrene concentrations, it could have suggested a toxic response. However, because it was only shown in images with the highest cell density, it suggests instead that pyrene utilization by the cells accounted for its low concentration. These images were those in which the rod-shaped cells were prevalent. There was no correlation between cell- and pyrene-occupied area in the Slurry FISH images.

In summary, it was not possible to infer pyrene utilization from the Slurry FISH images, due to the lack of a correlation between nearest neighbor distances, cell density, and pyrene concentration. However, correlation data from the Aggregate FISH images suggest that cell growth resulted in pyrene disappearance.

Two sample FISH images are shown below in Figures 5.19a and b. These images depict significant clustering of cells and pyrene, as evidenced by a nearest neighbor O/E ratio significantly less than one. Image 5.19a is from Slurry FISH; image b is from Aggregate FISH.
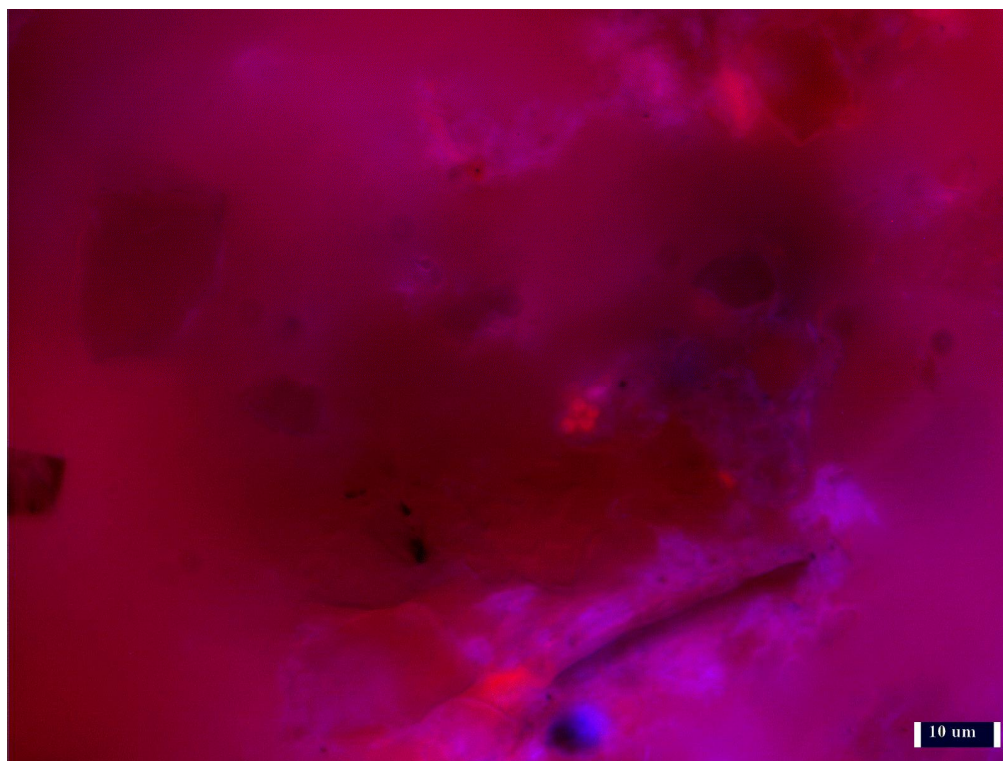
Figure 5.19a. Example of Slurry FISH Image with Significant Clustering of Objects (overlay of TRITC- and PYR-filtered images). Note cells (red) in center of image and presumptive pyrene crystal (blue) at bottom of image.
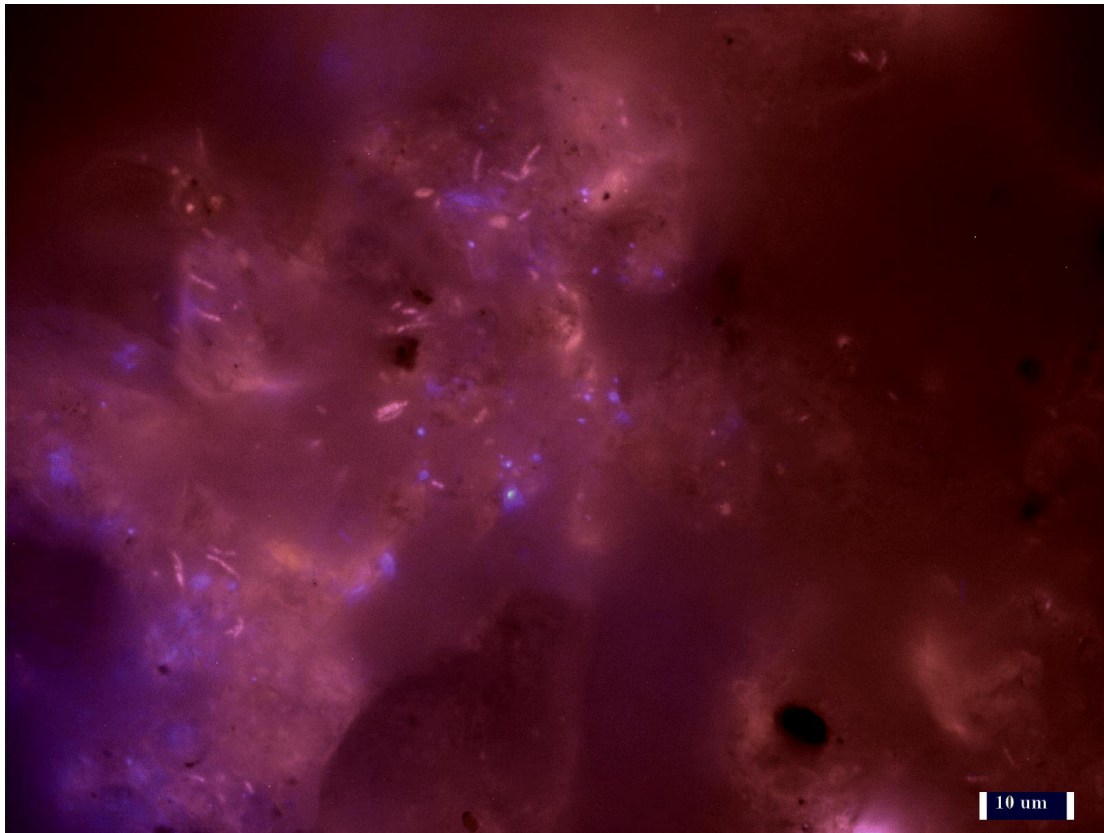
Figure 5.19b. Aggregate FISH Image Showing Significant Clustering of Objects (overlay of TRITC- and PYR-filtered images and their respective Red and Blue channels).

5.4.6.3 *daime*: spatial arrangement analysis of cells and pyrene

5.4.6.3.1 Pair cross-correlation values A summary of the average pair cross-correlation values is given below in Table 5.8. These values are plotted versus the lengths of dipole radii (distance) in Figures 5.20-5.22 below for replicate microcosms A-C, respectively. Within each figure (a) depicts Slurry FISH results, and (b) represents Aggregate FISH.

Table 5.8. Average Pair Cross Correlation Values Calculated at Given Distances from Pyrene for Each FISH Method.

Microcosm	< 5 μm		5-10 μm		All Distances	
	Slurry	Aggregate	Slurry	Aggregate	Slurry	Aggregate
A	3.21 ± 1.34	2.63 ± 1.80	3.18 ± 1.38	3.70 ± 1.38	1.63 ± 1.74	1.52 ± 1.58
B	3.85 ± 2.04	0.94 ± 0.69	3.12 ± 0.86	4.06 ± 2.02	1.66 ± 1.36	1.46 ± 1.37
C	1.74 ± 1.13	0.73 ± 0.48	1.15 ± 0.46	1.56 ± 0.28	1.56 ± 1.19	1.08 ± 0.70

194
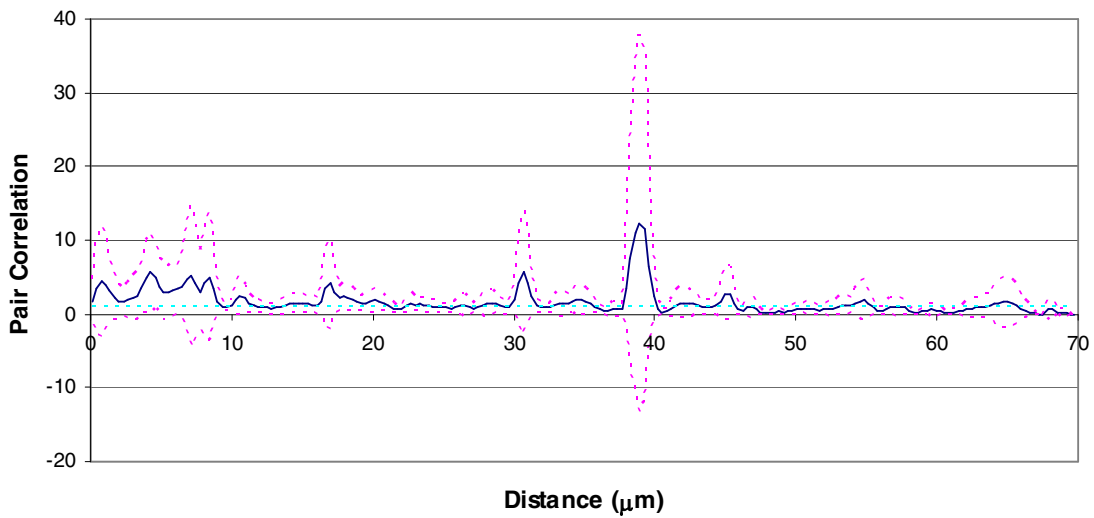
Figure 5.20a. Cross-correlation Values Plotted over Distance: Slurry FISH Images from Microcosm A. Pink dotted lines indicate ± 95% confidence intervals. The light blue dotted line represents a random distribution at a constant g(r) of one.
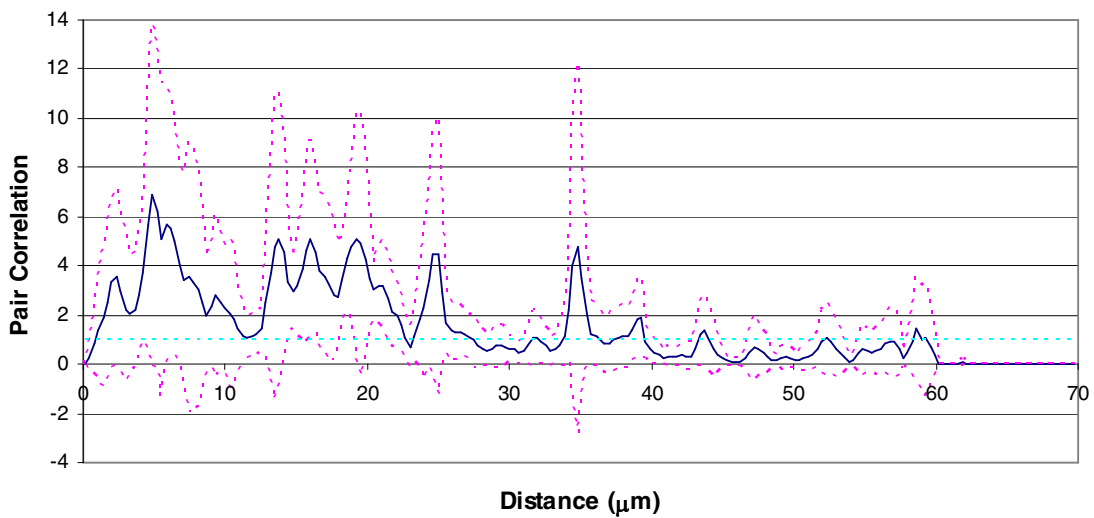
Figure 5.20b. Cross-correlation Values Plotted over Distance: Aggregate FISH Images from Microcosm A. Pink dotted lines indicate ± 95% confidence intervals. The light blue dotted line represents a random distribution at a constant g(r) of one.

Values from Slurry FISH images (Figure 5.20a) suggest weak clustering up to ~10 microns

and sporadic clustering at various long-range distances. Otherwise, values approach unity,

indicating randomness. The highest percentage of g(r) values that exceed one occur less than 5 microns from a pyrene crystal, suggesting that the organisms measured at this distance are not adversely affected by pyrene and that they might actually be utilizing it.

Values from Aggregate FISH (Figure 5.20b) suggest different clusters occurring between 0-12 microns and 12-23 microns, and at other mid-range distances. At greater distances, the pair correlation values reflect randomness to weak avoidance. The highest percentage of pair correlation values that exceed one occur between 5-10 microns. As with Slurry FISH, this suggests a lack of toxicity and/or utilization of the pyrene itself. Clustering in Slurry FISH images is more spread out over distance, whereas Aggregate FISH images exhibit more clustering at closer ranges. There was no significant difference between the overall g(r) values measured for Slurry FISH and Aggregate FISH or for the values generated at distances less than 10 microns.
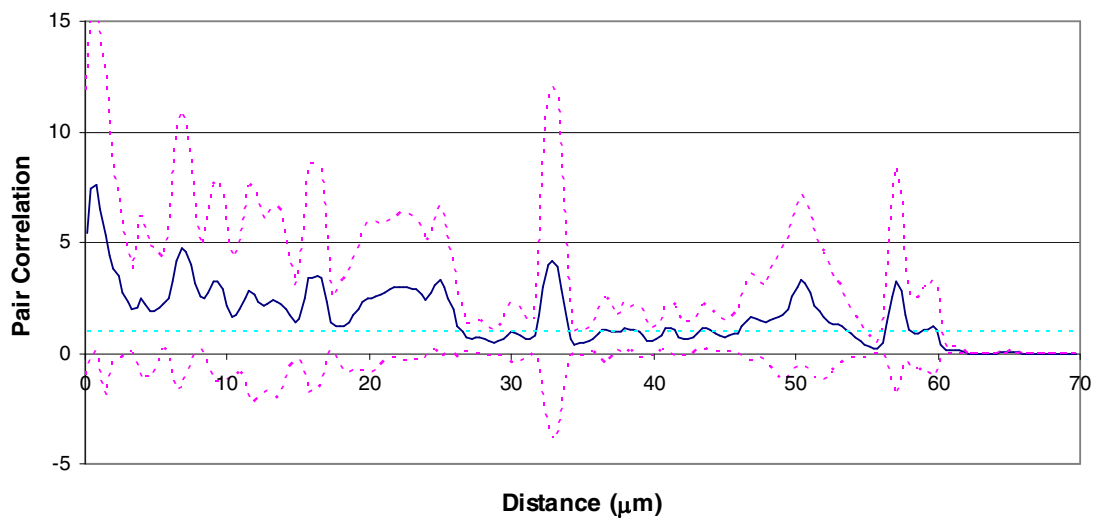
Figure 5.21a. Cross-correlation Values Plotted over Distance: Slurry FISH Images from Microcosm B. Pink dotted lines indicate ± 95% confidence intervals. The light blue dotted line represents a random distribution at a constant g(r) of one.

196
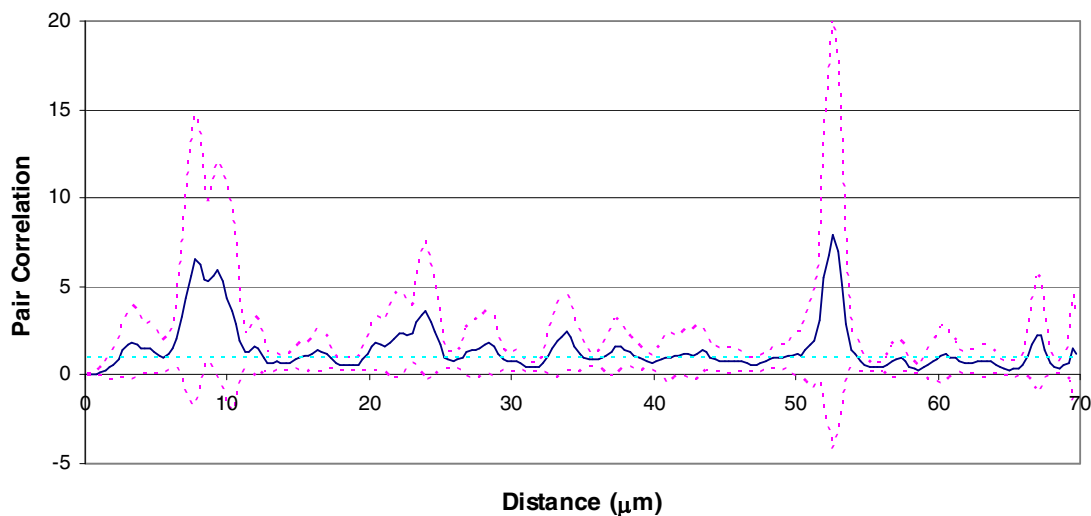
Figure 5.21b. Cross-correlation Values Plotted over Distance: Aggregate FISH Images from Microcosm B. Pink dotted lines indicate ± 95% confidence intervals. The light blue dotted line represents a random distribution at a constant $g(r)$ of one.

For Microcosm B, the $g(r)$ values for Slurry FISH images suggest weak clustering up to 27 microns, between 32-35 microns, 47-53 microns, and 57-58 microns. Otherwise, the values approach unity, suggesting randomness (Figure 5.21a). All $g(r)$ values generated at distances less than 20 microns are greater than one. Pair correlation values generated from Aggregate FISH images (Figure 5.21b) reflect weak clustering at sporadic distances, namely ~3-13 microns, 20-26 microns, 33-35 microns, and 51-55 microns. Otherwise, the values reflect a random distribution with $g(r)$ values close to one and weak repellant tendencies at greater distances. The highest percentage of $g(r)$ values that are greater than one occurs between 5-10 microns. Slurry FISH images from this microcosm show significantly more clustering at distances less than 5 microns than do Aggregate FISH images ($P < 0.001$) but no difference at greater distances.
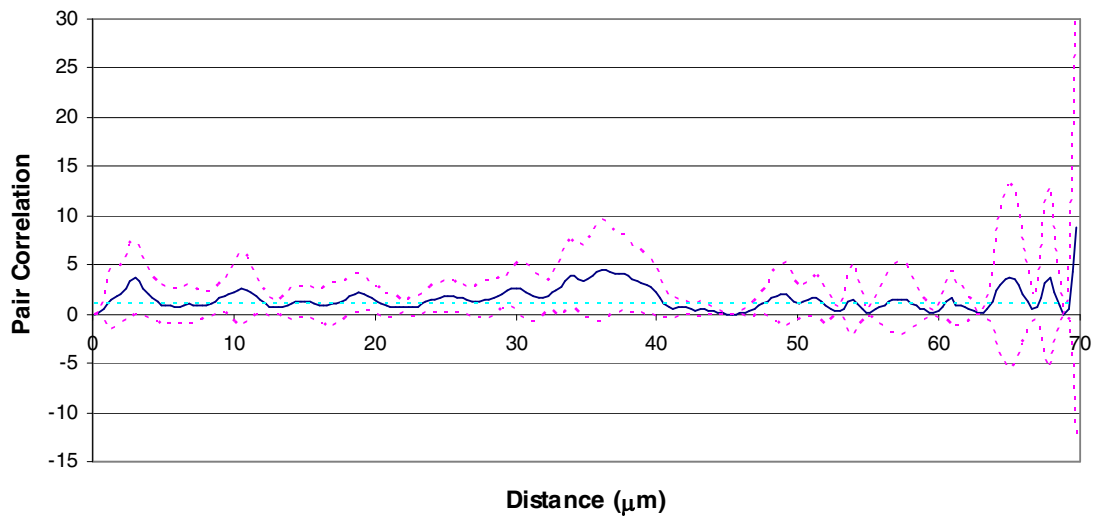
Figure 5.22a. Cross-correlation Values Plotted over Distance: Slurry FISH Images from Microcosm C. Pink dotted lines indicate ± 95% confidence intervals. The light blue dotted line represents a random distribution at a constant g(r) of one.
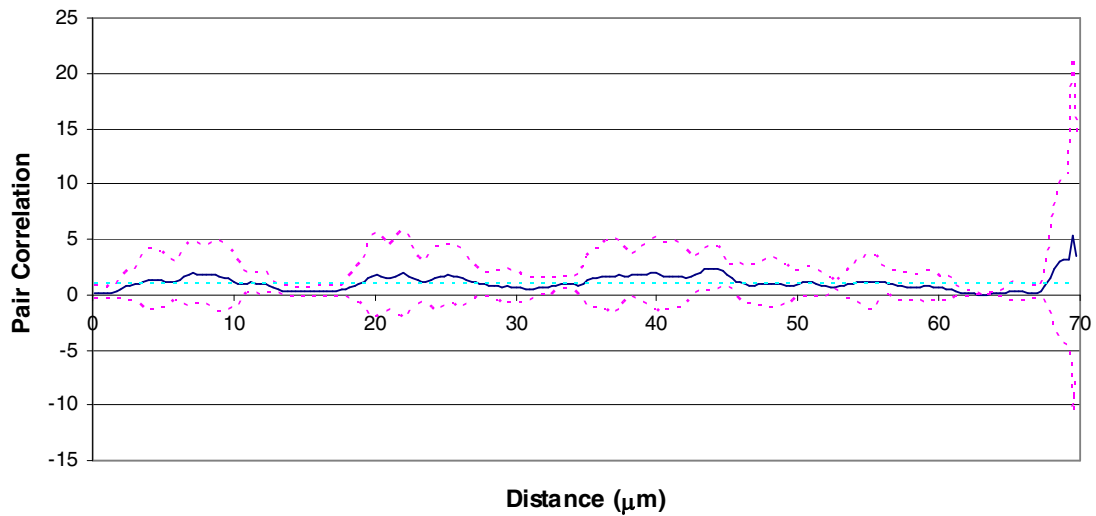
Figure 5.22b. Cross-correlation Values Plotted over Distance: Aggregate FISH Images from Microcosm C. Pink dotted lines indicate ± 95% confidence intervals. The light blue dotted line represents a random distribution at a constant g(r) of one.

Pair correlation values generated for Slurry FISH images from Microcosm C tend to be

greater than those for Aggregate FISH images (63.5% versus 47.6% of all g(r) values are

greater than one). Both Figures 5.22a and 5.22b show occasional weak clustering, but the overall g(*r*) values reflect random distributions for both sets of images. It should be noted that only one image from each set for microcosm C showed significant clustering, as measured by its O/E ratio. Therefore, the randomness observed in these samples is not surprising. The pair correlation values for this microcosm were significantly greater for Slurry FISH at distances less than 5 microns (P < 0.01) but were greater for Aggregate FISH at distances between 5-10 microns (P < 0.01).

Overall, pair correlation values were low, indicating weak clustering regardless of the method. Still, overall average g(*r*) values were significantly greater for Slurry FISH than Aggregate FISH (P < 0.001). As shown in the previous chapter, higher pair correlation values in Slurry FISH samples were probably due to the association of cells and/or pyrene with soil particles. Due to the high soil mass on the filters for this experiment, it was not possible to determine definitively if clustering in the Slurry FISH images was due to this association or not. Seven Slurry FISH images had a low enough mass of soil on the filter to check for this association. Out of these, 93.2 % of cells and 95.5% of pyrene crystals were soil-associated (i.e. located within one micron of a soil particle within the 2D image). However, the results clearly show that cells have a greater tendency to cluster at distances less than 5 microns from pyrene in Slurry FISH images and between 5-10 microns in Aggregate FISH images.

Whether the difference between 5 microns or 10 microns is relevant at the microbial scale in these microcosms is unknown. According to Bosma et al. (1997), the diffusion of a hydrophobic organic contaminant through soil can be estimated as 8.6 μm day^{-1}. Although this greatly oversimplifies the complex relationship between mass transfer and cell uptake, it

does suggest that the differences between Slurry FISH and Aggregate FISH clustering tendencies are meaningful. Since the original spatial relationships were destroyed by the formation of a slurry, the clustering tendencies below 5 microns in Slurry FISH images indicates that they are likely due to the association of cells and pyrene with soil particles. In the case of Aggregate FISH, the three-dimensional structure was minimally compromised during embedding; therefore, the clustering tendencies between 5-10 microns may more accurately depict the spatial relationships *in situ*, especially for non-adherent cells.

5.4.6.3.2 Frequency distributions of nearest neighbor values The percentage of cells at any given distance from a pyrene crystal, or the frequency distribution based on mean nearest neighbor distances, is given below in Figures 5.23-5.25 for replicate microcosms A-C, respectively. Within each figure, (a) depicts results for Slurry FISH, and (b) represents Aggregate FISH. Randomly distributed objects are depicted by a Poisson distribution; while a narrowed distribution reflects clustering (Kepner and Pratt, 1994; Russ, 2002). More than one underlying distribution within the histogram is not unusual (Russ, 2002) and could indicate patches of growth at varying distances. For bacteria in soil, these patches would be expected in areas of higher resource availability and once again point to the non-uniform nature of microbial distribution.
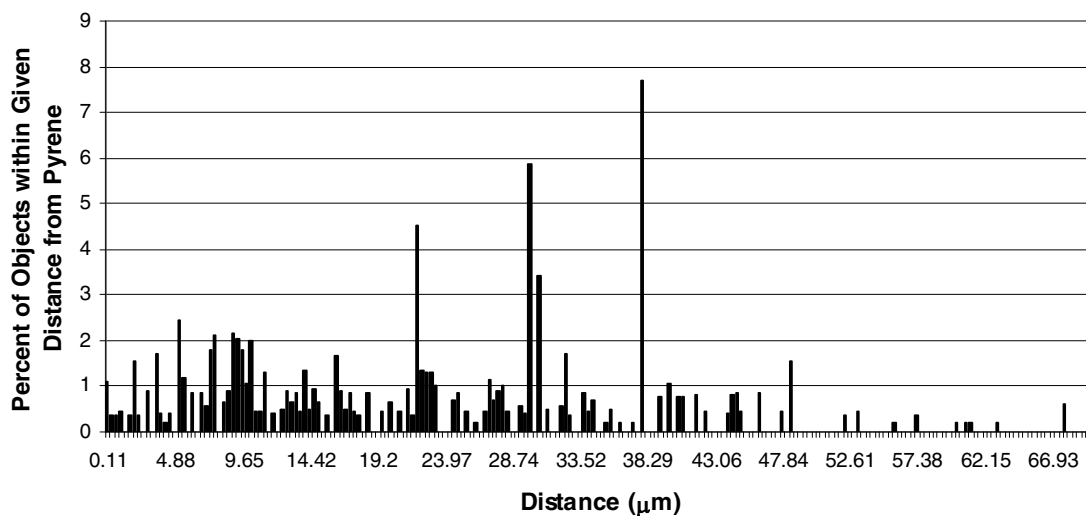
Figure 5.23a. Mean Nearest Neighbor Distribution versus Distance: Slurry FISH Images from Microcosm A.
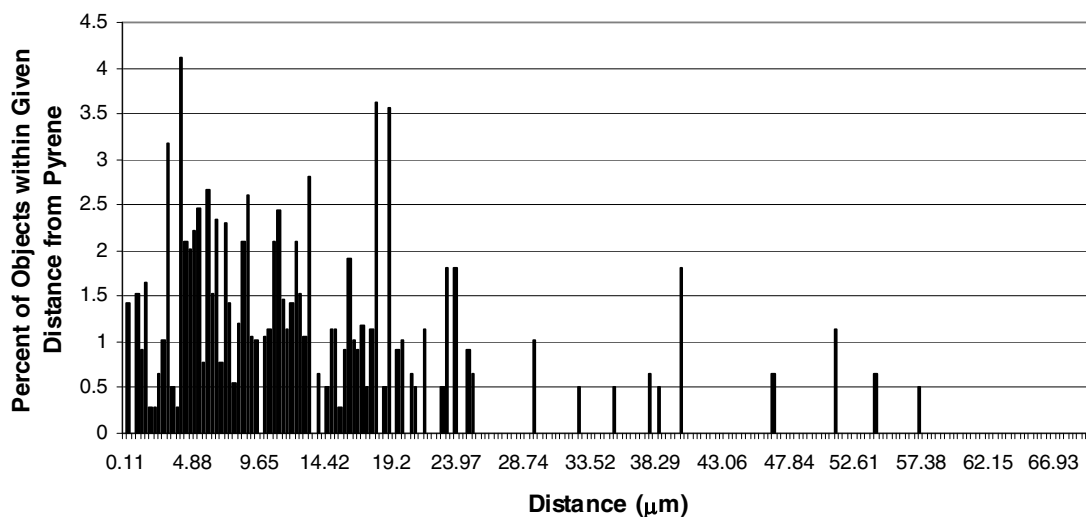
Figure 5.23b. Mean Nearest Neighbor Distribution versus Distance: Aggregate FISH Images from Microcosm A.

The histogram in Figure 5.23a is flat with occasional spikes in the percentages. There are

possibly 3 underlying subdistributions within the histogram: from 0 to 19 microns, between

19-26 microns, and from 26-37 microns. The histogram in Figure 5.23b is narrowed and

201

shifted to the left within 0-25 microns, suggesting clustering tendencies. Twenty-two percent of objects in this histogram are found within 5 microns of a pyrene crystal as compared to only 8% of cells in Figure 5.23a. Aggregate FISH images from microcosm A yielded a clustered histogram, as evidenced by its narrowing. Additionally, its shift to the left, i.e. 46% of the objects occur at distances less than 10 microns, suggests pyrene utilization. The relative flatness of the Slurry FISH histogram could suggest that the soil slurry was well mixed prior to filtering. The possible underlying distributions in this histogram are difficult to interpret, since the soil aggregate structure was not intact for FISH. If they reflect patchy cell growth, it is possible that cells either grew in clumps or were associated with soil particles.
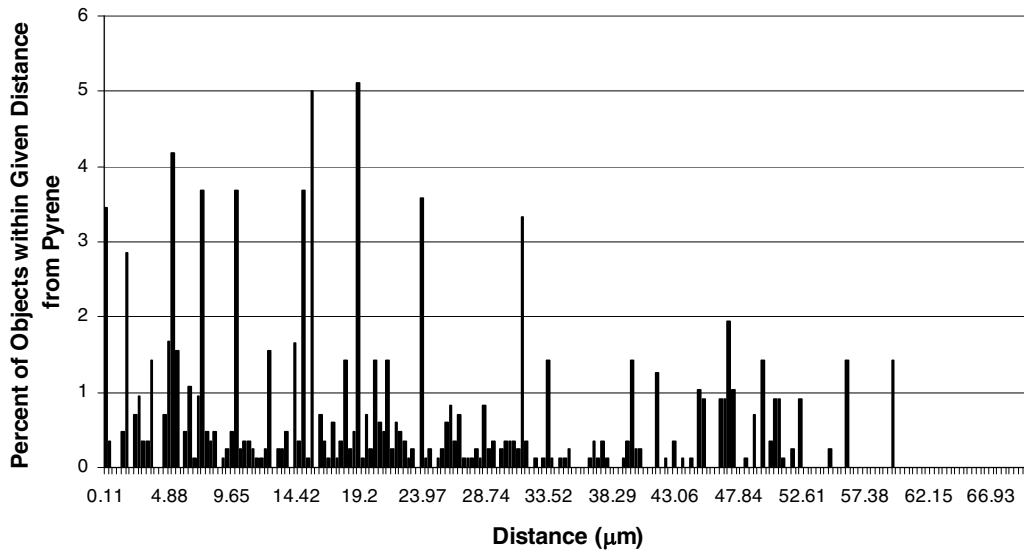
Figure 5.24a. Mean Nearest Neighbor Distribution versus Distance: Slurry FISH Images from Microcosm B.
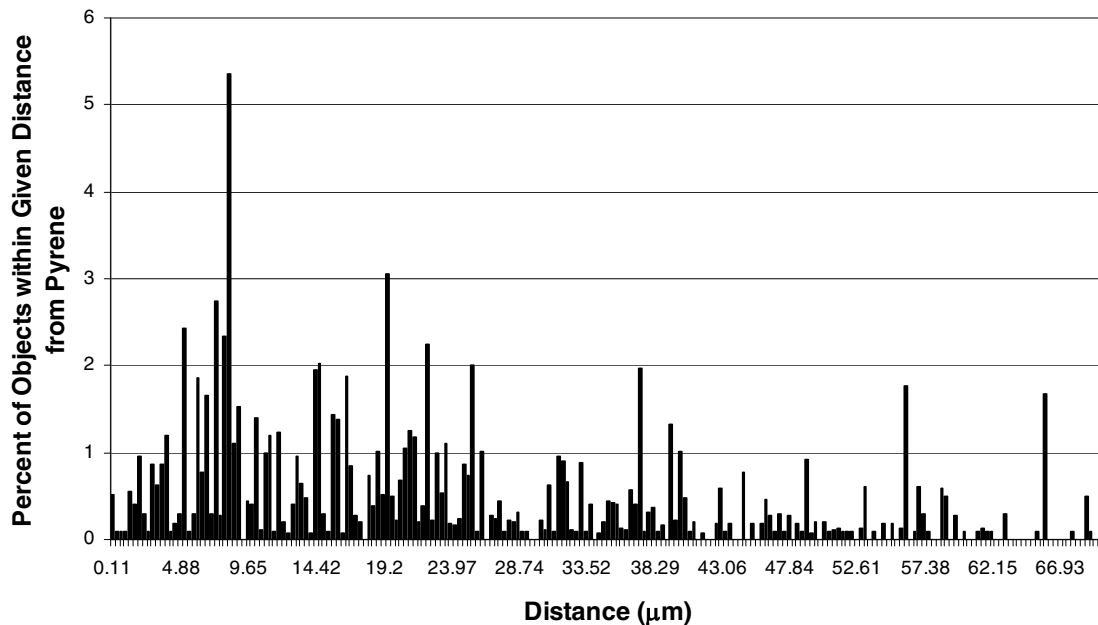
Figure 5.24b. Mean Nearest Neighbor Distribution versus Distance: Aggregate FISH Images from Microcosm B.

The histogram depicted in Figure 5.24a is very uneven, spiky, and disperse. There are questionable underlying distributions (0-12, 12-24, and 24-33 microns), but spikes in the percentages occur throughout the histogram. Figure 5.24b is more evenly distributed with possible underlying distributions between 0-18, 12-29, and 29-42 microns. Aggregate FISH images from microcosm B generated a more ordered, although still "spiky", histogram than their Slurry FISH counterpart. Roughly the same percentage of objects were located at a distance less than 10 microns from pyrene for each set of images (29% for Aggregate FISH and 31% for Slurry FISH); however, the percentage of objects in Slurry FISH images that were less than 5 microns from pyrene was near thrice that of Aggregate FISH images (19% versus 7%). Underlying distributions found in Aggregate FISH histograms could be interpreted as patches of cells growth at various distances from pyrene, given that the spatial relationship had been preserved. If this is the case, the highest percentage of cells (22%)

were between 5-10 microns from pyrene, whereas only 7% were located at a distance less

than 5 microns from pyrene.
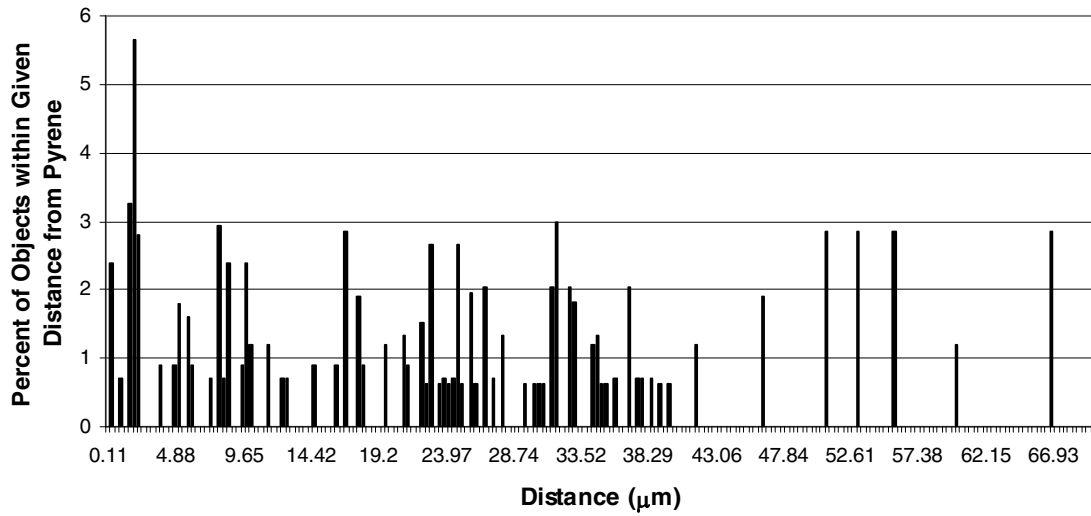
Figure 5.25a. Mean Nearest Neighbor Distribution versus Distance: Slurry FISH Images from Microcosm C.
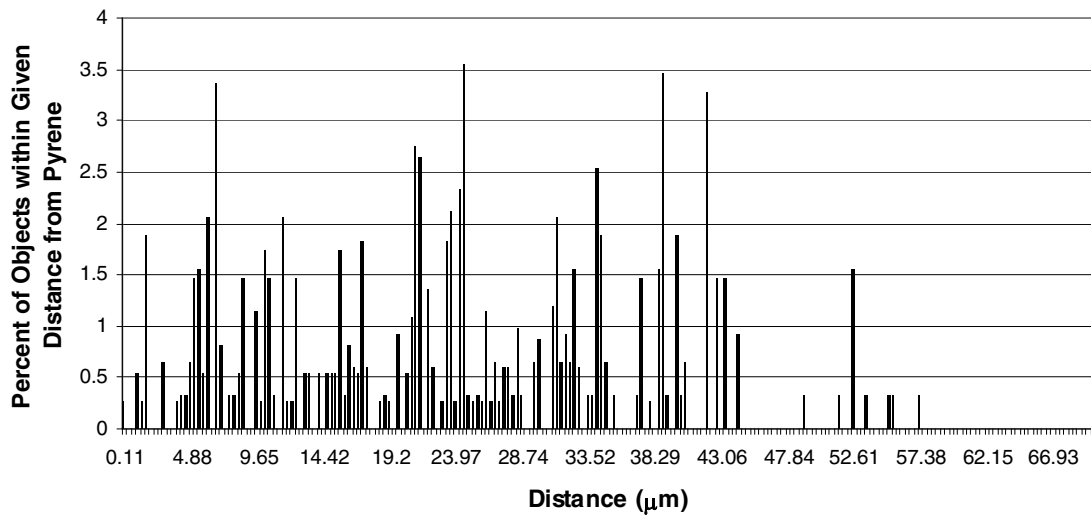
Figure 5.25b. Mean Nearest Neighbor Distribution versus Distance: Aggregate FISH Images from Microcosm C.

Both the histograms in Figures 5.25a and b are irregular, and it is difficult to tell whether

underlying distributions exist. Slurry FISH images from microcosm C resulted in a

histogram apparently even more irregular than its Aggregate FISH counterpart. However, a

larger percentage of cells were located less than 5 microns from pyrene (17%) in this

histogram than in the Aggregate FISH histogram (5%). It should be noted that 43% (3/7) of

the Aggregate FISH images from microcosm C contained no pyrene and could not be

included in the *daime* analysis.

One factor that has certainly affected these results is the percentage of objects involved in

a positive "hit"-- a dipole that touches both a pyrene crystal and a cell. The percentage of hit

objects was not different between the Slurry FISH images from all three microcosms (76%,

84%, and 88% for A, B, and C, respectively). In contrast, Aggregate FISH images generated

95%, 68%, and 78% hits for A, B, and C, respectively. A truly representative histogram

should obtain a hit percentage of 95% or above (*daime* version 1.1, H. Daims, 2005). This

could indicate why the histogram generated for Aggregate FISH from microcosm A images

is more even than the others and suggests that, perhaps, this tool is inadequate for measuring

the spatial relationships in the remainder of image sets.

Hits depend on the dipole lengths that are used. This study used lengths that increased by

~0.30-0.40 microns. Unfortunately, an attempt to use all suggested dipole lengths

(increments of 0.03-0.04 microns) was no more successful in generating a larger hit

percentage, and it required a vast amount of computing time (~9-10 hours/image). This is

likely a limitation of the *daime* software rather than the images themselves.

Overall, the Slurry FISH images generated histograms that were more irregular and

"spiky" than Aggregate FISH histograms, especially for microcosms A and B. This, in

contrast to the more ordered appearance of the Aggregate FISH histograms, suggests that the spatial arrangement of objects in the Slurry FISH images were destroyed during slurry formation. These spikes in percentages, coupled with the fact that percentages are higher at distances less than 5 microns from pyrene, suggests that there are clusters of cells adhering to the same soil particles as pyrene. This could indicate pyrene utilization. This finding is similar to that in the previous chapter and suggests that Slurry FISH is adequate for measuring spatial relationships at lesser distances when all objects are adherent to soil or to each other.

5.5 Conclusions

Pyrene spiked into a previously uncontaminated soil resulted in significant changes to the bacterial community over a five-month incubation period. As hypothesized, there was an overall decrease in richness and evenness, as evidenced by DGGE banding patterns. Diversity decreased even more after respiking microcosms with a second dose of pyrene. However, the community structures did not approach that of the contaminated soil from the Reilly site (CMN), as shown by pairwise similarity coefficients based on the DGGE profiles. This is probably due to 1) the lack of a non-aqueous phase, i.e. creosote, and the associated PAHs therein, 2) the lack of aging and, as a result, differential contaminant availability, and 3) the fact that the CMN was capped by 8 feet of topsoil at the time it was retrieved. Furthermore, the community did not recover its original structure at the end of the incubation period, suggesting that overall structure may not be an adequate endpoint for remediation purposes.

Mineralization of pyrene began after a two-week lag period. Maximum rates were comparable to those seen in the contaminated soil from the same site under similar incubation conditions, but the overall extent of mineralization in the PMN was greater.

One dominant band appeared in the DGGE profiles, pointing to the selection of pyrene-degrading organisms. This was verified by quantitative PCR using primer sets specific for Pyrene Groups 1-3. The increase in Pyrene Group 3 gene copy numbers correlated strongly with pyrene mineralization ($R^2 = 0.97$). The data suggest that the presence of a transient population of degraders, opportunistic or not, is a valid indicator of contaminant availability, and its disappearance could be utilized as an endpoint for remediation. The continued presence of PG3 in the samples suggested that pyrene was still present in the incubations or that cell numbers had not yet decreased to their original levels.

Overall, this study found that correlating community structure with mineralization data was sufficient to infer structure-function relationships without the use of more sophisticated techniques.

Although it seems obvious that the creation of a slurry should destroy the spatial arrangement of objects within soil, this was not immediately evident from the FISH results. In fact, stronger clustering tendencies existed at distances less than 5 microns from a pyrene crystal in Slurry FISH images than in Aggregate FISH when measured as pair correlation values. The clustering signals were strongest in Aggregate FISH images between 5-10 microns. This suggests that although the larger three-dimensional structure is destroyed by slurry formation, at a scale relevant to microbes (i.e. less than 5 microns), the relationship remains intact. This may be due to the association of both cells and pyrene with soil particles. FISH performed on an aggregate from microcosm A was able to suggest an

association between potentially pyrene-utilizing organisms and pyrene prevalence, as evidenced by its narrow histogram and high pair correlation values. Regression analysis for Aggregate FISH showed that at low pyrene prevalence, cell density was high but clustering tendencies were lower, whereas at high pyrene prevalence, the clustering tendencies were stronger. While this could indicate cell proliferation in the absence of pyrene, it could also indicate pyrene utilization by those same cells. In contrast, Slurry FISH showed no correlation between pyrene and cell density, a strong positive correlation between pyrene and nearest neighbor distances for microcosm A (more pyrene, less clustering) and a weakly negative one for microcosm B.

   Future endeavors should include the development of a probe specific for Pyrene Group 3 and the use of confocal laser scanning microscopy for a more accurate view of the soil aggregate. Additionally, this study might have benefited from the use of clone libraries at other time points (e.g. months 1 and 5; respiked samples).

6.0 Final Summary

The objectives of this study were 1) to compare the communities in an aged, PAH-contaminated soil and an uncontaminated soil from within the same site; 2) to see if the community in the uncontaminated soil would approach that in the contaminated soil after spiking either once or twice with pyrene; 3) to develop a method for retaining the aggregate structure of soil that was amenable to fluorescence *in situ* hybridization; and 4) to use that method to determine if spatial relationships existed between the spiked contaminant, pyrene, and the indigenous bacteria that might suggest utilization. The study found that: 1) the long-term PAH contamination of the CMN soil resulted in a bacterial community that was far less diverse than that of the uncontaminated PMN and contained only *Proteobacteria*; 2) spiking with pyrene irreversibly reduced community diversity, but resulted in the transient appearance of a group of Proteobacterial pyrene degraders that correlated with pyrene mineralization; 3) the Aggregate FISH method did not show clustering of bacteria with respect to pyrene as did its comparative Slurry FISH method, but the latter showed promise in inferring pyrene utilization from spatial relationships and was useful in describing differences between the contaminated soils.

Although conducting structural and spatial analyses of the microbial communities in PAH-contaminated soils were the goals of this research, it should not be forgotten to what end these findings must be applied--that is, the clean-up of contaminated sites. The findings of this study could help to focus remediation and monitoring activities on the relevant soil microbial populations.

Effective bioremediation of contaminated soil is dependent upon many factors, not the least of which is the indigenous microbial community. The structure and functional diversity of that community may be significantly different than they were prior to the contamination event(s). The community will have evolved by forced selection into one which has the capability to deal with its insult. Understanding the basis for this evolution will help to exploit the community's potential for bioremediation and assist in monitoring its progress.

Although seldom addressed, the spatial arrangement of microbial communities and contaminants in soil is important, especially if natural attenuation is the chosen remediation strategy. Contact between microbial life and contaminants may be limited, especially in the absence of water or another liquid interface. However, if colonization is shown to occur proximal to the contaminant, knowledge of which organism is involved will aid in the monitoring process and perhaps lead to means of enhancing its activity.

Microbial life is both figuratively and literally bound to the organized complex called soil (Young and Crawford, 2004). Thus, it stands to reason that changes in the soil, such as those resulting from contamination, should be reflected by changes in microbial community structure, function, or spatial distribution. This was the underlying premise for this work.

In the end, the microbes will have the last word.

--Louis Pasteur

APPENDIX I

Groupings of Contiguous Clone Sequences

Group Designation	Clone Sequences Contiguous at 97% Similarity	Clone Sequences Contiguous at 100% Similarity
1	3, 4, 5, 9, 30, 32, 36, 42, 44, 45, 47	4, 47
2	6, 13, 20, 21, 24, 25, 26, 31, 35, 37, 40, 43, 49, 50	6, 13, 21, 43, 49
3	7, 41	7, 41
4	11, 15	11, 15
5	1, 46	24, 25
6	23, 28, 29	3, 30

APPENDIX II

Optimization of Hybridization Buffer and Wash Solution for FISH
(The numbers represent the sum of color and luminance ratios for each image averaged over triplicate images, unless specified otherwise, or a range when only duplicate images were available.)

a. Optimization of Hybridization Buffer (HB) Composition and Wash Solution (SET) Salt Concentration using Pure Culture Mix.

HB / SET	No Formamide	Formamide
FITC		
5X	3.95 ± 0.86	3.88 ± 0.31
2.5X	3.56-5.19	3.38 ± 0.08
1X	4.08 ± 0.42	3.29 ± 0.10
TRITC		
5X	4.46 ± 0.35	4.70 ± 0.65
2.5X	3.80 ± 0.25	3.94 ± 0.49
1X	4.18 ± 0.23	4.06 ± 0.15

b. Optimization of Hybridization Buffer (HB) Composition and Wash Solution (SET) Salt Concentration using Slurried CMN Soil.

HB / SET	No Formamide	Formamide
FITC		
5X	2.53 ± 0.09	2.56 ± 0.10
2.5X	3.18 ± 0.57[4]	2.35-2.45
1X	2.36-2.84	2.25-2.31
TRITC		
5X	2.50 ± 0.14	2.41 ± 0.15[4]
2.5X	2.70 ± 0.21[4]	2.60-2.78
1X	2.92-0.12	2.46-2.52

c. Optimization of Hybridization Buffer (HB) and Wash Solution (SET) pH Using Pure Culture Mix.

SET \ HB	8.13	8.5	9.0	9.5
	FITC			
8.0	3.72-5.23	---	---	---
8.5	2.95[1]	---	---	---
9.0	4.76 ± 2.36[4]	5.62 ± 2.41[4]	---	---
9.5	6.13 ± 2.66	4.80-9.06	7.54 ± 1.64	5.63 ± 1.30
	TRITC			
8.0	4.33-4.46	---	---	---
8.5	3.89-4.40	---	---	---
9.0	5.98 ± 2.12[4]	6.77 ± 1.39[5]	---	---
9.5	5.26 ± 0.54	6.25 ± 1.30	7.09 ± 1.09	6.76 ± 1.63

d. Optimization of Hybridization Buffer (HB) and Wash Solution (SET) pH Using Slurried CMN Soil.

SET \ HB	8.13	8.5	9.0	9.5
	FITC			
8.0	2.02 ± 0.61	---	---	---
8.5	2.19 ± 0.22	---	---	---
9.0	1.73-2.16	2.12 ± 0.61	---	---
9.5	2.56 ± 0.17	2.39 ± 0.60	1.32[1]	2.05 ± 0.38
	TRITC			
8.0	2.16 ± 0.12	---	---	---
8.5	2.24 ± 0.04	---	---	---
9.0	2.30 ± 0.19	2.39 ± 0.38	---	---
9.5	2.13 ± 0.16	2.46 ±0.31	1.99-3.11	1.97 ± 0.19

REFERENCES

1. **Abed, R. M. M., N. M. D. Safi, J. Köster, D. de Beer, Y. El-Nahhal, J. Rullkötter, and F. Garcia-Pichel**. 2002. Microbial Diversity of a Heavily Polluted Microbial Mat and Its Community Changes following Degradation of Petroleum Compounds. Applied and Environmental Microbiology **68**:1674-1683.

2. **Acinas, S. G., L. A. Marcelino, V. Klepac-Ceraj, and M. F. Polz**. 2004. Divergence and Redundancy of 16S rRNA Sequences in Genomes with Multiple *rrn* Operons. Journal of Bacteriology **186**:2629-2635.

3. **Al-Tahhan, R. A., T. R. Sandrin, A. A. Bodour, and R. M. Maier**. 2000. Rhamnolipid-Induced Removal of Lipopolysaccharide from *Pseudomonas aeruginosa*: Effect on Cell Surface Properties and Interaction with Hydrophobic Substrates. Applied and Environmental Microbiology **66**:3262-3268.

4. **Alexander, D. B.** 1999. Bacteria and Archaea, p. 44-71. *In* D. M. Sylvia, J. J. Fuhrmann, P. G. Hartel, and D. A. Zuberer (eds.), Principles and Applications of Soil Microbiology. Prentice Hall, New Jersey.

5. **Alexander, M.** 2000. Aging, Bioavailability, and Overestimation of Risk from Environmental Pollutants. Environmental Science and Technology **34**:4259-4265.

6. **Altemüller, H.-J. and B. van Vliet-Lanoe**. 1990. Soil Thin Section Fluorescence Microscopy, p. 565-579. *In* L.A. Douglas (ed.), Soil Micromorphology: A Basic and Applied Science. Elsevier Science Publishers, New York.

7. **Altschul, S. F., T. L. Madden, A. A. Schaffer, J. Zhang, Z. Zhang, W. Miller, and D. J. Lipman**. 1997. Gapped BLAST and PSI-BLAST: A New Generation of Protein Database Search Programs. Nucleic Acids Research **25**:3389-3402.

8. **Amann, R.** 1995. In situ Identification of Microorganisms by Whole Cell Hybridization with rRNA-targeted Nucleic Acid Probes, p. 3.3.6. *In* A.D.L. Akkermans, J.D. van Elsas, and F. deBruijn (eds.), Molecular Microbial Ecology Manual. Kluwer Academic Publishers, Netherlands.

9. **Amann, R., B. M. Fuchs, and S. Behrens**. 2001. The Identification of Microorganisms by Fluorescence *in situ* Hybridization. Current Opinion in Biotechnology **12**:231-236.

10. **Amann, R. and W. Ludwig**. 2000. Ribosomal RNA-targeted Nucleic Acid Probes for Studies in Microbial Ecology. FEMS Microbiology Reviews **24**:555-565.

11. **Amann, R., J. Snaidr, M. Wagner, W. Ludwig, and K. Schleifer**. 1996. In Situ Visualization of High Genetic Diversity in a Natural Microbial Community. Journal of Bacteriology **178**:3496-3500.

12. **Amann, R. I., B. J. Binder, R. J. Olson, S. W. Chisholm, R. Devereux, and D. A. Stahl**. 1990b. Combination of 16S rRNA-Targeted Oligonucleotide Probes with Flow Cytometry

for Analyzing Mixed Microbial Populations. Applied and Environmental Microbiology **56**:1919-1925.

13. **Amann, R. I., L. Krumholz, and D. Stahl**. 1990a. Fluorescent-Oligonucleotide Probing of Whole Cells for Determinative, Phylogenetic, and Environmental Studies in Microbiology. Journal of Bacteriology **172**:762-770.

14. **Amann, R. I., W. Ludwig, and K. H. Schleifer**. 1995. Phylogenetic Identification and In Situ Detection of Individual Microbial Cells without Cultivation. Microbiological Reviews **59**:143-169.

15. **Amellal, N., J.-M. Portal, T. Vogel, and J. Berthelin**. 2001. Distribution and Location of Polycyclic Aromatic Hydrocarbons and PAH-degrading Bacteria within Polluted Soil Aggregates. Biodegradation **12**:49-57.

16. **Ashman, M. R., P. D. Hallett, and P. C. Brookes**. 2003. Are the Links Between Soil Aggregate Size Class, Soil Organic Matter and Respiration Rate Artifacts of the Fractionation Procedure? Soil Biology & Biochemistry **35**:435-444.

17. **Assmus, B., P. Hutzler, G. Kirchhof, R. Amann, J. R. Lawrence, and A. Hartmann**. 1995. In Situ Localization of *Azospirillum brasilense* in the Rhizosphere of Wheat with Fluorescently Labeled, rRNA-Targetd Oligonucleotide Probes and Scanning Confocal Laser Microscopy. Applied and Environmental Microbiology **61**:1013-1019.

18. **Atlas, R. M. and R. Bartha**. 1993. Microbial Ecology: Fundamentals and Applications. The Benjamin/Cummings Publishing Company, Inc., Redwood City, CA.

19. **Bakermans, C. and E. L. Madsen**. 2002. Diversity of 16S rDNA and Naphthalene Dioxygenase Genes from Coal-Tar-Waste-Contaminated Aquifer Waters. Microbial Ecology **44**:95-106.

20. **Bakker, D. P., B. R. Postmus, H. J. Busscher, and H. C. van der Mei**. 2004. Bacterial Strains Isolated from Different Niches can Exhibit Different Patterns of Adhesion to Substrata. Applied and Environmental Microbiology **70**:3758-3760.

21. **Barns, S. M., R. E. Fundyga, M. W. Jeffries, and N. R. Pace**. 1994. Remarkable Archaeal Diversity Detected in a Yellowstone National Park Hot Spring Environment. Proceedings of the National Academy of Science, USA **91**:1609-1613.

22. **Bastiaens, L., D. Springael, P. Wattiau, H. Harms, R. deWachter, H. Verachtert, and L. Diels** . 2000. Isolation of Adherent Polycyclic Aromatic Hydrocarbon (PAH)-Degrading Bacteria Using PAH-Sorbing Carriers. Applied and Environmental Microbiology **66**:1834-1843.

23. **Becker, J. M., T. Parkin, C. H. Nakatsu, J. D. Wilbur, and A. Konopka**. 2006. Bacterial Activity, Community Structure, and Centimeter-Scale Spatial Heterogeneity in Contaminated Soil. Microbial Ecology **51**:220-231.

24. **Bispo, A., M. J. Jourdain, and M. Jauzein**. 1999. Toxicity and Genotoxicity of Industrial Soils Polluted by Polycyclic Aromatic Hydrocarbons (PAHs). Organic Geochemistry **30**:947-952.

25. **Boffeta, P., N. Jourenkova, and P. Gustavsson**. 1997. Cancer Risk from Occupational and Environmental Exposure to Polycyclic Aromatic Hydrocarbons. Cancer Causes and Control **8**:444-472.

26. **Bond, W. J.** 1993. Keystone Species, p. 237-253. *In* E.-D. Schulze and H. A. Mooney (eds.), Biodiversity and Ecosystem Functions. Springer-Verlag, New York.

27. **Boonchan, S., M. L. Britz, and G. A. Stanley**. 2000. Degradation and Mineralization of High-Molecular Weight Polycyclic Aromatic Hydrocarbons by Defined Fungal-Bacterial Cocultures. Applied and Environmental Microbiology **66**:1007-1019.

28. **Borneman, J. and R. J. Hartin**. 2000. PCR Primers that Amplify Fungal rRNA Genes from Environmental Samples. Applied and Environmental Microbiology **66**:4356-4360.

29. **Borneman, J., P. W. Skroch, K. M. O'Sullivan, J. A. Palus, N. G. Rumjanek, J. L. Jansen, J. Nienhuis, and E. W. Triplett**. 1996. Molecular Microbial Diversity of an Agricultural Soil in Wisconsin. Applied and Environmental Microbiology **62**:1935-1943.

30. **Borneman, J. and E. W. Triplett**. 1997. Molecular Microbial Diversity in Soils from Eastern Amazonia: Evidence for Unusual Microorganisms and Microbial Population Shifts Associated with Deforestation. Applied and Environmental Microbiology **63**:2647-2653.

31. **Bosma, T. N. P., P. J. M. Middeldorp, G. Schraa, and A. J. B. Zehnder**. 1997. Mass Transfer Limitation of Biotransformation: Quantifying Bioavailability. Environmental Science and Technology **31**:248-252.

32. **Bossio, D. A., K. M. Scow, N. Gunapala, and K. J. Graham**. 1998. Determinants of Soil Microbial Communities: Effects of Agricultural Management, Season, and Soil Type on Phospholipid Fatty Acid Profiles. Microbial Ecology **36**:1-12.

33. **Bouchez, M., D. Blanchet, V. Bardin, F. Haeseler, and J.-P. Vandecasteele**. 1999. Efficiency of Defined Strains and of Soil Consortia in the Biodegradation of Polycyclic Aromatic Hydrocarbon (PAH) Mixtures. Biodegradation **10**:429-435.

34. **Bouchez, M., D. Blanchet, and Vandecasteele**. 1995. Degradation of Polycyclic Aromatic Hydrocarbons by Pure Strains and by Defined Strain Associations: Inhibition Phenomena and Cometabolism. Applied Microbiology and Biotechnology **43**:156-164.

35. **Bouchez, M., D. Blanchet, and Vandecasteele**. 1996. The Microbiological Fate of Polycyclic Aromatic Hydrocarbons: Carbon and Oxygen Balances for Bacterial Degradation of Model Compounds. Applied Microbiology and Biotechnology **45**:556-561.

36. **Bouvier, T. and P. A. del Giorgio**. 2003. Factors Influencing the Detection of Bacterial Cells using Fluorescence in situ Hybridization (FISH): A Quantitative Review of

Published Reports. FEMS Microbiology Ecology **44**:3-15.

37. **Braker, G., H. L. Ayala-del-Río, A. H. Devol, A. Fesefeldt, and J. M. Tiedje**. 2001. Community Structure of Denitrifiers, *Bacteria*, and *Archaea* along Redox Gradients in Pacific Northwest Marine Sediments by Terminal Restriction Fragment Length Polymorphism Analysis of Amplified Nitrite Reductase (*nirS*) and 16S rRNA Genes. Applied and Environmental Microbiology **67**:1893-1901.

38. **Breedveld, G. D. and D. A. Karlsen**. 2000. Estimating the Availability of Polycyclic Aromatic Hydrocarbons for Bioremediation of Creosote Contaminated Soils. Applied Microbiology Biotechnology **54**:255-261.

39. **Brinch, U. C., F. Ekelund, and C. S. Jacobsen**. 2002. Method for Spiking Soil Samples with Organic Compounds. Applied and Environmental Microbiology **68**:1808-1816.

40. **Briones, A. M., S. Okabe, Y. Umemiya, N.-B. Ramsing, W. Reichardt, and H. Okuyama**. 2003. Ammonia-oxidizing Bacteria on Root Biofilms and their Possible Contribution to N use Efficiency of Different Rice Cultivars. Plant and Soil **250**:335-348.

41. **Buckley, D. H. and T. M. Schmidt**. 2001. The Structure of Microbial Communities in Soil and the Lasting Impact of Cultivation. Microbial Ecology **42**:11-21.

42. **Bugg, T., J. M. Foght, M. A. Pickard, and M. R. Gray**. 2000. Uptake and Active Efflux of Polycyclic Aromatic Hydrocarbons by *Pseudomonas fluorescens* LP6a. Applied and Environmental Microbiology **66**:5387-5392.

43. **Bundt, M., F. Widmer, M. Pesaro, J. Zeyer, and P. Blaser**. 2001. Preferential Flow Paths: Biological "Hot Spots" in Soils. Soil Biology & Biochemistry **33**:729-738.

44. **Campbell, J. I. A., C. S. Jacobsen, and J. Sorensen**. 1995. Species Variation and Plasmid Incidence among Fluorescent *Pseudomonas* Strains Isolated from Agricultural and Industrial Soils. FEMS Microbiology Ecology **18**:51-62.

45. **Carmichael, L. M. and F. K. Pfaender**. 1997. Polynuclear Aromatic Hydrocarbon Metabolism in Soils: Relationship to Soil Characteristics and Preexposure. Environmental Toxicology and Chemistry **16**:666-675.

46. **Casamayor, E. O., C. Pedrós-Alió, G. Muyzer, and R. Amann**. 2002. Microheterogeneity in 16S Ribosomal DNA-Defined Bacterial Populations from a Stratified Planktonic Environment is Related to Temporal Changes and to Ecological Adaptations. Applied and Environmental Microbiology **68**:1706-1714.

47. **Cerniglia, C. E.** 1992. Biodegradation of Polycyclic Aromatic Hydrocarbons. Biodegradation **3**:351-368.

48. **Cerniglia, C. E.** 1984. Microbial Metabolism of Polycyclic Aromatic Hydrocarbons. Advances in Applied Microbiology **30**:31-71.

49. **Cerniglia, D. E., D. W. Kelly, J. P. Freeman, and D. W. Miller**. 1986. Microbial Metabolism of Pyrene. Chemico-biological Interactions **57**:203-216.

50. **Chen, S.-H. and M. D. Aitken**. 1999. Salicylate Stimulates the Degradation of High-Molecular Weight Polycyclic Aromatic Hydrocarbons by *Pseudomonas saccharophila* P15. Environmental Science and Technology **33**:435-439.

51. **Cheung, P.-Y. and B. K. Kinkle**. 2001. Mycobacterium Diversity and Pyrene Mineralization in Petroleum-Contaminated Soils. Applied and Environmental Microbiology **67**:2222-2229.

52. **Christensen, H., M. Hansen, and J. Sørensen**. 1999. Counting and Size Classification of Active Soil Bacteria by Fluorescence in situ Hybridization with an rRNA Oligonucleotide Probe. Applied and Environmental Microbiology **65**:1753-1761.

53. **Chung, N. and M. Alexander**. 1998. Differences in Sequestration and Bioavailability of Organic Compounds Aged in Dissimilar Soils. Environmental Science and Technology **32**:855-860.

54. **Cilia, V., B. Lafay, and R. Christen**. 1996. Sequence Heterogeneities Among 16S Ribosomal RNA Sequences, and Their Effect on Phylogenetic Analyses at the Species Level. Molecular Biology and Evolution **13**:451-461.

55. **Coates, J. D., R. Chakrabarty, S. M. O'Connor, C. Schmidt, and J. Thieme**. 2000. The Geochemical Effects of Microbial Humic Substances Reduction. Acta Hydrochimica Hydrobiologica **28**:420-427.

56. **Cohan, F. M.** 2001. Bacterial Species and Speciation. Systematic Biology **50**:513-524.

57. **Cohan, F. M.** 2002. What are Bacterial Species? Annual Reviews in Microbiology **56**:457-487.

58. **Coleman, D. C., J. Dighton, K. Ritz, and K. E. Giller**. 1994. Perspectives on the Compositional and Functional Analysis of Soil Communities, p. 261-. *In* K. Ritz, J. Dighton, and K. E. Giller (eds.), Beyond the Biomass. John Wiley & Sons, New York.

59. **Corgié S.C., T. Beguiristain, and C. Leyval**. 2004. Spatial Distribution of Bacterial Communities and Phenanthrene Degradation in the Rhizosphere of *Lolium perenne* L. Applied and Environmental Microbiology **70**:3552-3557.

60. **Cullander, C.** 1999. Fluorescent Probes for Confocal Microscopy. *In* S. Paddock (ed.), Methods in Molecular Biology: Confocal Microscopy Methods and Protocols **122**:59-73. Humana Press, Inc; Totowa, NJ.

61. **Daane, L. L., I. Harjono, G. J. Zylstra, and M. M. Häggblom**. 2001. Isolation and Characterization of Polycylcic Aromatic Hydrocarbon-Degrading Bacteria Associated with the Rhizosphere of Salt Marsh Plants. Applied and Environmental Microbiology **67**:2683-2691.

62. **Daims, H., S. Lücker, and M. Wagner**. 2006. *daime*, a Novel Image Analysis Program for Microbial Ecology and Biofilm Research. Environmental Microbiology **8**:200-213.

63. **Dean-Ross, D. and C. E. Cerniglia**. 1996. Degradation of Pyrene by *Mycobacterium flavescens*. Applied Microbiology and Biotechnology **46**:307-312.

64. **Dean-Ross, D., J. Moody, and C. E. Cerniglia**. 2002. Utilization of Mixtures of Polycyclic Aromatic Hydrocarbons by Bacteria Isolated from Contaminated Sediment. FEMS Microbiology Ecology **41**:1-7.

65. **Dechesne, A., C. Pallud, D. Debouzie, J. P. Flandrois, T. M. Vogel, J. P. Gaudet, and G. L. Grundmann**. 2003. A Novel Method for Characterizing the Microscale 3D Spatial Distribution of Bacteria in Soil. Soil Biology & Biochemistry **35**:1537-1546.

66. **Decho, A. W. and T. Kawaguchi**. 1999. Confocal Imaging of In Situ Natural Microbial Communities and Their Extracellular Polymeric Secretions Using Nanoplast Resin. BioTechniques **27**:1246-1252.

67. **Del Panno, M. T., I. S. Morelli, B. Engelen, and L. Berthe-Corti**. 2005. Effect of Petrochemical Sludge Concentrations on Microbial Communities During Soil Bioremediation. FEMS Microbial Ecology **53**:305-316.

68. **DeLong, E. F.** 1992. Archaea in Coastal Marine Environments. Proceedings of the National Academy of Science, USA **89**:5685-5689.

69. **DeSantis, T. Z., E. L. Brodie, J. P. Moberg, I. X. Zubieta, Y. M. Piceno, and G. L. Andersen**. 2007. High-Density Universal 16S rRNA Microarray Analysis Reveals Broader Diversity than Typical Clone Library When Sampling the Environment. Microbial Ecology **53**:371-383.

70. **Dionisi, H. M., C. S. Chewning, K. H. Morgan, F.-M. Menn, J. P. Easter, and G. S. Sayler**. 2004. Abundance of Dioxygenase Genes Similar to *Ralstonia* sp. Strain U2 *nagAc* is Correlated with Naphthalene Concentrations in Coal Tar-Contaminated Sediments. Applied and Environmental Microbiology **70**:3988-3995.

71. **Dojka, M. A., J. K. Harris, and N. R. Pace**. 2000. Expanding the Known Diversity and Environmental Distribution of an Uncultured Phylogenetic Division of Bacteria. Applied and Environmental Microbiology **66**:1617-1621.

72. **Dojka, M. A., P. Hugenholtz, S. K. Haack, and N. R. Pace**. 1998. Microbial Diversity in a Hydrocarbon- and Chlorinated-Solvent-Contaminated Aquifer Undergoing Intrinsic Bioremediation. Applied and Environmental Microbiology **64**:3869-3877.

73. **Doolittle, W. F.** 1999. Phylogenetic Classification and the Universal Tree. Science **284**:2124-2128.

74. **Dunbar, J., S. M. Barns, L. O. Ticknor, and C. R. Kuske**. 2002. Empirical and Theoretical Bacterial Diversity in Four Arizona Soils. Applied and Environmental

Microbiology **68**:3035-3045.

75. **Dunbar, J., L. O. Ticknor, and C. R. Kuske**. 2000. Assessment of Microbial Diversity in Four Southwestern United States Soils by 16S rRNA Gene Terminal Restriction Fragment Analysis. Applied and Environmental Microbiology **66**:2943-2950.

76. **Dykhuizen, D. E.** 1998. Santa Rosalia Revisited: Why are there so many species of bacteria? Antonie van Leeuwenhoek **73**:25-33.

77. **El Fantroussi, S., L. Verschuere, W. Verstraete, and E. M. Top**. 1999. Effect of Phenylurea Herbicides on Soil Microbial Communities Estimated by Analysis of 16S rRNA Gene Fingerprints and Community-Level Physiological Profiles. Applied and Environmental Microbiology **65**:982-988.

78. **Eriksson, M., G. Dalhammar, and W. W. Mohn**. 2002. Bacterial Growth and Biofilm Production on Pyrene. FEMS Microbiology Ecology **40**:21-27.

79. **Ettema, C. H. and D. A. Wardle**. 2002. Spatial Soil Ecology. TRENDS in Ecology & Evolution **17**:177-183.

80. **Feeney, D. S., J. W. Crawford, T. Daniell, P. D. Hallett, N. Nunan, K. Ritz, M. Rivers, and I. M. Young**. 2006. Three-Dimensional Microorganization of the Soil-Root-Microbe System. Microbial Ecology **52**:151-158.

81. **Felske, A., A. Wolterink, R. van Lis, W. M. de Vos, and A. D. L. Akkermans**. 1999. Searching for Predominant Soil Bacteria: 16S rDNA Cloning versus Strain Cultivation. FEMS Microbiology Ecology **30**:137-145.

82. **Fierer, N., J. P. Schimel, and P. A. Holden**. 2003. Influence of Drying-Rewetting Frequency on Soil Bacterial Community Structure. Microbial Ecology **45**:63-71.

83. **Fisk, A. C., S. L. Murphy, and R. L. Tate III**. 1999. Microscopic Observations of Bacterial Sorption in Soil Cores. Biology and Fertility of Soils **28**:111-116.

84. **Fleming, J. T., J. Sanseverino, and G. S. Sayler**. 1993. Quantitative Relationship Between Naphthalene Catabolic Gene Frequency and Expression in Predicting PAH Degradation in Soils at Town Gas Manufacturing Sites. Environmental Science and Technology **27**:1068-1074.

85. **Fox, G. E., K. R. Pechman, and C. R. Woese**. 1977. Comparative Cataloging of 16S Ribosomal Ribonucleic Acid: Molecular Approach to Procaryotic Systematics. International Journal of Systematic Bacteriology **27**:44-57.

86. **Fox, G. E., E. Stackebrandt, R. B. Hespell, J. Gibson, J. Maniloff, T. A. Dyer, R. S. Wolfe, W. E. Balch, R. S. Tanner, L. J. Magrum, L. B. Zablen, R. Blakemore, R. Gupta, L. Bonen, B. J. Lewis, D. A. Stahl, K. R. Leuhrsen, K. N. Chen, and C. R. Woese**. 1980. The Phylogeny of Prokaryotes. Science **209**:457-463.

87. **Friedrich, M., R. J. Grosser, E. A. Kern, W. P. Inskeep, and D. M. Ward**. 2000. Effect of Model Sorptive Phases on Phenanthrene Biodegradation: Molecular Analysis of Enrichments and Isolates Suggests Selection Based on Bioavailability. Applied and Environmental Microbiology **66**:2703-2710.

88. **Fromin, N., J. Hamelin, S. Tarnawski, D. Roesti, K. Jourdain-Miserez, N. Forestier, S. Teyssier-Cuvelle, F. Gillet, M. Aragno, and P. Ross**. 2002. Statistical Analysis of Denaturing Gradient Gel Electrophoresis (DGGE) Fingerprinting Patterns. Environmental Microbiology **4**:634-643.

89. **Frostegård, Å., S. Courtois, V. Ramisse, S. Clerc, D. Bernillon, F. Le Gall, P. Jeannin, X. Nesme, and P. Simonet**. 1999. Quantification of Bias Related to the Extraction of DNA Directly from Soils. Applied and Environmental Microbiology **65**:5409-5420.

90. **Gargas, A. and P. T. DePriest**. 1996. A Nomenclature for Fungal PCR Primers with Examples from Intron-containing SSU rDNA. Mycologia **88** :745-748.

91. **Garland, J. L., K. L. Cook, J. L. Adams, and L. Kerkhof**. 2001. Culturability as an Indicator of Succession in Microbial Communities. Microbial Ecology **42**:150-158.

92. **Gelsomino, A., A. C. Keijzer-Wolters, G. Cacco, and J. D. van Elsas**. 1999. Assessment of Bacterial Community Structure in Soil by Polymerase Chain Reaction and Denaturing Gradient Gel Electrophoresis. Journal of Microbiological Methods **38**:1-15.

93. **Gentry, T. J., D. C. Wolf, C. M. Reynolds, and J. J. Fuhrmann**. 2003. Pyrene and Phenanthrene Influence on Soil Microbial Populations. Bioremediation Journal **7**:53-68.

94. **Ginige, M. P., P. Hugenholtz, H. Daims, M. Wagner, J. Keller, and L. L. Blackall**. 2004. Use of Stable-Isotope Probing, Full-Cycle rRNA Analysis, and Fluorescence in situ Hybridization-Microautoradiography to Study a Methanol-Fed Denitrifying Microbial Community. Applied and Environmental Microbiology **70**:588-596.

95. **Giovannoni, S. J., T. B. Britschgi, C. L. Moyer, and K. G. Field**. 1990. Genetic Diversity in Sargasso Sea Bacterioplankton. Nature **345**:60-63.

96. **Girvan, M. S., J. Bullimore, J. N. Pretty, M. Osborn, and A. S. Ball**. 2003. Soil Type is the Primary Determinant of the Composition of the Total and Active Bacterial Communities in Arable Soils. Applied and Environmental Microbiology **69**:1800-1809.

97. **Gramss, G., K.-D. Voigt, and B. Kirsche**. 1999. Degradation of Polycyclic Aromatic Hydrocarbons with Three to Seven Aromatic Rings by Higher Fungi in Sterile and Unsterile Soils. Biodegradation **10**:51-62.

98. **Greene, E. A., J. G. Kay, K. Jaber, and L. G. V. G. Stehmeier**. 2000. Composition of Soil Microbial Communities Enriched on a Mixture of Aromatic Hydrocarbons. Applied and Environmental Microbiology **66**:5282-5289.

99. **Griffiths, B. S., M. Bonkowski, J. Roy, and K. Ritz**. 2001. Functional Stability, Substrate

Utilization and Biological Indicators of Soils Following Environmental Impact. Applied Soil Ecology **16**:49-61.

100. **Griffiths, B. S., H. L. Kuan, K. Ritz, L. A. Glover, A. E. McCaig, and C. Fenwick**. 2004. The Relationship between Microbial Community Structure and Functional Stability, Tested Experimentally in an Upland Pasture Soil. Microbial Ecology **47**:104-113.

101. **Grimm, A. C. and C. S. Harwood**. 1997. Chemotaxis of *Pseudomonas* spp. to the Polyaromatic Hydrocarbon, Naphthalene. Applied and Environmental Microbiology **63**:4111-4115.

102. **Grosser, R. J., M. Friedrich, D. M. Ward, and W. P. Inskeep**. 2000. Effect of Model Sorptive Phases on Phenanthrene Biodegradation: Different Enrichment Conditions Influence Bioavailability and Selection of Phenanthrene-Degrading Isolates. Applied and Environmental Microbiology **66**:2695-2702.

103. **Grundmann, G. L. and D. Debouzie**. 2000. Geostatistical Analysis of the Distribution of NH_4^+ and NO_2^--Oxidizing Bacteria and Serotypes at the Millimeter Scale along a Soil Transect. FEMS Microbiology Ecology **34**:57-62.

104. **Guerin, W. F. and S. A. Boyd**. 1992. Differential Bioavailability of Soil-Sorbed Naphthalene to Two Bacterial Species. Applied and Environmental Microbiology **58**:1142-1152.

105. **Gupta, R. S. and B. J. Soltys**. 1999. Lateral Gene Transfer, Genome Surveys, and the Phylogeny of Prokaryotes. Science **286**:1443a.

106. **Guthrie, E. A., J. M. Bortiatynski, J. D. H. van Heemst, J. E. Richman, K. S. Hardy, E. M. Kovach, and P. G. Hatcher**. 1999. Determination of [^{13}C]Pyrene Sequestration in Sediment Microcosms Using Flash Pyrolysis-GC-MS and ^{13}C NMR. Environmental Science & Technology **33**:119-125.

107. **Hall, K., C. D. Miller, D. L. Sorensen, A. J. Anderson, and R. C. Sims**. 2005. Development of a Catabolically Significant Genetic Probe for Polycyclic Aromatic Hydrocarbon-degrading *Mycobacteria* in Soil. Biodegradation **16**:475-484.

108. **Hammel, K. E., B. Kalyanaraman, and T. K. Kirk**. 1986. Oxidation of Polycyclic Aromatic Hydrocarbons and Dibenzo[p]-dioxins by *Phanerochaete chrysosporium* Ligninase. The Journal of Biological Chemistry **261**:16948-16952.

109. **Hansen, M., A. K. Nielsen, S. Molin, K. Hammer, and M. Kilstrup**. 2001. Changes in rRNA Levels during Stress Invalidates Results from mRNA Blotting: Fluorescence In Situ rRNA Hybridization Permits Renormalization for Estimation of Cellular mRNA Levels. Journal of Bacteriology **183**:4747-4751.

110. **Harris, P. J.** 1994. Consequences of the Spatial Distribution of Microbial Communities in Soil, p. 239-246. *In* K. Ritz, J. Dighton, and K. E. Giller (eds.), Beyond the Biomass. Wiley-Sayce.

111. **Hatzinger, P. B. and M. Alexander**. 1997. Biodegradation of Organic Compounds Sequestered in Organic Solids or in Nanopores within Silica Particles. Environmental Toxicology and Chemistry **16**:2215-2221.

112. **Hatzinger, P. B. and M. Alexander**. 1995. Effect of Aging of Chemicals in Soil on their Biodegradability and Extractability. Environmental Science and Technology **29**:537-545.

113. **Haugland, R. P.** 2002. Handbook of Fluorescent Probes and Research Products. Molecular Probes, Inc., Eugene, OR.

114. **Hearn, E. M., J. J. Dennis, M. R. Gray, and J. M. Foght**. 2003. Identification and Characterization of the *emhABC* Efflux System for Polycyclic Aromatic Hydrocarbons in *Pseudomonas fluorescens* cLP6a. Journal of Bacteriology **185**:6233-6240.

115. **Heider, J. and G. Fuchs**. 1997. Anaerobic Metabolism of Aromatic Compounds. European Journal of Biochemistry **243**:577-596.

116. **Heitkamp, M. A. and C. E. Cerniglia**. 1988. Mineralization of Polycyclic Aromatic Hydrocarbons by a Bacterium Isolated from Sediment below an Oil Field. Applied and Environmental Microbiology **54**:1612-1614.

117. **Hicks, R. E., R. I. Amann, and D. A. Stahl**. 1992. Dual Staining of Natural Bacterioplankton with 4',6-Diamidino-2-Phenylindole and Fluorescent Oligonucleotide Probes Targeting Kingdom-Level 16S rRNA Sequences. Applied and Environmental Microbiology **58**:2158-2163.

118. **Higgins, D. G. and P. M. Sharp**. 1988. CLUSTAL: a Package for Performing Multiple Sequence Alignment on a Microcomputer. Gene **73**:237-244.

119. **Ho, Y., M. Jackson, Y. Yang, J. G. Mueller, and P. H. Pritchard**. 2000. Characterization of Fluoranthene- and Pyrene-Degrading Bacteria Isolated from PAH-Contaminated Soils and Sediments. Journal of Industrial Microbiology & Biotechnology **24**:100-112.

120. **Holben, W.** 1997. Isolation and Purification of Bacterial Community DNA from Environmental Samples, p. pp. 431-436. *In* C. J. Hurst, G. R. Knudsen, M. J. McInerney, L. D. Stetzenbach, and M. V. Walter (eds.), Manual of Environmental Microbiology. ASM Press, Washington, DC.

121. **Hong, S. H., T. Y. Kim, and S. Y. Lee**. 2004. Phylogenetic Analysis Based on Genome-Scale Metabolic Pathway Reaction Content. Applied Microbiology and Biotechnology **65**:203-210.

122. **Huber, T., G. Faulkner, and P. Hugenholtz**. 2004. Bellerophon: A Program to Detect Chimeric Sequences in Multiple Sequence Alignments. Bioinformatics **20**:2317-2319.

123. **Huesemann, M. H., T. S. Hausmann, and T. J. Fortman**. 2002. Microbial Factors Rather Than Bioavailability Limit the Rate and Extent of PAH Biodegradation in Aged

Crude Oil Contaminated Model Soils. Bioremediation Journal **6**:321-336.

124. **Hugenholtz, P., C. Pitulle, K. L. Hershberger, and N. R. Pace**. 1998. Novel Division Level Bacterial Diversity in a Yellowstone Hot Spring. Journal of Bacteriology **180**:366-376.

125. **Hugenholtz, P., G. W. Tyson, R. I. Webb, A. M. Wagner, and L. L. Blackall**. 2001. Investigation of Candidate Division TM7, a Recently Recognized Major Lineage of the Domain Bacteria with no Known Pure-Culture Representatives. Applied and Environmental Microbiology **67**:411-419.

126. **Hughes, J. B., J. J. Hellman, T. H. Ricketts, and B. J. M. Bohannan**. 2001. Counting the Uncountable: Statistical Approaches to Estimating Microbial Diversity. Applied and Environmental Microbiology **67**:4399-4406.

127. **Huynen, M., B. Snel, and P. Bork**. 1999. Lateral Gene Transfer, Genome Surveys, and the Phylogeny of Prokaryotes. Science **286**:1443a.

128. **Ibekwe, M., S. K. Papiernik, J. Gan, S. R. Yates, C. Yang, and D. E. Crowley**. 2001. Impact of Fumigants on Soil Microbial Communities. Applied and Environmental Microbiology **67**:3245-3257.

129. **Insam, H.** 2001. Developments in Soil Microbiology Since the mid 1960s. Geoderma **100**:389-402.

130. **Iwabuchi, N., M. Sunairi, H. Anzai, M. Nakajima, and S. Harayama**. 2000. Relationships between Colony Morphotypes and Oil Tolerance in *Rhodococcus rhodocrous* . Applied and Environmental Microbiology **66**:5073-5077.

131. **Iwabuchi, N., M. Sunairi, M. Urai, C. Itoh, H. Anzai, M. Nakajima, and S. Harayama**. 2002. Extracellular Polysaccharides of *Rhodococcus rhodochrous* S-2 Stimulate the Degradation of Aromatic Components in Crude Oil by Indigenous Marine Bacteria. Applied and Environmental Microbiology **68**:2337-2343.

132. **Janecka, J., M. B. Jenkins, N. S. Brackett, L. W. Lion, and W. C. Ghiorse**. 2002. Characterization of a *Sinorhizobium* Isolate and Its Extracellular Polymer Implicated in Pollutant Transport in Soil. Applied and Environmental Microbiology **68**:423-426.

133. **Johnsen, A. R. and U. Karlson**. 2005. PAH Degradation Capacity of Soil Microbial Communities--Does It Depend on PAH Exposure? Microbial Ecology **50**:488-495.

134. **Johnsen, A. R., S. Schmidt, T. K. Hybholt, S. Henriksen, C. S. Jacobsen, and O. Andersen**. 2007. Strong Impact on the Polycyclic Aromatic Hydrocarbon (PAH)-Degrading Community of a PAH-Polluted Soil but Marginal Effect on PAH Degradation when Priming with Bioremediated Soil Dominated by Mycobacteria. Applied and Environmental Microbiology **73**:1474-1480.

135. **Johnsen, A. R., L. Y. Wick, and H. Harms**. 2005. Principles of Microbial PAH-

Degradation in Soil. Environmental Pollution **133**:71-84.

136. **Johnsen, A. R., A. Winding, U. Karlson, and P. Roslev**. 2002. Linking of Microorganisms to Phenanthrene Metabolism in Soil by Analysis of 13C-Labeled Cell Lipids. Applied and Environmental Microbiology **68**:6106-6113.

137. **Joner, E. J., S. C. Corgié, N. Amellal, and C. Leyval**. 2002. Nutritional Constraints to Degradation of Polycyclic Aromatic Hydrocarbons in a Simulated Rhizosphere. Soil Biology & Biochemistry **34**:859-864.

138. **Jones, M. D.** 2006. Thesis. University of North Carolina. Effect of Incubation Conditions on the Enrichment of Pyrene-Degrading Bacteria Identified by Stable Isotope Probing in a PAH-Contaminated Soil.

139. **Jones, M. D., D. R. Singleton, D. P. Carstensen, S. N. Powell, J. S. Swanson, F. K. Pfaender, and M. D. Aitken**. 2007. Effect of Incubation Conditions on the Enrichment of Pyrene-degrading Bacteria Identified by Stable Isotope Probing in an Aged, PAH-contaminated Soil. Microbial Ecology .

140. **Joynt, J., M. Bischoff, R. Turco, A. Konopka, and C. H. Nakatsu**. 2006. Microbial Community Analysis of Soils Contaminated with Lead, Chromium and Petroleum Hydrocarbons. Microbial Ecology **51**:209-219.

141. **Kanaly, R. A. and S. Harayama**. 2000. Biodegradation of High-Molecular-Weight Polycyclic Aromatic Hydrocarbons by Bacteria. Journal of Bacteriology **182**:2059-2067.

142. **Kaplan, C. W. and C. L. Kitts**. 2004. Bacterial Succession in a Petroleum Land Treatment Unit. Applied and Environmental Microbiology **70**:1777-1786.

143. **Kasai, Y., Y. Takahata, T. Hoaki, and K. Watanabe**. 2005. Phyisological and Molecular Characterization of a Microbial Community Established in Unsaturated, Petroleum-Contaminated Soil. Environmental Microbiology **7**:806-818.

144. **Kästner, M., M. Breuer-Jammali, and B. Mahro**. 1994. Enumeration and Characterization of the Soil Microflora from Hydrocarbon Contaminated Soil Sites Able to Mineralize Polycyclic Aromatic Hydrocarbons (PAH). Applied Microbiology and Biotechnology **41**:267-273.

145. **Kazunga, C. and M. Aitken**. 2000. Products from the Incomplete Metabolism of Pyrene by Polycyclic Aromatic Hydrocarbon-Degrading Bacteria. Applied and Environmental Microbiology **66**:1917-1922.

146. **Keith, L. H. and W. A. Telliard**. 1979. Priority Pollutants I- A Perspective View. Environmental Science & Technology **13**:416-423.

147. **Kepner, R. L. and J. R. Pratt**. 1994. Use of Fluorochromes for Direct Enumeration of Total Bacteria in Environmental Samples: Past and Present. Microbiological Reviews **58**:603-615.

225

148. **Kersters, K., P. de Vos, M. Gillis, J. Swings, P. van Damme, and E. Stackebrandt**. 2005. Introduction to the Proteobacteria, p. 3-37. *In* M. Dworkin, S. Falkow, E. Rosenberg, K.-H. Schleifer, and E. Stackebrandt (eds.), The Prokaryotes: A Handbook on the Biology of Bacteria. Springer, New York.

149. **Khan, A. A., R.-F. Wang, W.-W. Cao, D. R. Doerge, D. Wennerstrom, and C. E. Cerniglia**. 2001. Molecular Cloning, Nuleotide Sequence, and Expression of Genes Encoding a Polycyclic Aromatic Ring Dioxygenase from *Mycobacterium* sp. Strain PYR-1. Applied and Environmental Microbiology **67**:3577-3585.

150. **Khanna, M. and G. Stotzky**. 1992. Transformation of *Bacillus subtilis* by DNA Bound on Montmorillonite and Effect of DNase on the Transforming Ability of Bound DNA. Applied and Environmental Microbiology **58**:1930-1939.

151. **Kim, H. S. and F. K. Pfaender**. 2005. Effects of Microbially Mediated Redox Conditions on PAH-Soil Interactions. Environmental Science & Technology **39**:9189-9196.

152. **Kim, Y.-H., J. P. Freeman, J. D. Moody, K.-H. Engesser, and C. E. Cerniglia**. 2005. Effects of pH on the Degradation of Phenanthrene and Pyrene by *Mycobacterium vanbaalenii* PYR-1. Applied Microbiology and Biotechnology **67**:275-285.

153. **Klappenbach, J. A., J. M. Dunbar, and T. M. Schmidt**. 2000. rRNA Operon Copy Number Reflects Ecological Strategies of Bacteria. Applied and Environmental Microbiology **66**:1328-1333.

154. **Kleikemper, J., M. H. Schroth, W. V. Sigler, M. Schmucki, S. M. Bernasconi, and J. Zeyer**. 2002. Activity and Diversity of Sulfate-Reducing Bacteria in a Petroleum Hydrocarbon-Contaminated Aquifer. Applied and Environmental Microbiology **68**:1516-1523.

155. **Koch, A. L.** 1990. Diffusion: The Crucial Process in Many Aspects of the Biology of Bacteria. Advances in Microbial Ecology **11**:37-69.

156. **Kong, Y., J. L. Nielsen, and P. H. Nielsen**. 2005. Identity and Ecophysiology of Uncultured Actinobacterial Polyphosphate-Accumulating Organisms in Full-Scale Enhanced Biological Phosphorus Removal Plants. Applied and Environmental Microbiology **71**:4076-4085.

157. **Lane, D. J.** 1991. 16S/23S rRNA Sequencing, p. 115-175. *In* E. Stackebrandt and M. Goodfellow (eds.), Nucleic Acid Techniques in Bacterial Systematics. John Wiley & Sons, Inc., New York.

158. **Langworthy, D. E., R. D. Stapleton, G. S. Sayler, and R. H. Findlay**. 2002. Lipid Analysis of the Response of a Sedimentary Microbial Community to Polycyclic Aromatic Hydrocarbons. Microbial Ecology **43**:189-198.

159. **Lengeler, J. W., G. Drews, and H. G. Schlegel**. 1999. Biology of the Prokaryotes. Blackwell Science, New York.

160. **Leys, N. M., A. Ryngaert, L. Bastiaens, P. Wattiau, E. M. Top, W. Verstraete, and D. Springael**. 2005. Occurrence and Community Composition of Fast-growing *Mycobacterium* in Soils Contaminated with Polycyclic Aromatic Hydrocarbons. FEMS Microbiology Ecology **51**:375-388.

161. **Leys, N. M. E. J., A. Ryngaert, L. Bastiaens, W. Verstraete, E. M. Top, and D. Springael**. 2004. Occurrence and Phylogenetic Diversity of *Sphingomonas* Strains in Soils Contaminated with Polycyclic Aromatic Hydrocarbons. Applied and Environmental Microbiology **70**:1944-1955.

162. **Li, Y., W. A. Dick, and O. H. Tuovinen**. 2003. Evaluation of Fluorochromes for Imaging Bacteria in Soil. Soil Biology & Biochemistry **35**:737-744.

163. **Li, Y., W. A. Dick, and O. H. Tuovinen**. 2004. Fluorescence Microscopy for Visualization of Soil Microorganisms--a Review. Biology & Fertility of Soils **39**:301-311.

164. **Liang, Y., D. W. Britt, J. E. McLean, D. L. Sorensen, and R. C. Sims**. 2007. Humic Acid Effect on Pyrene Degradation: Finding an Optimal Range for Pyrene Solubility and Mineralization Enhancement. Applied Microbiology and Biotechnology **74**:1368-1375.

165. **Liesack, W., P. H. Janssen, F. A. Rainey, N. L. Ward-Rainey, and E. Stackebrandt**. 1997. Microbial Diversity in Soil: The Need for a Combined Approach Using Molecular and Cultivation Techniques, *In* Modern Soil Microbiology. Marcel Dekker, New York, New York.

166. **Liles, M. R., B. F. Manske, S. B. Bintrim, J. Handelsman, and R. M. Goodman**. 2003. A Census of rRNA Genes and Linked Genomic Sequences within a Soil Metagenomic Library. Applied and Environmental Microbiology **69**:2684-2691.

167. **Lloyd-Jones, G. and P. C. K. Lau**. 1997. Glutathione S-Transferase-Encoding Gene as a Potential Probe for Environmental Bacterial Isolates Capable of Degrading Polycyclic Aromatic Hydrocarbons. Applied and Environmental Microbiology **63**:3286-3290.

168. **Lloyd-Jones, G., A. D. Laurie, D. W. F. Hunter, and R. Fraser**. 1999. Analysis of Catabolic Genes for Naphthalene and Phenanthrene Degradation in Contaminated New Zealand Soils. FEMS Microbiology Ecology **29**:69-79.

169. **Lüdemann, H., I. Arth, and W. Liesack**. 2000. Spatial Changes in the Bacterial Community Structure along a Vertical Oxygen Gradient in Flooded Paddy Soil Cores. Applied and Environmental Microbiology **66**:754-762.

170. **Ludwig, W., S. H. Bauer, M. Bauer, I. Held, G. Kirchhof, R. Schulze, I. Huber, S. Spring, A. Hartmann, and K. H. Schleifer**. 1997. Detection and in situ Identification of Representatives of a Widely Distributed New Bacterial Phylum. FEMS Microbiology Letters **153**:181-190.

171. **Lunn, M., W. T. Sloan, and T. P. Curtis**. 2004. Estimating Bacteria Diversity from Clone Libraries with Flat Rank Abundance Distributions. Environmental Microbiology **6**:1081-

1085.

172. **Lünsdorf, H., R. W. Erb, W.-R. Abraham, and K. N. Timmis**. 2000. "Clay Hutches": a Novel Interaction between Bacteria and Clay Minerals. Environmental Microbiology **2**:161-168.

173. **Luthy, R. G., G. R. Aiken, M. L. Brusseau, S. D. Cunningham, P. M. Gschwend, J. J. Pignatello, M. Reinhard, S. J. Traina, Jr. W. J. Weber, and J. C. Westall**. 1997. Sequestration of Hydrophobic Organic Contaminants by Geosorbents. Environmental Science and Technology **31**:3341-3347.

174. **MacGregor, B. J., D. P. Moser, B. J. Baker, E. W. Alm, M. Maurer, K. H. Nealson, and D. A. Stahl**. 2001. Seasonal and Spatial Variability in Lake Michigan Sediment Small-Subunit rRNA Concentrations. Applied and Environmental Microbiology **67**:3908-3922.

175. **Macleod, C. J. A. and K. T. Semple**. 2002. The Adaptation of Two Similar Soils to Pyrene Catabolism. Environmental Pollution **119**:357-364.

176. **Macnaughton, S. J., T. Booth, T. M. Embley, and A. G. O'Donnell**. 1996. Physical Stabilization and Confocal Microscopy of Bacteria on Roots Using 16S rRNA Targeted, Fluorescent-labeled Oligonucleotide Probes. Journal of Microbiological Methods **26**:279-285.

177. **Macnaughton, S. J., J. R. Stephen, A. D. Venosa, G. A. Davis, Y. J. Chang, and D. C. White**. 1999. Microbial Population Changes during Bioremediation of an Experimental Oil Spill. Applied and Environmental Microbiology **65**:3566-3574.

178. **Madigan, M. T., J. M. Martinko, and J. Parker**. 2000. Brock Biology of Microorganisms. Prentice Hall, New Jersey.

179. **Madrid, V. M., G. T. Taylor, M. I. Scranton, and A. Y. Chistoserdov**. 2001. Phylogenetic Diversity of Bacterial and Archaeal Communities in the Anoxic Zone of the Cariaco Basin. Applied and Environmental Microbiology **67**:1663-1674.

180. **Magurran, A. E.** 1988. Ecological Diversity and its Measurement. Princeton University Press, Princeton, NJ.

181. **Marchesi, J. R., T. Sato, A. J. Weightman, T. A. Martin, J. C. Fry, S. J. Hiom, and W. G. Wade**. 1998. Design and Evaluation of Useful Bacterium-Specific PCR Primers that Amplify Genes Coding for Bacterial 16S RNA. Applied and Environmental Microbiology **64**:795-799.

182. **Margesin, R., D. Labbé, F. Schinner, C. W. Greer, and L. G. Whyte**. 2003. Characterization of Hydrocarbon-Degrading Microbial Populations in Contaminated and Pristine Alpine Soils. Applied and Environmental Microbiology **69**:3985-3092.

183. **Marshall, K. C.** 1980. Adsorption of Microorganisms to Soils and Sediments, *In* G. Bitton and K.C. Marshall (eds.), Adsorption of Microorganisms to Surfaces. John Wiley & Sons,

NY, NY.

184. **Martens, D. A. and Jr. W. T. Frankenberger**. 1992. Decomposition of Bacterial Polymers in Soil and their Influence on Soil Structure. Biology and Fertility of Soils **13**:65-73.

185. **Martin-Laurent, F., L. Philippot, S. Hallet, R. Chaussod, J. C. Germon, G. Soulas, and G. Catroux**. 2001. DNA Extraction from Soils: Old Bias for New Microbial Diversity Analysis Methods. Applied and Environmental Microbiology **67**:2354-2359.

186. **Maruyama, A., H. Ishiwata, K. Kitamura, M. Sunamura, T. Fujita, M. Matsuo, and T. Higashihara**. 2003. Dynamics of Microbial Populations and Strong Selection for *Cycloclasticus pugetii* following the Nakhodka Oil Spill. Microbial Ecology **46**:442-453.

187. **McCaig, A. E., L. A. Glover, and J. I. Prosser**. 1999. Molecular Analysis of Bacterial Community Structure and Diversity in Unimproved and Improved Upland Grass Pastures. Applied and Environmental Microbiology **65**:1721-1730.

188. **McCaig, A. E., L. A. Glover, and J. I. Prosser**. 2001. Numerical Analysis of Grassland Bacterial Community Structure under Different Land Management Regimens by Using 16S Ribosomal DNA Sequence Data and Denaturing Gradient Gel Electrophoresis Banding Patterns. Applied and Environmental Microbiology **67**:4554-4559.

189. **Menzie, C. A., B. B. Potocki, and J. Santodonato**. 1992. Exposure to Carcinogenic PAHs in the Environment. Environmental Science and Technology **26**:1278-1284.

190. **Mesarch, M. B., C. H. Nakatsu, and L. Nies**. 2000. Development of Catechol 2,3-Dioxygenase-Specific Primers for Monitoring Bioremediation by Competitive Quantitative PCR. Applied and Environmental Microbiology **66**:678-683.

191. **Meulenberg, R., H. H. M. Rijnaarts, H. J. Doddema, and J. A. Field**. 1997. Partially Oxidized Polycyclic Aromatic Hydrocarbons Show an Increased Bioavailability and Biodegradability. FEMS Microbiology Letters **152**:45-49.

192. **Meyer, O.** 1993. Functional Groups of Microorganisms, p. 67-96. *In* E.-D. Schulze and H. A. Mooney (eds.), Biodiversity and Ecosystem Function. Springer-Verlag, New York.

193. **Michelcic, J. R. and R. G. Luthy**. 1988. Degradation of Polycyclic Aromatic Hydrocarbon Compounds under Various Redox Conditions. Applied and Environmental Microbiology **54**:1182-1187.

194. **Miller, C. D., K. Hall, Y. N. Liang, K. Nieman, D. Sorensen, B. Issa, A. J. Anderson, and R. C. Sims**. 2004. Isolation and Characterization of Polycyclic Aromatic Hydrocarbon-Degrading Mycobacterium Isolates from Soil. Microbial Ecology **48**:230-238.

195. **Miller, D. N., J. E. Bryant, E. L. Madsen, and W. C. Ghiorse**. 1999. Evaluation and Optimization of DNA Extraction and Purification Procedures for Soil and Sediment

Samples. Applied and Environmental Microbiology **65**:4715-4724.

196. **Miller, P. E. and C. A. Scholin**. 1998. Identification and Enumeration of Cultured and Wild *Pseudo-Nitzschia* (Bacillariophyceae) Using Species-Specific LSU rRNA-Targeted Fluorescent Probes and Filter-Based Whole Cell Hybridization. Journal of Phycology **34**:371-382.

197. **Miyata, N., K. Iwahori, J. M. Foght, and M. R. Gray**. 2004. Saturable, Energy-Dependent Uptake of Phenanthrene in Aqueous Phase by *Mycobacterium* sp. Strain RJGII-135. Applied and Environmental Microbiology **70**:363-369.

198. **Møller, S., C. Sternberg, J. B. Andersen, B. B. Christensen, J. L. Ramos, M. Givskov, and S. Molin**. 1998. In Situ Gene Expression in Mixed-Culture Biofilms: Evidence of Metabolic Interactions between Community Members. Applied and Environmental Microbiology **64**:721-732.

199. **Moody, J. D., J. P. Freeman, D. R. Doerge, and C. E. Cerniglia**. 2001. Degradation of Phenanthrene and Anthracene by Cell Suspensions of *Mycobacterium* sp. Strain PYR-1. Applied and Environmental Microbiology **67**:1476-1483.

200. **Moore, E. R. B., B. J. Tindall, V. A. P. Martinsdos Santos, D. H. Pieper, J.-L. Ramos, and N. J. Palleroni**. 2005. Pseudomonas: Nonmedical, *In* M. Dworkin, S. Falkow, E. Rosenberg, K.-H. Schleifer, and E. Stackebrandt (eds.), The Prokaryotes: A Handbook on the Biology of Bacteria. Springer, New York.

201. **Morasch, B., H. H. Richnow, B. Schink, A. Vieth, and R. U. Meckenstock**. 2002. Carbon and Hydrogen Stable Isotope Fractionation during Aerobic Bacterial Degradation of Aromatic Hydrocarbons. Applied and Environmental Microbiology **68**:5191-5194.

202. **Moré, M. I., J. B. Herrick, M. C. Silva, W. C. Ghiorse, and E. L. Madsen**. 1994. Quantitative Cell Lysis of Indigenous Microorganisms and Rapid Extraction of Microbial DNA from Sediment. Applied and Environmental Microbiology **60**:1572-1580.

203. **Morris, C. E., M. Bardin, O. Berge, P. Frey-Klett, N. Fromin, H. Girardin, M.-H. Guinebretière, P. Lebaron, J. M. Thiéry, and M. Troussellier**. 2002. Microbial Biodiversity: Approaches to Experimental Design and Hypothesis Testing in Primary Scientific Literature from 1975 to 1999. Microbiology and Molecular Biology Reviews **66**:592-616.

204. **Moter, A. and U. B. Göbel**. 2000. Fluorescence in situ Hybridization (FISH) for Direct Visualization of Microorganisms. Journal of Microbiological Methods **41**:85-112.

205. **Mueller, J. G., P. J. Chapman, and P. H. Pritchard**. 1989. Action of a Fluoranthene-Utilizing Bacterial Community on Polycyclic Aromatic Hydrocarbon Components of Creosote. Applied and Environmental Microbiology **55**:3085-3090.

206. **Mummey, D., W. Holben, J. Six, and P. Stahl**. 2006. Spatial Stratification of Soil Bacterial Populations in Aggregates of Diverse Soils. Microbial Ecology **51**:404-411.

207. **Mummey, D. L. and P. D. Stahl**. 2004. Analysis of Soil Whole- and Inner-Microaggregate Bacterial Communities. Microbial Ecology **48**:41-50.

208. **Muyzer, G., E. C. de Waal, and A. G. Uitterlinden**. 1993. Profiling of Complex Microbial Populations by Denaturing Gradient Gel Electrophoresis Analysis of Polymerase Chain Reaction-Amplified Genes Coding for 16S RNA. Applied and Environmental Microbiology **59**:695-700.

209. **Muyzer, G. and K. Smalla**. 1998. Application of Denaturing Gradient Gel Electrophoresis (DGGE) and Temperature Gradient Gel Electrophoresis (TGGE) in Microbial Ecology. Antonie van Leeuwenhoek **73**:123-141.

210. **Nam, K. and M. Alexander**. 1998. Role of Nanoporosity and Hydrophobicity in Sequestration and Bioavailability: Tests with Model Solids. Environmental Science and Technology **32**:71-74.

211. **Neefs, J.-M., Y. van de Peer, L. Hendriks, and R. de Wachter**. 1990. Compilation of Small Ribosomal Subunit RNA Sequences. Nucleic Acids Research **18S**:2237-2317.

212. **Nieman, J. K. C., R. C. Sims, D. L. Sorensen, and J. E. McLean**. 2005. Humic Acid Toxicity in Biologically Treated Soil Contaminated with Polycyclic Aromatic Hydrocarbons and Pentachlorophenol. Archives of Environmental Contamination and Toxicology **49**:283-289.

213. **Nogales, B., E. R. B. Moore, E. Llobet-Brossa, R. Rossello-Mora, R. Amann, and K. N. Timmis** . 2001. Combined Use of 16S Ribosomal DNA and 16S rRNA to Study the Bacterial Community of Polychlorinated Biphenyl-Polluted Soil. Applied and Environmental Microbiology **67**:1874-1884.

214. **Norgerg, J., D. P. Swaney, J. Dushoff, J. Lin, R. Casagrandi, and S. A. Levin**. 2001. Phenotypic Diversity and Ecosystem Functioning in Changing Environments: A Theoretical Framework. Proceedings of the National Academy of Science, USA **98**:11376-11381.

215. **Nübel, U., B. Engelen, A. Felske, J. Snaidr, A. Wieshuber, R. I. Amann, W. Ludwig, and H. Backhaus**. 1996. Sequence Heterogeneities of Genes Encoding 16S rRNAs in *Paenibacillus polymyxa* Detected by Temperature Gradient Gel Electrophoresis. Journal of Bacteriology **178**:5636-5643.

216. **Nunan, N., K. Ritz, D. Crabb, K. Harris, K. Wu, J. W. Crawford, and I. M. Young**. 2001. Quantification of the in situ Distribution of Soil Bacteria by Large-Scale Imaging of Thin Sections of Undisturbed Soil. FEMS Microbiology Ecology **36**:67-77.

217. **Nunan, N., K. Wu, I. M. Young, J. W. Crawford, and K. Ritz**. 2002. In Situ Spatial Patterns of Soil Bacterial Populations, Mapped at Multiple Scales, in an Arable Soil. Microbial Ecology **44**:296-305.

218. **Nunan, N., K. Wu, I. M. Young, J. W. Crawford, and K. Ritz**. 2003. Spatial

Distribution of Bacterial Communities and their Relationships with the Micro-architecture of Soil. FEMS Microbial Ecology **44**:203-215.

219. **Ní Chadhain, S. M., R. S. Norman, K. V. Pesce, J. J. Kukor, and G. J. Zylstra**. 2006. Microbial Dioxygenase Gene Population Shifts During Polycyclic Aromatic Hydrocarbon Biodegradation. Applied and Environmental Microbiology **72**:4078-4087.

220. **Oda, Y., S.-J. Slagman, W. G. Meijer, L. J. Forney, and J. C. Gottschal**. 2000. Influence of Growth Rate and Starvation on Fluorescent in situ Hybridization of *Rhodopseudomonas palustris* . FEMS Microbiology Ecology **32**:205-213.

221. **Ogram, A.** 2000. Soil Molecular Microbial Ecology at Age 20: Methodological Challenges for the Future. Soil Biology & Biochemistry **32**:1499-1504.

222. **Ortega-Calvo, J.-J. and C. Saiz-Jimenez**. 1998. Effect of Humic Fractions and Clay on Biodegradation of Phenanthrene by a *Pseudomonas fluorescens* Strain Isolated from Soil. Applied and Environmental Microbiology **64**:3123-3126.

223. **Øvreås, L. and V. Torsvik**. 1998. Microbial Diversity and Community Structure in Two Different Agricultural Soil Communities. Microbial Ecology **36**:303-315.

224. **Parales, R. E., N. C. Bruce, A. Schmid, and L. P. Wackett**. 2002. Biodegradation, Biotransformation, and Biocatalysis (B3). Applied and Environmental Microbiology **68**:4699-4709.

225. **Parkin, T. B.** 1993. Spatial Variability of Microbial Processes in Soil--A Review. Journal of Environmental Quality **22**:409-417.

226. **Parkinson, A.** 2001. Biotransformation of Xenobiotics, p. 133-224. *In* C. D. Klaassen (ed.), Cassarett and Doull's Toxicology: The Basic Science of Poison. McGraw-Hill, New York.

227. **Penning, T. M., M. E. Burczynski, C.-F. Hung, K. D. McCoull, N. T. Palackal, and L. S. Tsuruda**. 1999. Dihydrodiol Dehydrogenases and Polycyclic Aromatic Hydrocarbon Activation: Generation of Reactive and Redox Active o-Quinones. Chemical Research in Toxicology **12**:1-18.

228. **Petersen, S. O. and M. J. Klug**. 1994. Effects of Sieving, Storage, and Incubation Temperature on the Phospholipid Fatty Acid Profile of a Soil Microbial Community. Applied and Environmental Microbiology **60**:2421-2430.

229. **Picard, C., C. Ponsonnet, E. N. X. Paget, and P. Simonet**. 1992. Detection and Enumeration of Bacteria in Soil by Direct DNA Extraction and Polymerase Chain Reaction. Applied and Environmental Microbiology **58**:2717-2722.

230. **Pietramellara, G., L. Dal Canto, C. Vettori, E. Gallori, and P. Nannipieri**. 1997. Effects of Air-Drying and Wetting Cycles on the Transforming Ability of DNA Bound on Clay Minerals. Soil Biology & Biochemistry **29**:55-61.

231. **Potter, C. L., J. A. Glaser, L. W. Chang, J. R. Neier, J. A. Dosani, and R. F. Herrmann**. 1999. Degradation of Polynuclear Aromatic Hydrocarbons under Bench-Scale Compost Conditions. Environmental Science & Technology **33**:1717-1725.

232. **Powell, S. N.** 2006. PhD Dissertation. University of North Carolina at Chapel Hill. Stable Isotope Probing of Salicylate-Degrading Bacteria in Polycyclic Aromatic Hydrocarbon-Contaminated Soil.

233. **Pravecek, T. L., R. F. Christman, and F. K. Pfaender**. 2005. Impact of Imposed Anaerobic Conditions and Microbial Activity on Aqueous-Phase Solubility of Polycyclic Aromatic Hydrocarbons from Soil. Environmental Toxicology and Chemistry **24**:286-293.

234. **Preston, S., B. S. Griffiths, and I. M. Young**. 1999. Links Between Substrate Additions, Native Microbes, and the Structural Complexity and Stability of Soils. Soil Biology and Biochemistry **31**:1541-1547.

235. **Ramirez, N., T. Cutright, and L.-K. Ju**. 2001. Pyrene Biodegradation in Aqueous Solutions and Soil Slurries by *Mycobacterium* PYR-1 and Enriched Consortium. Chemosphere **44**:1079-1086.

236. **Rappé, M. S. and S. J. Giovannoni**. 2003. The Uncultured Microbial Majority. Annual Reviews in Microbiology **57**:369-394.

237. **Raskin, L., J. M. Stromley, B. E. Rittman, and D. A. Stahl**. 1994. Group-specific 16S rRNA Hybridization Probes to Describe Natural Communities of Methanogens. Applied and Environmental Microbiology **60**:1232-1240.

238. **Ravenschlag, K., K. Sahm, C. Knoblauch, B. B. Jørgensen, and R. Amann**. 2000. Community Structure, Cellular rRNA Content, and Activity of Sulfate-Reducing Bacteria in Marine Arctic Sediments. Applied and Environmental Microbiology **66**:3592-3602.

239. **Raymond, J., O. Zhaxybayeva, J. P. Gogarten, S. Y. Gerdes, and R. E. Blankenship**. 2002. Whole-Genome Analysis of Photosynthetic Prokaryotes. Science **298**:1616-1620.

240. **Redmond, D. E.** 1970. Tobacco and Cancer: The First Clinical Report, 1761. The New England Journal of Medicine **282**:18-23.

241. **Reed, M. G. and C. V. Howard**. 1999. Stereological Estimation of Covariance Using Linear Dipole Probes. Journal of Microscopy **195**:96-103.

242. **Reid, B. J., G. L. Northcott, K. C. Jones, and K. T. Semple**. 1998. Evaluation of Spiking Procedures for the Introduction of Poorly Water Soluble Contaminants into Soil. Environmental Science and Technology **32**:3224-3227.

243. **Ressler, B. P., H. Kneifel, and J. Winter**. 1999. Bioavailability of Polycyclic Aromatic Hydrocarbons and Formation of Humic Acid-like Residues During Bacterial PAH Degradation. Applied Microbiology and Biotechnology **53**:85-91.

244. **Ringelberg, D. B., J. W. Talley, E. J. Perkins, S. G. Tucker, R. G. Luthy, E. J. Bouwer, and H. L. Fredrikson**. 2001. Succession of Phenotypic, Genotypic, and Metabolic Community Characteristics during In Vitro Bioslurry Treatment of Polycyclic Aromatic Hydrocarbon-Contaminated Sediments. Applied and Environmental Microbiology **67**:1542-1550.

245. **Röling, W. F. M., M. G. Milner, D. M. Jones, K. Lee, F. Daniel, R. J. P. Swannell, and I. M. Head**. 2002. Robust Hydrocarbon Degradation and Dynamics of Bacterial Communities during Nutrient-Enhanced Oil Spill Bioremediation. Applied and Environmental Microbiology **68**:5537-5548.

246. **Röling, W. F. M., B. M. van Breukelen, M. Braster, B. Lin, and H. W. Vvan Verseveld**. 2001. Relationships between Microbial Community Structure and Hydrochemistry in a Landfill Leachate-Polluted Aquifer. Applied and Environmental Microbiology **67**:4619-4629.

247. **Röling, W. F. M., I. R. Couto de Brito, R. P. J. Swannell, and I. M. Head**. 2004b. Response of Archaeal Communities in Beach Sediments to Spilled Oil and Bioremediation. Applied and Environmental Microbiology **70**:2614-2620.

248. **Röling, W. F. M., M. G. Milner, D. Martin Jones, F. Fratepietro, R. P. J. Swanell, F. Daniel, and I. M. Head**. 2004a. Bacterial Community Dynamics and Hydrocarbon Degradation during a Field-Scale Evaluation of Bioremediation on a Mudflat Beach Contaminated with Buried Oil. Applied and Environmental Microbiology **70**:2603-2613.

249. **Roper, J. C. and F. K. Pfaender**. 2005. Products of Laccase Catalyzed Reaction of 1-Hydroxypyrene. Toxicological & Environmental Chemistry **87**:583-593.

250. **Roper, J. C. and F. K. Pfaender**. 2001. Pyrene and Chrysene Fate in Surface Soil and Sand Microcosms. Environmental Toxicology and Chemistry **20**:223-230.

251. **Rosenberg, M., D. Gutnick, and E. Rosenberg**. 1980. Adherence of Bacteria to Hydrocarbons: A Simple Method for Measuring Cell-Surface Hydrophobicity. FEMS Microbiology Letters **9**:29-33.

252. **Rosner, B.** 1986. Fundamentals of Biostatistics. Duxbury Press, Boston, MA.

253. **Rosswall, T. and E. Kvillner**. 1978. Principal-Components and Factor Analysis for the Description of Microbial Populations. Advances in Microbial Ecology **2**:1-48.

254. **Russ, J. C.** 2002. The Image Processing Handbook. CRC Press LLC, Boca Raton, FL.

255. **Sanseverino, J., C. Werner, J. Fleming, B. Applegate, J. M. H. King, and G. S. Sayler**. 1993. Molecular Diagnostics of Polycyclic Aromatic Hydrocarbon Biodegradation in Manufactured Gas Plant Soils. Biodegradation **4**:303-321.

256. **Sarma, P. M., D. Bhattacharya, S. Krishnan, and B. Lal**. 2004. Degradation of Polycyclic Aromatic Hydrocarbons by a Newly Discovered Enteric Bacterium, *Leclercia*

adecarboxylata . Applied and Environmental Microbiology **70**:3163-3166.

257. **Saul, D. J., J. M. Aislabie, C. E. Brown, L. Harris, and J. M. Foght**. 2005. Hydrocarbon Contamination Changes the Bacterial Diversity of Soil from Around Scott Base, Antarctica. FEMS Microbial Ecology **53**:141-155.

258. **Sayler, G. S., K. Nikbakht, J. T. Fleming, and J. Packard**. 1992. Applications of Molecular Techniques to Soil Biochemistry, p. 131-172. *In* G. Stotzky and J.-M. Bollag (eds.), Soil Biochemistry. Marcel Dekker, Inc., New York.

259. **Schaechter, M., O. Maaløe, and N. O. Kjeldgaard**. 1958. Dependency on Medium and Temperature of Cell Size and Chemical Composition during Balanced Growth of *Salmonella typhimurium*. Journal of General Microbiology **19**:592-606.

260. **Schlöter, M., M. Lebuhn, T. Heulin, and A. Hartmann**. 2000. Ecology and Evolution of Bacterial Microdiversity. FEMS Microbiology Reviews **24**:647-660.

261. **Schwarzenbach, R. P., P. M. Gschwend, and D. M. Imboden**. 2003. Environmental Organic Chemistry. John Wiley & Sons, Inc., Hoboken, NJ.

262. **Schweigert, N., A. J. B. Zehnder, and R. I. L. Eggen**. 2001. Chemical Properties of Catechols and their Molecular Modes of Toxic Action in Cells, from Microorganisms to Mammals. Environmental Microbiology **3**:81-91.

263. **Seo, Y. J., H. S. Jeong, E.-K. Bang, G. T. Hwang, J. H. Jung, S. K. Jang, and B. H. Kim**. 2006. Cholesterol-Linked Fluorescent Molecular Beacons with Enhanced Cell Permeability. Bioconjugate Chemistry **17**:1151-1155.

264. **Sessitch, A., A. Weilharter, M. H. Gerzabek, H. Kirchmann, and E. Kandeler**. 2001. Microbial Population Structures in Soil Particle Size Fractions of a Long-Term Fertilizer Field Experiment. Applied and Environmental Microbiology **67**:4215-4224.

265. **Shannon, C. E. and W. Weaver**. 1963. The Mathematical Theory of Communication. The University of Illinois Press, Urbana, IL.

266. **Shillaber, C. P.** 1944. Photomicrography in Theory and Practice. John Wiley & Sons, Inc., NY, NY.

267. **Siciliano, S. D., N. Fortin, A. Mihoc, G. Wisse, Z. LaBelle, D. Beaumier, D. Ouellette, R. Roy, L. G. Whyte, M. K. Banks, P. Schwab, K. Lee, and C. W. Greer**. 2001. Selection of Specific Endophytic Bacterial Genotypes by Plants in Response to Soil Contamination. Applied and Environmental Microbiology **67**:2469-2475.

268. **Sikkema, J., J. A. M. de Bont, and B. Poolman**. 1995. Mechanisms of Membrane Toxicity of Hydrocarbons. Microbiological Reviews **59**:201-222.

269. **Singleton, D. R., S. N. Powell, R. Sangaiah, A. Gold, L. M. Ball, and M. D. Aitken**. 2005. Stable-isotope Probing of Bacteria Capable of Degrading Salicylate, Naphthalene, or

Phenanthrene in a Bioreactor Treating Contaminated Soil. Applied and Environmental Microbiology **71**:1202-1209.

270. **Singleton, D. R., R. Sangaiah, A. Gold, L. M. Ball, and M. D. Aitken**. 2006. Identification and Quantification of Uncultivated Proteobacteria Associated with Pyrene Degradation in a Bioreactor Treating PAH-Contaminated Soil. Environmental Microbiology **8**:1736-1745.

271. **Smalla, K., G. Wieland, A. Buchner, A. Zock, J. Parzy, S. Kaiser, N. Roskot, H. Heuer, and G. Berg**. 2001. Bulk and Rhizosphere Soil Bacterial Communities Studied by Denaturing Gradient Gel Electrophoresis: Plant-Dependent Enrichment and Seasonal Shifts Revealed. Applied and Environmental Microbiology **67**:4742-4751.

272. **Smit, E., P. Leeflang, S. Gommans, J. van den Broek, S. van Mil, and K. Wernars**. 2001. Diversity and Seasonal Fluctuations of the Dominant Members of the Bacterial Soil Community in a Wheat Field as Determined by Cultivation and Molecular Methods. Applied and Environmental Microbiology **67**:2284-2291.

273. **Smith, K. A. and J. R. M. Arah**. 1985. Anaerobic Micro-Environments in Soil and the Occurrence of Anaerobic Bacteria. Proceedings of the FEMS Symposium #33 247-261.

274. **Smith, M. J., G. Lethbridge, and R. G. Burns**. 1999. Fate of Phenanthrene, Pyrene, and Benzo[a]pyrene During Biodegradation of Crude Oil Added to Two Soils. FEMS Microbiology Letters **173**:445-452.

275. **Smith, V. H.** 2002. Effects of Resource Supplies on the Structure and Function of Microbial Communities. Antonie van Leeuwenhoek **81**:99-106.

276. **Snaidr, J., R. Amann, I. Huber, W. Ludwig, and K.-H. Schleifer**. 1997. Phylogenetic Analysis and In Situ Identification of Bacteria in Activated Sludge. Applied and Environmental Microbiology **63**:2884-2896.

277. **Snel, B., P. Bork, and M. A. Huynen**. 2002. Genomes in Flux: The Evolution of Archaeal and Proteobacterial Gene Content. Genome Research **12**:17-25.

278. **Sogin, S. J., M. L. Sogin, and C. R. Woese**. 1972. Phylogenetic Measurement in Procaryotes by Primary Structural Characterization. Journal of Molecular Evolution **1**:173-184.

279. **Sowers, K. R. S. H. J.** 1995. Archaea: A Laboratory Manual. Cold Spring Harbor Laboratory Press, Plainview, NY.

280. **Spain, J. C. and P. A. van Veld**. 1983. Adaptation of Natural Microbial Communities to Degradation of Xenobiotic Compounds: Effects of Concentration, Exposure Time, Inoculum, and Chemical Structure. Applied and Environmental Microbiology **45**:428-435.

281. **Stackebrandt, E., W. Frederiksen, G. M. Garrity, P. A. D. Grimont, P. Kämpfer, M. C. J. Maiden, X. Nesme, R. Rosselló-Mora, J. Swings, H. G. Trüper, L. Vauterin, A.**

C. Ward, and W. B. Whitman. 2002. Report of the Ad Hoc Committee for the Re-evaluation of the Species Definition in Bacteriology. International Journal of Systematic and Evolutionary Microbiology **52**:1043-1047.

282. **Stephen, J. R., Y.-J. Chang, Y. D. Gan, A. Peacock, S. M. Pfiffner, M. J. Barcelona, D. C. White, and S. J. MacNaughton**. 1999. Microbial Characterization of a JP-4 Fuel-contaminated Site Using a Combined Lipid Biomarker/Polymerase Chain Reaction-Denaturing Gradient Gel Electrophoresis (PCR-DGGE)-based Approach. Environmental Microbiology **1**:231-241.

283. **Stringfellow, W. T.** 1994. PhD Dissertation. University of North Carolina at Chapel Hill. The Physiology and Kinetics of Polynuclear Aromatic Hydrocarbon Degradation by Bacteria.

284. **Stringfellow, W. T. and L. Alvarez-Cohen**. 1999. Evaluating the Relationship between the Sorption of PAHs to Bacterial Biomass and Biodegradation. Water Research **33**:2535-2544.

285. **Sutherland, J. B., F. Rafii, A. A. Khan, and C. E. Cerniglia**. 1995. Mechanisms of Polycyclic Aromatic Hydrocarbon Degradation, p. 269-306. *In* L. Y. Young and C. E. Cerniglia (eds.), Microbial Transformation and Degradation of Toxic Organic Chemicals. John Wiley & Sons, Inc., New York.

286. **Sutherland, J. B., A. L. Selby, J. P. Freeman, F. E. Evans, and C. E. Cerniglia**. 1991. Metabolism of Phenanthrene by *Phanerochaete chrysosporium* . Applied and Environmental Microbiology **57**:3310-3316.

287. **Takai, K. and K. Horikoshi**. 2000. Rapid Detection and Quantification of Members of the Archaeal Community by Quantitative PCR Using Fluorogenic Probes. Applied and Environmental Microbiology **66**:5066-5072.

288. **Tang, W.-C., J. C. White, and M. Alexander**. 1998. Utilization of Sorbed Compounds by Microorganisms Specifically Isolated for that Purpose. Applied Microbiology and Biotechnology **49**:117-121.

289. **Tate III, R. L.** 2000. Soil Microbiology. John Wiley & Sons, Inc., New York.

290. **Thompson, I. P., M. J. Bailey, R. J. Ellis, N. Maguire, and A. A. Meharg**. 1999. Response of Soil Microbial Communities to Single and Multiple Doses of an Organic Pollutant. Soil Biology and Biochemistry **31**:95-105.

291. **Tilman, D.** 1993. Community Diversity and Succession: The Roles of Competition, Dispersal, and Habitat Modification, p. pp. 327-346. *In* E.-D. Schulze and H. A. Mooney (eds.), Biodiversity and Ecosystem Function. Springer-Verlag, New York.

292. **Tilman, D. and J. Knops**. 1997. The Influence of Functional Diversity and Composition on Ecosystem Processes. Science **277**:1300-1303.

293. **Torsvik, V., J. Goksøyr, and F. L. Daae**. 1990b. High Diversity in DNA of Soil Bacteria. Applied and Environmental Microbiology **56**:782-787.

294. **Torsvik, V., K. Salte, R. Sørheim, and J. Goksøyr**. 1990a. Comparison of Phenotypic Diversity and DNA Heterogeneity in a Population of Soil Bacteria. Applied and Environmental Microbiology **56**:776-781.

295. **Torsvik, V. L.** 1980. Isolation of Bacterial DNA from Soil. Soil Biology & Biochemistry **12**:15-21.

296. **Totsche, K. U., S. Jann, and I. Kogel-Knabner**. 2006. Release of Polycyclic Aromatic Hydrocarbons, Dissolved Organic Carbon, and Suspended Matter from Disturbed NAPL-Contaminated Gravelly Soil Material. Vadose Zone Journal **5**:469-479.

297. **Treves, D. S., B. Xia, J. Zhou, and J. M. Tiedje**. 2002. A Two-Species Test of the Hypothesis that Spatial Isolation Influences Microbial Diversity in Soil. Microbial Ecology **45**:20-28.

298. **Uyttebroek, M., P. Breugelmans, M. Janssen, P. Wattiau, B. Joffe, U. Karlson, J. J. Ortega-Calvo, L. Bastiaens, A. Ryngaert, M. Hausner, and D. Springael**. 2006a. Distribution of the *Mycobacterium* Community and Polycyclic Aromatic Hydrocarbons (PAHs) among Different Size Fractions of a Long-term PAH-Contamimnated Soil. Environmental Microbiology **8**:836-847.

299. **Uyttebroek, M., J.-J. Ortega-Calvo, P. Breugelmans, and D. Springael**. 2006b. Comparison of Mineralization of Solid-Sorbed Phenanthrene by Polycyclic Aromatic Hydrocarbon (PAH)-Degrading *Mycobacterium* spp. and *Sphingomonas* spp. Applied Microbiology and Biotechnology **72**:829-836.

300. **Vacca, D. J., W. F. Bleam, and W. J. Hickey**. 2005. Isolation of Soil Bacteria Adapted to Degrade Humic Acid-Sorbed Phenanthrene. Applied and Environmental Microbiology **71**:3797-3805.

301. **van Elsas, J. D. and K. Smalla**. 1995. Extraction of Microbial Community DNA from Soils, *In* Molecular Microbial Ecology Manual. Kluwer Academic Publishers, Netherlands.

302. **Vanderford, M.** 2001. PhD Dissertation. University of North Carolina at Chapel Hill. Influence of Metabolites and Co-Contaminants on the Biodegradation of Polycyclic Aromatic Hydrocarbons in Soils.

303. **Vertriani, C., H. W. Jannasch, B. J. MacGregor, D. Stahl, and A. Reysenbach**. 1999. Population Structure and Phylogenetic Characterization of Marine Benthic Archaea in Deep-Sea Sediments. Applied and Environmental Microbiology **65**:4375-4384.

304. **Vertriani, C., A. Reysenbach, and J. Doré**. 1998. Recovery and Phylogenetic Analysis of Archaeal rRNA Sequences from Continental Shelf Sediments. FEMS Microbiology Letters **161**:83-88.

305. **Viñas, M., M. Grifoll, J. Sabaté, and A. M. Solanas**. 2002. Biodegradation of a Crude Oil by Three Microbial Consortia of Different Origins and Metabolic Capabilities. Journal of Industrial Microbiology & Biotechnology **28**:252-260.

306. **von Wintzingerode, F., U. B. Gobel, and E. Stackebrandt**. 1997. Determination of Microbial Diversity in Environmental Samples: Pitfalls of PCR-based rRNA Analysis. FEMS Microbiology Reviews **21**:213-229.

307. **Vuilleumier, S.** 1997. Bacterial Glutathione S-Transferases: What are They Good for? Journal of Bacteriology **179**:1431-1441.

308. **Wagner, M., R. Amann, H. Lemmer, and K.-H. Schleifer**. 1993. Probing Activated Sludge with Oligonucleotides Specific for Proteobacteria: Inadequacy of Culture-Dependent Methods for Describing Microbial Community Structure. Applied and Environmental Microbiology **59**:1520-1525.

309. **Wagner, M., M. Horn, and H. Daims**. 2003. Fluorescence *in situ* Hybridization for the Identification and Characterization of Prokaryotes. Current Opinion in Microbiology **6**:302-309.

310. **Wagner, M., P. H. Nielsen, A. Loy, J. L. Nielsen, and H. Daims**. 2006. Linking Microbial Community Structure with Function: Fluorescence *in situ* Hybridization-Microautoradiography and Isotope Arrays. Current Opinion in Biotechnology **17**:83-91.

311. **Wagner, M., M. Schmid, S. Juretschko, K.-H. Trebesius, A. Bubert, W. Goebel, and K.-H. Schleifer**. 1998. In situ Detection of a Virulence Factor mRNA and 16S rRNA in *Listeria monocytogenes* . FEMS Microbiology Letters **160**:159-168.

312. **Walter, U., M. Beyer, J. Klein, and H.-J. Rehm**. 1991. Degradation of Pyrene by *Rhodococcus* sp. UW1. Applied Microbiology and Biotechnology **34**:671-676.

313. **Wang, G. C. Y. and Y. Wang**. 1997. Frequency of Formation of Chimeric Molecules as a Consequence of PCR Coamplification of 16S rRNA Genes from Mixed Bacterial Genomes. Applied and Environmental Microbiology **63**:4645-4650.

314. **Watanabe, K. and N. Hamamura**. 2003. Molecular and Physiological Approaches to Understanding the Ecology of Pollutant Degradation. Current Opinion in Biotechnology **14**:289-295.

315. **Weissenfels, W. D., H. J. Klewer, and J. Langhoff**. 1992. Adsorption of Polycyclic Aromatic Hydrocarbons (PAHs) by Soil Particles: Influence on Biodegradability and Biotoxicity. Applied Microbiology and Biotechnology **36**:689-696.

316. **Wick, L. Y., T. Colangelo, and H. Harms**. 2001. Kinetics of Mass Transfer-Limited Bacterial Growth on Solid PAHs. Environmental Science & Technology **35**:354-361.

317. **Wick, L. Y., A. R. de Munain, D. Springael, and H. Harms**. 2002. Responses of *Mycobacterium* sp. LB501T to the Low Bioavailability of Solid Anthracene. Applied

Microbiology and Biotechnology **58**:378-385.

318. **Wilcke, W.** 2000. Polycyclic Aromatic Hydrocarbons in Soil- A Review. Journal of Plant Nutrition and Soil Science **163**:229-248.

319. **Wilson, M. S. and C. M. E. L. Bakermans**. 1999. In Situ, Real-Time Catabolic Gene Expression: Extraction and Characterization of Naphthalene Dioxygenase mRNA Transcripts from Groundwater. Applied and Environmental Microbiology **65**:80-87.

320. **Woese, C. R.** 1998. The Universal Ancestor. Proceedings of the National Academy of Science, USA **95**:6854-6859.

321. **Woese, C. R. and G. E. Fox**. 1977. Phylogenetic Structure of the Prokaryotic Domain: The Primary Kingdoms. Proceedings of the National Academy of Science, USA **74**:5088-5090.

322. **Wolf, Y. I., I. B. Rogozin, N. V. Grishin, and E. V. Koonin**. 2002. Genome Trees and the Tree of Life. TRENDS in Genetics **18**:472-479.

323. **Wolfaardt, G. M., J. R. Lawrence, J. V. Headley, and R. D. Robarts**. 1994. Microbial Exopolymers Provide a Mechanism for Bioaccumulation of Contaminants. Microbial Ecology **27**:279-291.

324. **Wolfaardt, G. M., J. R. Lawrence, R. D. Robarts, and D. E. Caldwell**. 1995. Bioaccumulation of the Herbicide Diclofop in Extracellular Polymers and its Utilization by a Biofilm Community during Starvation. Applied and Environmental Microbiology **61**:152-158.

325. **Wollum, A. G.** 1999. Introduction and Historical Perspective, p. 3-20. *In* D. M. Sylvia, J. J. Fuhrmann, P. G. Hartel, and D. A. Zuberer (eds.), Principles and Applications of Soil Microbiology. Prentice Hall, New Jersey.

326. **Woodward, F. I.** 1993. How Many Species are Required for a Functional Ecosystem?, p. 271-292. *In* E.-D. Schulze and H. A. Mooney (eds.), Biodiversity and Ecosystem Function. Springer-Verlag, New York.

327. **Wu, G., Y. Feng, and S. A. Boyd**. 2003. Characterization of Bacteria Capable of Degrading Soil-Sorbed Biphenyl. Bulletin of Environmental Contamination and Toxicology **71**:768-775.

328. **Wünsche, L., L. Brüggemann, and W. Babel**. 1995. Determination of Substrate Utilization Patterns of Soil Microbial Communities: An Approach to Assess Population Changes After Hydrocarbon Pollution. FEMS Microbiology Ecology **17**:295-306.

329. **Xing, B. and J. J. Pignatello**. 1997. Dual-Mode Sorption of Low-Polarity Compounds in Glassy Poly(vinyl chloride) and Soil Organic Matter. Environmental Science & Technology **31**:792-798.

330. **Xing, B. and J. J. Pignatello**. 1996. Time-Dependent Isotherm Shape of Organic Compounds in Soil Organic Matter: Implications for Sorption Mechanism. Environmental Toxicology and Chemistry **15**:1282-1288.

331. **Yang, C.-H. and D. E. Crowley**. 2000. Rhizosphere Microbial Community Structure in Relation to Root Location and Plant Iron Nutritional Status. Applied and Environmental Microbiology **66**:345-351.

332. **Young, I. M. and J. W. Crawford**. 2004. Interactions and Self-Organization in the Soil-Microbe Complex. Science **304**:1634-1637.

333. **Yuan, S. Y., S. H. Wei, and B. V. Chang**. 2000. Biodegradation of Polycyclic Aromatic Hydrocarbons by a Mixed Culture. Chemosphere **41**:1463-1468.

334. **Yuste, L., M. E. Corbella, M. J. Turiégano, U. Karlson, A. Puyet, and F. Rojo**. 2000. Characterization of Bacterial Strains able to Grow on High Molecular Mass Residues from Crude Oil Processing. FEMS Microbiology Ecology **32**:69-75.

335. **Zablotowicz, R. M., R. E. Hoagland, M. A. Locke, and W. J. Hickey**. 1995. Glutathione S-transferase Activity and Metabolism of Glutathione Conjugates by Rhizosphere Bacteria. Applied and Environmental Microbiology **61**:1054-1060.

336. **Zehnder, A. J. B. and P. J. Colberg**. 1985. Anaerobic Biotransformation of Organic Carbon Compounds. Proceedings of the FEMS Symposium #33 275-291.

337. **Zhang, D., Y. Yang, L. A. Castlebury, and C. E. Cerniglia**. 1996. A Method for the Large Scale Isolation of High Transformation Efficiency Fungal Genomic DNA. FEMS Microbiology Letters **145**:261-265.

338. **Zhang, H., A. Kallimanis, A. Koukkou, and C. Drainas**. 2004. Isolation and Characterization of Novel Bacteria Degrading Polycyclic Aromatic Hydrocarbons from Polluted Greek Soils. Applied Microbiology Biotechnology **65**:124-131.

339. **Zhong, Y., T. Luan, X. Wang, C. Lan, and N. F. Y. Tam**. 2007. Influence of Growth Medium on Cometabolic Degradation of Polycyclic Aromatic Hydrocarbons by *Sphingomonas* sp. Strain PheB4. Applied Microbiology and Biotechnology **75**:175-186.

340. **Zhou, G., W.-Z. Whong, T. Ong, and B. Chen**. 2000. Development of a Fungus-specific PCR Assay for Detecting Low-level Fungi in an Indoor Environment. Molecular and Cellular Probes **14**:339-348.

341. **Zhou, J., M. A. Bruns, and J. M. Tiedje**. 1996. DNA Recovery from Soils of Diverse Composition. Applied and Environmental Microbiology **62**:316-322.

342. **Zhou, J., B. Xia, D. Treves, L.-Y. Wu, T. L. Marsh, R. V. O'Neill, A. V. Palumbo, and J. M. Tiedje**. 2002. Spatial and Resource Factors Influencing High Microbial Diversity in Soil. Applied and Environmental Microbiology **68**:326-334.

343. **Zhu, X. Y., J. Lubeck, and J. J. Kilbane II**. 2003. Characterization of Microbial Communities in Gas Industry Pipelines. Applied and Environmental Microbiology **69**:5354-5363.